Synthesis and characterisations of architecturally complex branched polymers

AGOSTINI, SERENA

Synthesis and characterisations of architecturally complex branched polymers

Serena Agostini

Department of Chemistry
Durham University

February 2014

Thesis submitted in fulfilment for the degree of Doctor of Philosophy

Serena Agostini

Synthesis and characterisations of architecturally complex branched polymers

Abstract

Well-defined branched polymers are fundamental in the understanding and prediction of the relationship between structure and properties. This work focused on two different types of branched polymers which we described in terms of their synthesis and characterisation. In particular we carried out a study on Hyperblocks and asymmetric three-arm stars. The combination of living anionic polymerisation and "macromonomer" approach was successfully used for the production of both types of branched polymers demonstrating the great versatility of this synthetic methodology. HyperBlocks were constructed from well-defined AB_2 macromonomers of polystyrene-polyisoprene-polystyrene while asymmetric three-arm stars involved the synthesis of well-defined polystyrene arms with different chain-end functionalities for the 'long' and the 'short' arm respectively. We have explored Williamson coupling reaction and copper (I)-catalysed azide-alkyne 'click' reaction for the final assembly of both HyperBlocks and three-arm stars. These materials were characterised by differential scanning calorimetry (DSC), transmission electron microscopy (TEM), mechanical tensile testing and temperature gradient interaction chromatography (TGIC). The characterisations in terms of morphology, thermal and mechanical properties carried out on HyperBlocks, macromonomers and the commercial thermoplastic elastomer (TPE) Kraton^{TM} D-1160 are here described and compared. Microphase separation with no long-range order was observed in the case of HyperBlocks and blends of the latter with the commercial TPE, suggesting that the highly branched structure frustrates and inhibit the formation of long-range order morphologies. Nevertheless the mechanical properties of HyperBlocks demonstrated to be superior to the properties of their well-defined linear precursors with long-range order morphologies. Analysis of the three-arm stars using the TGIC showed structural dispersity The ability of TGIC technique to separate polymers in terms of molecular weights allowed us to fully characterise the star polymers and quantify the impurities left after purification by fractionation.

Table of contents

CHAPTER 3 Characterisation of HyperBlocks

CHAPTER 4 Synthesis of Asymmetric Stars via the Macromonomer Approach

CHAPTER 5 Concluding remarks

List of Figures

List of Schemes

List of Tables

List of Abbreviations

AIBN	Azobisisobutyronitrile
ATRP	Atom Transfer Radical Polymerisation
B3OH	1,1-Tris(4-hydroxyphenyl)ethane
BHT	3,5-di-*tert*-butyl-4-hydroxytoluene
bp	boiling point
CMM	Couple-Monomer Methodology
CuAAC	Copper (I)-Catalysed Azide-Alkyne Cycloaddition
DB	Degree of Branching
DCM	Dichloromethane
DMF	Dimethylformamide
DMM	Double-Monomers Methodology
DMSO	Dimethylsulfoxide
dn/dc	Refractive index increment
DNA	Deoxyribonucleic Acid
DPE	Diphenylethylene
DPE-OSi	1,1-Bis(4-*tert*-butyldimethylsiloxyphenyl)ethylene
DP_n	Number Average Degree of Polymerisation
DP_w	Weight Average Degree of Polymerisation
DSC	Differential Scanning Calorimetry
DVB	Divinylbenzene
Et_2O	Diethyl ether
HB	Hyperbranched polymer
IC	Interaction Chromatography
IUPAC	International Union of Pure and Applied Chemistry
LCCC	Liquid Chromatography at Critical Condition
M_e	Entanglement Molecular Weight
M_n	Number Average Molecular Weight
M_w	Weight Average Molecular Weight
NMP	Nitroxide Mediated Polymerisation
NMR	Nuclear Magnetic Resonance
NP	Normal Phase
Đ	Dispersity
PDMS	Polydimethylsiloxane
PI	Polyisoprene
PS	Polystyrene
PS-PI	Polystyrene-Polyisoprene
PS-PI-PS	Polystyrene-Polyisoprene-Polystyrene
PTFE	Polytetrafluoroethylene
PTP	Proton-Transfer Polymerisation
RAFT	Reversible Addition-Fragmentation Transfer
RALS	Right Angle Light Scattering

RDRP	Reversible-Deactivation Radical Polymerisation
RI	Refractive Index
ROMBP	Ring-Opening Multibranching Polymerisation
RP	Reverse Phase
SBS	Polystyrene-Polybutadiene-Polystyrene polymer
SCFT	Self-Consistent Field Theory
SCROP	Self-Condensing Ring-Opening Polymerisation
SCVP	Self-Condensing Vinyl Polymerisation
SD	Standard Deviation
SEC	Size Exclusion Chromatography
sec-BuLi	*sec*-Buthyllithium
SHP	Segmented Hyperbranched Polymer
SIS	Polystyrene-Polyisoprene-Polystyrene polymer
SMM	Single-Monomer Methodology
t-BuOLi	Lithium *tert*-butoxide
TEM	Transmission Electron Microscopy
TEMPO	(2,2,6,6-tetramethylpiperidin-1-yl)oxyl
T_g	Glass Transition Temperature
TGIC	Temperature Gradient Interaction Chromatography
THF	Tetrahydrofuran
TLC	Thin Layer Chromatography
T_m	Melting Temperature
TMEDA	N,N,N',N'-tetramethylethylenediamine
TMP	1,1,1-Tris(hydroxymethyl)propane
TPE	Thermoplastic Elastomer
UTS	Ultimate Tensile Stress
P(S-I)	Poly(styrene-*block*-isoprene)
P(S-I-S)	Poly(styrene-*block*-isoprene-*block*-styrene)
P(S-I-S)a_b	Poly(styrene-*block*-isoprene-*block*-styrene)a_b The macromonomers synthesised in this work are named systematically P(S-I-S)a_b where *a* refers to the macromonomer molecular weight obtained by NMR analysis and *b* is the weight fraction (as a percentage) of polystyrene in the copolymer.
HBa_b	HyperBlock has been systematically named HBa_b where HB denotes HyperBlock, *a* stands for the molecular weight of the linear macromonomer precursor calculated by ^{1}H-NMR spectroscopy and *b* stands for the weight fraction of polystyrene in the macromonomer.
PSX	The short arms have been named PSX where X stands for the molecular weight in kg mol^{-1} calculated by SEC of the polystyrene arms.
StarX	The stars synthesised has been named StarX where X stands for the molecular weight in kg mol^{-1} calculated by SEC of the 'short' arm and, only for the symmetric star, of the 'long arm.

Statement of Copyright

Acknowledgements

I would like to express my sincere gratitude and special thanks to my supervisor Dr. Lian Hutchings for his continuous support, his patient, enthusiasm, motivation and many advises given to me during these years. Thanks for allowing me to work at this project and for the great help in the research and in the writing of this thesis.

I would also like to thank for their help and collaboration Dr. Richard Thompson, Durham University, Dr. Marianne Stol, Kraton™ Polymers Research in Amsterdam, and Dr. Christine Richardson, School of Biological and Biomedical Sciences in Durham, Mrs Onome Swader, Durham University and academic and non-academic staff in the Department of Chemistry at Durham University.

I thank the European project Dynacop for founding this research and all the people part of this project that I met during our meetings around Europe for their friendship and scientific help.

I would especially like to thank Dr Solomon Kimani for his huge help in the lab and his friendship. Without him and his motto “Life is too short” everything would have been much more difficult and much less funny.

At the end I would like to thank all present and past members in our research group, in particular Paul, Fabian, Lukas, Irina, Karina, Brunella, Tatiana and Gabriele. I also thank all my friends from the office CG156 for the good times spent together.

A special thank goes to my family that supported me during this period abroad, even if we were so far away from each other. Thanks to my special friends Federico, Claudia, Linda, Marianna, Sara and Martina that, even if not physically present, were always with me.

To my family,

Ivana and Sergio

Ilenia and Angelo

CHAPTER 1

Introduction

1.1 Well-defined polymers: properties and synthesis

The term polymer refers to a large class of natural and synthetic materials with a wide range of properties. They play an important role in everyday life: plastics, rubber, adhesives, fibers, coatings and natural biopolymers such as DNA and proteins are all essential for life. The first polymers used were natural products, especially cotton, starch, proteins and wool. The first synthetic polymer made was Bakelite, a resin of phenolformaldehyde produced in the first decade of the twentieth century. After that polymer science continued to develop and it led to the discovery of living anionic polymerisation by Szwarc[1] in the 1950's which gave rise to the possibility of producing polymers with controlled molecular weights, low dispersity and complex architectures. More recently, controlled radical polymerisation mechanisms e.g. ATRP, NMP, RAFT were discovered and improved in order to produce well-defined polymers with several architectures and functionalities. Branched polymers such as stars, graft copolymers, miktoarm stars, H-shaped polymers, dendrimers and hyperbranched polymers gained importance due to the interesting properties linked to their structures. The study of the relationship between properties and structure made the development of well-defined polymers more and more important.

The continuous research to produce novel polymers led to the screening of organic synthesis and to the application of organic reactions in polymers synthesis. Latest notable example of this interaction is given by the development of the concept of 'click' chemistry reported first in 2001 by Sharpless *et al.*[2] and now used extensively in the field of polymer science. The combination of living or controlled polymerisations with the newly developed synthetic strategy of the 'click' chemistry has favoured the development of polymers architectures.

1.2 Polymer synthesis

Polymers can be synthesised using different types of reactions.[3] It is possible to divide these reactions into two general groups, according to their mechanisms: step-growth polymerisation and chain-growth polymerisation. This subdivision makes a distinction between polymers prepared by the stepwise reaction of monomers and those formed by chain reactions.

A step-growth polymerisation can be described as a process that at the beginning involves one or more monomers having at least two reactive sites, i.e. functional groups. Two monomers can react together to give a dimer, a monomer may add to a trimer, or two dimers combine to form a tetramer and so on to form the polymer chains. From this, one can infer that polymerisation occurs by reaction between any of the reactive species not by addition of one monomer at a time. The monomer is consumed at the beginning of the reaction and step growth polymerisation does not need an initiator to start the reaction. The monomers can react with or without elimination of a byproduct: the former is the case of polycondensation reactions, the latter is the case of polyaddition reactions. It is possible to synthesise with this type of polymerisation polymers like polyester, polyamide, polyurethane, polysiloxane, polycarbonates, polyurea and polysulfides. The reactions involved are reactions to the carbonyl group or nucleophilic substitutions.

In the polymerisations that occur via a chain reaction, the monomers are usually converted into polymers by reaction of the double bond of substituted alkene monomers with a free radical or ionic initiator. The product, then, unlike that obtained from step-growth polymerisation, has the same chemical composition of the starting monomer, i.e., each unit in the chain is a complete monomer and not a residue as in the most step-growth reactions. In general when the polymerisation mechanism proceeds by the reaction of radicals, the reaction is called Free Radical Polymerisation, however, when it proceeds via reaction with ions, we have Anionic and Cationic Polymerisations. The chain grows by addition of one monomer unit at a time and the active species are always at the chain end. The complete polymerisation proceeds in three distinct stages: initiation, propagation and termination.

1.2.1 Free Radical Polymerisation

Free radical polymerisation[4] is a chain-growth polymerisation that yields polymers with high molecular weights in a very short time. The mechanism and kinetics of free radical polymerisation of vinyl compounds was described for the first time in 1937 by Flory.[5] It is a very common reaction for the industrial synthesis of polymers as it is applicable to a wide range of monomers, it is very tolerant of many functional groups (OH, NR_2, COOH) and the only requirement for its success is to exclude oxygen from the reaction bulk. The drawback of this kind of polymerisation is the impossibility of obtaining well-defined polymers in terms of molecular weight, composition and polymer architecture due to the lack of control that characterises the free radical polymerisations. The active species in this type of chain-growth polymerisation is a free radical. The radicals terminate at a very fast rate controlled only by the rate of diffusion of the radicals and this leads to the absence of control in the polymerisation. A free radical is an atomic or molecular fragment that comes from the homolytic rupture of a covalent bond; in that species the free electron is not involved in any covalent bonds. The presence of this free radical transforms the molecule or atom into a very reactive species that is capable of reacting with an olefinic monomer to generate a chain carrier that can retain its activity to propagate a macromolecular chain under the appropriate conditions. This type of synthesis is generally used for the polymerisation of vinyl monomers, for instance styrene, methyl methacrylate and vinyl chloride. Free radical polymerisations, being a chain-growth polymerisation, include the three steps of initiation, propagation and termination mentioned above.

Initiation

Initiation is the first step of the reaction. The radical can be formed in several radical-producing reactions[4]:

a) Thermal decomposition: it can be applied to organic peroxides (-O-O-), for example benzoyl peroxide (Equation 1.1), or azo compounds (-N=N-).

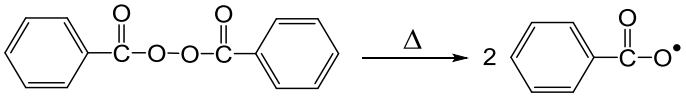

(1.1)

b) Photolysis: it can be applied to azo compounds, metal iodides and metal alkyls, for example, AIBN (Azobisisobutyronitrile) that is decomposed by radiation. (Equation 1.2)

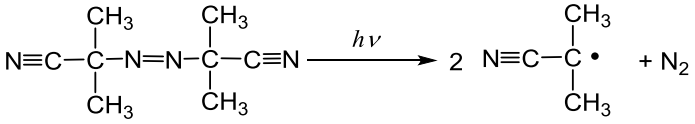

(1.2)

c) Redox reactions: for example the reaction between the ferrous ions and hydrogen peroxide in solution that produces hydroxyl radicals (Equation 1.3), but it is also possible to use alkyl hydroperoxides instead of hydrogen peroxide.

$$H_2O_2 + Fe^{2+} \rightarrow Fe^{3+} + OH^- + OH^{\cdot} \qquad (1.3)$$

Once formed, the radical is not stable and so it can react rapidly with a large number of unsaturated monomers reacting with the π bond. It is possible to have two types of reaction with the double bond due to the unsymmetrical nature of the double bond but one is the favoured because of stabilisation due to the resonance effect. (Scheme 1.1)

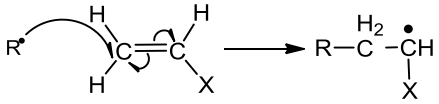

Scheme 1.1 Mechanism of a radical attack to a double bond.

The new radical species formed in this way is now able to react with another monomer forming the polymer chain in the so called *propagation step*.

Propagation

The chain propagation proceeds rapidly by addition of a monomer unit to the chain carrier. The active centre is displaced after every addition to the extremity of the growing chain. (Equation 1.4) The average life time of the growing chain is short, in the order of second or less.

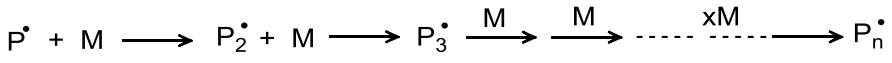

(1.4)

Termination

Termination occurs when the active radical at the chain end is deactivated, which means the end of the growth of the polymer chain. In theory, the chain could continue to propagate until all the monomer in the system has been consumed, but free radicals are very reactive and so they can react with other radicals to form inactive covalent bonds. Termination of chains can take place in several ways:

- reaction between two active chain ends
- reaction of an active chain end with an initiator radical
- transfer of the active centre to another molecule which may be a solvent, initiator or monomer (chain transfer)
- interaction with impurities or inhibitors

Free radical polymerisation leads to high molar-mass polymers as soon as the reaction starts, the monomer concentration decreases steadily throughout the reaction, only the active centre can react with the monomer and add units to the chain, and furthermore long reaction times increase the polymer yield, but not the molar mass of the polymer.

It is important to mention that this type of polymerisation is difficult to control because of the numerous, fast, irreversible, termination and chain transfer reactions that occur. It results in a product with a broad molecular weight distribution. Because of this free radical polymerisation is not a good method for producing well defined model polymers and it is not possible to produce well-defined block copolymers by free radical polymerisation. To obtain a better control on the polymers produced whilst maintaining the versatility of free radical polymerisation, a range of “controlled/living radical polymerisation” mechanisms have been developed.

1.2.2 Controlled Free Radical Polymerisation

Free radical polymerisation is characterised by the presence of chain termination and chain transfer reactions that lead to polymers with broad molecular weight distributions. In order

to gain control over the polymerisation mechanism and obtain well defined polymers, the free radical polymerisation mechanism has been modified leading to the development of a family of "controlled radical polymerisation" mechanisms, today called by IUPAC "reversible-deactivation radical polymerisation" (RDRP).[6] The aim of this new kind of polymerisation was to suppress the amount of termination in order to narrow the dispersity. This has been achieved in a variety of ways but in each case an equilibrium is introduced which promotes the reversible deactivation of the majority of the propagating species. The introduction of this dynamic equilibrium[7] allows control over the molecular weight of the polymers, imparts relatively low dispersity (Đ < 1.1 in some cases) and permits the synthesis of polymers with different functionalities and different architectures such as stars, combs, block copolymers or graft copolymers.

The reactions that belong to the group of controlled radical polymerisation are:

a) Atom Transfer Radical Polymerisation (ATRP)
b) Reversible Addition-Fragmentation Chain Transfer (RAFT)
c) Nitroxide Mediated radical Polymerisation (NMP)

ATRP and NMP can be represented by the following general equation (Equation 1.5).

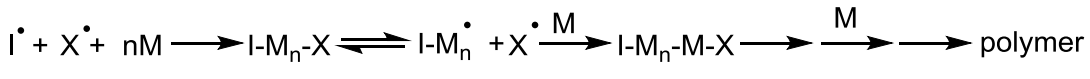

(1.5)

where I-X is the initiator used and M the monomer polymerised (n ≥ 1). The reaction is based on a rapid dynamic equilibrium between a very small amount of chain growing free radicals ($I\text{-}M_n^{\cdot}$) and a large excess of a dormant species ($I\text{-}M_n\text{-}X$).

1.2.2.1 ATRP

Atom Transfer Radical Polymerisations (ATRP) [8,9] are transition metal mediated controlled radical polymerisation reactions that were discovered at the same time in 1995 by the research groups of Matyjaszewski[10] and Sawamoto.[11] Many types of polymer architectures[12] can be synthesised by ATRP utilising commercially available starting materials under varied conditions and temperatures.

In these reactions metal catalysts are used in combination with aromatic ligands to achieve well-defined polymers with low molecular weight distribution. The mechanism involves the

transfer of a halogen atom (X) from the dormant species to the metal catalyst producing an active species (the radical). (Scheme 1.2)

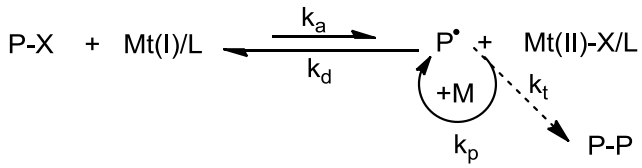

Scheme 1.2 Mechanism of the Atom Transfer Radical Polymerisation equilibrium.

The polymerisation proceeds through a reversible redox reaction that results in the oxidation of a transition metal (Mt(I)/L) when the polymer moves from the dormant species (P-X) to the active one ($P^{\cdot}$) by the transfer of the halogen to the same metal (Mt(II)-X/L). The metal catalyst is coordinated to multidentate ligands (L) that help the metal to abstract the halogen. It is important to notice that in the equilibrium reaction the deactivation reaction is kinetically favoured ($k_d >> k_a$) and that results in a very low concentration of the active species with all the consequences mentioned above. The termination reactions are minimised but not completely eliminated and this leads to limitations in control of the molecular weight and the dispersity of the polymers especially when attempting to make high molecular weight polymers or to drive reactions to high conversions. The product of the ATRP reaction is a potential initiator for a successive ATRP reaction because the polymers still have a halogen at the end of the chains. These conditions lead to the use of the polymers obtained via ATRP as a macroinitiator useful for the synthesis of block copolymers.
The limitations of ATRP reactions include problems with monomers containing functional groups that do not tolerate the reaction's conditions, i.e. carboxylic acids groups. In addition there is the problem due to the difficult removal of the metal catalyst and this constitutes a disadvantage of ATRP. This fact has a great impact on the use of ATRP for biotechnological applications where it is often required very low levels of metals. The presence of the metal in the final product is to be avoided for toxicological reasons.

1.2.2.2 RAFT

Reversible Addition-Fragmentation chain Transfer polymerisation (RAFT)[13,14] is a controlled radical polymerisation based on the use of dithio or trithio compounds as transfer agents. It was introduced by Rizzardo in 1998[15] and it is among the most successful controlled radical

polymerisation processes due to its applicability to a wide range of monomers. The mechanism of the reaction is shown in Scheme 1.3.

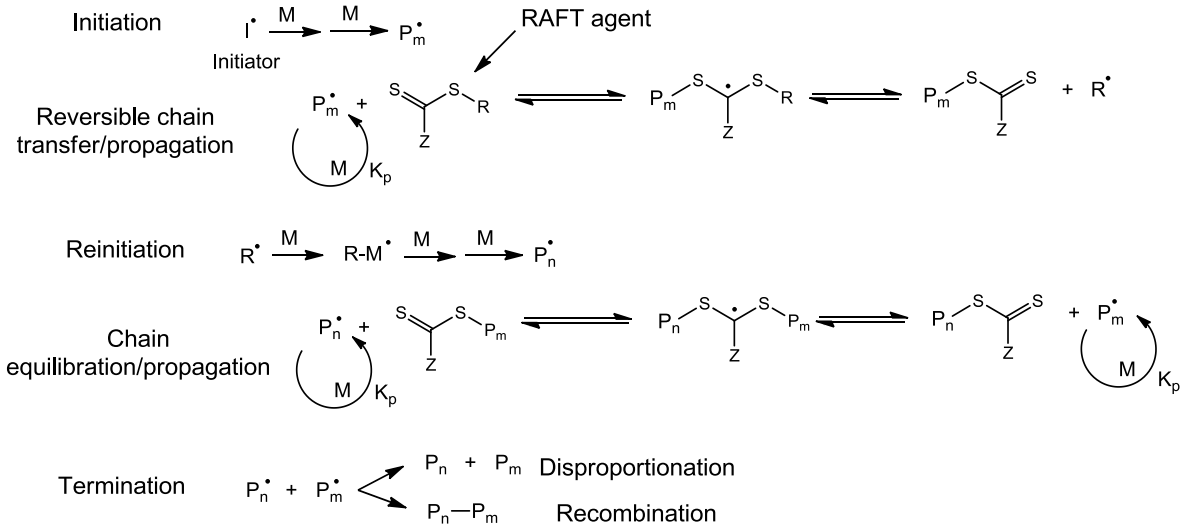

Scheme 1.3 Generic mechanism of RAFT Polymerisation.

The mechanism starts with the reaction between an initiator and the monomer. The initiators that can be used include AIBN or benzoyl peroxide, and the monomers can potentially be all the vinyl monomers possible. After this first step the RAFT agent, for example a thiocarbonylthio compound, reacts with the propagating radical ($P_m^{\cdot}$) and a new radical $R^{\cdot}$ is formed which acts as an initiator creating a new active polymer chain ($P_n^{\cdot}$). The new active chain reacts with the RAFT agent like the other propagating radical and a rapid equilibrium occurs between the active propagating radicals ($P_m^{\cdot}$ and $P_n^{\cdot}$) and the dormant polymeric RAFT agent. The two polymer chains $P_m^{\cdot}$ and $P_n^{\cdot}$ have the same probability to grow thanks to the thio intermediate facilitating the formation of polymers with low dispersity. Once the reaction is complete the polymer chains are stable in the dormant state and they possess the RAFT agent as end-group.

The choice of the RAFT agent is important for the control of the polymerisation. There are numerous types of RAFT agent that have being formulated during the development of RAFT. It is possible to find aromatic dithioesters (Z= aryl, alkyl or aralkyl), symmetric and non-symmetric trithiocarbonate, xanthate and dithiocarbamate RAFT agents.

The RAFT agent's efficiency is determined by the kind of monomer that is polymerised and by the type of substituent group Z and R as shown in Figure 1.1.

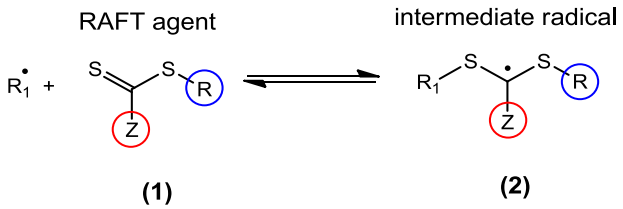

Figure 1.1 Equilibrium between the thiocarbonylthio RAFT agent (1) and the intermediated radical (2). Z and R are the two substituent groups that affect the efficiency of the RAFT agent.

Referring to Figure 1.1 R and R_1 are the free radical leaving groups and *Z* is the substituent group that affects the reactivity of the thiocarbonyl double bond of (1) and the stability of the intermediate radical (2). In general RAFT agents need to have a reactive C=S double bond, the intermediate radicals (2) that are formed in the reaction should not give side reactions and must quickly form the fragments; the second radical formed ($R^{\cdot}$) must be capable of efficient reinitiation of the polymerisation.

1.2.2.3 NMP

Nitroxide-Mediated Polymerisation (NMP)[16,17] is the third type of controlled radical polymerisation and uses a stable radical to reversibly transform the propagating active chains into a dormant species. This stable radical is a nitroxide and the active radical is thermally generated. The use of nitroxides was reported for the first time by Solomon and Rizzardo in 1982[18] for the radical polymerisation of styrene. The general NMP mechanism is shown in Scheme 1.4.

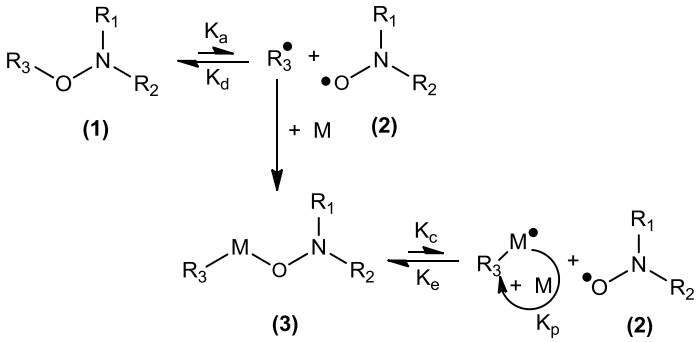

Scheme 1.4 Mechanism NMP that utilises the same alkoxyamine as initiator and ending group.

The polymerisation is based on the equilibrium between the dormant alkoxyamine (1) or (3) and the nitroxyl radical (2) with the active polymer radical ($R_3^{\cdot}$ or R_3-$M^{\cdot}$). The number of termination reactions like dimerization and disproportionation are suppressed by the low concentration of the active polymeric radicals. Typically alkoxyamines are the most widely used initiators and regulators in NMP, the reactions can be carried out in bulk or solution at

a temperature range of 90-130°C. The resulting polymers have an alkoxyamine as chain-end group and for this reason they can behave as suitable macromonomers for the synthesis of block copolymers. A common example of a nitroxide utilised in NMP polymerisations of styrene and styrene derivatives is the compound TEMPO (2,2,6,6-tetramethyl piperidinyl-1-oxy) which was used for the polymerisation of low dispersity polystyrene.[7] The synthesis used benzoyl peroxide as initiator and the polystyrene synthesised was characterised by a dispersity index of 1.2 to 1.3 that was lower than the theoretical value of 1.5 for a free radical process. However, TEMPO is not always the best nitroxide to use, the reactions give poor yields of polymer with byproducts and when used for the synthesis of other monomers such as acrylates, acrylamides or dienes it fails to retain control. New compounds similar in structure to TEMPO have been proposed and their efficiency improved NMP in terms of range of monomers polymerisable and reaction control. Among the numerous alkoxyamines[17] prepared, notable examples of these new initiator/regulator compounds are the phosphonate[19] and arene nitroxides[20].(Figure 1.2)

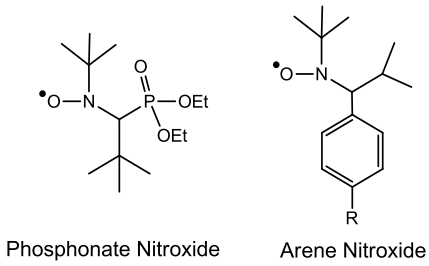

Figure 1.2 Structures of two nitroxides used in NMP: phosphonate and arene nitroxide where R= H, NH_2COOH.

They turned out to be better than the TEMPO derivatives and they successfully work in the NMP polymerisation of acrylates, acrylamides and acrylonitriles giving greater control of the molecular weight of the polymers.

1.2.3 Living Polymerisation

A living polymerisation[21] is a form of chain polymerisation where the steps of termination or chain transfer do not occur. Furthermore the rate of initiation is much higher than the rate of chain propagation which results in the growth of the polymer chains at a more constant rate than seen in traditional chain polymerisation. This characteristic leads to a very low dispersity index and a good control of compositional and structural parameters.

The technique of living polymerisation is one of the most effective for the synthesis of polymers with well-defined structures with a low degree of compositional heterogeneity. The concept of a living polymerisation was first demonstrated by Michael Szwarc in 1956[1] who carried out the anionic polymerisation of styrene using an alkali metal and naphthalene in THF. Subsequent to that other types of living polymerisation have been developed; for example living cationic polymerisation or ring opening metathesis polymerisation.[22]

It is possible to write a list of criteria that may be used to define whether a polymerisation is a living polymerisation:

1. The polymerisation proceeds until all of the monomer present is consumed and if other monomer is added, the polymerisation continues.
2. The number average molecular weight (M_n) is a linear function of conversion.

The M_n at complete conversion is represented by the Equation 1.6:

$$M_n = \frac{g\ of\ monomer}{moles\ of\ initiator} \quad (1.6)$$

And the M_n at an intermediate degree of conversion is (Equation 1.7):

$$M_n = \frac{g\ of\ consumed\ monomer}{moles\ of\ initiator} \quad (1.7)$$

If there are no chain transfer reactions, the plot of M_n versus conversion is linear and it remains linear even in the presence of termination reactions. For this reason, this criterion is not a rigorous test of a living polymerisation.

3. The number of polymer molecules and active centres is constant.

This criterion takes into account both chain transfer reactions that increase the number of polymer molecules, and chain terminations (by combination) that change also the number of polymer molecules. Like the second criterion it cannot be a rigorous test in itself for a living polymerisation.

4. The molecular weight can be controlled by the stoichiometry of the reaction.
5. Narrow molecular weight distribution polymers are produced (Đ).

It is possible to obtain low Đ when the rate of initiation is competitive with the rate of propagation, i.e. the chains grow for the same period of time. In addition it is necessary that all the active chain ends are equally susceptible to reaction with monomer and it is important that the propagation reaction is irreversible.

6. Block copolymers can be prepared by sequential monomer addition.

This is a good criterion to confirm the living nature of the polymerisation, because if termination reactions occur, the addition of a new monomer to the reaction can result in the presence of two different peaks in the SEC chromatogram, one of which is the same as before the addition and corresponds to the dead polymer chains; the second peak is the new one representative of the new block copolymer.

7. Chain-end functionalised polymers can be prepared in quantitative yield.

This is possible thanks to controlled termination reactions of living polymerisations using particular end-capping agent.

In conclusion all these criteria can be useful to understand if a polymerisation is living or not, but it is important to notice that they have to be used together. The reactions of termination and transfer can effectively show different consequences and the various criteria have different sensitivities to them.

1.2.3.1 Cationic Polymerisation[3]

Ionic polymerisations are defined as cationic when the active species responsible for the chain growth (Equation 1.8) is a positively charged species.

$$M + I^+ \rightarrow MI^+ \qquad (1.8)$$

Cationic polymerisations are chain growth polymerisations; therefore they have the common steps of initiation, propagation and termination. When they meet the seven criteria mentioned above, they can be defined living polymerisations. The initiator I^+ in the above reaction represents the electrophilic initiator of the cationic polymerisation. It is typically a strong Lewis acid but in general there are three groups of suitable initiators:

- Proton acid (HCl, H_2SO_4, $HClO_4$)
- Lewis acid (BF_3, $AlCl_3$, $SnCl_4$)
- Carbenium ion salts

The Lewis acids require a cocatalyst to act as a proton donor. For example, for boron trifluoride we have:

$$BF_3 + ROH \leftrightarrows [BF_3OR]^-H^+ \qquad (1.9)$$

where R can be: H, alkyl or aryl groups.

Generally we can write:

$$MX_n + SH \leftrightarrows [SMX_n]^- H^+ \quad (1.10)$$

The unit that goes forward to the second part of the initiation reaction is the electrophilic species, H^+. This reaction can be represented by the classical electrophilic addition of Scheme 1.5.

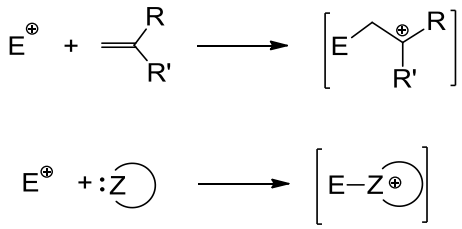

Scheme 1.5 Electrophilic addition reactions with Z= O, S, N, P.

And so in the case of BF_3 initiation can be represented by the following reaction:

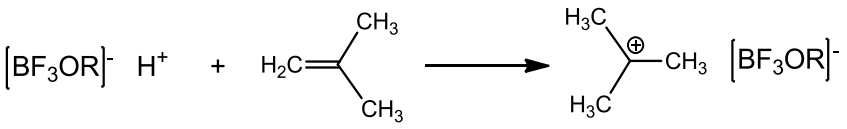

(1.11)

The monomers used in cationic polymerisation are vinyl or cyclic monomers. The side groups in these compounds are very important because the formation and stabilisation of a carbocation depends largely on the nature of these side groups. They have to stabilise the positive charge formed during the initiation step and then the propagation step. (Figure 1.3)

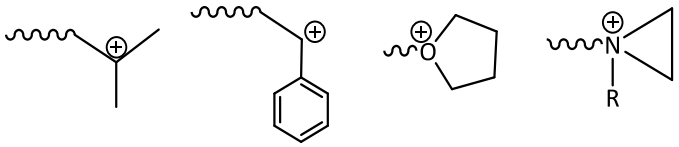

Figure 1.3 Example of stable carbocations (active species) involved in cationic polymerisation.

The reaction mechanism depends on these types of monomers but it also depends on the temperature, the solvent and the counterion. The number of solvents that are possible to use is restricted. Among these there are non-polar solvents like toluene and cyclohexane, polar solvents like nitroalkane solvents and in addition solvents with intermediate polarity like chloroform and dichloromethane. Generally the solvents have to be neutral or at least to have a weak acid character because a nucleophilic environment would act against the active species inhibiting the cationic polymerisation. For the same reason it is also crucial to avoid any basic impurities and moisture. Termination can occur by a unimolecular rearrangement of the ion pair (Scheme 1.6-1) or by a bimolecular transfer reaction with a monomer (Scheme 1.6-2).

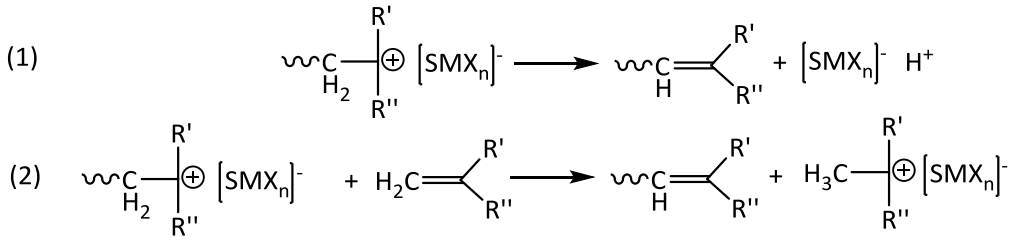

Scheme 1.6 Scheme of termination reactions in cationic polymerisation: 1) unimolecular rearrangement, 2) bimolecular transfer reaction.

1.2.3.2 Anionic Polymerisation

Ionic polymerisations are defined anionic polymerisation[21] when the active species is a negatively charged species. Two general ways of showing the anionic polymerisation of a monomer M is shown below where MI^- is an anion and $M^{\bullet -}$ a radical anion.

$$M + I^- \rightarrow MI^- \quad (1.12)$$

$$M + e^- \rightarrow M^{\bullet -} \quad (1.13)$$

Anionic polymerisation belongs to the chain polymerisation reactions group and as well as the cationic polymerisations it is possible to observe the same steps of initiation, propagation and termination. Particularly attention has to be paid to the last step mentioned, since in reality anionic polymerisation is a living polymerisation and there is no inherent termination step. Living polymerisation was first reported by Szwarc[1] in 1956 through the synthesis of polystyrene in THF using sodium naphthalene. The mechanism of the reaction is shown in Scheme 1.7.

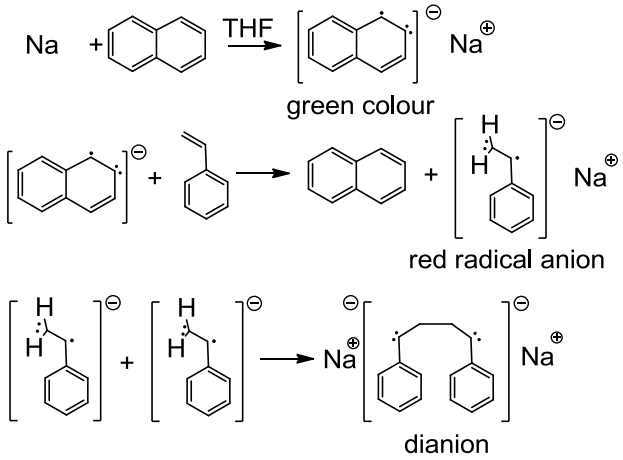

Scheme 1.7 Anionic polymerisation of styrene with sodium naphthalide.

The first step is the formation of the green naphthalene anion radical. The addition of styrene leads to electron transfer from the naphthyl radical to the monomer to form the red

styryl radical anion. This radical anion goes through a rapid coupling to form a dianion that is capable of propagating from both ends. The propagating carbanions can be deactivated by a variety of functional groups and traces of environmental impurities such as water, oxygen and carbon dioxide. The reaction is very sensitive to tiny quantities of these compounds and thus the system must be free of any acidic proton, the solvent must be aprotic and the reagents must be very pure. An inert atmosphere is required with no air, CO_2 or O_2 and in practice reactions must be carried out under inert atmospheres or even better with the use of high vacuum techniques.

The absence of termination reactions in living anionic polymerisation is useful for the synthesis of block copolymers or polymers with functionalised end group. As mentioned before, this is possible by the addition of a second monomer in the case of block copolymers or in the second case, a new compound that is itself incorporated to form a useful end group.

Anionic polymerisation permits us to obtain well-defined polymers in terms of molecular weight, molecular weight distribution, microstructure and chain end functionality, but the choice of the monomer, solvent, initiator and reaction conditions is crucial.

Monomers

There are a limited number of monomers that can be polymerised by anionic polymerisation. These monomers may be divided into two groups: vinyl, diene and carbonyl-type monomers that have one or more double bonds, and cyclic monomers.

As mentioned before when discussing cationic polymerisation, the monomer has to be able to stabilise the negative charge formed in the initiation step. The delocalisation of the charge (Figure 1.4) creates stable carbanions.

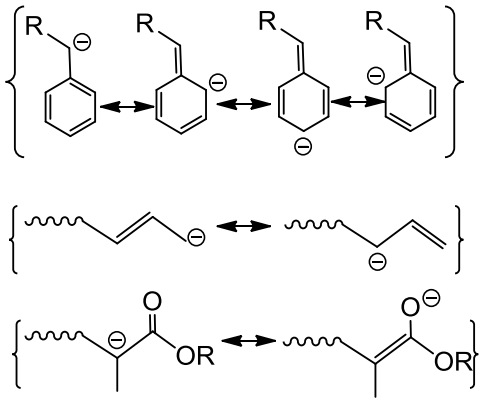

Figure 1.4 Stabilisation of the charge for the first group of monomers: vinyl, diene and carbonyl-type

Regarding the cyclic monomer, the active centres carry the negative charge on the heteroatom and the structure is stable. (Figure 1.5)

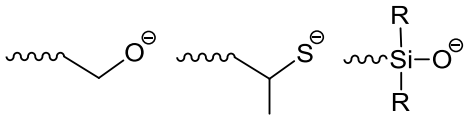

Figure 1.5 Carbanions made starting from cyclic monomers.

Some of the monomers used for anionic polymerisation are reported in Figure 1.6.

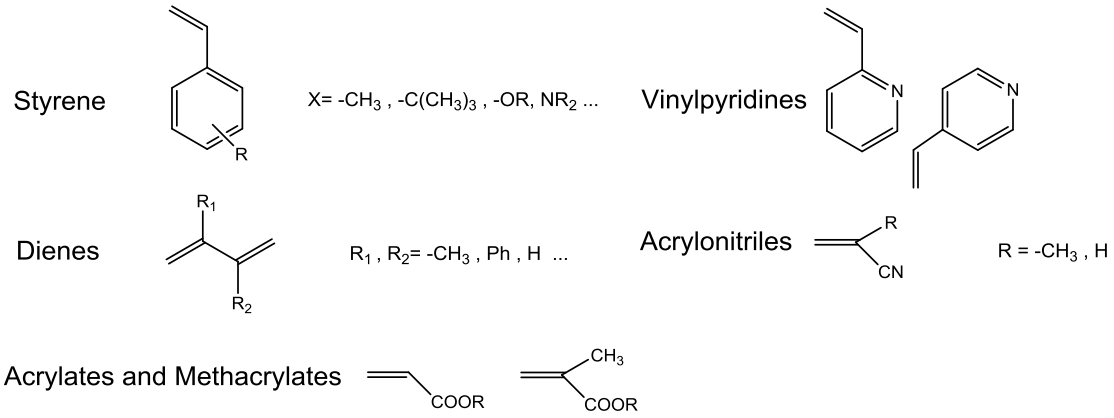

Figure 1.6 Monomers used in anionic polymerisations.

All those monomers with polar substituents like carbonyl, cyano and nitro groups are not the most suitable reagents for anionic polymerisation because they are affected by side reactions with initiators and propagating anions. The functional group with acidic hydrogen can be protected to avoid termination during the anionic polymerisation. The protected groups ideal for the monomer have to be stable during the reaction and easily removed after polymerisation. For instance silyl groups can be useful to protect hydroxyl, phenol and amine groups and a mild acid hydrolysis is enough for the deprotection.

Among the monomers that can be used in anionic polymerisation, styrene is one of the most widely used. The butyllithium-initiated polymerisation of styrene can be observed in Scheme 1.8.

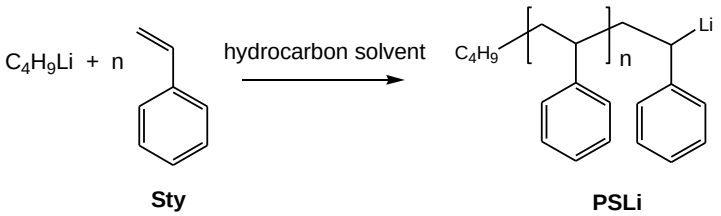

Scheme 1.8 Synthesis of Polystyrene by anionic polymerisation.

Styrene can be polymerised in hydrocarbon or polar aprotic solvents and it can have substituents on the aromatic ring with protection groups, if required, leading to functionalised polystyrene. In addition 1,3-diene monomers can be polymerised by anionic polymerisation. The microstructure of the resulting polymer can vary depending on the counterion, solvent, temperature and chain-end concentration. For instance, lithium as a counterion leads to predominantly 1,4-polydienes in hydrocarbon solvents.

Initiator

There are several types of initiators: alkali metals, radical anions and alkyllithium compounds. Alkali metals initiators can polymerise styrenes and 1,3-dienes. The polymerisation is a heterogeneous process occurring on the surface of the metal. Radical anions are generated in the reaction between alkali metals (Li, Na, K, Rb, Cs) and aromatic hydrocarbons in polar aprotic solvents. The reaction by Szwarc (Scheme 1.7)[1] is an example of this type of initiators. The monomers that can polymerise in the presence of radical anions initiators include styrenes, dienes, epoxides and cyclosiloxanes. The microstructure for the resulting polydienes is predominantly 1,2- and 3,4-microstructure due to the necessity of polar aprotic solvents for the radical anions. In addition polar solvents accelerate the rate of propagation and it decreases the difference between that and the rate of initiation; as a result the molecular weight distribution is broader than in other anionic polymerisations. Even if these first two types of initiators have been used and can still be used for anionic polymerisation, in the overwhelming majority of cases the alkyllithium are preferably used.

Alkyllithium initiators are commercially available in hydrocarbon solution (hexane, cyclohexane). Several types of alkyllithium initiators are available for the living anionic polymerisation of monomers like styrene and dienes. Each of this initiator has a different reactivity toward the monomers and this reactivity depends on their degree of association/aggregation in solution. In general the less associated initiators are more reactive than the more associated. For instance, menthyllithium, which has a degree of aggregation of two, is the more reactive, followed by *sec*-buthyllithium provided with a degree of aggregation of four. The less reactive is *n*-buthyllithium which is characterised by a degree of aggregation of six. Regarding the rate of initiation, this parameter is directly

dependent upon the degree of aggregation. The kinetics of the initiation step exhibits an order dependence on the initiator concentration that varies from unity to a fractional order. In the case of the polymerisation of styrene in benzene by using *n*-butyllithium as initiator the kinetics of the initiation reaction is shown in Equation 1.14.

$$R_i = k_i K_d [BuLi]^{1/6} [M] \qquad (1.14)$$

where k_i is the kinetics constant of the initiation reaction, K_d is the constant of the dissociation reaction of the aggregated initiator (Equation 1.15) and M the monomer polymerised (styrene).

$$(RLi)_6 \overset{K_d}{\rightleftharpoons} 6\ RLi \qquad (1.15)$$

The kinetics shows a first-order dependence on the concentration of the monomer but a one-sixth-order dependence on the initiator. The fractional unit has been explained with the fact that the reactive species is the unassociated form of the initiator, proved also by the fact that *n*-butyllithium in benzene is aggregated into hexamers.

The rate of propagation is similarly dependent upon the degree of aggregation of the propagating species and this in turn also depends on the monomer polymerised and the solvent used; aromatic solvents tend to dissociate the aggregates and so they lead to higher reactivity of the initiator than in aliphatic solvents. Completely unaggregated initiators can be observed in polar solvents such as THF, but ethers can react with both the organometallic initiators and the growing polymer chains giving termination reactions.

The most commonly used alkyllithium initiators are the butyl lithiums: *sec*-BuLi, *n*-BuLi, *i*-BuLi. They are utilised in the polymerisation of styrene and dienes, giving a high percentage of 1,4-microstructure (in non-polar solvents) for polydienes. *Sec*-BuLi is a good initiator for styrene because of its rate of initiation that is very much higher than the rate of propagation. *n*-BuLi is characterised by a high degree of association, usually hexameric, and it needs higher temperature of reaction or addition of polar additives that enhance the rate of initiation. These initiators can also be used for the synthesis of random copolymers of styrene and dienes. Problems arise from the difference in terms of monomers reactivity and it is necessary to add small amount of Lewis base (e.g. THF) or alkali metal alkoxide to ensure the production of random rather than blocky copolymers. To avoid a big change in the microstructure of the polydiene the alkali metal alkoxide are preferred to Lewis base additives.

An interesting aspect of the use of lithium initiators is the possibility to synthesise end-functionalised polymers and macromonomers simply by initiating the polymerisations with an alkyllithium containing a functional group. The polymer created will have the functionality at one end chain and it can be useful for the preparation of block copolymers or star branched polymers. All the functional groups that are not stable in the reaction condition can be protected as mentioned before. Examples of these initiators are shown in Figure 1.7.

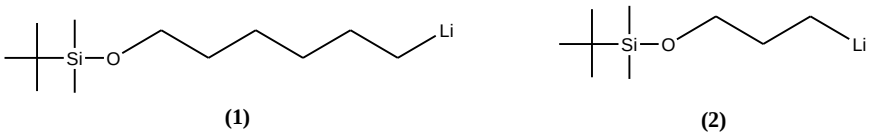

(1) **(2)**

Figure 1.7 Protected initiators 6-(*t*-butyldimethylsiloxy)hexyllithium (1) and 3-(*t*-butyldimethylsiloxy)propyllithium (2).

1.3 Block copolymers and thermoplastic elastomers[3]

A block copolymer contains a linear arrangement of blocks constituted by two or more different monomers. The blocks are generally incompatible and undergo phase separation which has consequences for their properties in solution and in the solid-state. Since they contain segments of different polymers, they can show both new properties and properties common to each type of homopolymer. For example a block copolymer of A-B type can possess both the glass transition temperatures (T_g) characteristic of the two separate blocks. Block copolymers have a natural tendency toward phase separation due to the incompatibility of the constituent blocks. However, the covalent connection between the incompatible blocks impedes the macroscopic phase separation observed for polymer blends and so the incompatibility between the two blocks results in microphase separation into self-organised nanostructured materials with several possible morphologies. The classical morphologies are: spheres, cylinders, gyroids and lamellae (Figure 1.8).[23] Their formation depends on the Flory-Huggins interaction parameter χ, the degree of polymerisation and the volume fraction of the monomers constituting the block copolymer.[24] The experimental techniques that may help in the characterisation in terms of morphologies include small-angle X-ray scattering and electron microscopy.

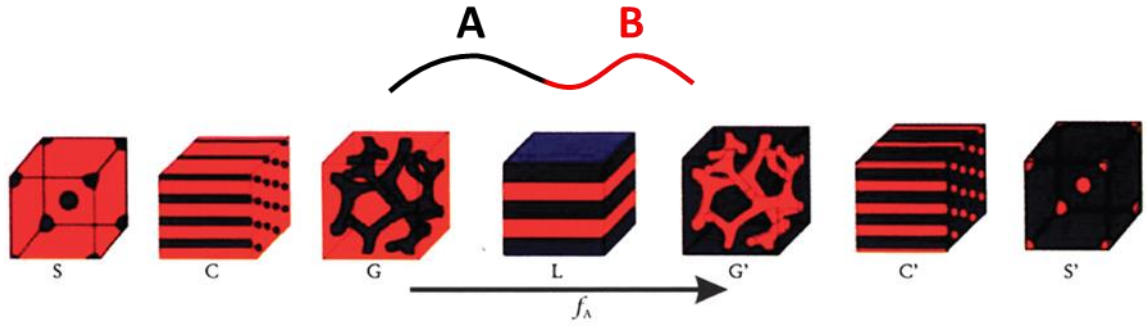

Figure 1.8 Solid-state morphologies of block copolymers, A and B blocks. The four equilibrium morphologies represented are: spheres (S and S'), cylinders (C and C'), gyroids (G and G') and lamellae (L). f_A is the composition parameter in terms of the polymer block A.(Reproduced from Ref 23 with permission of The Royal Society of Chemistry)

During the synthesis of the block copolymers the choice of monomers, the molecular weight of the blocks and the block architecture can influence deeply the resulting morphology. The properties of the resulting block copolymers usually change in accordance with the morphology for example, the mechanical properties of copolymers with both rubbery and glassy domains depend fundamentally upon phase separated morphology.

ABA triblock copolymers in which A is a glassy thermoplastic block and B is an elastomeric rubbery block, are known as thermoplastic elastomers (TPEs).[24] This class of polymer is produced commercially on a very large scale and TPEs are important industrial polymers. They combine the physical properties of elastomeric rubbers, like flexibility and impact resistance, with the strength and easy processability of thermoplastics. There are several types of thermoplastic elastomers with a general structure comprising of two glassy end blocks connected by an amorphous elastomeric polydiene block. The properties of thermoplastic elastomers depend on the properties and volume fraction of the individual phases and on the resultant morphology. The desirable mechanical properties (rubber elasticity and tensile strength) of thermoplastic elastomers are provided by transient "physical crosslinks", formed by discrete glassy phases embedded in a continuous elastomer phase. In fact the glassy blocks tend to aggregate in domains that act as cross-linking points anchoring the central elastomeric polydiene blocks at both the ends. (Figure 1.9)

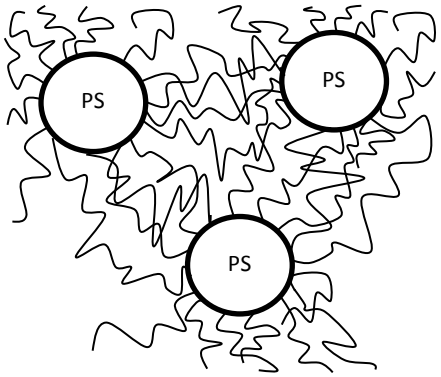

Figure 1.9 Representation of glassy domains of polystyrene in an elastomeric matrix of a TPE.

Polystyrene-block-polydiene-block-polystyrene based TPEs (ABA block copolymers) have been commercialised and studied in detail. An example of this type of TPE is manufactured by Kraton™ Polymers comprising of polystyrene (A blocks) and a rubber block (B block) that can be polyisoprene or polybutadiene. When the TPE is heated above the T_g of the styrene block, the "cross-links" made by the glassy state of the polystyrene softens and the material flows allowing the polymer to be processed by molding and extrusion into any desired form. On cooling, the TPE will regain its elastomeric properties as the glassy domains reform. Kraton™ polymers can be used in blends with other materials to provide a large number of useful products with a variety of applications such as adhesives or medical compounds.

In this work we will describe the synthesis of the highly branched block copolymers called HyperBlocks. In a previous study[25] a single sample of HyperBlock demonstrated the possibility of HyperBlocks to be a new class of branched thermoplastic elastomers. They are constructed from linear macromonomers that consist of ABA triblock copolymers of polystyrene and polyisoprene. The single sample of a HyperBlock previously prepared was investigated in terms of its mechanical properties and morphology. The solid-state morphology of the HyperBlock was investigated by transmission electron microscopy (TEM) and in order to understand the impact of the branched architecture on the morphology, the HyperBlock was compared with the linear ABA macromonomer precursor as well as a commercial linear polymer made of PS-PI-PS triblock copolymer and a three arm star copolymer PS-PI with a content of polystyrene respectively 20% and 30%. The linear precursor PS-PI-PS macromonomer with a styrene content of 40% underwent microphase separation and showed well defined cylindrical morphology with long-range order. However, the HyperBlock derived from this linear copolymer also underwent phase separation but showed no long-range order; a lack of order was attributed to inhibition by the highly branched architecture – see Figure 1.10.

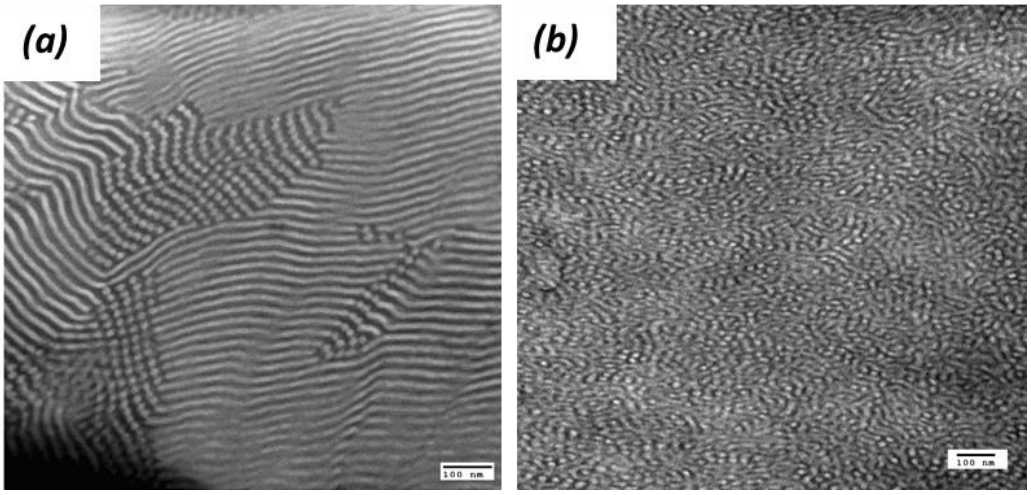

Figure 1.10 TEM of AB_2 macromonomer (a) and of HyperBlock (b)[25] "Reprinted (adapted) with permission from (Hutchings L. R., Dodds J. M., Rees D., Kimani S. M., Wu J. J., Smith E. *Macromolecules* **2009**, *42*, 8675-8687). Copyright (2009) American Chemical Society."

Mechanical (tensile) testing was carried out on the pure HyperBlock and also on the HyperBlock in blends with the commercial Kraton™ TPEs which showed interesting mechanical properties. The pure HyperBlock had a higher ultimate tensile stress and a lower strain at break than the commercial TPEs but when the HyperBlock was used as an additive

in a blend (10% w/w with Kraton^{TM} linear TPE) it improved the mechanical properties: both the elongation at break and the ultimate tensile stress were higher. (Figure 1.11)

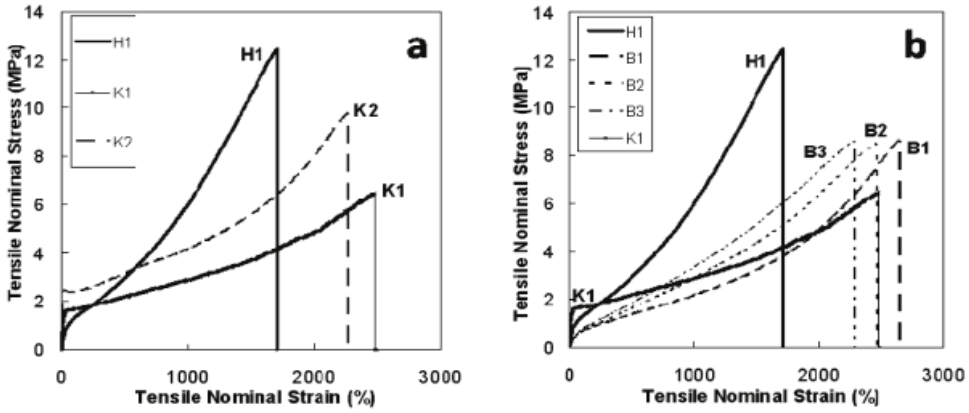

Figure 1.11 Tensile stress-strain behavior for HyperBlock (*H1*), Kraton polymers (*K1*, *K2*), blends of H1 and K1 containing 10% H1 (*B1*), 20% H1 (*B2*) and 30% H1 (*B3*).[25] "Reprinted (adapted) with permission from (Hutchings L. R., Dodds J. M., Rees D., Kimani S. M., Wu J. J., Smith E. *Macromolecules* **2009**, *42*, 8675-8687). Copyright (2009) American Chemical Society."

The properties of the blend were not intermediate between the two constituents of the blends and the principle aims of this project are;

- to gain a wider understanding of the effect of the branched architecture upon the solid-state morphology of HyperBlocks
- to understand the relationship between molecular weight and composition of the linear macromonomer precursors and the phase separated morphology of HyperBlocks
- to understand the impact of morphology and composition upon the mechanical properties of HyperBlocks and Hyperblock/Kraton Linear blends

This will be achieved through the synthesis and characterisation of a series of HyperBlocks prepared from ABA macromonomers in which the block copolymer composition and molecular weight are systematically varied.

1.4 Branched Polymers

In 2007 Frey emphasised the great importance of branched polymers in both polymer science and bioscience writing in an editorial of the journal *Macromolecular Chemistry and Physics* "Life is branched".[26] In fact, an important structural feature which plays a big part in determining polymer properties is the polymer architecture. A branched polymer is a material where the main chains are connected to other chains through the presence of branch points. This leads to a greater number of chain ends than in linear polymers. The importance of branching in polymers has grown dramatically starting with Flory who in 1948 synthesised star polymers by polycondensation of AB monomers and multifunctional co-reactants RA_b or RB_b creating stars with *b* number of arms from the radical core R.[27] If during the past branched polymers were considered only products of peripheral interest, today the concept of controlled branching in the development of new polymers and functional materials has assumed a very significant role in polymer science. The presence of branching and (multiple) chain-end functionalities confers to the polymers interesting properties, more compact structures, improved solubility and reduced viscosity in solution and melt in comparison to linear polymers.

1.4.1 Star-branched Polymers

A star-branched polymer consists of a single branch point to which several linear chains are connected. This is the simplest structure that can be found within branched polymers and their synthesis can be carried out using various polymerisation mechanisms. In order to produce the arms techniques such as anionic polymerisation[21,28] and controlled free radical polymerisations[29] can be used, and one of two general strategies to produce the star polymers are adopted: "core-first" and "arm-first" (Figure 1.12).

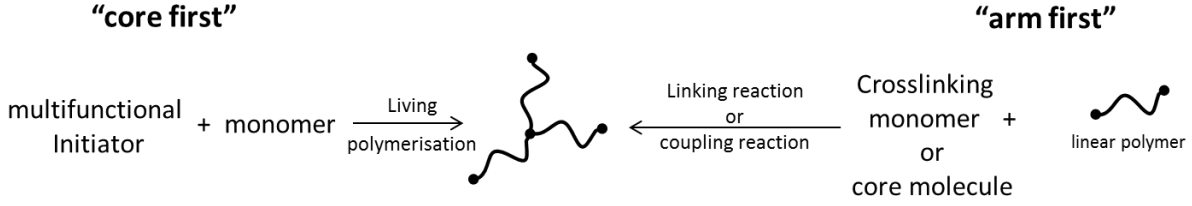

Figure 1.12 Two different methodologies for the synthesis of star polymers: "core-first" and "arm-first".

The "core-first" method[30] involves the use of a multifunctional initiator (core) from which the arms start to grow. The number of arms per star polymer is determined by the number of initiating functionalities on each initiator but this method has some problems. For example the molecular weights of each arm may not be homogeneous due to the different reactivity of each initiating group and the molecular weight of the arms cannot be measured independently of the star unless the link between arms and core is subsequently chemically cleaved. In the "arm-first" method, the linear arms of the star polymers are synthesised first followed by coupling of the arms to form the star. There are a number of different coupling methods that can be used. One of the most widely exploited approaches, which has been used successfully in combination with living anionic polymerisation, utilises multifunctional silyl halides such as chlorosilanes[31-34] as linking agents that work by terminating multiple chains. Since the silanes have a fixed number of functional groups the resulting stars are well defined with a number of arms equal to the number of functionalities on the silane. A similar approach can be exploited to prepare stars by the coupling of arms synthesised by controlled free radical polymerisation mechanisms for example ATRP[35] and RAFT.[36] Nevertheless the combination of ATRP and the “arm first” approach still requires efficient coupling reactions between the core molecule and the arms in order to have well defined stars. The azide-alkyne ‘click’ reaction was found to be an efficient coupling reaction and it was used for the first time in combination with ATRP by Matyjaszewski *et al.* for the synthesis of polystyrene stars.[37] Difunctional monomers such as divinylbenzene (DVB)[38] can also be used as coupling agents to prepare star shaped polymers by the “arm-first” methods. Such compounds work through the addition of living polymeric chains to the vinyl groups without termination and that result in a cross-linked core that contains as many living anions as arms that are coupled. However the use of difunctional monomers can lead to an increase in the dispersity of the resulting stars due to the formation of stars with an imprecise number of arms and the possibility of star-star coupling. The “arm first” approach offers the distinct advantage that the molecular weight of the arms can be analysed prior to the coupling reactions but this approach is not without some drawbacks. Generally speaking the coupling reaction requires the use of an excess of arms to ensure the complete coupling to the core and that implies subsequent additional purification (fractionation) steps will be required.

Star polymers have many interesting properties, arising from their compact structure and globular shape and for decades have been used as a model branched polymers to help to understand the relationship between molecular architecture and physical properties. The synthesis of simple star shaped polymers has been extended to the formation of polymers with more complex architectures. For instance the molecular weights of the arms have been varied to make asymmetric stars[39] or the introduction of branches in the arm to create polymers like "comb stars"[40] where the arms are comb-branched polymers, or "umbrella stars"[41] where at the end of the arms there are several branches attached. The introduction of arms of different polymers leads to another type of stars called "miktoarm stars"[41-43] that have very different aggregation behaviour in selective solvents.

1.4.2 Graft/Comb Polymers

Graft polymers contain polymer chains that are incorporated as side chains onto a backbone polymer chain.[44] The grafted arms can themselves have various architectures; they can be linear or branched chains, stars or dendritic units. Graft copolymers are generally prepared by three different synthetic strategies: the grafting "onto", grafting "from" and macromonomer method (grafting "through").

The grafting "onto" method[45] involves the synthesis of the backbone and the arms in two separate reactions thereby allowing the separate characterisation of the backbone and the arms. The backbone has sites on the main chain which can react with the polymeric arms in a subsequent coupling reaction to yield the graft polymer. An example of this methodology is given by the synthesis of poly(butadiene-*g*-styrene) graft copolymer by Hadjichristidis *et al.*[46] During the first step of this work anionic polymerisation was used to produce the polybutadiene backbone. Chlorosilane groups were subsequently added along the linear polymer by the hydrosilylation reaction of $(CH_3)_2SiHCl$ with the double bonds. The polystyrene arms were then attached by reaction of the living polystyryllithium chains with the Si-Cl groups present along the backbone.

In the grafting "from" method, the active sites have to be created on the polymer chain and they have to be able to initiate the growth of the chain branches with another monomer. In this method the number of branches is given by the number of active sites along the backbone but the characterisation of both the two types of polymer chains, backbone and

branches, is not possible. The synthesis of PMMA-*g*-poly(β-butyrolactone) copolymer is an example of this technique.[47]

In the grafting "through" method the arms are introduced by the use of macromonomers which are synthesised first and then copolymerised with another monomer to form the backbone. The molar ratio of the comonomer and the macromonomer is the main factor that determines the average number of arms attached to the backbone although in all of the above described methods the resulting polymers will contain molecules with a distribution of side chains. Poly(methyl methacrylate)-*graft*-polystyrene has been synthesised by grafting "through" methodology.[48] Polystyrene macromonomer was synthesised by living anionic polymerisation and end-capped with p-vinylbenzyl chloride. Afterwards it was copolymerised by free radical polymerisation utilising AIBN with methyl methacrylate that forms the backbone of the graft polymer.

1.4.3 H-shaped Polymers

In H-shaped polymers the architecture becomes a little more complicated than in star polymers due to the introduction of a second branch point.

For example, H-shaped polystyrene with two trifunctional branch points was synthesised by Roovers[49] using anionic polymerisation in a three step reaction (Scheme 1.9). Step (1) involved the synthesis of the arms using *sec*-BuLi as an initiator and in step (2) chains of living polystyrene undergo reaction with CH_3SiCl_3 – it is important to control the stoichiometry during this step. The central backbone (crossbar) chain was synthesised with sodium naphthalenide as a difunctional initiator in step (3). The final step was the addition of the arms to the central body.

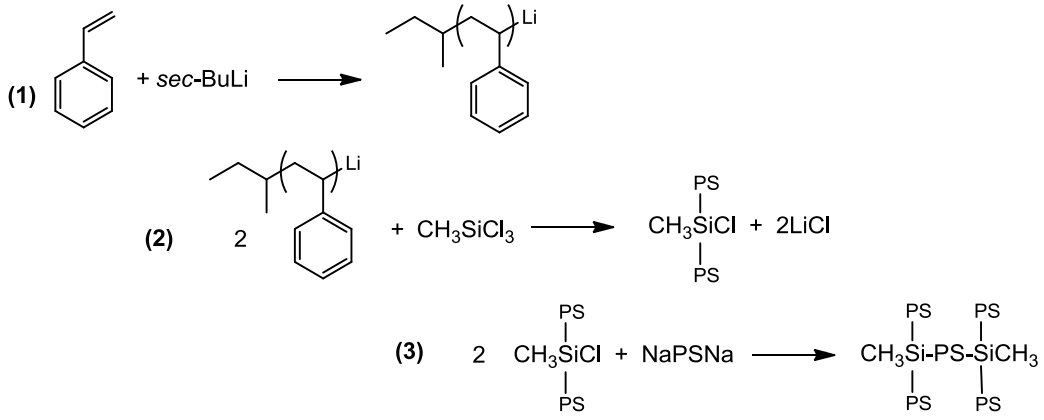

Scheme 1.9 Synthesis of H-Shaped polystyrene by anionic polymerisation with trifunctional chlorosilane.

1.5 Dendritically Branched Polymers

Dendritically branched polymers[50] are a diverse class of polymers that includes several types of highly branched three-dimensional macromolecules such as dendrimers, hyperbranched polymers, dendrons, dendrigraft and dendronized polymers.(Figure 1.13)

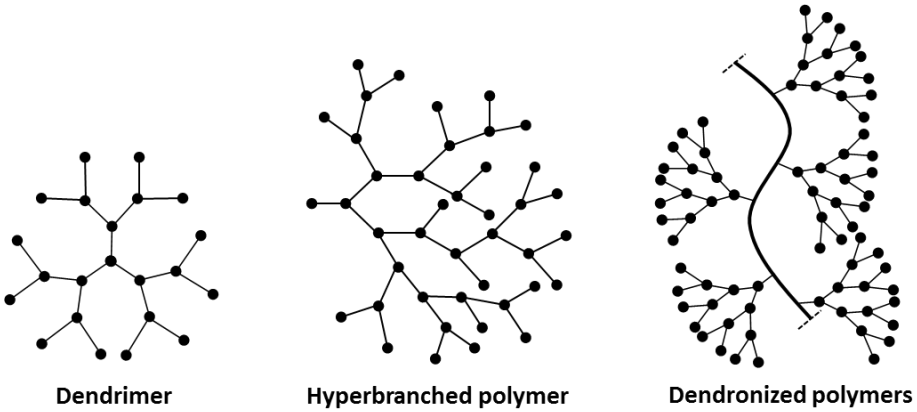

Figure 1.13 Schematic representation of dendritically branched polymers.

They are characterised by novel architectures that make them interesting materials for several applications. They show a higher number of terminal groups, lower viscosity and higher solubility than the corresponding linear polymers. Within this class of polymers dendrimers represent the perfect dendritically branched polymers characterised by a degree of branching (DB) of 1.0. Hyperbranched polymers instead are irregular dendritically branched polymers with a lower and variable DB. In the following section we will define briefly dendrimers and we will focus on the description of hyperbranched polymers that are the main study of this thesis.

1.5.1 Dendrimer-like

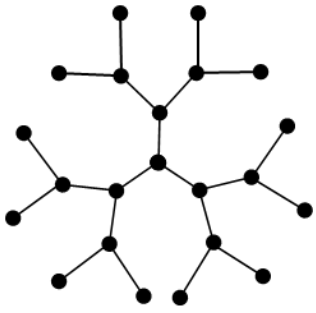

Dendrimers are perfectly branched and monodisperse polymers. The term “dendrimer” derives from the Greek words *dendron*, meaning tree-like, and *meros*, meaning part. Dendritic macromolecules[51] are hyperbranched structures emanating from a central core and containing a large number of terminal groups. They are monodisperse and highly-branched globular molecules. Their unique architectural, structural and functional features make them a potential significant contribution in several areas of physical and biological sciences

and engineering, from drug delivery to nanofabrication.[52] There are two synthetic approaches for the synthesis of dendrimers, the divergent and the convergent growth approaches. The divergent synthesis[53] usually involves the sequential addition of AB_n monomers to a core. AB_n is a monomer structure meaning that the monomer has (1+n) functionalities to form branch points. The probability of defects in this synthesis is very high and it increases with the number of generations created. The convergent growth approach[54,55] starts at the periphery and well-defined dendrons are prepared and coupled to a multifunctional core molecule. This method was introduced in an attempt to solve the problems encountered in the divergent methods and it aims to obtain structures with less defects. The synthesis of dentritic polymers is very time-consuming due to the fact that many steps are required along with purifications and protection and deprotection reactions. Some improvements from the point of view of the synthesis were achieved with the discovery of the azide-alkyne and the thiol-ene 'click' reaction.[56] The great versatility and tolerance toward functional groups characteristic of 'click' chemistry are providing in the last years a new way for the synthesis of dendrimers.[57]

1.5.2 Hyperbranched Polymers

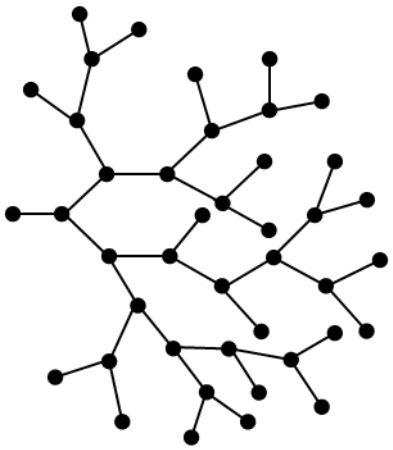

Hyperbranched polymer

Another class of dendritically branched polymers is represented by *hyperbranched polymers*[58] that are characterised by a very high branching density, irregular structure and high number of chain-end functionalities. These highly branched polymers result from one-pot synthesis and the loss of control in this process leads to a big variation in the degree of branching and as a consequence to a very broad molecular weight distributions. Even if this type of synthesis does not allow the production of a perfect structure, it is suitable for large scale production. Therefore hyperbranched (HB) polymers with their unique chemical and physical properties find industrial applications for instance in additives, coatings, drug and gene delivery and nanotechnology. The commercial success of hyperbranched polymers is due mainly to the easy of synthesis and so the possibility to produce cheaply these

materials. In addition the commercial success is also due to characteristics such as the high branching density, high number of chain-end functionalities and irregular structure that results in an excellent solubility, low solution viscosity and modified melt rheology.

1.5.2.1 History

The first time that the term 'hyperbranched polymer' appeared in literature was in 1990 when Kim and Webster reported the synthesis of hyperbranched polyphenylene from AB_2 monomers.[59,60] Before this successful work, the synthesis of highly branched polymers was studied theoretically by Flory who in 1952 demonstrated that the polycondensation of AB_n monomers (where A and B are two mutually reactive functionalities and $n \geq 2$) could be used to create highly branched polymers without the occurrence of gelation.[61] After this theoretical work a highly branched polymer was obtained by copolymerisation of AB and AB_2 monomers by Kricheldorf in 1982.[31] But it was only after the work of Kim and Webster that the hyperbranched polymers started to attract the attention of the polymer society and develop considerably in the last few decades.

1.5.2.2 Synthesis methodologies

Several approaches have been taken for the synthesis of hyperbranched polymers during the development of these particular materials. As mentioned in the review on hyperbranched polymers written by Gao *et al.* [62] it is possible to identify two different groups of HB polymers synthesis methodologies. The first group is the single-monomer methodology (SMM) and the second is the double-monomers methodology (DMM).

1) Single-monomer methodology (SMM)

In this category the synthesis of HB polymers is carried out by using monomers of the type AB_n ($n \geq 2$) whereby the reactive functionalities are located on a single monomer molecule. Several types of reactions may be used and some are listed below:

- Polycondensation reactions
- Polyaddition reactions
- Self-condensing vinyl polymerisation (SCVP)

- Self-condensing ring-opening polymerisation (SCROP) or ring-opening multibranching polymerisation (ROMBP)
- Proton-transfer polymerisation (PTP)

The *polycondensation* approach is the classical way used to synthesise hyperbranched polymers with AB_n ($n \geq 2$) monomers as starting materials as first reported by Flory.[61] This type of synthesis resembles a step-growth polymerisation of AB_n monomers and the developing oligomers with no crosslinking reactions. AB_2 are the most common monomers used but also AB_3, AB_4 and AB_6 monomers have been employed. An important aspect of this kind of synthesis is the reactivity of the monomers: A must react selectively with B and B functionalities must have equal reactivity in order to succeed in the synthesis of HB polymers with high molar masses and without side products resulting from cyclisation reactions. At the beginning due to the availability of the monomers the polyesters were the most widely investigated class of HB polymers by polycondensation. A general reaction scheme for this type of polymerisation is represented in Figure 1.14. The resulting hyperbranched polymer presents an unreacted functionality A called focal unit, branch points corresponding to a group of all reacted B functionalities (called also dendritic units), terminal unreacted B groups and linear units where only one functionality B has reacted.

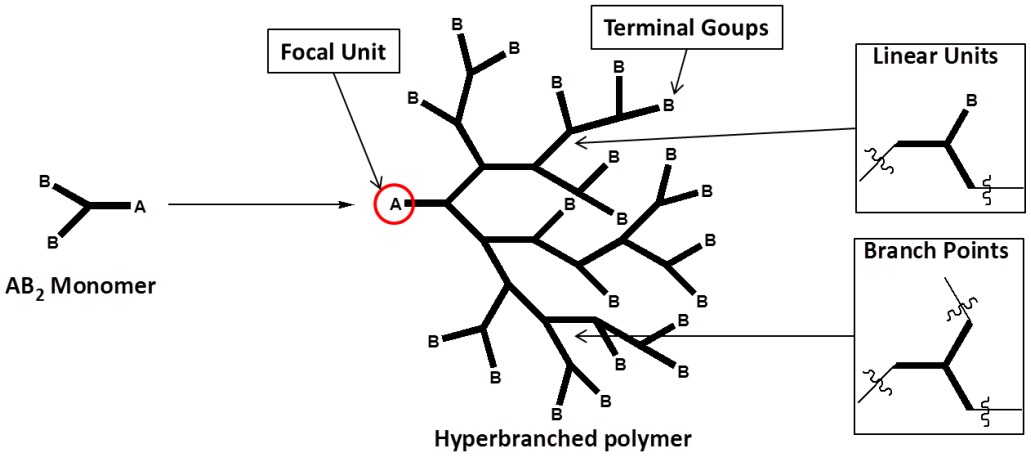

Figure 1.14 Scheme of the polycondensation of AB_2 monomers for the synthesis of hyperbranched polymers. In the hyperbranched structure it is possible to individuate different units: focal unit A, terminal groups B, linear units and branched points.

Further investigations into the polycondensation method for the synthesis of hyperbranched polymers brought to the development of a new method created in order to control the molecular weight and avoid side reactions. Thus to the polymerisation of AB_n monomers, a B_n ($n \geq 2$) core molecule was added and the molecular weight that could be reached

becomes dependent upon the ratio between AB_n and B_n. The resulting HB polymer no longer retains the focal unit A. An example of this method is given by the polymerisation of 2,2-bis(hydroxymethyl)propionic acid (AB_2) in the presence of trimethylolpropane (B_3 core molecule).[63] In this process the monomer is added continuously during the reaction time, maintaining a very low monomer concentration in the reaction mixture. This technique makes possible the production of much more ordered HB polymers with high degree of branching, controlled molecular weights and narrower molecular weight distributions. This method is today called the "slow monomer addition" method for the synthesis of hyperbranched polymers and it is employed with several variants as described by Satoh in his recent review.[64]

Self-condensing vinyl polymerisations (SCVP) are based on the use of AB vinyl monomers called 'inimers' due to the fact that they carry both an initiating group B and a polymerisable vinyl group A. The polymerisation (Scheme 1.10) is carried out in a one-pot reaction and it involves the activation of the initiating group followed by the addition of this active species to the vinyl group. This reaction leads to the propagation step where the vinyl group (propagating centre) continues reacting and each polymer chain-end can contains in this way two reactive sites making possible the formation of a branch point in each repeating units.

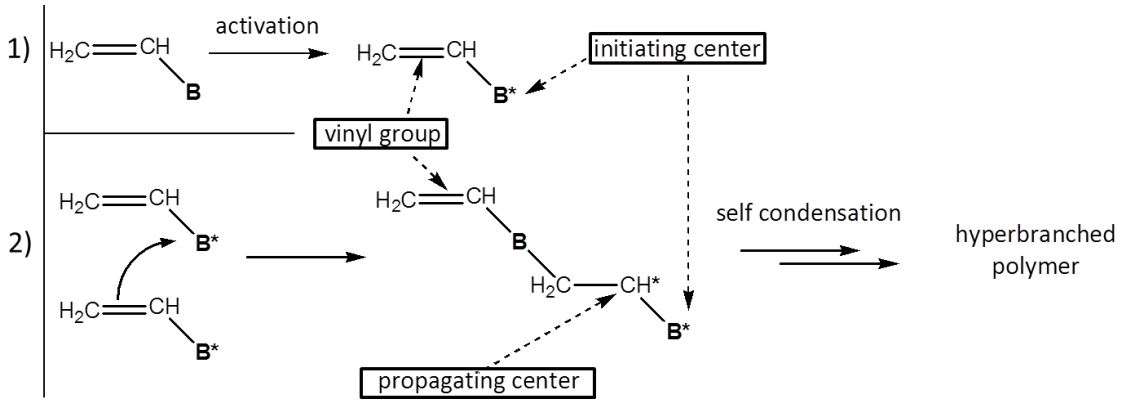

Scheme 1.10 Scheme of self-condensing vinyl polymerisation of inimers: 1) activation step, 2) propagation step.

This type of synthesis for hyperbranched polymers was first reported by Frechét *et al.* in 1995.[65] The HB polymer was synthesised by cationic polymerisation using 3-[(1-chloroethyl)ethenyl]benzene as the monomer, in the presence of the Lewis acid $SnCl_4$. The monomer is an AB monomer with the alkyl halide functionality as A initiating group and the vinyl group as B. SCVP can also be used with other types of polymerisations, for instance controlled radical polymerisations as ATRP, RAFT and NMP.[66-68] Some problems connected

to this type of HB synthesis are due to side reactions that can give gelation, the dispersity is very high and the degree of branching cannot be calculated directly by NMR spectroscopy.

The *ring-opening multibranching polymerisation* (ROMBP) or self-condensing ring-opening polymerisation (SCROP) uses a slightly different monomer (but a similar concept) to SCVP methodology. The monomer comprises of a heterocyclic group instead of a vinyl group in the inimers. A variety of HB polymers have been synthesised by this approach including polyamines[69], polyethers[70] and polyesters[71,72]. Scheme 1.11 shows a general scheme reaction for ROMBP polymerisation.

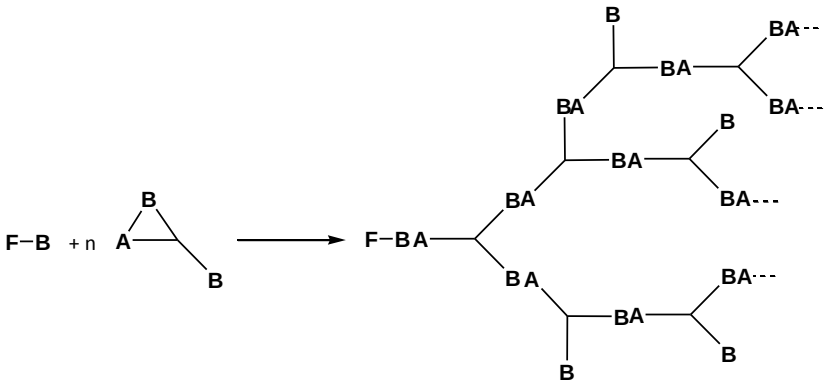

Scheme 1.11 Scheme of ROMBP synthesis of hyperbranched polymers. F-B represents a monofunctional initiator employed in the polymerisation and the cyclic monomer resembles the AB_2 monomer used in the polycondensation methodology for the synthesis of hyperbranched polymers.

An example of this type of polymerisation can be found in the synthesis of hyperbranched polyglycerols reported by Frey *et al.*[70] They combined the ROMBP method with living anionic polymerisation obtaining narrow molecular weight distributions (Đ = 1.1-1.4) through a very versatile way. The monomer used, glycidol, acted as a latent AB_2 monomer which is the type of monomer commonly used in ROMBP. The anionic polymerisation of this hydroxy epoxide, glycidol is shown in Scheme 1.12.

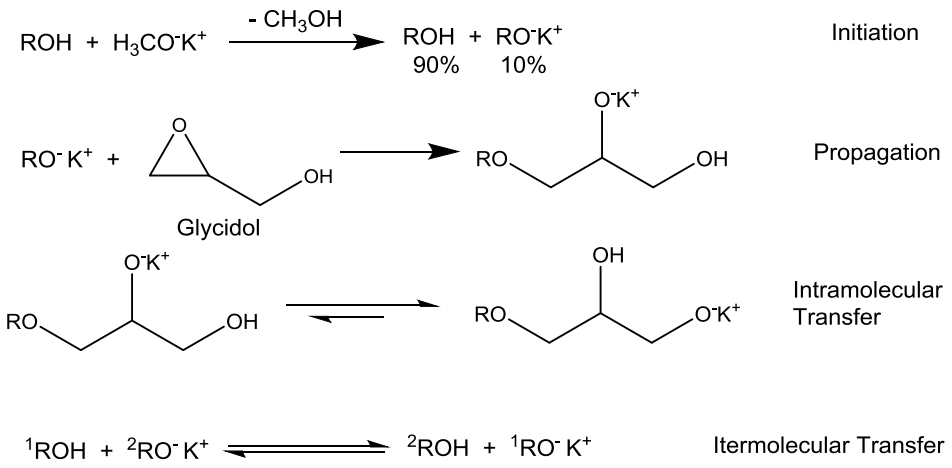

Scheme 1.12 Anionic polymerisation of the monomer glycidol.

The initiating moiety ROH, is for the most part (90%) in a dormant state in order to have a better control of the molecular weight and dispersity following the concept of low concentration of active species during polymerisation typical of controlled free radical polymerisations. Although at any given point the majority of the OH groups are dormant the potassium counterion can 'hop' between oxygen atoms with relative ease ensuring propagation can continue via all potential sites. Thus the inter- and intramolecular transfer of the active site, the alkoxide, makes possible the formation of chain branching during the polymerisation. The ROH initiator used by Frey *et al.* was a trifunctional initiator i.e. the 1,1,1-tris(hydroxymethyl)propane (TMP) that behaved as a core unit and lowered the dispersity values of the resulting polymers. In addition the monomer was added slowly to the reaction (slow monomer addition methodology) in order to offer further control of the polymerisation and suppress cyclisation. The resulting polymer with numerous hydroxyl end groups contains dendritic, linear and terminal units as is typical of hyperbranched polymers with more possible structures due to the fact that the glycidol monomer had two possible unsymmetrical reactive sites.

The *proton-transfer polymerisation* is used to produce epoxy or hydroxyl functionalised hyperbranched polymers.[73,74] The reaction proceeds following the scheme shown below (Scheme 1.13).

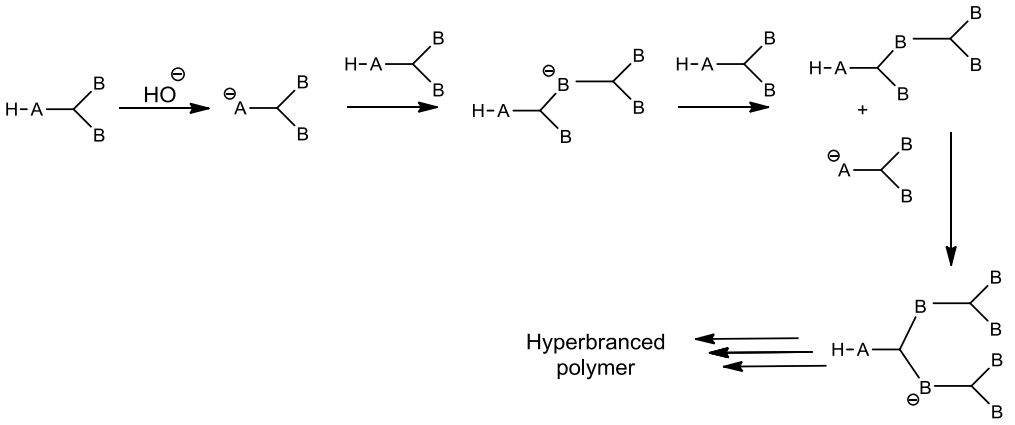

Scheme 1.13 Hyperbranched polymer synthesis by proton-transfer polymerisation.

The initiation step is carried out by the use of a hydroxide ion which abstracts a proton and in turn leads to the formation of a nucleophile. After nucleophilic addition to a second monomer, a proton transfer generates a neutral dimer and a new nucleophile able to react with another monomer. Each subsequent propagation step involves a proton transfer step and leads to the formation of the hyperbranched polymer. The initiation step and activation of the propagating species are faster than the nucleophilic propagation step, allowing the growth of the polymer and not the start of a new polymer chain by the nucleophilic centre. The monomers used belong to the AB_2 types and they contain generally hydroxyl (A) and epoxide groups (B).

2) Double-monomers methodology (DMM)

In this category the hyperbranched polymers are synthesised by using two monomers or specific monomer pairs. One of the DMM methods is the polymerisation of A_2 and B_n ($n > 2$) monomers. The most common approach in this group is the $A_2 + B_3$ methodology. A and B monomers are provided with two and three functionalities respectively and in Flory's[61] ideal condition all A as well as B functionalities have equal reactivity in the monomers and in the growing polymer chains. In addition ideally A groups can react only with B groups and the reaction proceeds in the total absence of intramolecular cyclisation. The advantage of using the $A_2 + B_3$ methodology instead of the AB_n methodology is found in the type of monomer involved. The AB_n monomers very often need to be synthesised whereas the A_2 and B_3 monomers are more commercially available making the synthesis of hyperbranched polymers less problematic and more cost effective on an industrial scale. The disadvantage of this approach is that the possibility of gelation exists. To avoid gelation it is necessary to

work at low monomer concentration, use the slow monomer addition method or stop the reaction before the critical point of gelation.

The combination of the A_2 + B_3 methodology with the single-monomer methodology described before leads to another example within the DMM techniques which is called the couple-monomer methodology (CMM) for the synthesis of hyperbranched polymers. The AB_n monomers are formed in situ from pairs of monomers that have functional groups with differing reactivity. This new method was introduced in order to improve the A_2 + B_3 methodology adding to it the classical AB_n polycondensation method and maintaining the advantage of using commercially available monomers. There are several variants possible within this method but a general scheme can be seen in Scheme 1.14.

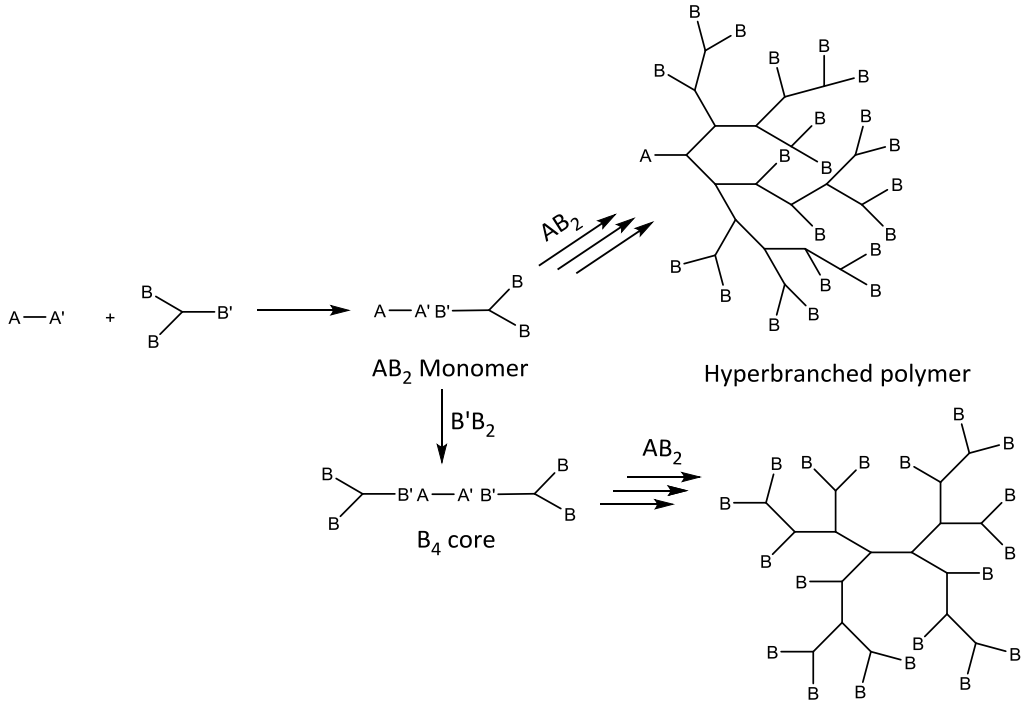

Scheme 1.14 CMM method for the synthesis of hyperbranched polymers. The monomers chosen for the polymerisation are AA' and B'B_2 one of the variant approach of the CMM.

The scheme shows the case in which the monomers are AA' and B'B_2 where A' and B' functionalities have higher reactivity compared with A and B respectively. A' and B' react with each other preferentially and lead to the in situ formation of the AB_2 monomer (A-(A'B')-B_2) that can go through self-polycondensation and give the hyperbranched polymer. There is also the possibility of the formation of a B_4 core molecule due to the reaction between the AB_2 molecules and a B'B_2 monomer. In this last case the B_4 core molecules are important for lower dispersity values and the resulting hyperbranched polymer is provided with a core. The review from Gao[62] describes all the possible variations from (AA' + A'B_2)

and an example of hyperbranched polymer synthesised by CMM is given by Gao *et al.*[75] that produced hyperbranched poly(urea urethane)s by the A_2+ CB_n variant approach (n ≥ 2). The A groups were isocyanato functionalities, C was an amino group and B were hydroxyl groups. A and C reacted together to form in situ the AB_n monomer or the core molecules B_n that led with further reactions to the hyperbranched polymer as mention above.

1.5.2.3 Long-chain hyperbranched polymers

The different methodologies described above represent the general methods used for the synthesis of conventional hyperbranched polymers. However one interesting variation to this type of hyperbranched polymers is the introduction of linear units between the branch points, which results in the reduction of the degree of branching and the branching density. This new class of hyperbranched polymers is called long-chain or segmented hyperbranched polymers.[51] The branch points can be separated by linear homopolymers or block copolymer chains[76,77] (Figure 1.15) and some examples include the synthesised polymers dendrigrafts[78], comb-burst polymer[79] and HyperMacs[80].

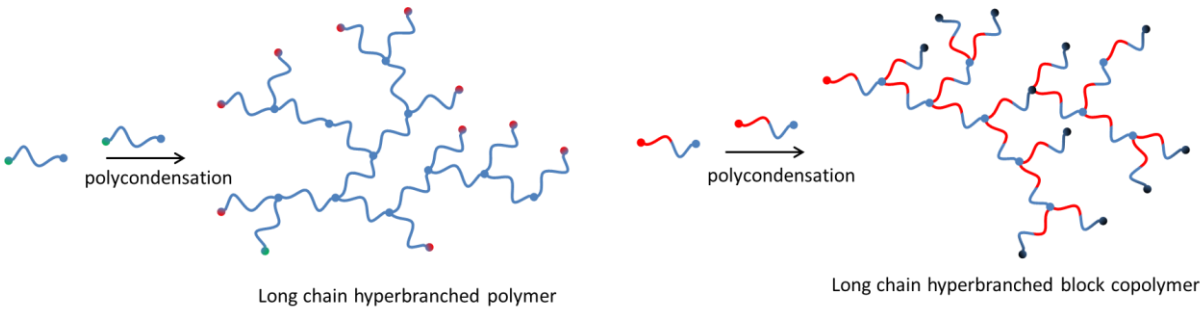

Figure 1.15 Scheme of HB polymers synthesis with the 'macromonomer' approach. On the left the macromonomer is a linear homopolymer with A group (green) and B_2 groups (blue). On the right the macromonomer is a block copolymer with A group (red) and B_2 groups (blue).

The introduction of a linear segment between branching points can be obtained by several methods: the self-condensing vinyl polymerisation (SCVP) approach[81,82] or the use of polymeric monomers – the so-called 'macromonomer' approach – via an A_2 + B_3 or AB_2 methodology that uses linear polymeric chains as monomers rather than small molecules. The first approach mentioned above involving self-condensing vinyl polymerisation was adopted by Gao *et al.* in order to synthesise multifunctional segmented hyperbranched polymers (SHPs). [82,83] It was observed how the introduction of new functionalities along the branch segments was easier due to the presence of the linear segments between the branch

points which decreased the compact structure of the classical HB polymers. The post-functionalisation of SHPs was carried out in order to create new hyperbranched polymers which were water-soluble and chain-clickable for their potential use in several applications such as, for instance, drug delivery or antibacterial materials. The SCVP approach was combined with RAFT and the hyperbranched polymers were obtained from the copolymerisation of an inimer and a comonomer. Gao *et al.* synthesised poly(tertiary amino methacrylate)s with tertiary amino group[82] or epoxy groups[83] at each repeating units that were then converted by several types of reaction including 'click' reactions. There are relatively few examples of the employment of A_2 + B_3 approach but one notable example is found in the synthesis of poly(ether ester)s by Long *et al.*[84] that utilised the oligomer poly(propylene glycol) as an A_2 macromonomer and trimethyl 1,3,5-benzenetricarboxylate as a B_3 monomer. The AB_2 approach for the introduction of very short linear segments between branching points was carried out first in the synthesis of hyperbranched poly(ethylene glycol)s[85] and in the synthesis of hyperbranched copolyesters[71]. The 'macromonomer' AB_2 approach for the synthesis of hyperbranched polymers, in which the linear segments were polymer chains, sometimes with very high molecular weights, was first employed by Hutchings *et al.* for the synthesis of the long-chain hyperbranched polystyrenes called HyperMacs[80,86]. Macromonomers are macromolecular materials provided with polymerisable end groups and their synthesis is the first step in the preparation of HyperMacs. This approach gives the advantage of control over the molecular weight of the long chains between branching points. Characteristic of this kind of HB polymers synthesis is the very fast increase in molecular weight and size of the materials in each generation. In particular the synthesis of HyperMacs was carried out by step-growth polymerisation of polystyrene AB_2 macromonomers which were prepared by living anionic polymerisation. Macromonomers were in this way well-defined in terms of molecular weights and dispersity. In the earliest examples the end-group reactive functionalities were two phenols (B) and a halide (chloride or bromide) group (A). The polycondensation of the polystyrene AB_2 macromonomers was carried out via Williamson coupling reaction but in general also other types of reactions are possible like esterifications[71] and hydrosilylation reactions[87]. It was also reported the synthesis of long-chain hyperbranched polystyrene resembling the HyperMacs by the use of 'click' reaction chosen as coupling reaction. The macromonomers were synthesised by ATRP using an heterofunctional initiator provided with two propargyl

groups and a bromide group which was converted into azide group after the ATRP polymerisation.[88] HyperMacs were synthesised afterwards also from polybutadiene and poly(methyl methacrylate) by the same research group that also brought some modifications in the synthethic procedure.[25] In the same work was also introduced a new class of HyperMacs, HyperBlocks, which were the font of inspiration of the present work. A single sample of a HyperBlock was synthesised in a large scale and analysed by TEM and tensile testing to obtain information about solid-state morphology and mechanical properties. The macromonomer used in this case was an ABA triblock copolymer of polystyrene and polyisoprene with chain-end functionalities suitable for the Williamson coupling reaction for the synthesis of HyperBlocks. There are a growing number of other workers who have used block copolymers in the synthesis of HB copolymers and a few examples can be found in the literature of highly branched block copolymers[71,77]. An example is given by the HB polymers by Perrier *et al.* based on linear-diblocks of dimethyl acrylamide and styrene which were synthesised by RAFT and then used as macromonomers in a 'click' reaction[89]. With HyperBlocks[25,90] Hutchings *et al.* introduced the alternating blocks structure in the field of hyperbranched polymers.

1.5.2.4 Properties

The modification of the architecture and chemical composition of HB polymers by varying parameters such as the degree of branching, chain end groups, molecular weights, molecular weight distribution and of particular relevance to the current work, chain length and composition between branch points, can have a great impact upon the properties of the resulting materials. As a result the materials can combine the properties of linear and branched polymers or may gain entirely new properties behaving in between the extremes of a linear and a dendritic polymer. Properties such as rheology and the ability to form chain entanglements[86], self-assembly into particular morphologies and mechanical properties can be affected by the presence of these spacers and the branching architecture. The impact of the hyperbranched architecture upon self-assembly properties in water acetone mixtures was studied by Perrier *et al.*[89] who synthesised HB block copolymers of polystyrene and poly(dimethyl acrylamide). The HB polymers constructed of hydrophobic and hydrophilic blocks formed self-assembled structures different from the ones displayed by the

corresponding linear polymers, showing how the hyperbranched architecture affects substantially the self-assembly of the polymers. In fact, while the linear block copolymers assembled into micellar structures with hydrodynamic sizes of ca. 10 nm, the HB polymers formed large aggregates with sizes of ca. 100 nm.

Rheology is fundamentally important in polymer processing and its dependence upon polymer architecture has been studied for several types of polymers and for many years. Investigations carried out in order to understand the effect of architecture revealed that long-chain branching in polymers influences the rheological properties in the melt. Long-chain HB polystyrene polymers, HyperMacs, were studied from a point of view of their rheological properties.[86] It was noticed how the highly branched structure frustrates the formation of entanglements even when the overall molecular weight of individual polymer molecules were well above the entanglement molecular weight (M_e) of polystyrene. Chain entanglement was only observed (as a plateau region in the rheology master curve) when the molecular weight of the linear macromonomers were above the M_e of polystyrene.

Hyperbranched polymers with their unique properties and structures have the potential of being employed in many fields. The most well-known applications areas are coatings, additives and resin nanocomposites where it is possible to find HB polymers already in commercial use. In addition applications can be also observed in biological and medical fields as gene and drug delivery, biodegradable materials and modification of surfaces.[91]

1.5.3 'Click' Reaction

The synthesis of polymers with complex branched architectures often relies upon the use of efficient chain coupling reactions and in the recent years 'click' chemistry proved to be a particularly popular and successful example. 'Click' reactions are in fact very attractive for polymers thanks to the mild reaction conditions, the high yields and the tolerance to many functional groups.

The term "click chemistry" was introduced for the first time by Sharpless *et al.* in 2001 to represent a new modular approach to synthesis.[2] The source of inspiration that lead to the concept of 'click' chemistry was Nature. Looking at Nature's way of creating new compounds, it was observed that carbon-carbon (C-C) and carbon heteroatoms (C-X) bonds formations were used for the synthesis of materials with strong preference toward the

latter. Nature's carbon-carbon chemistry requires unique enzymes and complicated synthetic pathways resulting in synthetic challenges for chemists. An example can be found in the pharmaceutical industry with the complex synthesis of compounds chosen for medical purposes like drugs.[92] C-X bonds are on the other hand found in the most important molecules of life like polypeptides (Figure 1.16-1), polynucleotides (Figure 1.16-2) and polysaccharides.

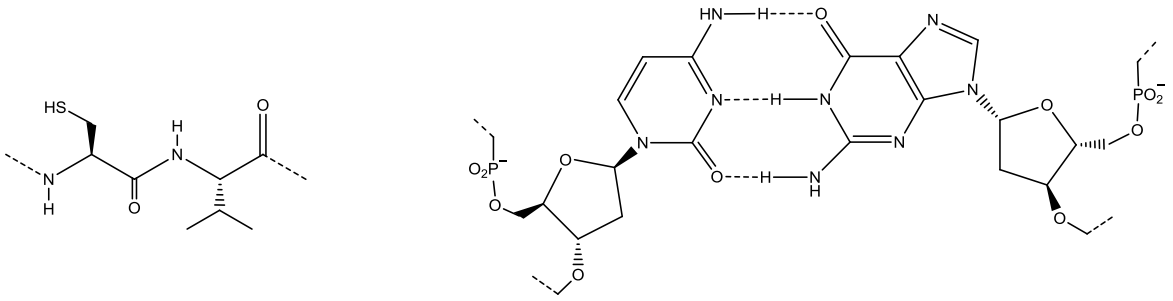

Polypeptides (1) Polynucleotides (2)

Figure 1.16 Examples of C-X found in nature: (1) Polypeptides and (2) polynucleotides.

It was also observed how Nature could make large molecules from a restricted number of small building blocks. Taking into account these observations of Nature's way of synthesis, the aim was to develop a new strategy to create compounds provided with useful properties via the best synthetic procedure that couples together small units, keeping in mind the concept expressed by Hammond in 1968:

"*The most fundamental and lasting objective of synthesis is not production of new compounds, but production of properties.*"

George S. Hammond, Norris Award Lecture, 1968.

For a reaction to be classified as a 'click' reaction has to fulfil several criteria[2]:

1. It must be modular and wide in scope.
2. It must give high yields.
3. It must generate only inoffensive byproducts that can be removed by non-chromatographic processes, for example crystallisation or distillation.
4. It must be stereospecific, but not necessarily enantioselective.
5. The reaction conditions must be simple.
6. It must be insensitive to O_2 and H_2O.
7. It must use only readily available starting materials and reagents.
8. It must use no solvents or benign solvents like H_2O.

9. It must be possible to isolate the obtained product in a simple way.
10. Reactions being “atom efficient”

‘Click’ chemistry simplifies the synthesis of materials using “spring loaded” reactants to give a particular product through reactions provided with high thermodynamic driving force (>20 kcal/mol) and high reaction rates. The list that follows shows the reactions that meet the above criteria and aim at the production of new carbon-heteroatom bonds by using pre-formed carbon-carbon bonds as found in materials like olefins and acetylenes.[2,93](Figure 1.17)

1. Cycloaddition reactions: 1,3-dipolar cycloaddition reactions, Diels-Alder reactions.[94]
2. Nucleophilic substitution chemistry: ring-opening reactions with strained heterocyclic electrophiles (epoxides, aziridines, aziridinium ions, cyclic sulfates, cyclic sulfamidates, episulfonium ions).
3. Carbonyl chemistry of the non-aldol type: synthesis of oxime ethers, aromatic heterocycles, hydrazones, amides ureas and thioureas.
4. Addition to carbon-carbon multiple bonds: epoxidation[95], dihydroxylation[96], aziridination[97], sulfenyl halide addition and also Michael addition reactions.

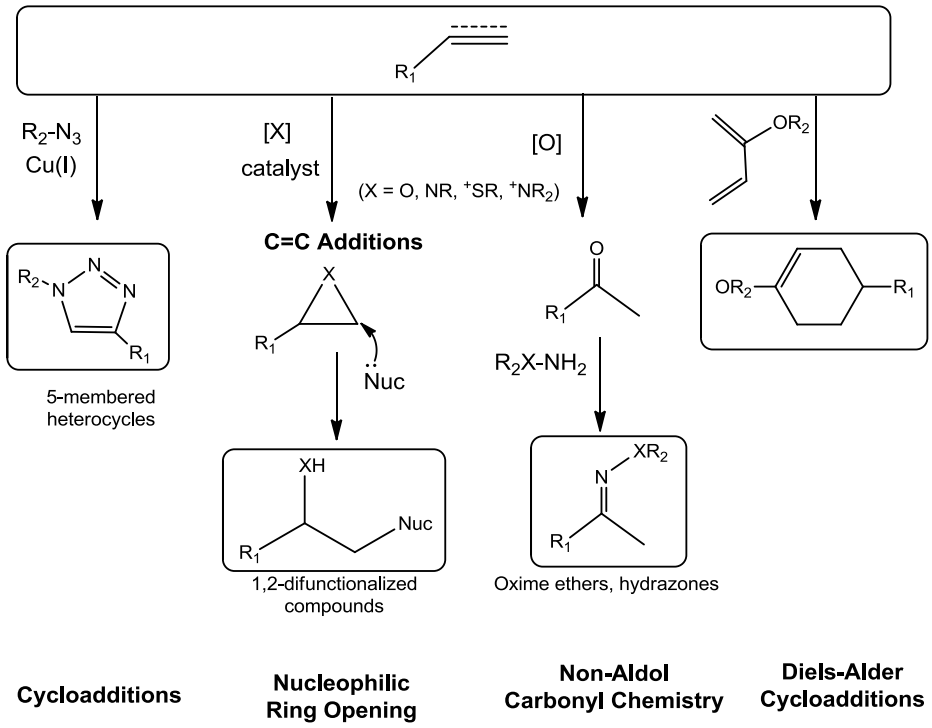

Figure 1.17 ‘Click’ reactions: synthesis of new carbon-heteroatom bonds from unsaturated compounds.

Cycloaddition reactions involving heteroatoms symbolise better than other types of reaction the 'click' chemistry approach. Hetero-Diels-Alder and 1,3-dipolar cycloadditions produce a large set of five- and six-membered heterocycles from two unsaturated reactants. Within the 1,3-dipolar cycloadditions, the Huisgen dipolar cycloaddition of azides and alkynes[98] is worth of note - defined by Sharpless *et al.* as the "cream of the crop" of 'click' chemistry[2].

1.5.3.1 Azide-alkyne 'click' reaction

The family of Huisgen 1,3-dipolar cycloadditions includes many reactions where two unsaturated reactants form five-membered heterocycles. The reaction between an azide and an alkyne to give 1,2,3-triazoles belongs to this type of reactions and it is the most popular reaction in the field of 'click' chemistry. (Scheme 1.15)

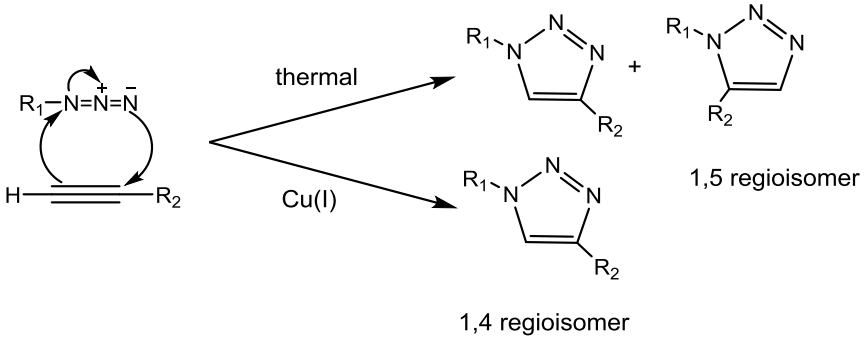

Scheme 1.15 The Huisgen 1,3-Dipolar cycloaddition of an azide and a terminal alkyne.

The azide functionality makes this kind of reaction very suitable for 'click' chemistry thanks to their great stability toward many of the organic synthesis conditions, H_2O and O_2. Despite the great versatility derived from the use of the azide, this reaction required elevated temperature, long reaction time and the resulting product was a mixture of the two possible regioisomers 1,4 and 1,5-triazole. Its importance increased thanks to the discovery that the use of copper(I) could accelerate the reaction and more importantly, made this a regiospecific process. As shown in Scheme 1.15 the thermal cycloaddition is non-regiospecific but copper(I)-catalysed reaction gives only the 1,4-regioisomer of the 1,2,3-triazole. The copper catalysed azide-alkyne cycloaddition (CuAAC) was reported at the same time by two different research groups in 2002: Tornøe *et al.*[99] and Rostovtsev *et al.*[100]. Its use spread out over several fields as for example cell surface engineering[101], carbohydrate chemistry[102], block copolymers and polymers with complex architectures[51] as, for instance, dendrimers[103]. The azide and alkyne functional groups are highly energetic and they have

the ability to remain unaltered during a large number of organic reactions and in biological environments. The resulting 1,2,3-triazole rings are formed irreversibly and exothermically, they are almost impossible to oxidise, reduce or hydrolyse. In addition 1,2,3-triazoles are not only a passive linker but it has shown biological function[104] such as the ability to protect proteins from copper soluble compounds[105].

Rostovtsev *et al.*[100] synthesised 1,2,3-triazoles from several azides and terminal acetylenes in a mixture of H_2O an *tert*-butanol at room temperature. The catalytic system used was copper(II) sulfate pentahydrate and sodium ascorbate[106] as reductant (Scheme 1.16). The choice of generating the copper(I) in situ by reduction of copper(II) salts was mainly due to the higher purity and lower cost of the copper(II) salts.

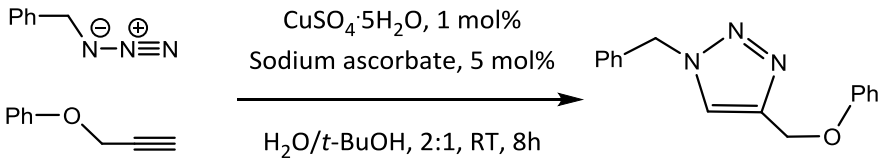

Scheme 1.16 Cu(I)-catalysed 1,3-dipolar cycloaddition of phenyl propargyl ether and benzylazide in aqueous solution.

The reaction proved tolerant to a wide variety of substituents on both the azide and the acetylene. The use of copper(I) salts is also possible and CuI, $CuOTf.C_6D_6$ and $[Cu(NCCH_3)_4][PF_6]$ have been used with no reducing agent. The reaction is still conducted in H_2O but it requires a co-solvent like acetonitrile and a nitrogen base as 2,6-lutidine, pyridine, triethylamine or diisopropylethylamine. In these conditions the reaction does not go as well as the one using copper(II) salts, in fact by-products occur and the exclusion of oxygen may be required for a purer product. Although azides can be very dangerous materials, they are a very important functional group for 'click' chemistry.[2] The azide group is in fact very stable during organic reactions and towards dimerization and hydrolysis in the presence of O_2 and H_2O.[107] The azide functionality has to be introduced onto the organic molecule of interest and sodium azide (NaN_3) is the principal source of the azide functionality. Particular care has to be taken when working with NaN_3 because its toxicity is very similar to that of sodium cyanide (NaCN).[108] In addition azides, and in particular low molecular weight azides, are highly energetic materials and potentially explosive and dangerous when used with metals and halogenated solvents.

1.5.3.2 Applications

'Click' chemistry entered the world of polymer science as a useful alternative to classical coupling reactions like esterification, etherification and many others. The stability of the azide and alkyne groups towards many reaction conditions turned out to be a useful characteristic of the copper mediated azide-alkyne cycloaddition reaction allowing the presence of other functionalities in the compounds to be coupled together. The exploitation of this reaction in polymer science was first reported for the synthesis of dendrimers by Wu *et al.*[103] and has subsequently be reported for the synthesis of several other classes of polymers (e.g. stars, block copolymers, cyclic polymers and hyperbranched polymers).[56,109] 'Click' coupling has also been exploited to introduce functionality into polymers by chain-end reactions,[110] side-chain functionalization and in step growth polymerisation. CuAAC is widely used in combination with ATRP due to several aspects that make the two techniques very compatible. The halogen end groups resulting from the ATRP polymerisation can easily be converted into azide groups that are then reacted with alkyne groups introduced by the use of functionalised initiators. In addition the reaction conditions for the two reactions are very similar making possible the synthesis of polymers in a one-pot reaction.

Even if the CuAAC is still the most widely used 'click' reaction in polymer synthesis, it is important to mention that also other types of 'click' reactions have also been investigated like Diels-Alder and thiol based 'click' reactions pursuing the need of metal free 'click' reactions.[56]

1.5.3.3 'Click' reaction and Hyperbranched Polymers

'Click' reactions have been used for the synthesis of hyperbranched polymers as well as for the monodisperse dendrimers due to the excellent control and good yields. Hyperbranched poly(1,2,3-triazole)s were synthesised by using AB_2 monomers with one (A) azide group and two (B) terminal alkyne groups. Poly([1,2,3]-triazole)s were synthesised in a one-pot reaction by Voit *et al*. who used the 1,3-dipolar cycloaddition reaction with AB_2 monomers *via* both thermally driven and catalytic (copper catalyst) approaches.[111] Long-chain hyperbranched polystyrenes analogous to the HyperMacs[80] synthesised by Hutchings *et al* using Williamson coupling reaction, have also been synthesised by step polymerisation using 'click' coupling chemistry of AB_2 macromonomers with azide and terminal propargyl groups. The

macromonomers were synthesised by ATRP and subsequently modified with the introduction of the clickable groups.[88] In addition to CuAAC 'click' chemistry, thiol-yne 'click' chemistry has also been applied for the synthesis of hyperbranched polymers from both small molecules and linear macromonomers synthesised by RAFT.[112] The thiol-yne reaction consists of the addition of a thiol to an alkyne forming an alkene that reacts with another thiol forming an unsaturated species. The hyperbranched polymers are synthesised with AB_2 macromonomers that carry the thiol group as A group and the two B groups are each π bond in the alkyne group. (Scheme 1.17)

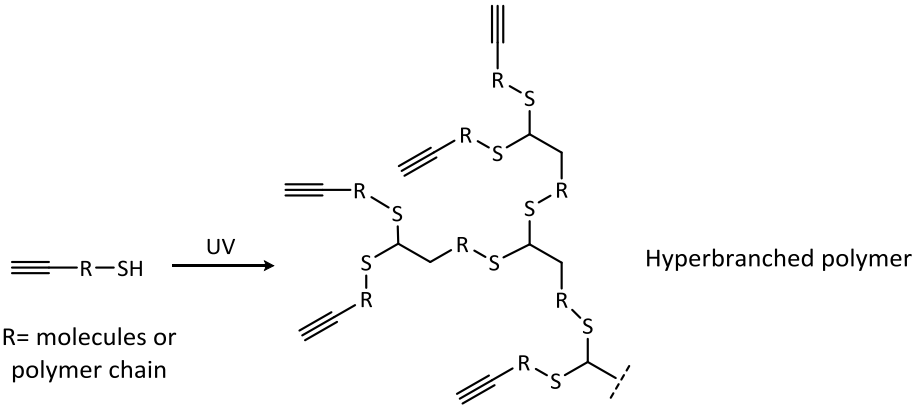

Scheme 1.17 Synthesis of hyperbranched polymers by thiol-yne reaction. The AB_2 monomer can be a single molecule or a macromonomer with a thiol on one end and an alkyne on the other end.

This method was also carried out for macromonomers which were diblock copolymers resulting in hyperbranched polymers with alternating blocks.[89] The reaction produced hyperbranched polymers with high conversions in a short time and high degree of branching.

1.6 Aims and Objectives

The presence of branches in a polymer has a significant impact on the properties of the materials. Varying the molecular weight, molecular weight distribution and the degree of long-chain branching can affect deeply the behaviour of a polymer and significant amounts of work has been directed towards understanding the relationship between the polymer architecture and properties.

In the present study we want to understand how the polymer architectures of block copolymers are related to their microphase separated morphology and mechanical properties.

We aim:

1) to synthesise and characterise a series of highly branched block copolymers that we call HyperBlocks
2) to use the 'macromonomer' approach and living anionic polymerisation techniques in order to synthesise and fully characterise AB_2 PS-PI-PS macromonomers - linear precursors to the branched HyperBlocks
3) to obtain a series of AB_2 macromonomers where we systematically vary:
   - the molecular weight (50 kg mol^{-1} – 150 kg mol^{-1})
   - the composition (PS 20 wt. % – 40 wt. %)
4) to produce highly branched polymers – HyperBlocks – from the AB_2 macromonomers by using two different coupling reactions
5) to investigate the effect of the branched architecture on the solid-state morphology of HyperBlocks
6) to compare the solid-state morphology of the HyperBlocks with the morphology of the linear precursors and blends of HyperBlocks with a commercial thermoplastic elastomer
7) to investigate the effect of the variation of the above mentioned parameters – molecular weight and composition - on the mechanical properties of macromonomers, HyperBlocks and blends

In addition we will carry out the synthesis of a different type of branched polymers, i.e. asymmetric three-arm stars. The objectives are:

1) to produce model materials for rheological studies

2) to synthesise a series of symmetric and asymmetric three-arm stars with two arms of the same molecular weight (90 kg mol^{-1}) and the third arm with a molecular weight that varies from 10 kg mol^{-1} to 90 kg mol^{-1}
3) to synthesise the polymer stars by utilising the 'macromonomer' approach and living anionic polymerisation for a full characterisation of the arms and the final stars
4) to analyse the crude and purified three-arms star by TGIC (Temperature Gradient Interaction Chromatography) in order to investigate the purity of the materials and compare this new technique with the very well-known SEC (Size Exclusion Chromatography).

1.7 References

(1) Szwarc M., Levey M., Milkovich R. *J. Am. Chem. Soc.*, **1956**, *78*, 2656-2657
(2) Kolb H. C., Finn M. G., Sharpless K. B. *Angew. Chem. Int. Ed.*, **2001**, *2001*, 2004-2021
(3) Cowie J. M. G., Arrighi V., *Polymers: Chemistry and Physics of Modern Materials*, CRC Press, (**2008**)
(4) Braun D. *Int. J. Polym. Sci.*, **2009**, *2009*, 1-10
(5) Flory J. P. *J. Am. Chem. Soc.*, **1937**, *59*, 241-253
(6) Jenkins A. D., Jones R. G., Moad G. *Pure Appl. Chem.*, **2010**, *82*, 483-491
(7) Georges M. K., Veregin R. P. N., Kazmaier P. M., Hamer G. K. *Macromolecules*, **1993**, *26*, 2987-2988
(8) Matyjaszewski K., Xia J. *Chem. rev.*, **2001**, *101*, 2921-2990
(9) Matyjaszewski K. *Macromolecules*, **2012**, *45*, 4015-4039
(10) Wang J.-S., Matyjaszewski K. *J. Am. Chem. Soc.*, **1995**, *117*, 5614-5615
(11) Kato M., Kamigaito M., Sawamoto M., Higashimura T. *Macromolecules*, **1995**, *28*, 1721-1732
(12) Coessen V. M. C., Matyjaszewski K. *J. Chem. Ed.*, **2010**, *87*, 916-919
(13) Moad G., Rizzardo E., Thang S. H. *Aus. J. Chem.*, **2012**, *65*, 985-1076
(14) Moad G., Rizzardo E., Thang S. H. *Acc. Chem. Res.*, **2008**, *41*, 1133-1142
(15) Chiefari J., Chong Y. K., Ercole F., Krstina J., Jeffery J., Le T. P. T., Mayadunne R. T. A., Meijs G. F., Moad C. L., Moad G., Rizzardo E., Thang S. H. *Macromolecules*, **1998**, *31*, 5559-5562
(16) Hawker C. J., Bosman A. W., Harth E. *Chem. Rev.*, **2001**, *101*, 3661-3688
(17) Tebben L., Studer A. *Angew Chem Int Ed Engl*, **2011**, *50*, 5034-68
(18) Moad G., Rizzardo E., Solomon D. H. *Macromolecules*, **1982**, *15*, 909-914
(19) Benoit D., Grimaldi S., Robin S., Finet J.-P., Tordo P., Gnanou Y. *J. Am. Chem. Soc.*, **2000**, *122*, 5929-5939
(20) Benoit D., Chaplinski V., Braslau R., Hawker C. J. *J. Am. Chem. Soc.*, **1999**, *121*, 3904-3920
(21) Hsieh H. L., Quirk R. P., *Anionic Polymerization: Principles and Practical Applications*, Marcel Dekker I.: (**1996**)
(22) Bielawski C. W., Grubbs R. H. *Prog. Polym. Sci.*, **2007**, *32*, 1-29
(23) Mai Y., Eisenberg A. *Chem. Soc. Rev.*, **2012**, *41*, 5969-5985
(24) Bates F. S., Fredrickson G. H. *Annu. Rev. Phys. Chem.*, **1990**, *41*, 525-557
(25) Hutchings L. R., Dodds J. M., Rees D., Kimani S. M., Wu J. J., Smith E. *Macromolecules*, **2009**, *42*, 8675-8687
(26) Frey H. *Macrom. Chem. and Phys.*, **2007**, *208*, 1613-1614
(27) Schaefgen J. R., Flory P. J. *J. Am. Chem. Soc.*, **1948**, *70*, 2709-2718
(28) Hadjichristidis N., Pitsikalis M., Pispas S., Iatrou H. *Chem. Rev.*, **2001**, *101*, 3747-3792
(29) Gao H., Matyjaszewski K. *Prog. Polym. Sci.*, **2009**, *34*, 317-350
(30) Angot S., Murthy S. K., Taton D., Gnanou Y. *Macromolecules*, **1998**, *31*, 7218-7225
(31) Hadjichristidis N., Fetters L. J. *Macromolecules*, **1980**, *13*, 191-193
(32) Roovers J., Zhou L.-L., Toporowski P. M., van der Zwan M., Iatrou H., Hadjichristidis N. *Macromolecules*, **1993**, *26*, 4324-4331
(33) Frater D. J., Mays J. W., Jackson C., Sioula S., Efstradiadis V., Hadjichristidis N. *J. Polym. Sci., Part B: Polym. Phys.*, **1997**, *35*, 587-594

(34) Hutchings L. R., Richards R. W. *Polym. Bull.*, **1998**, *41*, 283-289
(35) Li Y., Zhang B., Hoskins J. N., Grayson S. M. *J. Polym. Sci., Part A: Polym. Chem.*, **2012**, *50*, 1086-1101
(36) Ferreira J., Syrett J., Whittaker M., Haddleton D., Davis T. P., Boyer C. *Polym.Chem.*, **2011**, *2*, 1671-1677
(37) Gao H., Matyjaszewski K. *Macromolecules*, **2006**, *39*, 4960-4965
(38) Bi L.-K., Fetters L. J. *Macromolecules*, **1976**, *9*, 732-742
(39) Pennisi R. W., Fetters L. J. *Macromolecules*, **1988**, *21*, 1094-1099
(40) Schappacher M., Deffieux A. *Macromolecules*, **2000**, *33*, 7371-7377
(41) Hadjichristidis N. *J. Polym. Sci.: Part A: Polym. Chem.*, **1999**, *37*, 857-871
(42) Whittaker M. R., Urbani C. N., Monteiro M. J. *J. Am. Chem. Soc.*, **2006**, *128*, 11360-11361
(43) Wu Z., Liang H., Lu J. *Macromolecules*, **2010**, *43*, 5699-5705
(44) Gido S. P., Lee C., Pochan D. J. *Macromolecules*, **1996**, *29*, 7022-7028
(45) Zhang H., Li Y., Zhang C., Li Z., Li X., Wang Y. *Macromolecules*, **2009**, *42*, 5073-5079
(46) Xenidou M., Hadjichristidis N. *Macromolecules*, **1998**, *31*, 5690-5694
(47) Kowalczuk M., Adamus G., Jedlinski Z. *Macromolecules*, **1994**, *27*, 572-575
(48) Tanaka S., Uno M., Teramachi S., Tsukhara Y. *Polymer*, **1995**, *36*, 2219-2225
(49) Roovers J., Toporowski P. M. *Macromolecules*, **1981**, *14*, 1174-1178
(50) Carlmark A., Hawker C., Hult A., Malkoch M. *Chem. Soc. Rev.*, **2009**, *38*, 352-62
(51) Konkolewicz D., Monteiro M. J., Perrier S. b. *Macromolecules*, **2011**, *44*, 7067-7087
(52) Fréchet J. M. J. *J. Polym. Sci.: Part A: Polym. Chem.*, **2003**, *41*, 3713-3725
(53) Tomalia D. A., Baker H., Dewald J., Hall M., Kallos G., Martin S., Roeck J., Ryder J., P. S. *Polym. J.*, **1985**, *17*, 117-132
(54) Hawker C., Fréchet J. M. J. *J. Chem. Soc., Chem. Commun.*, **1990**, 1010-1013
(55) Hawker C. J., Fréchet J. M. J. *J. Am. Chem. Soc.*, **1990**, *112*, 7638-7647
(56) Kempe K., Krieg A., Becer C. R., Schubert U. S. *Chem. Soc. Rev.*, **2012**, *41*, 176-191
(57) Urbani C. N., Bell C. A., Lonsdale D., Whittaker M. R., Monteiro M. J. *Macromolecules*, **2008**, *41*, 76-86
(58) Voit B., Lederer A. *Chem. Rev.*, **2009**, *109*, 5924-5973
(59) Kim Y. H., Webster O. W. *J. Am. Chem. Soc.*, **1990**, *112*, 4592-4593
(60) Kim Y. H., Webster O. W. *Macromolecules*, **1992**, *25*, 5561-5572
(61) Flory P. J. *J. Am. Chem. Soc.*, **1952**, *74*, 2718-2723
(62) Gao C., Yan D. *Prog. Polym. Sci.*, **2004**, *29*, 183-275
(63) Malmstrom E., Johansson M., Hult A. *Macromolecules*, **1995**, *28*, 1698-1703
(64) Satoh T. *Int. J. Polym. Sci.*, **2012**, *2012*, 1-8
(65) Fréchet J. M. J., Henmi M., Gitsov I., Aoshima S., Leduc M. R., Grubbs B. R. *Science*, **1995**, *269*, 1080-1083
(66) Hawker C. J., Fréchet J. M. J., Grubbs R. B., Dao J. *J. Am. Chem. Soc.*, **1995**, *117*, 10763-10764
(67) Gaynor S. G., Edelman S., Matyjaszewski K. *Macromolecules*, **1996**, *29*, 1079-1081
(68) Carter S., Rimmer S., Sturdy A., Webb M. *Macromol. Biosci.*, **2005**, *5*, 373-378
(69) Suzuki M., Ii A., Saegusa T. *Macromolecules*, **1992**, *25*, 7071-7072
(70) Sunder A., Hanselmann R., Frey H., Mulhaupt R. *Macromolecules*, **1999**, *32*, 4240-4246
(71) Trollsås M., Kelly M. A., Claesson H., Siemens R., Hedrick J. L. *Macromolecules*, **1999**, *32*, 4917-4924

(72) Liu M., Vladimirov N., Fréchet J. M. J. *Macromolecules*, **1999**, *32*, 6881-6884
(73) Chang H.-T., Fréchet J. M. J. *J. Am. Chem. Soc.*, **1999**, *121*, 2313-2314
(74) Gong C., Fréchet J. M. J. *Macromolecules*, **2000**, *33*, 4997-4999
(75) Gao C., Yan D. *Macromolecules*, **2003**, *36*, 613-620
(76) Paulo C., Puskas J. E. *Macromolecules*, **2001**, *34*, 734-739
(77) Peleshanko S., Gunawidjaja R., Petrash S., Tsukruk V. V. *Macromolecules*, **2006**, *29*, 4756-4766
(78) Teertstra S. J., Gauthier M. *Prog. Polym. Sci.*, **2004**, *29*, 277-327
(79) Tomalia D. A., Hedstrand D. M., Ferritto M. S. *Macromolecules*, **1991**, *24*, 1435-1438
(80) Hutchings L. R., Dodds J. M., Roberts-Bleming S. J. *Macromolecules*, **2005**, *38*, 5970-5980
(81) Rikkou-Kalourkoti M., Matyjaszewski K., Patrickios C. S. *Macromolecules*, **2012**, *45*, 1313-1320
(82) Han J., Li S., Tang A., Gao C. *Macromolecules*, **2012**, *45*, 4966-4977
(83) Li S., Han J., Gao C. *Polym. Chem.*, **2013**, *4*, 1774-1787
(84) Unal S., Long T. E. *Macromolecules*, **2006**, *39*, 2788-2793
(85) Hawker C. J., Chu F., Pomery P. J., Hill D. J. T. *Macromolecules*, **1996**, *29*, 3831-3838
(86) Clarke N., Luca E. D., Dodds J. M., Kimani S. M., Hutchings L. R. *Eur. Polym. J.*, **2008**, *44*, 665-676
(87) López-Villanueva F.-J., Wurm F., Kilbinger A. F. M., Frey H. *Macrom. Rapid Commun.*, **2007**, *28*, 704-709
(88) Kong L.-Z., Sun M., Qiao H.-M., Pan C.-Y. *J. Polym. Sci., Part A: Polym. Chem.*, **2010**, *48*, 454-462
(89) Konkolewicz D., Poon C. K., Gray-Weale A., Perrier S. *Chem. Commun.*, **2011**, *47*, 239-241
(90) Hutchings L. R. *Soft Matter*, **2008**, *4*, 2150-2159
(91) Yan D., Gao C., Frey H., *HYPERBRANCHED POLYMERS, Synthesis, Properties and Applications*, John Wiley & Sons, Inc., (**2011**)
(92) Prashad A. S., Vlahos N., Fabio P., Feigelson G. B. *Tetrahedron Lett.*, **1998**, *39*, 7035-7038
(93) Kolb H. C., Sharpless K. B. *Drug Disc. To.*, **2003**, *8*, 1128-1137
(94) Jørgensen K. A. *Angew. Chem. Int. Ed.*, **2000**, *39*, 3558-3588
(95) Adolfsson H., Converso A., Sharpless K. B. *Tetrahedron Lett.*, **1999**, *40*, 3991-3994
(96) Kolb H. C., VanNieuwenhze M. S., Sharpless K. B. *Chem. Rev.*, **1994**, *94*, 2483-2547
(97) Gontcharov A. V., Liu H., Sharpless K. B. *Org. Lett.*, **1999**, *1*, 783-786
(98) Huisgen R. *Pure Appl. Chem.*, **1989**, *61*, 613-628
(99) Tornøe C. W., Christensen C., Meldal M. *J. Org. Chem.*, **2002**, *67*, 3057-3064
(100) Rostovtsev V. V., Green L. G., Fokin V. V., Sharpless K. B. *Angew. Chem. Int. Ed.*, **2002**, *41*, 2596-2599
(101) Link J. A., Tirell D. A. *J. Am. Chem. Soc.*, **2003**, *125*, 11164-11165
(102) Fazio F., Bryan M. C., Blixt O., Paulson J. C., Wong C.-H. *J. Am. Chem. Soc.*, **2002**, *124*, 14397-14402
(103) Wu P., Feldman A. K., Nugent A. K., Hawker C. J., Scheel A., Voit B., Pyun J., Frechet J. M., Sharpless K. B., Fokin V. V. *Angew. Chem. Int. Ed.*, **2004**, *43*, 3928-3932
(104) Hartzel L. W., Benson F. R. *J. Am. Chem. Soc.*, **1954**, *76*, 667-670
(105) Wang Q., Chan T. R., Hilgraf R., Fokin V. V., Sharpless K. B., Finn M. G. *J. Am. Chem. Soc.*, **2003**, *125*, 3192-3193

(106) Davies M. B. *Polyhedron*, **1992**, *11*, 285-321
(107) Saxon E., Bertozzi C. R. *Science*, **2000**, *287*, 2007-2010
(108) Bräse S., Gil C., Knepper K., Zimmermann V. *Angew. Chem. Int. Ed.*, **2005**, *44*, 5188-5240
(109) Fournier D., Hoogenboom R., Schubert U. S. *Chem. Soc. Rev.*, **2007**, *36*, 1369-1380
(110) Malkoch M., Schleicher K., Drockenmuller E., Hawker C., Russell T. P., Wu P., Fokin V. V. *Macromolecules*, **2005**, *38*, 3663-3678
(111) Scheel A. J., Komber H., Voit B. I. *Macromol. Rapid Commun.*, **2004**, *25*, 1175-1180
(112) Konkolewicz D., Gray-Weale A., Perrier S. *J. Am. Chem. Soc.*, **2009**, *131*, 18075-18077

CHAPTER 2

Synthesis of HyperBlocks

2.1 Introduction

The synthesis of a series of long-chain hyperbranched polymers called HyperBlocks is presented here and discussed. HyperBlocks are a novel class of branched thermoplastic elastomers (TPE) reported for the first time in 2009 by Hutchings *et al*.[1] HyperBlocks are made from macromonomers that are triblock copolymers of polystyrene and polyisoprene in the form of ABA block copolymers. Polystyrene-polyisoprene-polystyrene triblock copolymers find significant commercial application as thermoplastic elastomers as for example the commercial polymers Kraton™ D (SIS). The 'physical crosslinks' that impart good mechanical properties (rubber elasticity and tensile strength) to the linear TPEs are enhanced by 'covalent branch points' between the linear segments in the HyperBlocks. In fact HyperBlocks are made from PS-PI-PS linear polymers joined together by covalent bonds resulting in a very highly branched architecture that influences the physical properties of the material. During the previous work a single HyperBlock sample was produced and investigations were carried out on the solid-state morphology and mechanical properties in order to understand the effect of the hyperbranched architecture on these properties.

HyperBlocks were synthesised via a 'macromonomer' approach that enabled the synthesis and complete characterisation of well-defined linear (macromonomer) polymers which become the linear polymer segments between the branch points in the final HyperBlock. The macromonomers are α,ω,ω'–trifunctional AB_2 macromonomers and they are the linear precursor building blocks used to construct the HyperBlocks. According to this approach the macromonomers were synthesised in a preliminary step using living anionic polymerisation. Such a synthetic strategy offers the possibility to obtain a high degree of control over the molecular weight, dispersity, microstructure and composition of the macromonomers. In addition the use of living anionic polymerisation made possible the introduction of chain-end functionalities that were subsequently modified in order to introduce suitable groups for the HyperBlocks synthesis by coupling reactions.

HyperBlocks were then produced in a one-pot reaction by coupling the macromonomers together using two different classes of reaction. The coupling reactions exploited in this work were the Williamson coupling reaction, as previously described[1], and the azide-alkyne 'click' reaction.

Each polymer synthesised was characterised by Size Exclusion Chromatography (SEC) and Nuclear Magnetic Resonance (NMR) spectroscopy to obtain molecular weight and copolymer composition data. Differential Scanning Calorimetry (DSC) was used to characterise the polymers in terms of their thermal properties. Further analyses by Transmission Electron Microscopy (TEM) were carried out in order to study the solid-state morphology of the HyperBlocks and blends of the HyperBlocks with a commercial linear PS-PI-PS thermoplastic elastomer Kraton^{TM}. Mechanical properties were studied by tensile testing on the pure HyperBlocks and on blends with the commercial TPE. (see Chapter 3 – Characterisation of HyperBlocks)

2.2 Aims

The presence of branches in a polymer has a significant impact on the properties of the materials. Varying the molecular weight, molecular weight distribution and the degree of long-chain branching can affect substantially the behaviour of a polymer and significant amounts of work has been directed towards understanding the relationship between the polymer architecture and properties such as rheology.[2,3] However, in the present study we are attempting to understand how the polymer architecture of block copolymers impact upon their solid state morphology and in turn their mechanical properties and we aim to synthesise a series of highly branched block copolymers that we call HyperBlocks. In a preliminary study a single sample of a HyperBlock was prepared and it was discovered that HyperBlocks have the potential to be thermoplastic elastomers with excellent properties however the branched architecture undoubtedly had an impact upon physical properties. The aforementioned sample underwent microphase separation but the resulting morphology showed no long-range order. However, far from having a negative impact upon mechanical properties, the single HyperBlock had properties which were at worst comparable to commercial TPEs. In the present study we aim to synthesise and analyse a family of HyperBlocks with systematic variation in molecular weight and copolymer composition. Moreover, we will prepare blends of HyperBlock with commercial thermoplastic elastomers in order to understand the relationship between the branched architecture and the physical and mechanical properties and in particular the impact of low concentrations of HyperBlock upon the blend properties.

The initial work reported herein focused on attempts to improve the previously reported synthetic methodology in order to obtain triblock copolymers (macromonomers) with more highly controlled molecular parameters i.e. molecular weight and molecular weight distribution. The objective of this work was the synthesis of two sets of AB_2 macromonomers – the linear precursors to the branched HyperBlocks – synthesised by living anionic polymerisation and comprising of a triblock copolymer of polystyrene, polyisoprene and polystyrene. The first set of macromonomers has a fixed composition of 30% (by weight fraction) polystyrene but a range of molecular weights. The molecular weights chosen were M_n= 50,000 g mol^{-1}, 100,000 g mol^{-1} and 150,000 g mol^{-1}. The second set of macromonomers

has a fixed molecular weight of (approximately) 100,000 g mol^{-1} and a variable composition. The weight fraction of styrene in these cases was decided to be 20%, 30% and 40%.

Each macromonomer was made on a large scale, about 50 g, so that it would be possible to convert the macromonomers into HyperBlocks and then compare the characterisation of both the linear and hyperbranched copolymers.

The characterisation of the materials was carried out to investigate thermal properties (DSC), mechanical analysis (tensile testing) and morphology (TEM) in order to understand the relationship between the architecture and physical properties. The results of the characterisation studies are reported in Chapter 3.

2.3 Results and discussion

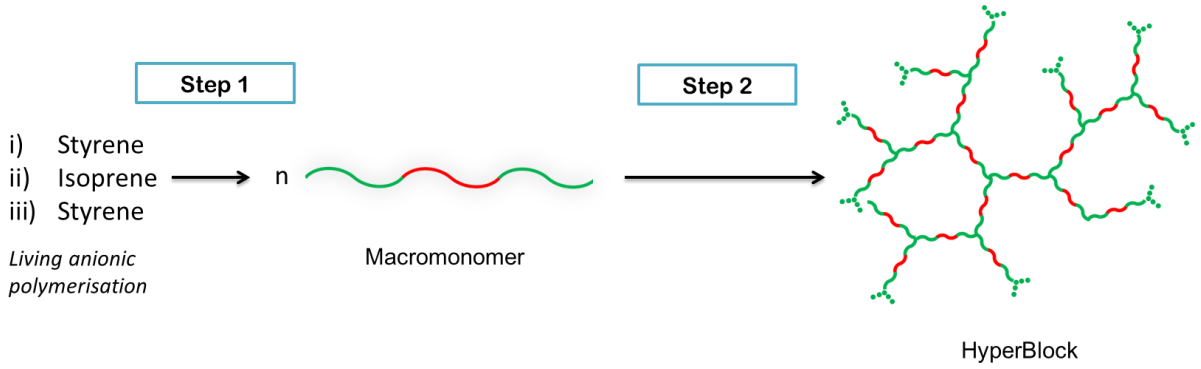

Figure 2.1 Schematic representation of the HyperBlocks synthesis via the 'macromonomer' approach using styrene and isoprene as monomers.

HyperBlocks are synthesised via a 'macromonomer' approach in a two-step procedure. (Figure 2.1) The first step consists of the synthesis of linear macromonomers by living anionic polymerisation. The second step involves the synthesis of the hyperbranched polymers called HyperBlocks by reacting together the macromonomers through coupling reactions.

2.3.1 Synthesis of AB_2 Macromonomers

The macromonomers are linear ABA triblock copolymers where polystyrene constitutes the outer A blocks and polyisoprene constitutes the central B block of the polymer chain (PS-PI-PS). A series of macromonomers have been synthesised by living anionic polymerisation which is the best polymerisation technique for the control of polymer characteristics such as molecular weight and dispersity. The macromonomer synthesis carried out in this work was based upon a methodology described in a previous paper from Hutchings *et al.*[1] and it involves three steps at the end of which we obtain an AB_2 macromonomer triblock copolymers with reactive chain-end functionalities; one A functionality and two B functionalities. These functionalities facilitate the subsequent coupling reactions for the synthesis of HyperBlocks. The first step involves the anionic polymerisation of the monomers using a functionalised (protected alcohol) initiator and an end-capping reaction with a difunctional (protected phenol) diphenylethylene derivative to give a protected AB_2 macromonomer. The remaining two steps involve deprotection of the protected functionalities and modification of the functional A and B groups as appropriate. The macromonomers synthesised in this work are named systematically P(S-I-S)a_b where *a*

refers to the macromonomer molecular weight obtained by NMR analysis and *b* is the weight fraction (as a percentage) of polystyrene in the copolymer – thus P(S-I-S)59_33 is a poly(styrene-isoprene-styrene) copolymer with a molecular weight (M_n) of 59 000 g mol^{-1} and a weight fraction of 33% polystyrene.

2.3.1.1 Protected Macromonomer P(S-I-S)

The sequential polymerisation of styrene and isoprene were carried out under high-vacuum at room temperature with benzene as a solvent. The synthesis involves four separate steps as shown below (Scheme 2.1).

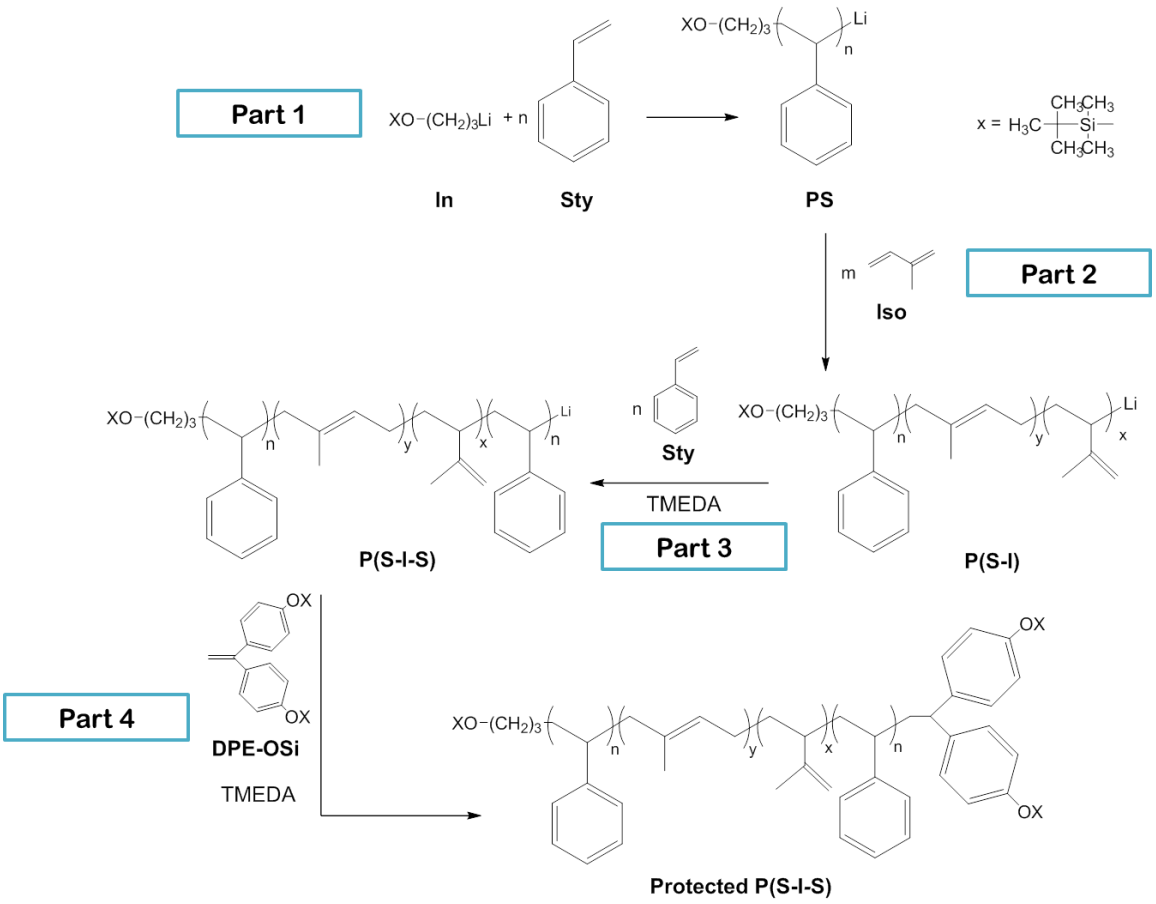

Scheme 2.1 Synthesis of protected AB_2 macromonomers: Part 1 is the polystyrene synthesis constituting the first block, Part 2 is the synthesis of the second block by addition of isoprene, Part 3 is the synthesis of the third block by addition of styrene and Part 4 is the end-capping reaction.

The procedure previously reported for the synthesis of macromonomer is described below.

Part 1: 3-(*tert*-butyldimethylsiloxy)-1-propyllithium (In) was added to the solution of styrene in benzene. The addition of the initiator created a change in colour of the solution which became orange/red.

Part 2: After 12 hrs to allow complete consumption of the styrene, a small sample was removed for characterisation followed by the addition of isoprene monomer. Upon addition of isoprene, the solution changed colour again becoming a pale yellow. After three days of reaction at room temperature the change in viscosity of the solution demonstrated that the polymerisation had successfully continued upon the addition of the second monomer – a second sample was removed for characterisation.

Part 3: at this point, prior to the addition of the second batch of styrene, *N,N,N',N'*-tetramethylethylenediamine (TMEDA) was added to ensure rapid re-initiation of the polymerisation of styrene by the polyisoprenyl lithium chain end. Addition of the styrene for the third block resulted in a change of colour from yellow rapidly back to the orange/red colour of living polystyryllithium as in Part 1. The reaction was stirred for three hours to ensure the complete reaction.

Part 4: this step consists of the end-capping of the living polymer through the addition of a functionalised diphenylethylene derivative carrying two protected phenol groups (1,1-*bis*(4-*tert*-butyldimethylsiloxyphenyl)ethylene) (DPE-OSi) thereby adding the B functionalities to the AB_2 macromonomer polymer chain. The colour of the solution changed to a dark red colour upon addition of the DPE-OSi and the reaction was stirred at room temperature for five days.

2.3.1.1.1 Modified procedure

In the previously described procedure, the initiator employed, 3-(*tert*-butyldimethylsiloxy)-1-propillithium, carries a protected alcohol group that allows the introduction of the first functionality at one end of the polymer chains. However, the initiator is also a *n*-alkyl lithium initiator and in the absence of any Lewis base additives, initiation is slow and the dispersity of the first PS block in the previously reported work was broad – 1.45[1]. The cause can be found in the slow rate of initiation with respect to the rate of propagation due to the high aggregation state of the initiator in the solution. However, it is also known that the addition of a Lewis base such TMEDA in a molar ratio of 1:1 with respect to the initiator serves to break up the alkyl lithium aggregates, increasing the rate of initiation and decreasing the dispersity, which in turn gives polymers with much lower dispersity.[4] Whilst the addition of TMEDA may therefore seem like an obvious step to take, the omission of TMEDA in this case was required for the polymerisation of isoprene in the next step of the macromonomer

synthesis. Polyisoprene synthesised in benzene preferably has a high degree of 1,4-microstructure and this is prevented in the presence of TMEDA.[5] In general dienes can form four isomeric microstructures. (Figure 2.2)

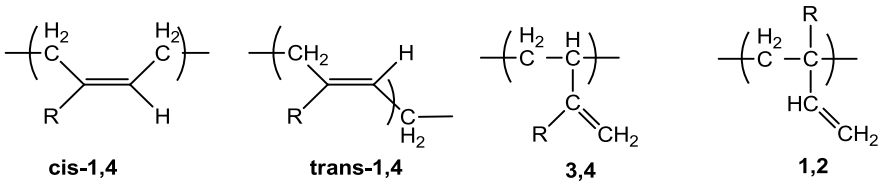

Figure 2.2 Possible microstructures assumed by polyisoprene in different reaction conditions.

The polydiene microstructure is very sensitive to the metal counterion, solvent and the presence of Lewis base. In the anionic polymerisation of dienes the use of lithium as counterion provides polydienes with high 1,4-microstructure and for isoprene a microstructure of at least 90 % 1,4 enchainment can be achieved. This microstructure results in polydienes with a low glass transition temperature (T_g) and good elastomeric properties at room temperature and above. The characteristic of lithium to form 1,4-polydienes is completely lost when the reaction is carried out in a polar solvent instead of in non-polar hydrocarbons such a benzene. Moreover, when using hydrocarbon solvents, even small amounts of Lewis bases can dramatically change the microstructure. In fact the presence of Lewis base modifies the charge distribution, the chain end configuration, and the distribution of contact ion pairs that determine the resulting microstructure. So in the previous work it was preferred to omit TMEDA in order to retain a high 1,4-microstructure in the polyisoprene block and accepting a higher dispersity in the first block of polystyrene.

In an attempt to improve the dispersity of the first block whilst retaining the desired high 1,4 microstructure in the second block we decided to reconsider the use of a Lewis base additive. Initially we considered the use of alkali metal alkoxides, which have been used previously in the synthesis of the triblock copolymer poly(styrene-*block*-butadiene-*block*-styrene) utilising a dilithium initiator which also resulted in slow initiation and high Đ in the absence of additives.[6] The addition of lithium *sec*-butoxide was shown to solve the problem of high dispersity values and it did not have a significant effect on the polybutadiene microstructure. However, the presence of lithium butoxide in the polymerisation of styrene in benzene with *n*-butyl lithium initiator decreased dramatically the initiation rate.[7] Moreover, the effect of lithium butoxide on the polymerisation of isoprene also resulted in an undesirable depression of the propagation rate that decreases by a factor that varies

from 0.65 to 0.25 depending on the ratio of *t*-BuOLi over polyisopropyllithium.[8] It was therefore decided that the addition of alkali metal alkoxide would not have been a very good way to proceed, in fact even if lithium butoxide might solve the problem of the dispersity, the resulting reaction rates were too low to be practical. Instead, we decided to investigate the use of a volatile Lewis base which could be removed by distillation at the end of the polymerisation of styrene and before the addition of isoprene. We investigated the use of THF and diethyl ether and we compared the results with the ones obtained by using TMEDA which can solve the problem of the dispersity but is not volatile (bp 122°C). It is well known that the effect of THF upon the rate of initiation is big: a study on the polymerisation of styrene in benzene with the addition of THF[9] showed a big increase in rate of initiation at a mole ratio of less than 10:1 of THF with respect to the initiator which would be expected to solve the problem of high dispersity. However in the polymerisation of isoprene the use of THF[10] leads to a big change in the microstructure which goes from a largely 1,4-microstructure to a largely 3,4-microstructure. The same effect is provoked by the addition of any polar additives. For that reason it was deemed necessary to carry out the polymerisation of styrene in the presence of such an additive but also to be able to evacuate the additive before the addition of isoprene.

Three small scale (2 g) polymerisations were carried out focusing only upon the synthesis of the first two blocks (part 1 and 2 in Scheme 2.1). The polymerisation of styrene was only carried out for about an hour and not overnight as mentioned in the paper[1] because ether type additives such as THF can react with the living polystyryl anions to decrease the concentration of the active chains and to terminate the chains growth.[5] In addition these additives tend to increase the rate of propagation and so the reaction reaches completion in a short time. In each case the mole ratio of additive to lithium was 5:1. The molecular weight, dispersity and microstructure of the resulting polymers are reported below in Table 2.1.

Table 2.1 Molecular weight, dispersity and microstructure of the PS first blocks and P(S-I) diblock copolymers obtained by living anionic polymerisation with the addition of the three different additives.

Polymers	PS Block		P(S-I) block			*3,4-microstructure (%)*	*Additives*
	M_n (g·mol^{-1})	Đ	M_n (g·mol^{-1}) (a)	M_n (g·mol^{-1}) (b)	Đ		
P(S-I)60	10500	1.14	34300	60400	1.04	12	THF
P(S-I)36	-	-	25700	35500	1.03	>61	TMEDA
P(S-I)180	30900	1.27	39200	180400	1.11	8	Et_2O

(a) Data obtained by SEC in THF using a value of dn/dc= 0.185
(b) Data obtained by ^{1}H-NMR spectroscopy in $CDCl_3$.

It can be seen from the data in Table 2.1 that the best result is obtained by the addition of THF that gives the best dispersity value whilst retaining a reasonable microstructure. The content of 3,4-microstructure in the polymer has been calculated by ^{1}H-NMR analysis carried out on each polymer. A typical spectrum of a poly(styrene-isoprene) block copolymer is shown in Figure 2.3.

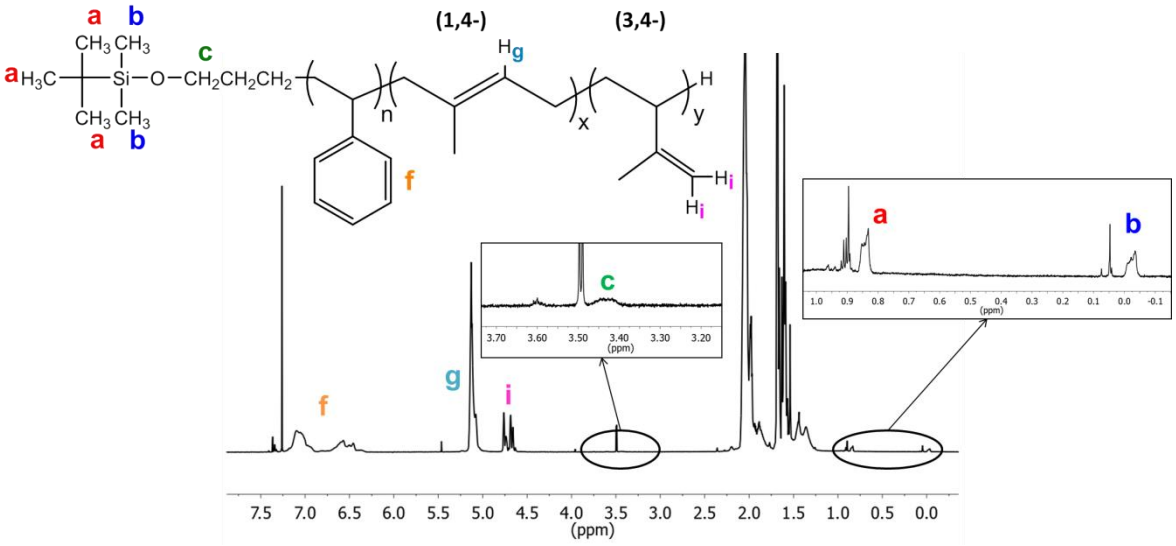

Figure 2.3 ^{1}H-NMR spectrum of P(S-I)60 in $CDCl_3$ (700MHz).

Observing the spectrum it is possible to identify some of the main peaks characteristic of the subsequently synthesised polystyrene-polyisoprene-polystyrene triblock macromonomer. The characteristic peaks of the initiator carrying a primary alcohol functionality protected by a silyl group can be observed at δ 0.0 ppm [$(C\underline{\mathbf{H}}_3)_2SiO$], at δ 0.8-0.9 ppm [$(C\underline{\mathbf{H}}_3)_3C$-Si] and at δ 3.4-3.5 ppm [$C\underline{\mathbf{H}}_2OSi$] for the protons adjacent to the protected primary alcohol. The characteristic peaks of the alkene protons of the polyisoprene block are found in the range δ 4.5 – 5.5 ppm. The peaks representing the 1,4-microstructure are visible in $CDCl_3$ at δ 5-5.2 ppm [$(CH_3)C$=C$\underline{\mathbf{H}}$] and the peaks corresponding to 3,4-microstructure are found at δ 4.6-4.8

ppm [$(CH_3)C=C\underline{\mathbf{H}}_2$].[11] In Figure 2.4 we compare the ^{1}H-NMR spectra of P(S-I)60 and P(S-I)36 having a content of 3,4-microstructure of 12% and 61% respectively. The overlay of the spectra shows the change of the peaks representing the microstructure of the polyisoprene block.

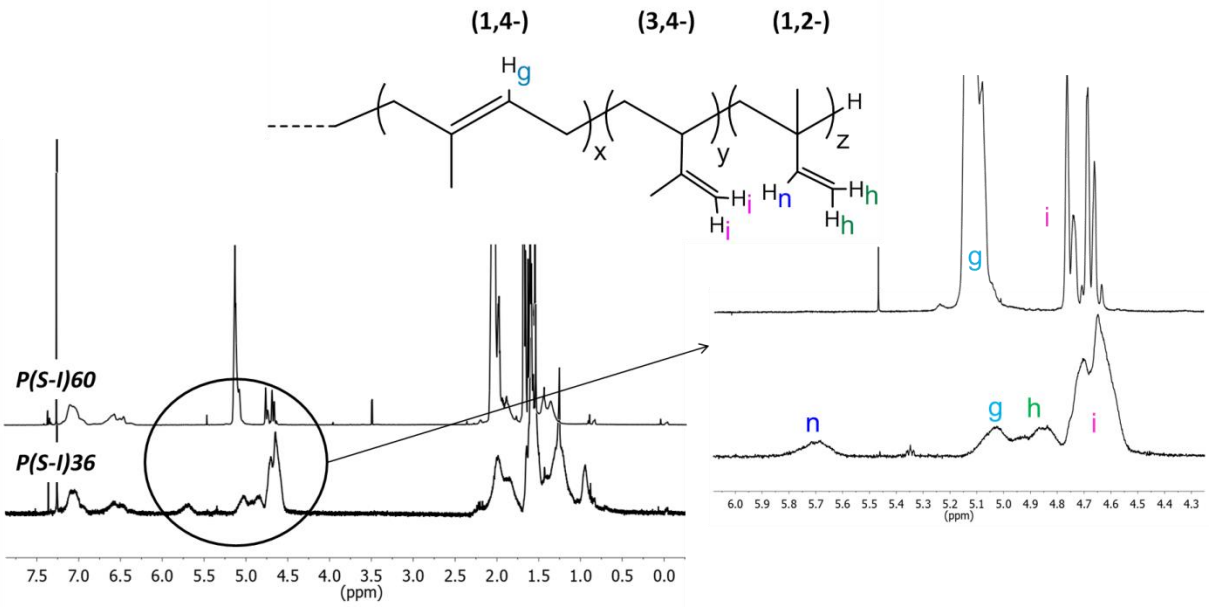

Figure 2.4 Comparison of ^{1}H-NMR spectra of P(S-I)60 and P(S-I)36 in $CDCl_3$ (700MHz and 400MHz respectively). Expansion of the peaks corresponding to the polyisoprene block.

It is clear that there is almost a total loss of 1,4-microstructure which is replaced by 3,4- and 1,2-microstructure. The peaks representing the 1,2-microstructure can be observed at δ 5.6-5.8 ppm [$C\underline{\mathbf{H}}=CH_2$] and at δ 4.8-4.9 ppm [$CH=C\underline{\mathbf{H}}_2$].[12] The poor results obtained for P(S-I)36 in terms of microstructure derive from the difficulty in removing all the TMEDA from the reaction at the end of the polymerisation of styrene. Removal of the polar additive was attempted by distilling out of the flask the solvents and then adding fresh, dry benzene, repeating this procedure at least three times. It has to be considered that the boiling points of the three additives are quite different and the TMEDA has the highest one: THF 66°C, TMEDA 122°C and Et_2O 35°C. So it is highly likely that for THF and Et_2O additives the three distillation cycles with benzene were enough to remove the overwhelming majority of the polar additives and permitted the polymerisation of isoprene in their absence. It is equally likely that TMEDA was not completely removed. In previous polymerisations carried out in non-polar hydrocarbon solvents, polymers with 90% (or more) 1,4 microstructure have been observed. It is possible that in these cases, traces of polar solvent remain during the polymerisation of isoprene despite the washing cycles.

Following these initial trials to optimise the dispersity and microstructure it was decided to scale up the reaction. The aim was to synthesise a 50 g batch of macromonomer in order to have enough material for the synthesis of HyperBlocks and for the characterisation on both the HyperBlock and the macromonomer. THF was used as the Lewis base additive as described above. However, the larger scale reaction did not yield the same result as previously obtained and the ability to retain the 1,4-microstructure was lost in the scale up of the reaction. Despite repeated distillation cycles with benzene, THF could not be removed completely and the resulting polymer P(S-I-S)59_33 presented a content of 32% of 3,4-microstructure.

In addition to their failure to remove all the THF, the repeated distillation cycles created another problem in the synthesis. They increased the possibility to add to the reaction some impurities, even if the fresh benzene used was always kept under vacuum and dried with calcium hydride. Impurities in anionic polymerisation result in the termination of the living polymer chains; for the macromonomer synthesised in this way it was always possible to observe a small (but significant) amount of dead chains of polystyrene in the SEC curves at 16.12min. (Figure 2.5)

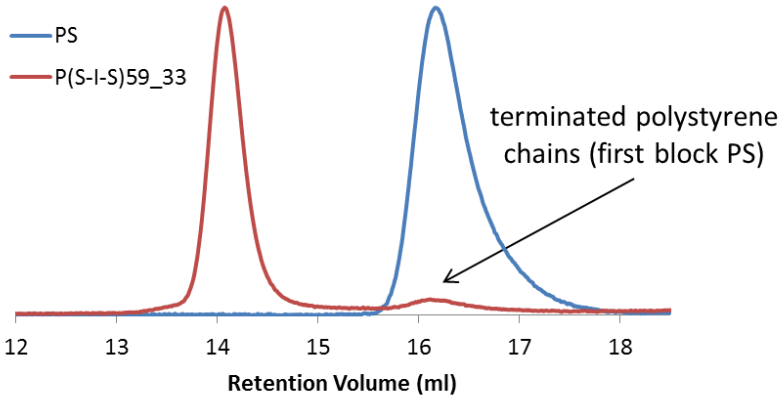

Figure 2.5 SEC (refractive index (RI) detector) chromatogram of the macromonomer P(S-I-S)59_33 (red line) overlaid with the SEC chromatogram of the first polystyrene block PS sampled before the isoprene addition and after the distillation cycles (blue line).

For all these reasons and above all for the loss of the desired polyisoprene microstructure, we decided to adopt the previously established procedure without the addition of any Lewis base.

2.3.1.1.2 Macromonomers specifications

A series of AB_2 macromonomers have been synthesised by the method described above without any polar additive additions. We characterised each macromonomer and the constituting blocks by sampling of the reaction after the polymerisation of each block and before each subsequent addition of monomers to the polymerisation.

Analysis of the macromonomers and the samples taken during the polymerisation were carried out by SEC and ^{1}H-NMR spectroscopy. SEC analysis highlighted the success of the anionic polymerisation (Figure 2.6) and allowed the determination of the molecular weight of each block.

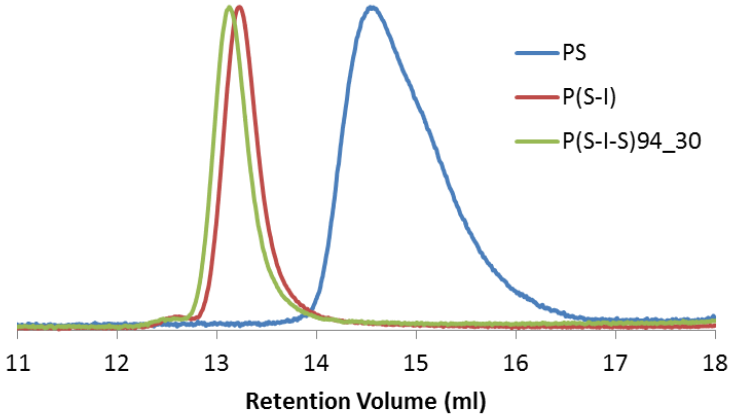

Figure 2.6 SEC chromatogram (RI detector) of P(S-I-S)94_30: from the right polystyrene block PS, diblock copolymer P(S-I) and final triblock copolymer i.e. the macromonomer.

The increase in molecular weight of the polymer after each addition step is demonstrated by the shift (from right to left) of the SEC curves from the homopolymer polystyrene (first block PS) to the triblock copolymer P(S-I-S).

A typical ^{1}H-NMR spectrum of the synthesised AB_2 macromonomers P(S-I-S) is shown in Figure 2.7 which also shows the spectra for the samples taken representing the PS and P(S-I) polymers. From these data it is possible to calculate the composition of the macromonomer and weight fraction of polystyrene in the macromonomer, the molecular weight (M_n), the microstructure of the polyisoprene block and the degree of end-capping.

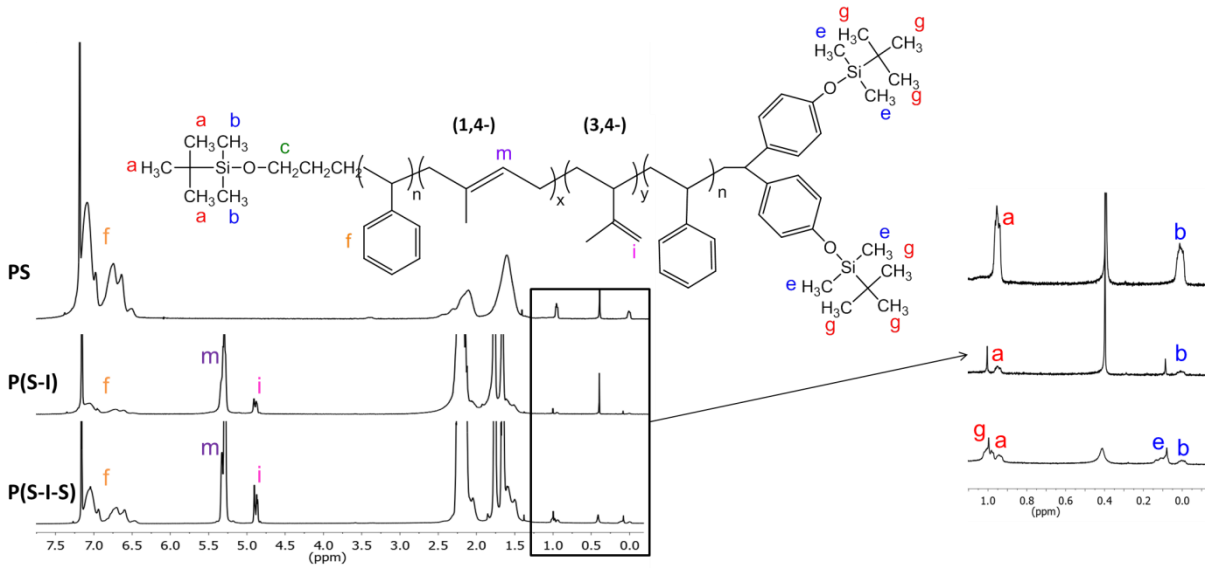

Figure 2.7 ^{1}H-NMR spectra in C_6D_6 (synthesis of the macromonomer P(S-I-S)114_23, 400MHz) of the samples taken during the polymerisation before each monomer addition. On the right expanded picture of the peaks corresponding to the protection groups introduced through the initiator and the end-capping agent.

Starting from the top of the overlaid spectra in Figure 2.7 it is possible to observe the spectrum of the first block (PS), the diblock copolymer P(S-I) and the final product i.e. the end-capped triblock copolymer P(S-I-S). In the final stage of the synthesis the AB_2 macromonomer is end-capped with the functionalised diphenylethylene derivative (DPE-OSi). This reaction is very slow so it was stirred for 5 days before termination with nitrogen sparged methanol. DPE-OSi (in common with all DPE monomers) is too sterically bulky to propagate and so it was possible to add an excess of it (with respect to lithium) to the reaction to ensure a complete reaction with chain ends. The signals corresponding to the protected DPE-OSi group attached to the polymer chains are at δ 0.1 ppm [(C**H**$_3$)$_2$Si] and at δ 1.0 ppm [(C**H**$_3$)$_3$C-Si] that lie close to the signals given by the initiator molecule that has the same silyl protection group for the -OH functionality. From these peaks it is possible to calculate the degree of end-capping which represents the percentage of chains functionalised.

The degree of end-capping, the microstructure of the polyisoprene block and the composition of the macromonomers can be calculated using ^{1}H-NMR analysis. Table 2.2 shows the percentage of the end-capped polymer chains calculated considering the two peaks at δ 0.1 ppm and δ 0.0 ppm corresponding to [(C**H**$_3$)$_2$Si] of the silyl protection group present in both the initiator and the end-capping DPE-OSi. The table also shows the microstructure of the polyisoprene block and the weight fraction of polystyrene of the macromonomers. These data were obtained by considering the peaks representing the

hydrogen atoms on the double bond in the polyisoprene block ([$(CH_3)C=C\underline{\mathbf{H}}$], [$(CH_3)C=C\underline{\mathbf{H}}_2$] at δ 4.5-5.5 ppm) and the peaks corresponding to the aromatic hydrogens of the polystyrene blocks (δ 6.3-7.4 ppm).

Table 2.2 Data calculated by ^{1}H-NMR analysis: percentages of end-capping, content of polystyrene and 1,4-microstructure of AB_2 macromonomers.

Macromonomers	*end-capping (%)*	*1,4-PI (%)*	*PS (%)*
P(S-I-S)153_20	94	93	20
P(S-I-S)183_20	86	93	20
P(S-I-S)114_23	93	93	23
P(S-I-S)153_30	70	93	30
P(S-I-S)94_30	67	93	30
P(S-I-S)65_31	80	93	31
P(S-I-S)82_41	85	93	41

NMR spectroscopy in C_6D_6 was used to calculate the microstructure of the polyisoprene by comparing the integrals of the peaks at δ 5-5.2 and δ 4.6-4.8 ppm of the 1,4 and 3,4 polyisoprene respectively.

The peaks of the protons [$(C\underline{\mathbf{H}}_3)_2Si$] considered for the estimation of the percentage of end-capping at δ 0.1 ppm and δ 0.0 ppm should have integral values in a ratio of 2:1 (DPE-OSi:In) in order to represent a quantitatively end-capped polymer. The calculated degree of end-capping varies from a value of 67% to 94% but in most cases is in excess of 80%. A high degree of end-capping is important due to the fact that DPE-OSi is the source of the two B functionalities necessary for the coupling reactions that yield the HyperBlocks.

The results in terms of molecular weight obtained from SEC and ^{1}H-NMR analysis for the series of macromonomers synthesised are shown in the following Table 2.3.

Table 2.3 Molecular weight and dispersity of the first block PS, the diblock copolymer P(S-I) and the final macromonomer calculated by ^{1}H-NMR spectroscopy and SEC.

Macromonomers	*PS* M_n(g mol^{-1}) (a)	(b)	Đ	*P(S-I)* M_n(g mol^{-1}) (a)	(b)	Đ	*P(S-I-S)* M_n(g mol^{-1}) (a)	(b)	Đ
P(S-I-S)153_20	15000	14700	1.26	52400	136900	1.07	60300	152600	1.06
P(S-I-S)183_20	17400	20100	1.24	81500	163800	1.04	93100	183000	1.04
P(S-I-S)114_23	11700	14800	1.29	40100	99700	1.11	44400	113900	1.10
P(S-I-S)94_30	14000	14400	1.32	50200	79600	1.06	61100	93900	1.06
P(S-I-S)153_30	23100	25500	1.22	96600	131100	1.05	119200	152800	1.06
P(S-I-S)65_31	9300	8300	1.24	26800	54300	1.06	33600	64900	1.05
P(S-I-S)82_41	16000	17400	1.33	36600	64300	1.10	46300	81500	1.07

(a) Data obtained by SEC in THF using a value of dn/dc= 0.185

(b) Data obtained by ^{1}H-NMR spectroscopy in $CDCl_3$ and C_6D_6.

During the synthesis, the same amount of styrene was used for the synthesis of the two blocks so that the two blocks at the extremity of the macromonomers should have the same

length. From the data in the table we can work out the values for each block of PS and PI. Polystyrene blocks have M_n in the range of 9.3-23.1 kg·mol^{-1} for the first block (SEC data) and 10.6-21.7 kg·mol^{-1} for the second block (NMR data). Polyisoprene block has a M_n in the range 45-146.4 kg·mol^{-1} (NMR data).

In Table 2.3 we report two sets of data for the molecular weight of each polymer analysed. The molecular weights of the first column were obtained by triple detection SEC in THF using a dn/dc of 0.185 typical of polystyrene in THF (value obtained from Viscotek). This technique allowed us to have the exact molecular weight for the first PS block but not very accurate values for the PS-PI and PS-PI-PS copolymers. The parameter dn/dc represents the change in refractive index of the solution as a function of the solute concentration. In the literature it is possible to find values of dn/dc for several polymer/solvent systems. The dn/dc is dependent on the monomer, the temperature, the solvent, the wavelength of the light source and the molecular weight. For homopolymers the dependence of dn/dc on the molecular weight is small; in the case of copolymers the change in composition and the presence of more than one type of monomer affect deeply the dn/dc. The inaccuracy in the results obtained by SEC for the molecular weights using a dn/dc of 0.185 are due to the presence of the polyisoprene blocks and the change in composition of each polymer analysed.

The values of molecular weight in the second column were obtained by ^{1}H-NMR spectroscopy. It is possible to calculate the molecular weight of the first PS block by NMR spectroscopy comparing the integrals of the aromatic signals of the polystyrene block and the integral of the [C**H**$_2$OSi] signal given by the initiator. These data are quoted in table 2.3 however, the molecular weights of the subsequent P(S-I) and P(S-I-S) block copolymers were obtained instead by using the definite value of M_n of the first PS block obtained by SEC and the integrals of the peaks of the aromatic protons of the polystyrene block and the integrals of the methylene protons of the polyisoprene block. Whilst the two sets of values in Table 2.3 are in a good agreement in the case of the first block PS, they differ considerably for the diblock and triblock copolymers. However the data obtained by NMR spectroscopy is in good agreement with the target molecular weight for each block based on the amount of monomer used. A summary table (Table 2.4) of the two sets of molecular weights calculated by ^{1}H-NMR spectroscopy and predicted by using the amount of monomers added to the polymerisation for the diblock copolymer P(S-I) and the final macromonomers is given below.

Table 2.4 Molecular weight data of the intermediate diblock copolymer and the final macromonomers calculated by ^{1}H-NMR spectroscopy and by taking into account the amount of monomers used.

Macromonomers	*P(S-I)* M_n (g mol^{-1})		*P(S-I-S)* M_n (g mol^{-1})		*Target* M_n *P(S-I-S)* (g mol^{-1})
	(a)	(b)	(a)	(b)	
P(S-I-S)153_20	136900	136600	152600	152700	100000
P(S-I-S)183_20	163800	157900	183000	175600	150000
P(S-I-S)114_23	99700	105100	113900	117200	100000
P(S-I-S)94_30	79600	79300	93900	93500	150000
P(S-I-S)153_30	131100	131700	152800	153600	150000
P(S-I-S)65_31	54300	53600	64900	63400	50000
P(S-I-S)82_41	64300	64200	81500	80800	100000

(a) Data obtained by ^{1}H-NMR spectroscopy in $CDCl_3$ and C_6D_6.
(b) Theoretical values obtained by using the amount of monomers used and the molecular weight of the first PS block obtained by SEC.

Figure 2.8 shows the good agreement between these two sets of data and the discrepancy with the data obtained by SEC analysis for the molecular weights of each final macromonomer P(S-I-S).

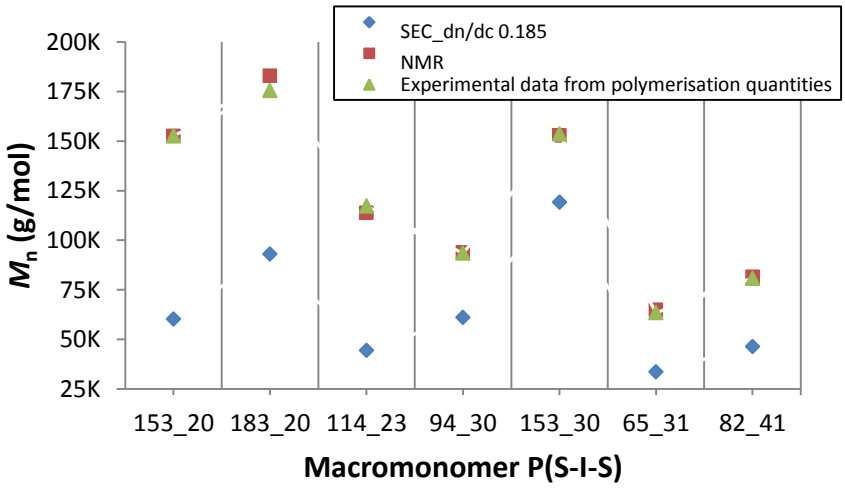

Figure 2.8 Comparison between M_n calculated in three different ways: by SEC with a dn/dc of 0.185 of polystyrene (blue line), by ^{1}H-NMR spectroscopy (red line) and by considering the amount of monomers added during the polymerisation and the molecular weight obtained by SEC of the first polystyrene block (green line).

As already observed in the previous work[1] the molecular weights calculated by ^{1}H-NMR spectroscopy are the highest values that differ substantially from the SEC data obtained by using dn/dc of 0.185. The calculation of the target molecular weight was based on the molecular weight obtained by SEC for the first block of polystyrene. This data is considered to be exact thanks to the calibration of SEC based on polystyrene standards and to the use of dn/dc of polystyrene as mentioned above and confirmed by the good agreement found with the NMR results (Table 2.3). Knowing the amount of monomer added during the living anionic polymerisation it was then possible the prediction of the molecular weight for each block.

2.3.1.2 Modification of the protected AB_2 macromonomers

The next step in the macromonomer synthesis in preparation for the subsequent HyperBlocks synthesis is the deprotection of the primary alcohol functionality and the two phenol functionalities introduced by the initiator and the end-capping agent respectively. The deprotection reaction was carried out by hydrolysis under mild acid conditions (Scheme 2.2)

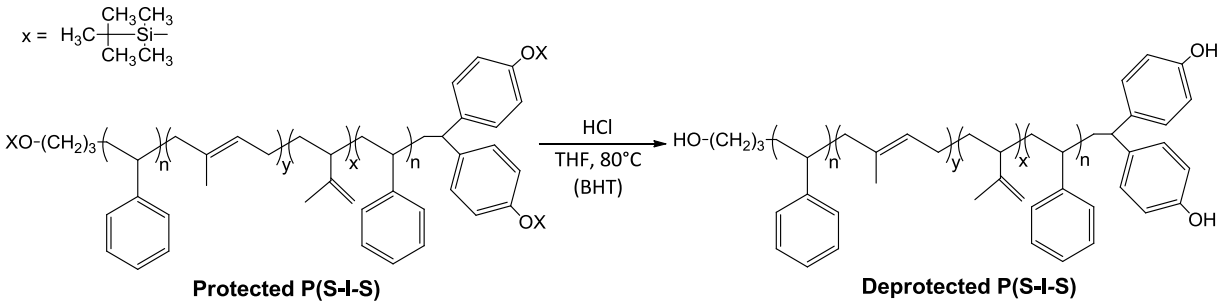

Scheme 2.2 Deprotection of the primary alcohol functionality and the two phenol functionalities at both the ends of the polymer chains of the AB_2 macromonomers.

The macromonomers were dissolved in THF and a small amount of 3,5-di-*tert*-butyl-4-hydroxytoluene (BHT) was added in order to prevent oxidative degradation and coupling of the polyisoprene blocks. However, it should be noted that BHT is a phenolic antioxidant and has to be removed completely afterwards as it can inhibit, via competition, the coupling reaction for the synthesis of the HyperBlocks. The progress of the reaction was followed by ^{1}H-NMR spectroscopy which showed the decrease of the peaks corresponding to the *tert*-butyldimethylsilyl protection groups until their complete removal. The peaks corresponding to these groups are at: 1.0 ppm [$ArOSi(CH_3)_2C(C\underline{\mathbf{H}}_3)_3$], 0.8-0.9 ppm [$CH_2OSi(CH_3)_2C(C\underline{\mathbf{H}}_3)_3$], 0.1 ppm [$ArOSi(C\underline{\mathbf{H}}_3)_2C(CH_3)_3$], 0.0 ppm [$CH_2OSi(C\underline{\mathbf{H}}_3)_2C(CH_3)_3$]. (Figure 2.9)

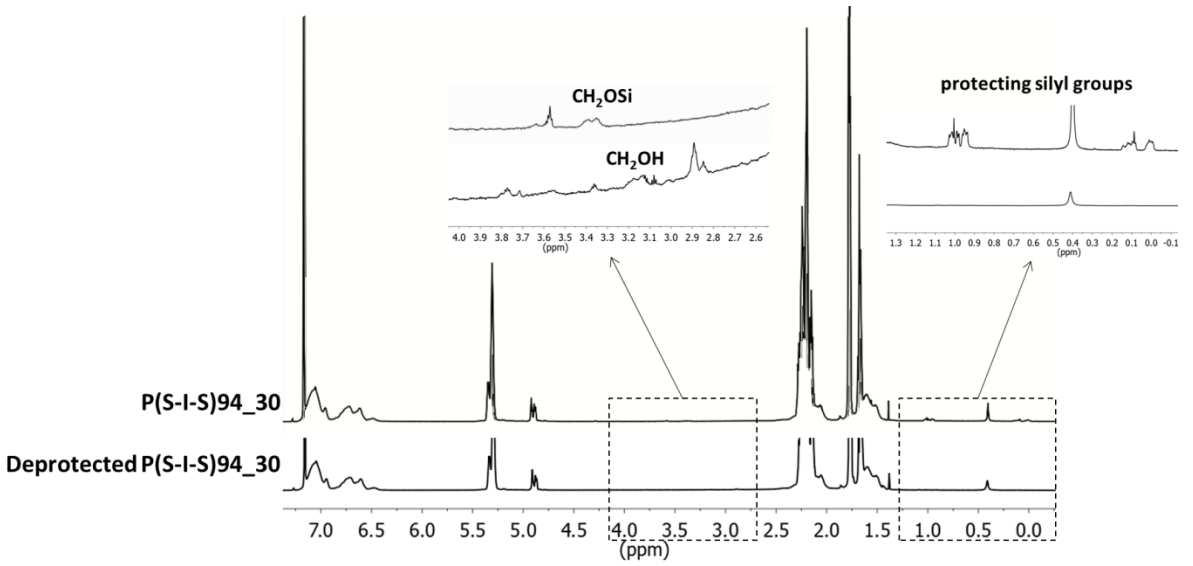

Figure 2.9 Spectra ^{1}H-NMR (700 MHz) in C_6D_6 of protected and deprotected AB_2 macromonomer P(S-I-S)94_30. Expansion of the spectra in correspondence of the main peaks of the chain end functionalities: primary alcohol and phenol functionalities protected by silyl groups.

It is also possible to observe the shift of the protons of the end group [C**H**$_2$-OSi] from δ 3.3-3.4 ppm to δ 3.15 ppm of the deprotected primary alcohol [C**H**$_2$OH] highlighting the completion of the deprotection of the alcohol groups. (Figure 2.9) At the end of the reaction the macromonomers are completely protonated and the efficiency of the reaction is excellent with yields greater than 96%.

2.3.1.2.1 Bromination of the primary alcohol for Williamson coupling reaction

In order to couple AB_2 macromonomers via a Williamson coupling reaction in the HyperBlocks synthesis it is necessary to convert the single primary alcohol group into an alkyl halide group. Bromide was chosen as the preferred alkyl halide (leaving group) based on previous investigations.[1,13] The bromination was carried out using carbon tetrabromide and triphenylphosphine (CBr_4/PPh_3) via the Appel reaction. (Scheme 2.3)

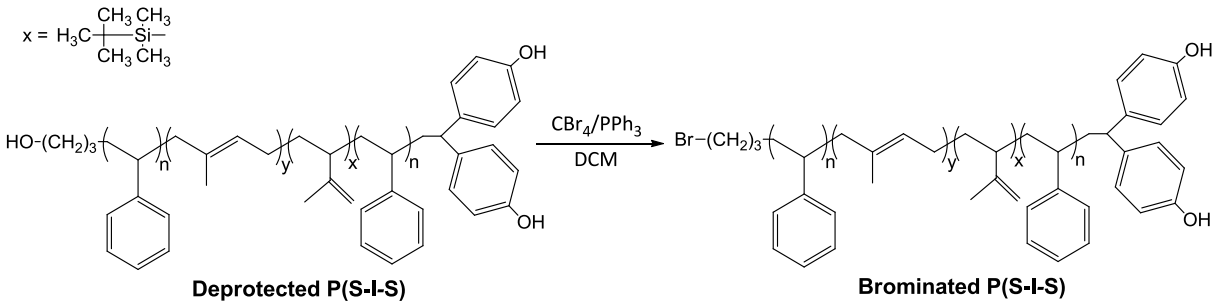

Scheme 2.3 Conversion of the primary alcohol functionality of the AB_2 macromonomer to a bromide functionality.

As for the previously described deprotection reaction, the bromination reaction was followed by ^{1}H-NMR spectroscopy where the signal of [C**H**$_2$OH] (δ 3.15 ppm) disappeared and was replaced by a new peak at δ 2.7-2.8 ppm of [C**H**$_2$Br]. (Figure 2.10)

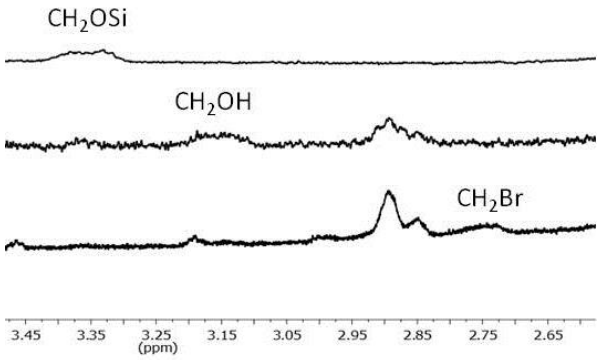

Figure 2.10 Overlay of ^{1}H-NMR spectra in C_6D_6 (700 MHz and 400 MHz) of protected, deprotected and brominated P(S-I-S)82_41. Shift of the peak of the end group functionality during the transformation from protected alcohol [C**H**$_2$OSi] to primary alcohol [C**H**$_2$OH] and finally to alkyl bromide [C**H**$_2$Br].

The signals shown in Figure 2.10 are very weak due to the high molecular weight values of the polymers that do not allow the single unit of the chain end functionality to be very visible on the spectrum. For this reason they cannot be used in a quantitative way and it results merely in a qualitative analysis.

2.3.1.2.2 Introduction of the chain end functionalities for azide-alkyne 'click' reaction

The second type of coupling reaction employed in the synthesis of HyperBlocks, the azide-alkyne 'click' reaction, requires two different chain-end functionalities in the AB_2 macromonomers. It is necessary to introduce at the polymer chain ends a single azide functionality and two alkyne functionalities by converting the bromide 'A' functionality and the two phenol 'B' functionalities. These conversions are carried out in two steps: first we carried out the conversion of the bromide into azide and subsequently we converted the phenol groups into alkyne groups as shown in Scheme 2.4.

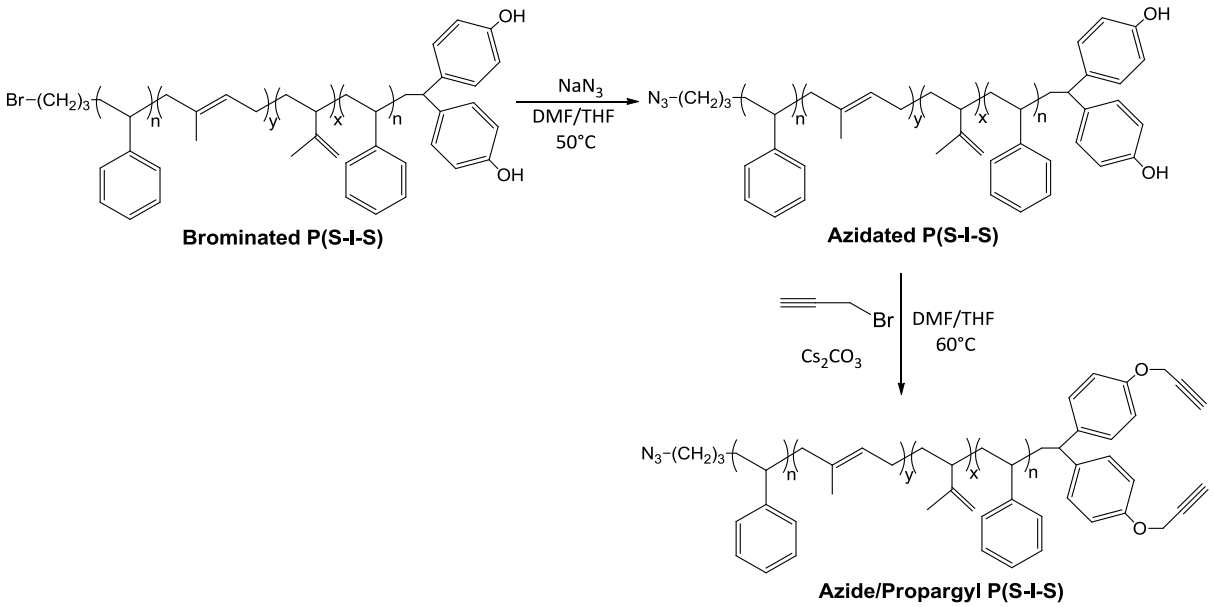

Scheme 2.4 Reaction scheme of the preparation of the macromonomer for 'click' coupling reaction: first step is the conversion of the bromide into azide, second step is the conversion of the phenol functionalities into two propargyl groups.

The order of conversion was as shown above due to the type of reaction used for the conversion of the phenol functionalities. The second reaction, being in fact a Williamson coupling reaction, would have shown a competition between the two bromide functionalities present in the mixture: namely the bromide group at the chain end of the macromonomers and the propargyl bromide. In order to avoid the formation of hyperbranched polymers during the functionalisation reaction, the bromide of the macromonomers chains needed to be converted before the conversion to propargyl groups of the phenol functionalities.

First step

The bromide functionality modification was carried out using sodium azide (NaN_3) in a solvent mixture of DMF and THF. This mixed solvent was used since DMF is an excellent solvent for carrying out the azidation step (to promote S_N2 nucleophilic substitution) and THF is required to fully solubilise the macromonomer since DMF is a non-solvent for polyisoprene. The procedure followed was developed previously in our laboratory by Kimani *et al.*[14] that converted a bromide group of an analogous end-functionalised polybutadiene synthesised by living anionic polymerisation using the same functionalised initiator as is used in this study.

The progress of the conversion reaction was checked by ^{1}H-NMR spectroscopy. The peak under observation was the peak at δ 2.7-2.8 ppm corresponding to the protons next to the

bromide functionality [C**H**$_2$Br], which decreased and eventually disappeared when the bromide was completely converted. The appearance of a new peak for the [C**H**$_2$N$_3$] group could not be observed due to the shift of the peak to lower ppm coinciding with the region (δ 2.6-1.2 ppm) where the peaks of the protons of the main chain of the macromonomer are more intense.

Second step

The conversion of the phenol functionalities into alkyne groups was carried out via a Williamson coupling reaction with propargyl bromide in the presence of cesium carbonate (Cs_2CO_3) (Scheme 2.4). The solvent used was a mixture of DMF and THF in order to favour the nucleophilic substitution reaction and the solubility of the polymers. ^{1}H-NMR spectroscopy was used to monitor the progress of the reaction as seen before for the reaction of conversion of the primary alcohol into azide. The NMR analysis showed the appearance of the peaks at δ 4.1-4.3 ppm due to the protons next to the alkyne functionalities [C**H**$_2$C≡CH]. (**Figure 2.11**)

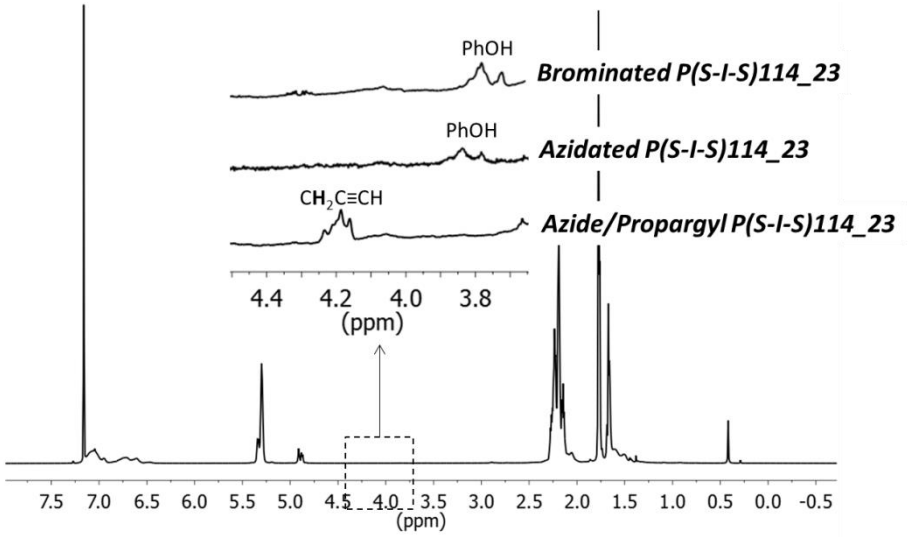

Figure 2.11 ^{1}H-NMR spectra in C_6D_6 (700 MHz) of the macromonomer P(S-I-S)114_23. Inset: comparison of the spectra in the range of δ 4.5-3.9 ppm obtained after bromination, azidation reaction and propargyl functionalisation. The peaks observed refer to the protons [PhO**H**] and [C**H**$_2$C≡CH].

As shown in Figure 2.11 the broad peak at δ 3.7-3.9 ppm corresponding to the phenolic protons [PhO**H**] is maintained after bromination and azidation reaction even if the signal is very weak and in some cases it was difficult to be observed. However after reaction with propargyl bromide, its disappearance is an additional proof of the success of the propargyl functionalisation of the polymer. The signal given by the proton of the alkyne group [C≡C**H**]

does not appear in the spectrum due to the presence of the strong peaks of the polymer chain present in the same region (δ 1.2-2.6 ppm).

2.3.2 Synthesis of HyperBlocks

After the successful synthesis of well-defined AB_2 macromonomers by living anionic polymerisation and the introduction of suitable chain-end functionalities (A and B), we carried out the synthesis of the hyperbranched polymers, HyperBlocks, by using two separate coupling mechanisms. The macromonomers were coupled by a Williamson coupling reaction and/or by copper (I) catalysed azide-alkyne 'click' reaction. These two different approaches are described and compared below for the synthesis of several HyperBlocks. Each HyperBlock has been systematically named HBa_b where HB denotes HyperBlock, *a* stands for the molecular weight of the linear macromonomer precursor calculated by ^{1}H-NMR spectroscopy and *b* stands for the weight fraction of polystyrene in the macromonomer.

2.3.2.1 HyperBlocks via Williamson coupling reaction

The AB_2 macromonomers described above carrying a single bromide 'A' functionality and two phenol 'B' functionalities allow the synthesis of HyperBlocks via a Williamson coupling reaction. Williamson coupling reaction is a nucleophilic substitution reaction between an alcohol and a halide that results in an ether linkage. (Scheme 2.5)

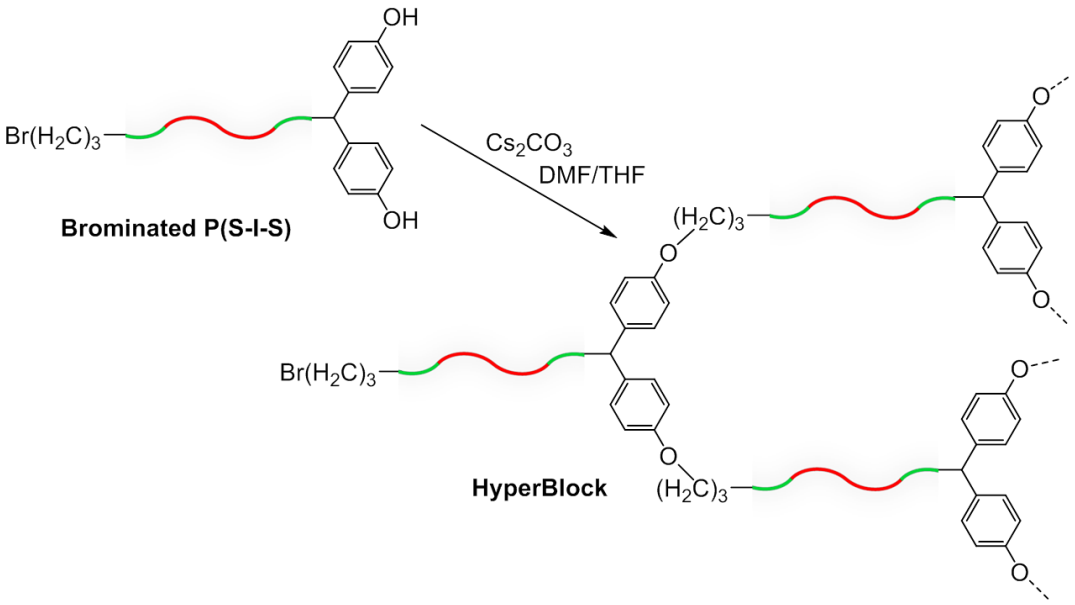

Scheme 2.5 Williamson coupling reaction for the synthesis of HyperBlocks.

The alkyl bromide at one end of the macromonomer chain acts as the leaving group and the phenol functionalities on the other chain end acts as the nucleophile in this reaction. The reaction conditions applied in this synthesis were developed in previously reported investigations[1,4,13] which optimised solvents, temperature, solution concentration, leaving group and type of base employed. The solvent mixture used was THF and DMF as used before for the azide and propargyl functionalisation of the macromonomer. The solution was 10% by wt. of macromonomer in THF/DMF (50/50 by volume). The use of a mixed solvent was employed to promote the polymer solvency by using THF and to favour the nucleophilc substitution by using DMF. Williamson coupling reactions are in fact promoted by aprotic solvents with high dielectric constants as, for instance, DMF (dieletric constant 36.7 at 25°C). Particular attention was paid to the purity of these solvents. THF was dried and degassed over Na/benzophenone and stored under vacuum; DMF was stored over molecular sieves. Purified solvents are necessary in Williamson coupling reaction in order to minimise any side reactions. The base cesium carbonate (Cs_2CO_3) was used in a molar ratio of 1:10 with respect to the macromonomer and the temperature chosen was 60°C with the exception of HB65_31 that was synthesised at 40°C for reasons explained hereafter. The progress of the coupling reaction was followed by extracting small samples periodically and subjecting them to SEC analysis as shown in Figure 2.12.

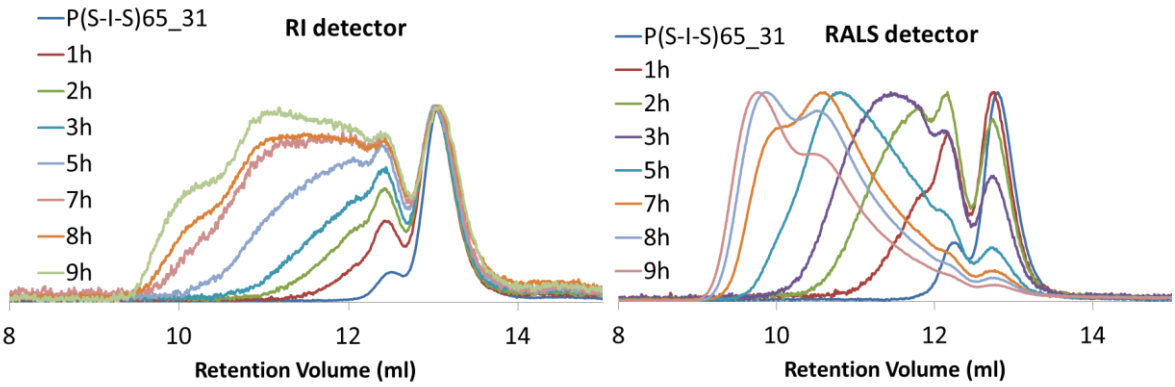

Figure 2.12 SEC chromatograms of a small scale synthesis of HyperBlock starting from the macromonomer P(S-I-S)65_31. Samples taken at different times during the reaction carried out at 40°C, 50:50 DMF/THF 10% wt/v solution.

Figure 2.12 shows typical refractive index (RI) and right-angle light scattering (RALS) SEC traces obtained for samples taken during the HyperBlock synthesis. On the right of each chromatogram it is possible to observe a sharp peak at a retention volume of about 13 ml corresponding to the macromonomer P(S-I-S)65_31. The macromonomer shows on the left a small peak (12.5 ml) due to the coupling of two macromonomer chains (dimer) during the termination step of the living anionic polymerisation due to the presence of impurities. Observing the RI response it can be seen that the peak representing the dimer (two coupled macromonomer chains) is already present after the first hour of reaction and the extent of coupling continues to increase in each sample taken during the reaction time. That part of the distribution emerging at lower elution volumes (9.5-12.0 ml) on the left of the macromonomer peak (13 ml) represents the formation of the hyperbranched polymer HyperBlock. The peak of the macromonomer is present in each chromatogram and indicates that there is still uncoupled macromonomers in the reaction mixture. The presence of unreacted macromonomer could be explained in part by the presence of macromonomer which has not undergone successful end-capping with DPE-OSi although even in this case macromonomer could still be incorporated into growing HyperBlocks through the bromide group. However in previous similar studies carried out both in our labs and others[15], residual, unreacted macromonomer is always observed. The coupling reaction of P(S-I-S)65_31 was carried out at 40°C instead of 60°C in order to slow down the rate of reaction. It was found that when this macromonomer was coupled at 60°C the rate of coupling was of such high efficiency that in few hours (4 h) the coupling reaction produced very high molecular weight, highly branched polymers. As a result the resulting Hyperblock was no longer completely soluble in solvent like THF in which it looked like a swollen gel due to the

high molecular weight chains produced during the coupling. We do not believe that the polymer is crosslinked since there is not mechanism to promote crosslinking through the coupling of an AB_2 macromonomer even if the presence of side reactions and impurities that bring to crosslinked materials is still possible. Moreover we believe that the polymer has a very high molecular weight – probably with some fraction of the polymer having a molecular weight of many millions $g \cdot mol^{-1}$. This observation has been made before during the synthesis of polystyrene HyperMacs.[2]

A series of HyperBlocks have been synthesised with the following results. (Table 2.5)

Table 2.5 Data for the HyperBlocks synthesised by Williamson coupling reaction. Molecular weights calculated by SEC using dn/dc of polystyrene in THF (0.185).

Macromonomer	***HyperBlocks***	M_n **(g·mol^{-1})**	DP_n	M_w **(g·mol^{-1})**	DP_w	**Đ**
P(S-I-S)65_31	HB65_31	220600	6.6	826400	23.3	3.75
	HB65_31	218200	6.5	959000	27.1	4.40
P(S-I-S)82_41	HB82_41[(a)]	390100	8.4	807700	16.3	2.07
	HB82_41[(a)]	354500	7.7	664800	13.4	1.88
P(S-I-S)183_20	HB183_20	216500	2.3	791900	8.2	3.66
P(S-I-S)94_30	HB94_30[(a)]	344200	5.6	637300	9.8	1.85
	HB94_30[(a)]	384700	6.3	709600	10.9	1.84
P(S-I-S)153_30	HB153_30	453500	3.8	1007000	8.0	2.22

(a) Data from SEC analysis in THF at a flow rate of 0.75 ml/min.

The HyperBlocks produced in this work proved to be polydisperse in terms of both molecular weight and architecture – as expected. Each HyperBlock is characterised by a value of Dp_n and Dp_w that are used to describe the extent of the coupling reaction. Dp is the degree of macromonomer polymerisation and it represents the number of macromonomers reacted and coupled together to form the HyperBlocks. Dp_n and Dp_w are the number-average and weight-average degree of polymerisation respectively and they are calculated as reported below:

$$Dp_n = \frac{M_n \text{ (HyperBlock)}}{M_n \text{ (Macromonomer)}} \qquad Dp_w = \frac{M_w \text{ (HyperBlock)}}{M_w \text{ (Macromonomer)}}$$

Each coupling reaction was carried out twice on a similar scale to establish reproducibility of the reaction and in order to avoid the loss of the entire amount of material in case of oxidative degradation of the macromonomer during the reaction caused by the accidental presence of oxygen in the reaction vessel. The two reactions yielded very similar HyperBlocks which have subsequently been solution blended together to form a single

sample of HyperBlock. In some cases only half of the batch of macromonomer has been coupled via a Wlliamson coupling reaction and hence only one set of molecular weight data is presented in Table 2.5. In these cases the other half of the batch of macromonomer has been converted to HyperBlocks via the second type of coupling reaction, the azide-alkyne 'click' reaction, which will be described later in this chapter.

Where two (identical) coupling reactions have been carried out on the same macromonomer, the reproducibility of the results obtained can be better observed in the diagram below (Figure 2.13) where the degree of polymerisation Dp_n and Dp_w have been plotted and compared for each Williamson coupling reaction.

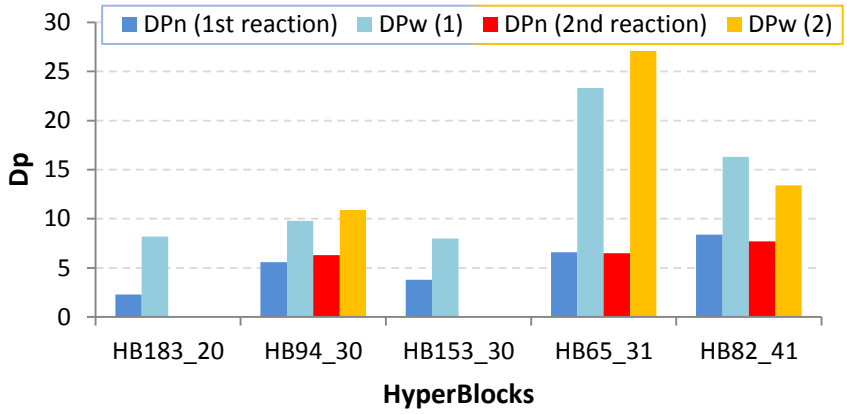

Figure 2.13 Diagram of degree of polymerisation Dp_n and Dp_w of HyperBlocks synthesised by Williamson coupling reaction.

In the case of HyperBlocks HB94_30, HB65_31 and HB82_41 both the reactions gave similar results in terms of molecular weight and dispersity. This allowed us to blend the two batch of HyperBlocks together in order to obtain a reasonably amount of material to be used for further characterisations.

A further observation that can be made when considering all of the results of coupling reactions with the different macromonomers, is that the highest degree of coupling were obtained for HB65_31, i.e. the coupling of the macromonomer P(S-I-S)65_31. The degree of polymerisation (Dp_n 6.6-6.5 and Dp_w 23.3-27.1) and the dispersity (3.75-4.40) are higher than the ones obtained in the coupling of the other macromonomers. It is also noteworthy that although the synthesis of HyperBlock HB65_31, proved to give the highest extent of coupling in the current study, this result is not quite as good as the HyperBlock obtained in the previous work[1]. In optimising the best conditions for the coupling reaction, Hutchings *et al*. obtained a sample of HyperBlock with Dp_n 10.5 and Dp_w 31.8 from a small scale reaction (1-2 g). We also obtained a similar result in the current work for HB65_31 when the coupling

was carried out on a small scale (2 g) at 60 °C (DP_n 10.3 and Dp_w 29.6). However, when the reaction was stopped the polymer resembled a gel which showed very limited solubility as already mentioned. For this reason we tried to modify the reaction conditions in order to obtain a soluble polymer and be able to stop the reaction at a lower degree of coupling. The temperature was decreased to 40°C to slow down the reaction rate enabling reaction to be stopped before the formation of insoluble products.

It can be seen from Figure 2.13 and Table 2.5 that the degree of polymerisation (extent of macromonomer coupling) decreases in this order: HB65_31> HB82_41 > HB94_30 > HB153_30 ≈ HB183_20 – a trend which coincides with an increase in the molecular weight of the linear precursor of each HyperBlock. Therefore a possible explanation for the decrease in the extent of coupling reaction may be the increase in molecular weight of the coupled macromonomer. There may be two factors which support this hypothesis. Firstly, the higher molecular weight macromonomers will tend to increase the viscosity of the reaction solution, resulting in a reduction of chain mobility and less efficient stirring/poorer mixing could be responsible for the lower degree of polymerisation. In addition the concentration of the reactive groups A and B of the macromonomers in the reaction mixture decreases with the increase in molecular weight which results in a lower rate of reaction.

Furthermore, the extent of coupling observed in the present study are not so very different to the previously report data which was carried out on a macromonomer with a molecular weight M_n of 64.1 kg mol^{-1} (NMR data), very close to the value of HB65_31 but with a different content of polystyrene (40% in comparison with 31% of HB65_31). The coupling reaction in both cases gave similar degree of polymerisation as mention above even if with HB65_31 we met problems with the solubility of the resulting hyperbranched polymer.

The scaling up of the coupling reaction appeared to create a further problem in the synthesis of HyperBlocks in common with the previous work in which it was observed that scaling up (20 g) the coupling of the macromonomer resulted in a lower degree of coupling. The previously synthesised HyperBlock had a Dp_n of 6.7 and a Dp_w of 16.5 when produced on a 20 g scale cf. Dp_n of 10.5 and a Dp_w of 31.8 when coupled on a 2 g scale. In the present study this problem was minimised by carrying out reactions using a maximum of 15 g of macromonomer. This scale allowed us to maintain a similar degree of polymerisation as that obtained in the small scale reactions carried out as trial reactions.

The success of the coupling reaction can also be influenced by the extent of the end-capping reaction carried out on each macromonomers. A high degree of end-capping ensures a high concentration of AB_2 macromonomer chains with the two phenol (B) groups and the bromide (A) functionality available for the formation of HyperBlocks. A lower percentage of end capped polymer chains results in a higher concentration of macromonomers in which the B groups are absent which will undoubtedly result in the production of HyperBlocks with low degree of polymerisation.

Finally, as is now obvious, the coupling reactions are characterised by a significant increase in molecular weight of the product and as a consequence the solubility of the samples taken during the reaction time decreases considerably. This makes the preparation of samples for SEC analysis more difficult due to the need for longer time for solubilisation of the samples. Therefore the time required for the analysis did not always allow us to stop the reaction at the same optimal degree of polymerisation and prior to formation of insoluble gel as reported above for the small scale reaction.

2.3.2.2 HyperBlocks via azide-alkyne ‘click’ reaction

The azide-alkyne ‘click’ reaction was the second type of coupling reaction investigated in this work for the synthesis of HyperBlocks. In this type of coupling the macromonomers are joined together by an addition reaction (Scheme 2.6) between the azide functionality and the alkyne functionality introduced at the chain ends during the macromonomer preparation. The reaction leads to the formation of a 1,2,3-triazole linkage that replaces the ether linkage formed in a Williamson coupling reaction.

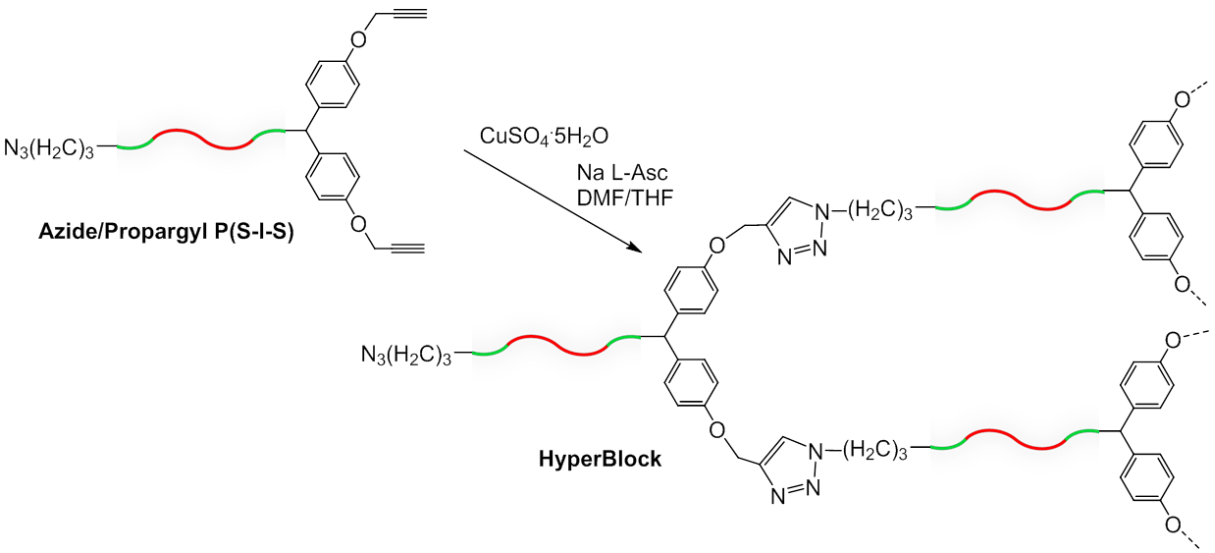

Scheme 2.6 Azide-alkyne 'click' reaction for the synthesis of HyperBlocks.

The macromonomer was dissolved in a mixture of THF and DMF (50/50 ratio) and in the presence of copper(II) sulfphate pentahydrate ($CuSO_4 \cdot 5H_2O$) as the catalyst and sodium ascorbate (Na L-Asc) as the *in situ* reducing agent needed to generate the copper Cu(I).[14] These two compounds were added in few drops of water which corresponded to ca. 0.8% of the solvent mixture. As for the Williamson coupling reaction, the progress of the reaction was followed by sampling the reaction and characterising the samples by SEC.

The HyperBlocks synthesised by 'click' coupling reaction are listed in the following table.

Table 2.6 Data for the HyperBlocks synthesised by azide-alkyne 'click' reaction.

Macromonomer	*HyperBlocks*	M_n (g·mol^{-1})	DP_n	M_w (g·mol^{-1})	DP_w	Đ
P(S-I-S)153_20	HB153_20	299900	5.0	743800	11.7	2.48
	HB153_20	261600	4.3	677800	10.6	2.59
P(S-I-S)114_23	HB114_23	256500	5.8	562200	11.5	2.19
	HB114_23	142800	3.2	593600	12.2	4.15
P(S-I-S)183_20	HB183_20	320600	3.4	497400	5.1	1.55
P(S-I-S)153_30	HB153_30[(a)]	455300	3.8	661800	5.3	1.45

(a) Data from SEC analysis in THF at a flow rate of 0.75 ml/min.

As observed in the case of the synthesis by Williamson coupling reaction, where two identical coupling reactions were carried out (for both HB153_20 and HB114_23) the results were rather similar results, as shown in both Table 2.6 and Figure 2.14 below.

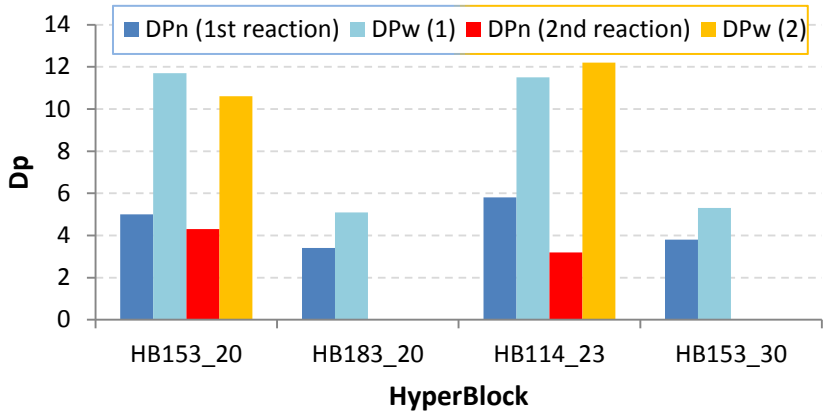

Figure 2.14 Diagram of degree of polymerisation Dp_n and Dp_w of HyperBlocks synthesised by azide-alkyne 'click' coupling reaction.

In common with the Williamson coupling reaction, 'click' coupling reaction gave good results for relatively low molecular weight macromonomers, as shown by the higher degrees of polymerisation obtained for HB114_23 and HB153_20 in comparison with HB183_20. The reason of the low Dp obtained for HB153_30 is not clear. The molecular weight of the linear precursor was the same of HB153_20 and the only differences were the content in polystyrene (20% and 30% respectively) and the end-capping percentage (94% and 70% respectively). Therefore an explanation for the difference in Dp between HB153_20 and HB153_30 is likely to be the lower degree of end-capping of the macromonomer for HB153_30.

Similar observations about the likely efficiency of 'click' coupling reactions can be made as were made for Williamson coupling reactions. The solubility, macromonomer molecular weight, concentration of reactive groups A and B, reaction scale and macromonomer end-capping all influence the extent of the coupling reaction.

2.3.2.3 HyperBlocks: comparison between Williamson and 'click' coupling reaction

The synthesis of HyperBlocks was carried out utilising two different strategies, as described above, the Williamson coupling reaction and the azide-alkyne 'click' coupling reaction. The majority of the HyperBlocks were synthesised by Williamson coupling reaction that, thanks to the optimisations achieved in the previous work, proved to be a very efficient route. HB65_31, HB82_41 and HB94_30 showed relatively high values for the degree of polymerisation (extent of coupling) however the coupling reactions showed decreasing effectiveness with increasing molecular weight of the macromonomer. In order to obtain

polymers with higher degrees of branching from higher molecular weight macromonomers, we investigated the widely used azide-alkyne 'click' reaction. This route for the coupling of macromonomers had been already employed with good efficiency for the synthesis of asymmetric three-arm stars (Chapter 4). The 'click' coupling reaction for star polymer synthesis appeared to be more efficient and reproducible than Williamson coupling reaction and the popularity of using 'click' coupling reactions in the wider literature for the synthesis of branched polymers[16] convinced us to investigate this route also for the synthesis of HyperBlocks.

P(S-I-S)153_20 and P(S-I-S)114_23 were coupled on a large scale by 'click' coupling reaction only and the results were comparable to analogous reactions carried out using Williamson coupling reactions of low molecular weight macromonomers (Table 2.5 and Table 2.6). Macromonomers P(S-I-S)183_20 and P(S-I-S)153_30 were the only macromonomers coupled on a large scale by both the two strategies. Table 2.7 compares the two HyperBlocks obtained in the two different coupling reactions.

Table 2.7 Comparison of molecular weight, dispersity and degree of polymerisation of HyperBlocks synthesised by Williamson and 'click' coupling reactions.

Macromonomer	*HyperBlocks*	M_n (g·mol^{-1})	DP_n	M_w (g·mol^{-1})	DP_w	Đ
P(S-I-S)183_20	HB183_20[(b)]	216500	2.3	791900	8.2	3.66
	HB183_20[(c)]	320600	3.4	497400	5.1	1.55
P(S-I-S)153_30	HB153_30[(b)]	453500	3.8	1007000	8.0	2.22
	HB153_30[(a)(c)]	455300	3.8	661800	5.3	1.45

(a) Data from SEC analysis in THF at a flow rate of 0.75 ml/min.
(b) HyperBlocks synthesised by Williamson coupling reaction.
(c) HyperBlocks synthesised by azide-alkyne 'click' reaction.

The degree of polymerisation and the dispersity show slightly better results for the HyperBlock synthesised by Williamson coupling reaction. For both the two types of coupling, in an attempt to obtain a higher extent of reaction, the macromonomers were allowed to react for a long time (between 20 and 40 hours) but it did not influence the results. Further addition of catalyst in the case of 'click' reaction did not lead to any improvements in the extent of the reaction as was seen for the synthesis of star polymers described in Chapter 4.

A series of six HyperBlocks was finally prepared by blending together the polymers obtained in both the two reactions carried out for each macromonomer: Williamson coupling reaction and/or azide-alkyne 'click' reaction. In Table 2.8 we report the molecular weight, degree of

polymerisation and dispersity data for each single HyperBlock obtained after blending of the various batches.

Table 2.8 Data for the final HyperBlocks analysed by SEC analysis by using the dn/dc of the polystyrene in THF.

Macromonomer	***HyperBlocks***	M_n (g·mol^{-1})	DP_n	M_w (g·mol^{-1})	DP_w	Đ
P(S-I-S)183_20	HB183_20	269600	2.9	779700	8.1	2.89
P(S-I-S)114_23	HB114_23	144300	3.3	590000	12.1	4.09
P(S-I-S)94_30	HB94_30	329700	5.4	757800	11.7	2.30
P(S-I-S)153_30	HB153_30	398500	3.3	992100	7.9	2.49
P(S-I-S)65_31	HB65_31	156400	4.7	870700	24.6	5.57
P(S-I-S)82_41	HB82_41	308300	6.7	808500	16.3	2.62

These HyperBlocks were further analysed in terms of solid state morphology, thermal and mechanical properties.

2.4 Experimental

2.4.1 Materials

Benzene (Aldrich, HPLC grade, ≥ 99%), styrene (Sigma-Aldrich, ≥ 99%), isoprene (Sigma-Aldrich), dichloromethane (in-house purification) were all dried and degassed over calcium hydride (CaH_2) (Acros Organics, 93%) and stored under high vacuum. 3-*tert*-butyldimethylsiloxy-1-propyllithium in cyclohexane (InitiaLi 103, FMC Corporation), triphenylphosphine (Sigma-Aldrich) and carbon tetrabromide (Sigma-Aldrich, 99%), cesium carbonate (Sigma-Aldrich), sodium azide (Sigma-Aldrich ≥ 99.5%), copper(II) sulphate pentahydrate ($CuSO_4 \cdot 5H_2O$) (Sigma-Aldrich), (+)-sodium L-ascorbate (Sigma-Aldrich), 3,5-di-*tert*-butyl-4-hydroxytoluene (BHT) (Sigma-Aldrich) and N,N,N'N'-tetramethylethylenediamine were used as received. Dimethyl formamide (DMF) (Sigma-Aldrich 99.8%) was stored over molecular sieves 3Å (Sigma-Aldrich) under an inert atmosphere. Di-*n*-butylmagnesium (Sigma-Aldrich) 1.0M solution in heptanes, *n*-butyllithium (Sigma-Aldrich) 2.0M solution in pentane and *sec*-butyllithium (Sigma-Aldrich) 1.4M solution in cyclohexane, were used as received. Propargyl bromide (Sigma-Aldrich) 80 wt. % solution in toluene was used as received. Tetrahydrofuran (THF), methanol (AR grade) and hydrochloric acid (~36 wt. %) (all Fischer Scientific) were used as received. Tetrahydrofuran (Fisher Scientific, AR grade) was also dried and degassed over Na benzophenone and stored under high vacuum as for diethyl ether (Fisher Scientific, AR grade). 1,1-Bis(4-*tert*-butyldimethylsiloxyphenyl)ethylene (DPE-OSi) was synthesised in two steps from dihydroxybenzophenone according to the procedure of Quirk and Wang.[17]

2.4.2 Synthesis of Poly(styrene-isoprene) diblock copolymers

The following reactions involving living anionic polymerisation were all carried out using a specially designed reaction vessel colloquially known as a "christmas tree" (Figure 2.15)

Figure 2.15 Living anionic polymerisation reaction vessel called 'christmas tree'.

This vessel allows polymerisations to be carried out under high vacuum conditions in the total absence of impurities.

2.4.2.1 Synthesis of P(S-I)60 in the presence of THF

Benzene (50 ml) and styrene (2.43 g, 23.33 mmol) were distilled under vacuum into the 250 ml reaction flask of the christmas tree. To the monomer solution was injected through a septum, tetrahydrofuran (THF) (132 µl, 1.63 mmol) in a molar ratio of 5:1 with respect to the initiator. The solution was titrated with *sec*-butyl lithium until a persistent pale yellow colour was achieved. After that the initiator 3-*tert*-butyldimethylsiloxy-1-propyllithium 0.55 M in cyclohexane (590 µl, 0.324 mmol) was injected into the flask. The reaction was stirred at room temperature for 1 hour and 10 minutes. A small sample of polymer solution was removed and collected in a side arm of the reactor and terminated with nitrogen-sparged methanol. The sample was analysed by NMR spectroscopy and SEC.

At this point the solvent (benzene and THF) was distilled out of the flask and replaced with fresh, dry benzene (100 ml), the living polymer was redissolved before the solvent was distilled out again. This process was repeated a further two times to ensure the complete elimination of the THF from the reaction. After the addition of fresh benzene (100 ml) distilled under vacuum, isoprene (11.09 g, 0.163 mol) was added and the reaction was stirred at room temperature for 3 days.

The reaction was terminated with nitrogen-sparged methanol. The polymer was precipitated into methanol, redissolved in THF, precipitated again into methanol and then dried under vacuum. The polymer was characterised by ^{1}H-NMR spectroscopy and SEC. Yield >97%.

PS block M_n= 10500 g mol^{-1}, M_w= 12000 g mol^{-1}, Đ= 1.14

P(S-I) block M_n= 34300 g mol^{-1}, M_w= 35600 g mol^{-1}, Đ= 1.04

^{1}H-NMR ($CDCl_3$, δ in ppm): 3.4-3.5 [C**H**$_2$OSi], 1.0 [Si(CH$_3$)$_2$C(C**H**$_3$)$_3$], 0.0 [CH$_2$OSi(C**H**$_3$)$_2$C(CH$_3$)$_3$].

2.4.2.2 Synthesis of P(S-I)36 in the presence of TMEDA

P(S-I)36 was prepared following the same method as described above in section 2.4.2.1 except that *N,N,N',N'*-tetramethylethylenediamine (202 µl, 1.35 mmol) in a molar ratio of 5:1 respect to the initiator was added (instead of THF) to the mixture of benzene (50 ml) and styrene (2.02 g, 19.40 mmol). The other reagents were: initiator 3-*tert*-butyldimethylsiloxy-1-propyllithium in 0.55 M cyclohexane (490 µl, 0.270 mmol) and isoprene (9.54 g, 0.140 mol).

The polymer was characterised by ^{1}H-NMR spectroscopy and SEC. Yield >97%.

P(S-I) block M_n= 25700 g mol^{-1}, M_w= 26400 g mol^{-1}, Đ=1.03

^{1}H-NMR ($CDCl_3$, δ in ppm): 3.4-3.5 [C**H**$_2$OSi], 1.0 [Si(CH$_3$)$_2$C(C**H**$_3$)$_3$], 0.0 [CH$_2$OSi(C**H**$_3$)$_2$C(CH$_3$)$_3$].

2.4.2.3 Synthesis of P(S-I)180 in the presence of Et_2O

P(S-I)180 was prepared following the same method as described above in section 2.4.2.1 except that diethyl ether (150 µl, 1.43 mmol) in a molar ratio of 5:1 with respect to the initiator was added (instead of THF) to a mixture of benzene (50 ml) and styrene (2.14 g, 20.55 mmol). The other reagents were: initiator 3-*tert*-butyldimethylsiloxy-1-propyllithium in 0.55 M cyclohexane (519 µl, 0.285 mmol) and isoprene (10.7 g, 0.157 mol). The polymer has been characterised by ^{1}H-NMR spectroscopy and SEC. Yield > 97%.

PS block M_n= 30900 g mol^{-1}, M_w= 39300 g mol^{-1}, Đ= 1.27

P(S-I) block M_n= 39200 g mol^{-1}, M_w= 43600 g mol^{-1}, Đ= 1.11

^{1}H-NMR ($CDCl_3$, δ in ppm): 3.4-3.5 [C**H**$_2$OSi], 1.0 [Si(CH$_3$)$_2$C(C**H**$_3$)$_3$], 0.0 [CH$_2$OSi(C**H**$_3$)$_2$C(CH$_3$)$_3$].

2.4.3 Synthesis of Poly(styrene-isoprene-styrene) triblock AB_2 Macromonomers

2.4.3.1 Synthesis of P(S-I-S)59_33 in the presence of THF

Benzene (75 ml) and styrene (7.74 g, 74.32 mmol) were distilled under vacuum into the 1L reaction flask of a christmas tree. Styrene was further purified by the addition of di-*n*-butylmagnesium (0.5 ml) to destroy any remaining protic impurities before distilling it into the christmas tree. To the monomer solution was added tetrahydrofuran (THF) in a molar ratio of 5:1 with respect to the initiator (420 µl, 5.18 mmol). The initiator, 3-*tert*-butyldimethylsiloxy-1-propyllithium in 0.55 M cyclohexane (1.9 ml, 1.045 mmol) was injected through a septum into the flask. The reaction was stirred at room temperature for 1 hour and 10 minutes. A small sample of polymer solution was removed and collected in a side arm of the reactor and was terminated with nitrogen-sparged methanol. The sample was analysed by ^{1}H-NMR spectroscopy and SEC.

At this point benzene and THF were removed as described above to ensure the complete elimination of the THF from the reaction flask. After the addition of fresh benzene (300 ml) by distillation under vacuum, isoprene (36.2 g, 0.531 mol) was added and the reaction was stirred at room temperature for 3 days to ensure complete conversion. Isoprene was further purified before addition to the flask by the addition of *n*-butyllithium (50 µl) to eliminate any remaining impurities.

After complete conversion of the isoprene, a sample of the polymer solution was collected for ^{1}H-NMR and SEC analysis, as previously described. To the polymer solution was then injected TMEDA (0.155 ml, 1.03 mmol) through a septum in a molar ratio of (1:1) with respect to the initiator, followed by styrene (7.99 g, 76.72 mmol), which had been further purified by the addition of di-*n*-butylmagnesium (0.5 ml). The styrene was distilled under vacuum into the christmas tree and the reaction was stirred at room temperature for 3 hours. To the solution was then added 1,1-*bis*(4-*tert*-butyldimethylsiloxyphenyl)ethylene (DPE-OSi) (0.6880 g, 1.56 mmol) as a solution in benzene in a molar ratio of (1.5:1) with respect to the initiator. Before the injection, the desired amount of DPE-OSi was weighed into a flask which was sealed and evacuated. Benzene was distilled in under vacuum and removed to azeotropically dry the DPE-OSi before the DPE-OSi was redissolved in benzene.

To this was added TMEDA (0.155 ml, 1.03 mmol) and the mixture titrated (to remove impurities) with *sec*-butyllithium until a faint but persistent red colour was seen. Following addition of DPE-OSi to the living polymer, the end capping reaction was stirred at room temperature for 5 days and then terminated with nitrogen-sparged methanol. The polymer was precipitated into methanol, redissolved in THF, precipitated again into methanol and then dried under vacuum. The polymer has been characterised by ^{1}H-NMR spectroscopy and SEC. Yield > 97%.

PS block M_n= 7700 g mol^{-1}, M_w= 8700 g mol^{-1}, Đ=1.13

P(S-I) block M_n= 45100 g mol^{-1}, M_w= 46700 g mol^{-1}, Đ=1.04

P(S-I-S) block M_n= 56100 g mol^{-1}, M_w= 58000 g mol^{-1}, Đ=1.04

^{1}H-NMR ($CDCl_3$, δ in ppm): 3.4-3.5 [C**H**$_2$OSi], 3.5 [**H**C(Ph)$_2$], 1.0 [Si(CH$_3$)$_2$C(C**H**$_3$)$_3$], 0.1 [ArOSi(C**H**$_3$)$_2$C(CH$_3$)$_3$], 0.0 [CH$_2$OSi(C**H**$_3$)$_2$C(CH$_3$)$_3$].

2.4.3.2 Synthesis of P(S-I-S) without additives

All the macromonomers were synthesised by the following procedure. The amount of initiator and monomers used were varied in order to obtain a series of macromonomers differing in molecular weight and polystyrene content.

2.4.3.2.1 Synthesis of P(S-I-S)65_31

AB_2 P(S-I-S)65_31 was prepared following the same method as described above in 2.4.3.1 but without the addition of THF in the first step. The solution was made of benzene (500 ml) and styrene (7.45 g, 71.53 mmol). The initiator 3-*tert*-butyldimethylsiloxy-1-propyllithium in 0.55 M cyclohexane (1.8 ml, 0.99 mmol) was injected. The reaction was stirred overnight and then a sample was collected for analysis. Isoprene (35.47 g, 0.52 mol) was added and the reaction was stirred at room temperature for 3 days. The second sample was taken and TMEDA (0.150 ml, 1 mmol) was injected. Then styrene (7.87 g, 75.56 mmol) was added and left to react for 3 hours.

Finally 1,1-*bis*(4-*tert*-butyldimethylsiloxyphenyl)ethylene (DPE-OSi) (0.88 g, 1.99 mmol) was added to the solution. The reaction was stirred at room temperature for 5 days. Yield >97%.

PS block M_n= 9300 g mol^{-1}, M_w= 11600 g mol^{-1}, Đ=1.24

P(S-I) block M_n= 26800 g mol^{-1}, M_w= 28400 g mol^{-1}, Đ=1.05

P(S-I-S) block M_n= 33600 g mol^{-1}, M_w= 35400 g mol^{-1}, Đ=1.05

^{1}H-NMR (C_6D_6, δ in ppm): 3.4-3.5 [C**H**$_2$OSi], 3.5 [**H**C(Ph)$_2$], 1.0 [Si(CH$_3$)$_2$C(C**H**$_3$)$_3$], 0.1 [ArOSi(C**H**$_3$)$_2$C(CH$_3$)$_3$], 0.0 [CH$_2$OSi(C**H**$_3$)$_2$C(CH$_3$)$_3$].

2.4.3.2.2 Synthesis of P(S-I-S)82_41

AB_2 P(S-I-S)82_41 was prepared following the same method as described above in 2.4.3.2.1. The solution was of benzene (500 ml) and styrene (11.13 g, 106.87 mmol). The initiator 3-*tert*-butyldimethylsiloxy-1-propyllithium in 0.55 M cyclohexane (2 ml, 1.1 mmol) was injected. The reaction was stirred overnight and then a sample was removed for analysis. Isoprene (33.54 g, 0.492 mol) was added and the reaction was stirred at room temperature for 3 days. The second sample was taken before TMEDA (0.0835 ml, 0.557 mmol) was injected. The styrene (11.56 g, 110.99 mmol) was added and left to react for 3 hours.

Finally 1,1-*bis*(4-*tert*-butyldimethylsiloxyphenyl)ethylene (DPE-OSi) (0.50 g, 1.14 mmol) was added to the solution. The reaction was stirred at room temperature for 5 days. Yield >97%.

PS block M_n= 16000 g mol^{-1}, M_w= 21300 g mol^{-1}, Đ=1.33

P(S-I) block M_n= 36600 g mol^{-1}, M_w= 40100 g mol^{-1}, Đ=1.10

P(S-I-S) block M_n= 46300 g mol^{-1}, M_w= 49700 g mol^{-1}, Đ=1.07

^{1}H-NMR ($CDCl_3$, δ in ppm): 3.4-3.5 [C**H**$_2$OSi], 3.5 [**H**C(Ph)$_2$], 1.0 [Si(CH$_3$)$_2$C(C**H**$_3$)$_3$], 0.1 [ArOSi(C**H**$_3$)$_2$C(CH$_3$)$_3$], 0.0 [CH$_2$OSi(C**H**$_3$)$_2$C(CH$_3$)$_3$].

2.4.3.2.3 Synthesis of P(S-I-S)153_20

AB_2 P(S-I-S)153_20 was prepared following the same method as described above in 2.4.3.2.1. The solution was of benzene (500 ml) and styrene (5.26 g, 50.50 mmol). The initiator 3-*tert*-butyldimethylsiloxy-1-propyllithium in 0.4 M cyclohexane (1.4 ml, 0.56 mmol) was injected. The reaction was stirred overnight and then a sample was removed for analysis. Isoprene (42.63 g, 0.626 mol) was added and the reaction was stirred at room temperature for 3 days. The second sample was taken before TMEDA (0.079 ml, 0.527 mmol) was injected. The styrene (5.63 g, 54.06 mmol) was added and left to react for 3 hours.

Finally 1,1-*bis*(4-*tert*-butyldimethylsiloxyphenyl)ethylene (DPE-OSi) (0.47 g, 1.07 mmol) was added to the solution. The reaction was stirred at room temperature for 5 days. Yield >97%.

PS block M_n= 15000 g mol^{-1}, M_w= 18800 g mol^{-1}, Đ=1.26

P(S-I) block M_n= 52400 g mol^{-1}, M_w= 56300 g mol^{-1}, Đ=1.07

P(S-I-S) block M_n= 60300 g mol^{-1}, M_w= 63700 g mol^{-1}, Đ=1.06

^{1}H-NMR ($CDCl_3$, δ in ppm): 3.4-3.5 [C**H**$_2$OSi], 3.5 [**H**C(Ph)$_2$], 1.0 [Si(CH$_3$)$_2$C(C**H**$_3$)$_3$], 0.1 [ArOSi(C**H**$_3$)$_2$C(CH$_3$)$_3$], 0.0 [CH$_2$OSi(C**H**$_3$)$_2$C(CH$_3$)$_3$].

2.4.3.2.4 Synthesis of P(S-I-S)183_20

AB_2 P(S-I-S)183_20 was prepared following the same method as described above in 2.4.3.2.1. The solution was of benzene (500 ml) and styrene (5.33 g, 51.18 mmol). The initiator 3-*tert*-butyldimethylsiloxy-1-propyllithium in 0.474 M cyclohexane (1.2 ml, 0.57 mmol) was injected. The reaction was stirred overnight and then a sample was removed for analysis. Isoprene (43.03 g, 0.632 mol) was added and the reaction was stirred at room temperature for 3 days. The second sample was taken before TMEDA (0.080 ml, 0.534 mmol) was injected. The styrene (5.43 g, 52.14 mmol) was added and left to react for 3 hours.

Finally 1,1-*bis*(4-*tert*-butyldimethylsiloxyphenyl)ethylene (DPE-OSi) (0.47 g, 1.07 mmol) was added to the solution. The reaction was stirred at room temperature for 5 days. Yield >97%.

PS block M_n= 17400 g mol^{-1}, M_w= 21400 g mol^{-1}, Đ=1.24

P(S-I) block M_n= 81500 g mol^{-1}, M_w= 84900 g mol^{-1}, Đ=1.04

P(S-I-S) block M_n= 93100 g mol^{-1}, M_w= 96700 g mol^{-1}, Đ=1.04

^{1}H-NMR ($CDCl_3$, δ in ppm): 3.4-3.5 [C**H**$_2$OSi], 3.5 [**H**C(Ph)$_2$], 1.0 [Si(CH$_3$)$_2$C(C**H**$_3$)$_3$], 0.1 [ArOSi(C**H**$_3$)$_2$C(CH$_3$)$_3$], 0.0 [CH$_2$OSi(C**H**$_3$)$_2$C(CH$_3$)$_3$].

2.4.3.2.5 Synthesis of P(S-I-S)114_23

AB_2 P(S-I-S)114_23 was prepared following the same method as described above in 2.4.3.2.1. The solution was of benzene (500 ml) and styrene (5.09 g, 48.87 mmol). The initiator 3-*tert*-butyldimethylsiloxy-1-propyllithium in 0.474 M cyclohexane (1.1 ml, 0.52 mmol) was injected. The reaction was stirred overnight and then a sample was removed for analysis. Isoprene (40.62 g, 0.596 mol) was added and the reaction was stirred at room temperature for 3 days. The second sample was taken before TMEDA (0.076 ml, 0.507 mmol) was injected. The styrene (5.28 g, 50.70 mmol) was added and left to react for 3 hours.

Finally 1,1-*bis*(4-*tert*-butyldimethylsiloxyphenyl)ethylene (DPE-OSi) (0.45 g, 1.02 mmol) was added to the solution. The reaction was stirred at room temperature for 5 days. Yield >97%.

PS block M_n= 11700 g mol^{-1}, M_w= 15100 g mol^{-1}, Đ=1.29

P(S-I) block M_n= 40100 g mol^{-1}, M_w= 44500 g mol^{-1}, Đ=1.11

P(S-I-S) block M_n= 44400 g mol^{-1}, M_w= 48700 g mol^{-1}, Đ=1.10

^{1}H-NMR ($CDCl_3$, δ in ppm): 3.4-3.5 [C**H**$_2$OSi], 3.5 [**H**C(Ph)$_2$], 1.0 [Si(CH$_3$)$_2$C(C**H**$_3$)$_3$], 0.1 [ArOSi(C**H**$_3$)$_2$C(CH$_3$)$_3$], 0.0 [CH$_2$OSi(C**H**$_3$)$_2$C(CH$_3$)$_3$].

2.4.3.2.6 Synthesis of P(S-I-S)94_30

AB_2 P(S-I-S)94_30 was prepared following the same method as described above in 2.4.3.2.1. The solution was of benzene (500 ml) and styrene (7.61 g, 73.07 mmol). The initiator 3-*tert*-butyldimethylsiloxy-1-propyllithium in 0.30 M cyclohexane (1.5 ml, 0.45 mmol) was injected. The reaction was stirred overnight and then a sample was removed for analysis. Isoprene (35.51 g, 0.341 mol) was added and the reaction was stirred at room temperature for 3 days. The second sample was taken before TMEDA (0.051 ml, 0.340 mmol) was injected. The styrene (7.73 g, 74.22 mmol) was added and left to react for 3 hours.

Finally 1,1-*bis*(4-*tert*-butyldimethylsiloxyphenyl)ethylene (DPE-OSi) (0.30 g, 0.68 mmol) was added to the solution. The reaction was stirred at room temperature for 5 days. Yield >97%.

PS block M_n= 14000 g mol^{-1}, M_w= 18500 g mol^{-1}, Đ=1.32

P(S-I) block M_n= 50200 g mol^{-1}, M_w= 53400 g mol^{-1}, Đ=1.06

P(S-I-S) block M_n= 61100 g mol^{-1}, M_w= 64900 g mol^{-1}, Đ=1.06

^{1}H-NMR ($CDCl_3$, δ in ppm): 3.4-3.5 [C**H**$_2$OSi], 3.5 [**H**C(Ph)$_2$], 1.0 [Si(CH$_3$)$_2$C(C**H**$_3$)$_3$], 0.1 [ArOSi(C**H**$_3$)$_2$C(CH$_3$)$_3$], 0.0 [CH$_2$OSi(C**H**$_3$)$_2$C(CH$_3$)$_3$].

2.4.3.2.7 Synthesis of P(S-I-S)153_30

AB_2 P(S-I-S)153_30 was prepared following the same method as described above in 2.4.3.2.1. The solution was of benzene (500 ml) and styrene (7.72 g, 74.12 mmol). The initiator 3-*tert*-butyldimethylsiloxy-1-propyllithium in 0.47 M cyclohexane (0.73 ml, 0.34 mmol) was injected. The reaction was stirred overnight and then a sample was removed for analysis. Isoprene (36.31 g, 0.53 mol) was added and the reaction was stirred at room temperature for 3 days. The second sample was taken before TMEDA (0.051 ml, 0.340

mmol) was injected. The styrene (7.32 g, 70.28 mmol) was added and left to react for 3 hours.

Finally 1,1-*bis*(4-*tert*-butyldimethylsiloxyphenyl)ethylene (DPE-OSi) (0.30 g, 0.68 mmol) was added to the solution. The reaction was stirred at room temperature for 5 days. Yield >97%.

PS block M_n= 23100 g mol^{-1}, M_w= 28200 g mol^{-1}, Đ=1.22

P(S-I) block M_n= 96600 g mol^{-1}, M_w= 101500 g mol^{-1}, Đ=1.05

P(S-I-S) block M_n= 119200 g mol^{-1}, M_w= 125800 g mol^{-1}, Đ=1.06

^{1}H-NMR ($CDCl_3$, δ in ppm): 3.4-3.5 [C**H**$_2$OSi], 3.5 [**H**C(Ph)$_2$], 1.0 [Si(CH$_3$)$_2$C(C**H**$_3$)$_3$], 0.1 [ArOSi(C**H**$_3$)$_2$C(CH$_3$)$_3$], 0.0 [CH$_2$OSi(C**H**$_3$)$_2$C(CH$_3$)$_3$].

2.4.4 Deprotection of AB_2 Macromonomer P(S-I-S)

A typical procedure for the deprotection of each AB_2 macromonomer is described below.

Protected AB_2 macromonomer P(S-I-S)59_33 (50 g, 0.89 mmol) was dissolved in 500 ml of THF. To the solution was added concentrated HCl (2.67 ml, 26.74 mmol) in a 10:1 molar ratio with respect to the protected alcohol groups of the macromonomer and the solution was stirred under reflux at 80°C overnight. The completion of the reaction was confirmed by ^{1}H-NMR analysis, before the reaction mixture was cooled. The deprotected polymer was recovered by precipitation into methanol, redissolved in THF, precipitated again and dried under vacuum. Yield >96%.

^{1}H-NMR (C_6D_6, δ in ppm): 3.15 [C**H**$_2$OH], 3.7-3.8 [**H**OPh]

2.4.5 Bromination of deprotected AB_2 Macromonomer P(S-I-S)

A typical procedure for the bromination of each AB_2 macromonomer is described below.

In a 250 ml flask, the deprotected AB_2 macromonomer P(S-I-S)59_33 (5 g, 0.089 mmol) and triphenyl phosphine (PPh_3) (0.5 g, 0.19 mmol) were azeotropically dried three times with benzene under vacuum before dry dichloromethane (DCM) (50 ml) was added to form a 10% w/v solution. Into another flask, carbon tetrabromide (CBr_4) (0.077 g, 0.23 mmol) was dried in the same way and DCM (5 ml) was added by vacuum distillation before the flask was brought to atmospheric pressure with nitrogen. The CBr_4 solution was injected through a septum to the macromonomer/PPh_3 solution at a temperature of 0°C achieved with a

water/ice bath. After addition of the CBr_4 solution the reaction was allowed to rise to room temperature and then stirred at room temperature for 24 hours. A sample was removed to check the completion of the reaction with ^{1}H-NMR analysis before recovering the polymer by precipitation into methanol. Yields >97%.

^{1}H-NMR (C_6D_6, δ in ppm): 2.75 [C**H**$_2$Br]

2.4.6 AB_2 Macromonomer P(S-I-S) conversion of the bromide to azide functionality

A typical procedure for the conversion of the bromide to azide functionality of AB_2 macromonomers P(S-I-S)153_20, P(S-I-S)114_23, P(S-I-S)183_20 and P(S-I-S)153_30 is described below.

In a 500 ml flask, brominated macromonomer P(S-I-S)153_20 (21.36 g, 0.35 mmol) was dissolved in a mixture of DMF (107 ml) and THF (107 ml) to form a 10% w/v solution and heated at 50°C. To the polymer solution was added sodium azide (0.116 g, 1.78 mmol) in a 5:1 molar ratio with respect to the macromonomer and the solution stirred overnight. The completion of the reaction was confirmed by ^{1}H-NMR analysis. The azide functionalised polymer was recovered by precipitation into methanol, redissolved in THF, precipitated again and dried under vacuum. Yield 99%.

^{1}H-NMR (C_6D_6, δ in ppm): disappearance of the peak at 2.7-2.8 [C**H**$_2$Br].

2.4.7 AB_2 Macromonomer P(S-I-S) conversion of phenol functionalities to alkyne functionalities

A typical procedure for the conversion of phenol functionalities into alkyne functionalities for AB_2 macromonomers P(S-I-S)153_20, P(S-I-S)114_23, P(S-I-S)183_20 and P(S-I-S)153_30 is described below.

In a 500 ml flask under an inert atmosphere of nitrogen, azide-functionalised macromonomer P(S-I-S)114_23 (12.31 g, 0.28 mmol) and cesium carbonate (0.23 g, 0.71 mmol) were dissolved in a mixture of THF (50 ml) and DMF (50 ml) to form a 12% w/v solution. To the macromonomer solution was then added propargyl bromide (0.132 g, 1.11 mmol). The reaction was heated with an oil bath to 60°C and the reaction stirred overnight.

The completion of the reaction was confirmed by ^{1}H-NMR analysis. The polymer was recovered by precipitation into methanol, redissolved in THF, precipitated again and dried under vacuum. Yield 98%.

^{1}H-NMR (C_6D_6, δ in ppm): 4.1-4.3 [C**H**$_2$C≡CH].

2.4.8 Synthesis of HyperBlocks

2.4.8.1 Synthesis of HB65_31

2.4.8.1.1 Williamson Coupling Reaction

In a 250 ml flask under an inert atmosphere of nitrogen, AB_2 macromonomer P(S-I-S)65_31 with a bromide 'A' group (11.81 g, 0.35 mmol) and cesium carbonate (1.15 g, 3.53 mmol) were dissolved in 120 ml of THF/DMF 50:50 v/v to form a 10% w/v solution. The reaction was heated with an oil bath to 40°C and the reaction stirred with a mechanical stirrer. The progress of the reaction was followed by SEC analysis and when no more increase in the molecular weight was observed the reaction was said to be complete. The polymer was recovered by precipitation into methanol with the addition of a small amount of BHT antioxidant, redissolved in THF, precipitated again and dried under vacuum.

HB65_31: M_n= 218200 g mol^{-1}, M_w= 959000 g mol^{-1}, Đ 4.39, Yield 99%.

A second reaction with the same macromonomer P(S-I-S)65_31 was carried out with the following amount of materials: P(S-I-S)65_31 (10.01 g, 0.30 mmol), Cs_2CO_3 (0.99 g, 3.04 mmol) and 100 ml of THF/DMF 50:50 v/v to form a 10% w/v solution with a temperature of 40°C.

HB65_31: M_n= 220600 g mol^{-1}, M_w= 826400 g mol^{-1}, Đ 3.75, Yield 99%.

The resulting two HyperBlocks were combined into a single sample by co-dissolving the two polymers in THF and the blend was recovered by precipitation. The combined sample was characterised by SEC to obtain the molecular weight distribution.

HB65_31: M_n= 156400 g mol^{-1}, M_w= 870700 g mol^{-1}, Đ 5.57

2.4.8.2 Synthesis of HB82_41

2.4.8.2.1 Williamson Coupling Reaction

HyperBlock HB82_41 was prepared by Williamson coupling reaction following the same method as described above in 2.4.8.1.1. P(S-I-S)82_41 brominated macromonomer (4.48 g, 0.097 mmol) and cesium carbonate (0.32 g, 0.98 mmol) were dissolved in 45 ml of THF/DMF 50:50 v/v to form a 10% w/v solution. The reaction was conducted at 60°C.

HB82_41: M_n= 390100 g mol^{-1}, M_w= 807700 g mol^{-1}, Đ 2.07, Yield 99%. (0.75 ml/min)

A second coupling reaction was carried out with P(S-I-S)82_41 (5.32 g, 0.11 mmol), Cs_2CO_3 (0.38 g, 1.17 mmol) and 53 ml of THF/DMF 50:50 v/v to form a 10% w/v solution at a temperature of 60°C.

HB82_41: M_n= 354500 g mol^{-1}, M_w= 664800 g mol^{-1}, Đ 1.88, Yield 99%. (SEC 0.75 ml/min)

The resulting two HyperBlocks were combined into a single sample by co-dissolving the two polymers in THF and the blend was recovered by precipitation. The combined sample was characterised by SEC to obtain the molecular weight distribution.

HB82_41: M_n= 308300 g mol^{-1}, M_w= 808500 g mol^{-1}, Đ 2.62

2.4.8.3 Synthesis of HB153_20

2.4.8.3.1 Azide-Alkyne 'click' Reaction

In a 250 ml flask under an inert atmosphere of nitrogen, AB_2 macromonomer P(S-I-S)153_20 (10.03 g, 0.17 mmol) with one azide 'A' group and two alkyne 'B' groups was dissolved in 100 ml of THF/DMF 50:50 v/v to form a 10% w/v solution. The reaction was heated with an oil bath to 30°C and the reaction mixture stirred with a mechanical stirrer. To the solution was added first sodium ascorbate (0.13 g, 0.66 mmol) and then the catalyst $CuSO_4 \cdot 5H_2O$ (0.085 g, 0.34 mmol) in few drops of water. The progress of the reaction was followed by SEC analysis. After 23h further amounts of sodium ascorbate (0.066 g, 0.33 mmol) and catalyst $CuSO_4 \cdot 5H_2O$ (0.042 g, 0.17 mmol) were added to the reaction. When no more increase in the molecular weight was observed the reaction was said to be complete. The polymer was recovered by precipitation into methanol, redissolved in THF, precipitated again and dried under vacuum. Yield 99%.

HB153_20: M_n= 299900 g mol^{-1}, M_w= 743800 g mol^{-1}, Đ 2.48.

A second 'click' coupling reaction was carried out with P(S-I-S)153_20 (10.27 g, 0.17 mmol), sodium ascorbate (0.13 g, 0.66 mmol), $CuSO_4 \cdot 5H_2O$ (0.085 g, 0.34 mmol) and 100 ml of THF/DMF 50:50 v/v to form a 10% w/v solution. No further addition of catalytic system was required before the end of the reaction.

HB153_20: M_n= 261600 g mol^{-1}, M_w= 677800 g mol^{-1}, Đ 2.59.

2.4.8.4 Synthesis of HB183_20

2.4.8.4.1 Williamson Coupling Reaction

HyperBlock HB183_20 was prepared by Williamson coupling reaction following the same method as described above in 2.4.8.1.1. P(S-I-S)183_20 brominated macromonomer (12.80 g, 0.14 mmol) and cesium carbonate (0.45 g, 1.38 mmol) were dissolved in 128 ml of THF/DMF 50:50 v/v to form a 10% w/v solution. The reaction was conducted at 60°C.

HB183_20: M_n= 216500 g mol^{-1}, M_w= 791900 g mol^{-1}, Đ 3.66, Yield 97%.

2.4.8.4.2 Azide-Alkyne 'click' Reaction

HyperBlock HB183_20 was prepared by an azide-alkyne 'click' coupling reaction following the same procedure as described above in 2.4.8.3.1. P(S-I-S)183_20 (12.29 g, 0.13 mmol), sodium ascorbate (0.10 g, 0.50 mmol), $CuSO_4 \cdot 5H_2O$ (0.068 g, 0.27 mmol) and 120 ml of THF/DMF 50:50 v/v to form a 10% w/v solution. No further addition of catalytic system was required before the end of the reaction.

HB183_20: M_n= 320600 g mol^{-1}, M_w= 497400 g mol^{-1}, Đ 1.55, Yield 96%.

The resulting two HyperBlocks were combined into a single sample by co-dissolving the two polymers in THF and the blend was recovered by precipitation. The combined sample was characterised by SEC to obtain the molecular weight distribution.

HB183_20: M_n= 269600 g mol^{-1}, M_w= 779700 g mol^{-1}, Đ 2.89.

2.4.8.5 Synthesis of HB114_23

2.4.8.5.1 Azide-Alkyne 'click' Reaction

HyperBlock HB114_23 was prepared by an azide-alkyne 'click' coupling reaction following the same procedure as described above in 2.4.8.3.1. P(S-I-S)114_23 (10.02 g, 0.23 mmol), sodium ascorbate (0.18 g, 0.91 mmol), $CuSO_4 \cdot 5H_2O$ (0.11 g, 0.44 mmol) and 100 ml of

THF/DMF 50:50 v/v to form a 10% w/v solution at a temperature of 40°C. No further addition of catalytic system was required before the end of the reaction.

HB114_23: M_n= 256500 g mol^{-1}, M_w= 562200 g mol^{-1}, Đ 2.19, Yield 98%.

A second reaction was carried out with P(S-I-S)114_23 (13.11 g, 0.30 mmol), sodium ascorbate (0.24 g, 1.21 mmol), $CuSO_4 \cdot 5H_2O$ (0.15 g, 0.60 mmol) and 100 ml of THF/DMF 50:50 v/v to form a 10% w/v solution. No further addition of catalytic system was required before the end of the reaction.

HB114_23: M_n= 142800 g mol^{-1}, M_w= 593600 g mol^{-1}, Đ 4.16.

The resulting two samples of HyperBlock were combined into a single sample by co-dissolving the two polymers in THF and the blend was recovered by precipitation. The combined sample was characterised by SEC to obtain the molecular weight distribution.

HB114_23: M_n= 144300 g mol^{-1}, M_w= 590000 g mol^{-1}, Đ 4.09

2.4.8.6 Synthesis of HB94_30

2.4.8.6.1 Williamson Coupling Reaction

HyperBlock HB94_30 was prepared by Williamson coupling reaction following the same procedure as described above in 2.4.8.1.1. P(S-I-S)94_30 brominated macromonomer (12.30 g, 0.20 mmol) and cesium carbonate (0.66 g, 2.03 mmol) were dissolved in 120 ml of THF/DMF 50:50 v/v to form a 10% w/v solution. The reaction was conducted at 60°C.

HB94_30: M_n= 344200 g mol^{-1}, M_w= 637300 g mol^{-1}, Đ 1.85, Yield 99%.(SEC 0.75 ml/min)

A second reaction was carried out with P(S-I-S)94_30 (14.78 g, 0.24 mmol), Cs_2CO_3 (0.79 g, 2.39 mmol) and 148 ml of THF/DMF 50:50 v/v to form a 10% w/v solution at a temperature of 60°C.

HB94_30: M_n= 384700 g mol^{-1}, M_w= 709600 g mol^{-1}, Đ 1.84, Yield 99%.(SEC 0.75 ml/min)

The resulting two HyperBlocks were combined into a single sample by co-dissolving the two polymers in THF and the blend was recovered by precipitation. The combined sample was characterised by SEC to obtain the molecular weight distribution.

HB94_30: M_n= 329700 g mol^{-1}, M_w= 757800 g mol^{-1}, Đ 2.30

2.4.8.7 Synthesis of HB153_30

2.4.8.7.1 Williamson Coupling Reaction

HyperBlock HB153_30 was prepared by Williamson coupling reaction following the same method as described above in 2.4.8.1.1. P(S-I-S)153_30 brominated macromonomer (12.76 g, 0.11 mmol) and cesium carbonate (0.35 g, 1.07 mmol) were dissolved in 128 ml of THF/DMF 50:50 v/v to form a 10% w/v solution. The reaction was conducted at 60°C.

HB153_30: M_n = 453500 g mol^{-1}, M_w= 1007000 g mol^{-1}, Đ 2.22, Yield 99%.

2.4.8.7.2 Azide-Alkyne 'click' Reaction

HyperBlock HB153_30 was prepared by an azide-alkyne 'click' coupling reaction following the same procedure as described above in 2.4.8.3.1. P(S-I-S)153_30 (11.43 g, 0.096 mmol), sodium ascorbate (0.076 g, 0.38 mmol), $CuSO_4 \cdot 5H_2O$ (0.048 g, 0.19 mmol) and 114 ml of THF/DMF 50:50 v/v to form a 10% w/v solution. After 23h further amounts of sodium ascorbate (0.038 g, 0.19 mmol) and then catalyst $CuSO_4 \cdot 5H_2O$ (0.024 g, 0.095 mmol) were added to the reaction.

HB153_30: M_n= 455300 g mol^{-1}, M_w= 661800 g mol^{-1}, Đ 1.45, Yield 97%. (SEC 0.75 ml/min)

The resulting two HyperBlocks were combined into a single sample by co-dissolving the two polymers in THF and the blend was recovered by precipitation. The combined sample was characterised by SEC to obtain the molecular weight distribution.

HB153_30: M_n= 398500 g mol^{-1}, M_w= 992100 g mol^{-1}, Đ 2.49.

2.4.9 Characterisation

2.4.9.1 Size Exclusion Chromatography (SEC)

Measurements of molecular weight and dispersity of the polymers synthesised were carried out by Size Exclusion Chromatography (SEC) on a Viscotek TDA 302 with triple detectors: refractive index, light scattering and viscosity. The columns used were PLgel 2 x 300 mm 5 µm mixed C, that have a linear range of molecular weight from 200-2,000,000 g mol^{-1}. The solvent was THF, the flow rate was 1.0 ml/min at a temperature of 35 °C. The calibration was carried out with a narrow molecular weight polystyrene standard purchased from Polymer Laboratories. A value of 0.185 (obtained from Viscotek) was used for the dn/dc of polystyrene. All data reported in this work are obtained by using triple detection calibration.

2.4.9.2 Nuclear Magnetic Resonance (NMR)

^{1}H-NMR spectra were measured on Varian VNMRS 700 MHz or Burker DRX-400 MHz spectrometer using either C_6D_6, DMSO or $CDCl_3$ as solvents.

2.5 Conclusions

We have described here the synthesis of a series of hyperbranched polymers called HyperBlocks via the 'macromonomer' approach. Using this approach we synthesised several AB_2 macromonomers of ABA triblock copolymers of polystyrene-polyisoprene-polystyrene via living anionic polymerisation that allowed us to obtain well-defined polymers in terms of molecular weight, dispersity, microstructure and composition. The introduction of the chain-end functionalities A and B was also possible thanks to the use of a functionalised initiator (3-*tert*-butyldimethylsiloxy-1-propyllithium) and an end-capping agent (1,1-*bis*(4-*tert*-butyldimethylsiloxyphenyl)ethylene) during the subsequent living anionic polymerisation of styrene and isoprene monomers. In the synthesis of the macromonomers we obtained polymers with a varying content of polystyrene (from 20 to 41 wt. %) and a varying molecular weight (from ca. 65000 to 183000 $g \cdot moli^{-1}$). The 50 g large scale reactions carried out allowed us to obtain enough polymer for the synthesis of HyperBlocks and the characterisation studies described later. We have reported a modified procedure for the macromonomers synthesis in order to improve the dispersity of the first block of polystyrene. The addition of THF in a small scale reaction resulted to decrease the Đ to 1.14 and upon its successive removal it did not change the microstructure of the second block of polyisoprene. Although the success obtained with this procedure, during the scale up of the reaction (50 g) it was found difficult to remove completely the additive THF resulting in a change of polyisoprene microstructure.

We have shown that the conversion of the linear macromonomers into HyperBlocks could be carried out efficiently by both Williamson coupling reaction and the azide-alkyne 'click' reaction. We reported the chemical modification of the end groups of the AB_2 macromonomers, carried out in order to obtain the suitable end group functionalities for these two types of coupling reactions. The protected primary alcohol functionality was deprotected and converted into a bromide group and into an azide group. The protected phenol functionalities were deprotected and converted to alkyne functionalities. The Williamson coupling reaction proved once again to be a very good strategy for the synthesis of hyperbranched polymers; the 'click' coupling reaction surprisingly gave slightly lower value of degree of polymerisation (extent of monomer coupling) and the additional two steps for the conversion of the chain-end functionalities of the macromonomers make this

type of coupling less appealing for the synthesis of HyperBlocks. Finally HyperBlocks synthesised by the two different types of coupling reactions were highly polydisperse in terms of molecular weight and molecular architecture as expected. HyperBlocks and the precursor macromonomers were subjected to SEC and NMR analysis in order to fully characterise the polymers. The six HyperBlocks prepared were subjected to further characterisation studies (Chapter 3) showed a degree of polymerisation DP_n between 2.9 and 6.7 and DP_w between 7.9 and 24.6, high values of Đ and molecular weights M_w equal and above 600 $kg \cdot mol^{-1}$.

2.6 References

(1) Hutchings L. R., Dodds J. M., Rees D., Kimani S. M., Wu J. J., Smith E. *Macromolecules*, **2009**, *42*, 8675-8687
(2) Dodds J. M., Hutchings L. R. *Macromol. Symp.*, **2010**, *291-292*, 26-35
(3) Dodds J. M., De Luca E., Hutchings L. R., Clarke N. *J. Polym. Sci., Part B: Polym. Phys.*, **2007**, *45*, 2762-2769
(4) Hutchings L. R., Dodds J. M., Roberts-Bleming S. J. *Macromolecules*, **2005**, *38*, 5970-5980
(5) Hsieh H. L., Quirk R. P., *Anionic Polymerization: Principles and Practical Applications*, Marcel Dekker I.: (**1996**)
(6) Quirk R. P., Ma J.-J. *Polym. Inter.*, **1991**, *24*, 197-206
(7) Roovers J. E. L., Bywater S. *Trans. Faraday Soc.*, **1966**, *62*, 1876-1880
(8) Roovers J. E. L., Bywater S. *Macromolecules*, **1968**, *1*, 328-331
(9) Bywater S., J. W. D. *Can. J. Chem.*, **1962**, *40*, 1564-1570
(10) J. W. D., Bywater S. *Can. J. Chem.*, **1964**, *42*, 2884-2892
(11) Sato H., Tanaka Y. *J. Polym. Sci.: Polym. Chem. Ed.*, **1979**, *17*, 3551-3558
(12) Chen Y. H. *Anal. Chem.*, **1962**, *34*, 1134-1136
(13) Clarke N., Luca E. D., Dodds J. M., Kimani S. M., Hutchings L. R. *Eur. Polym. J.*, **2008**, *44*, 665-676
(14) Kimani S. M., Hardman S. J., Hutchings L. R., Clarke N., Thompson R. L. *Soft Matter*, **2012**, *8*, 3487
(15) López-Villanueva F.-J., Wurm F., Kilbinger A. F. M., Frey H. *Macromol. Rapid Commun.*, **2007**, *28*, 704-709
(16) Kempe K., Krieg A., Becer C. R., Schubert U. S. *Chem. Soc. Rev.*, **2012**, *41*, 176-191
(17) Quirk R. P., Yuechuan W. *Polym. Int.*, **1993**, *31*, 51-59

CHAPTER 3

Characterisation of HyperBlocks

The purpose of the synthesis carried out during this work was to create a series of HyperBlocks with varying molecular weight and composition and subsequently to analyse the materials from different points of view. We are interested in the impact of the hierarchical branched architecture upon the physical and mechanical properties of HyperBlocks and to this end the materials were characterised by differential scanning calorimetry (DSC), transmission electron microscopy (TEM) and tensile testing.

3.1 Thermal Analysis

Thermal analysis is a technique employed in order to study the properties of a polymer as they change with temperature. Thermal transitions of a polymer, i.e. the changes that take place when the polymer is heated, include crystallisation, melting and glass transition. The glass transition is the transformation accompanying an increase in temperature whereby a polymer changes from a glassy, brittle solid to a rubber-like viscous liquid state and it occurs at the glass transition temperature (T_g). The internal macroscopic organisation of the polymer chains influences the type(s) of thermal transition that can be observed for a material. In the theoretical case of a pure crystalline polymer, a melting point (T_m) would be observed (and not a glass transition) due to the melting of the crystallite, i.e. the three-dimensional structure formed by highly ordered chains. Crystallites are destroyed by heating and the polymer becomes a disordered liquid. If the polymer is amorphous, its chains are randomly arranged and disordered even in the solid state and it undergoes a glass transition at T_g, above which the polymer behaves as a viscous liquid. For a semi-crystalline polymer, with varying proportion of ordered (crystalline) and disordered (amorphous) regions, it is possible to observe both T_g and T_m, where T_g is only observed for the amorphous regions that undergoes glass transition and T_m for the crystalline portion. The glass transition temperature is an important characteristic for a polymer. At the glass transition we can observe abrupt changes in the physical properties of the polymers in particular mechanical properties and for amorphous polymers, the polymer may only be processed above T_g when the polymer is in a viscous liquid state. Many polymers are used in applications which depend on the use of the materials at temperatures below and/or above the T_g. For these reasons the determination of T_g of polymers is important and relevant for the potential applications of polymeric materials such as thermoplastic elastomers upon which this work

is focused. ABA thermoplastic elastomers (TPEs) being block copolymers, are characterised by the presence of two T_gs corresponding respectively to the glass transition of the two types of polymers A and B from which they are formed. These versatile materials act like cross-linked elastomers at a temperature in between the two T_gs and at temperature higher than the T_g of the hard block, they soften and they can be processed and shaped. By cooling TPEs regain their elastomeric properties and can be softened again by re-heating. Several types of techniques are employed for the thermal analysis and during this work we utilised differential scanning calorimetry (DSC).

3.1.1 Differential Scanning Calorimetry (DSC)

Differential scanning calorimetry is a technique which investigates the thermal transitions in materials. In a DSC experiment the material under examination is placed in a sample pan and the amount of energy required to heat the sample pan at the same temperature rate as reference (empty) pan is measured. The analysis gives quantitative and qualitative information about all those changes in the polymer that involve exothermic and endothermic process or change in heat capacity.

During this work two different experiments were run on the ABA macromonomers and HyperBlocks in order to observe the thermal behaviour of both polyisoprene and polystyrene blocks. A typical DSC thermogram of a polystyrene/polyisoprene ABA triblock copolymer macromonomer is shown below. (Figure 3.1) The resulting thermogram was obtained by scanning the samples form -90°C to 150°C at a scan rate of 20°C/min.

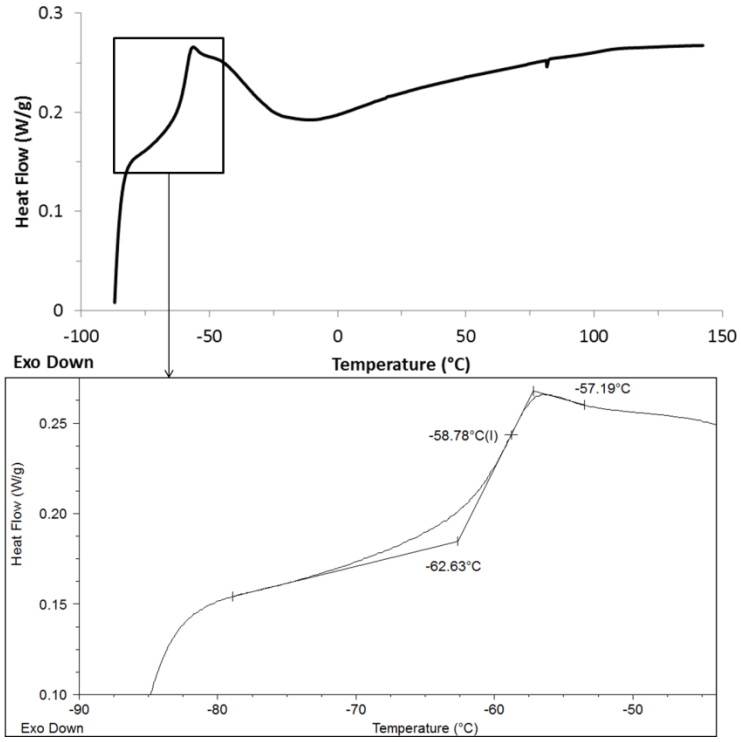

Figure 3.1 On the top DSC thermogram of macromonomer P(S-I-S)153_30 and below the expanded thermogram in correspondence of the glass transition of polyisoprene. Heating cycle: from -90°C to 150°C at 20°C/min.

In this thermogram it is possible to observe only one of the two thermal transitions expected for a block copolymer of PS and PI. The observed T_g corresponds to the T_g of the polyisoprene block and it is found at low temperature (midpoint value: -59°C). The presence of the T_g of the polystyrene block was not observed for any samples analysed using a heating cycle of 20°C/min due to the low styrene content (20-40%) of each triblock copolymer – the T_g being a low energy transition at the best of times. Therefore the samples were scanned in a different temperature range (from 20°C to 200°C) at a faster heating rate (400°C/min) in order to make possible the observation of the polystyrene T_g. A typical thermogram obtained at the higher heating rate is shown in Figure 3.2.

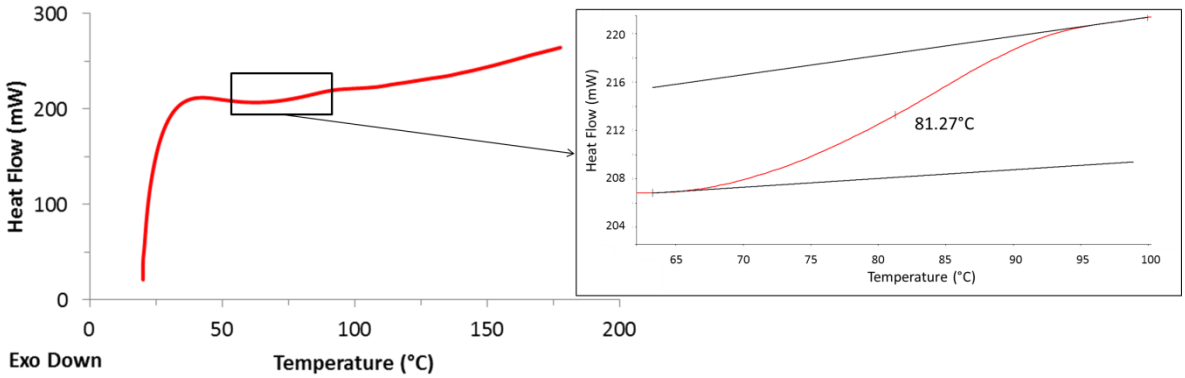

Figure 3.2 On the left DSC thermogram of macromonomer P(S-I-S)82_41 and on the right the same thermogram expanded in corresponance of polystyrene T_g transition. The heating cycle represented is from 20°C to 200°C at 400°C/min.

The T_g observed at higher temperature values (midpoint value: 81°C) compared to polyisoprene T_g (-59°C) corresponds to the polystyrene glass transition.

In Table 3.1 are listed the T_g values obtained for each macromonomer and HyperBlock analysed.

Table 3.1 T_gs values and PS content for each macromonomer and corresponding HyperBlock analysed by DSC. The T_gs values listed are at the midpoint for each thermogram.

Macromonomer	**PS (%)**	**Low T_g [(b)] (°C)**	**High T_g [(c)] (°C)**	***HyperBlocks***	**Low T_g [(b)] (°C)**	**High T_g [(c)] (°C)**
P(S-I-S)82_41	41	-59	81	HB82_41	-57	81
P(S-I-S)65_31	31	-57	82	HB65_31	-59	79
P(S-I-S)94_30	30	-58	-	HB94_30	-57	80
P(S-I-S)153_30[(a)]	30	-59	86	HB153_30	-58	90
P(S-I-S)114_23	23	-58	87	HB114_23	-57	85
P(S-I-S)183_20	20	-58	81	HB183_20	-57	84

(a) A third T_g at high temperature was observed: 116.82°C.
(b) These data were obtained by using a heating rate of 20°C/min.
(c) These data were obtained by using a heating rate of 400°C/min

T_g is typically influenced by several characteristics of polymers including the molar mass, the molecular structure, backbone flexibility and the presence of branching and cross-linking present in a polymer.[1] For instance, the influence of chain flexibility can be observed when comparing the T_g of poly(dimethylsiloxane) (PDMS) **(1)** (-123°C) and poly(2,6-dimethyl-1,4-phenylene oxide) **(2)** (211°C).

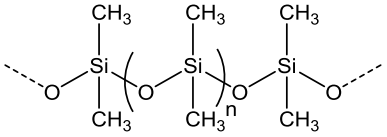

Poly(dimethylsiloxane)
(1)

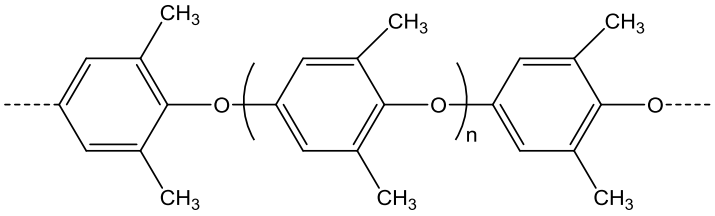

Poly(2,6-dimethyl-1,4-phenylene oxide)
(2)

T_g decreases when the polymer has flexible chains as in the case of PDMS and higher values are achieved when rigid chains form the polymers as in the case of poly(2,6-dimethyl-1,4-phenylene oxide). The molecular structure is also another important factor that influences T_g, for example the steric bulk of substituents to the polymer backbone in a polymer increases the T_g. Polystyrene **(3)** T_g has a high value (100°C)[2] due to the aromatic rings which impede the free rotation of the chains and more thermal energy is needed to allow the chain motion. When the styrenic rings are substituted by the much less bulky substituent group -CH_3, as in the case of polypropylene **(4)**, a much lower T_g (-20°C) is observed. The

polymer chains in polypropylene are in fact more free and the chain motion requires much less thermal energy.

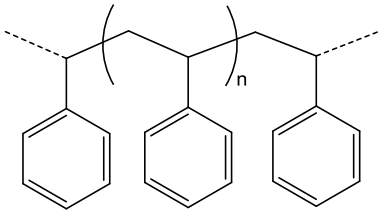

Polystyrene
(3)

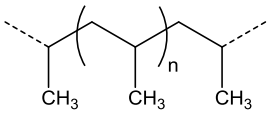

Polypropylene
(4)

Another parameter that influences the T_g is the microstructure and this is of particular relevance to polyisoprene. Polymers containing double bonds can have *cis* or *trans* conformations and in particular 1,3-polydienes can have various combinations of *cis*, *trans*, 1,2- or 1,4-microstructures and in the case of isoprene, 3,4 microstructure (Chapter 2 – Figure 2.2). This is clearly demonstrated by the several different values of T_g reported for polyisoprene with varying microstructure. The *cis* and *trans* configurations give two different values of T_g for 1,4-polyisoprene microstructure with a T_g of -73°C (*cis*) and ca. -60°C (*trans*).[2,3] The presence of the two other possible microstructures (1,2- and 3,4-) can affect the T_g of the polyisoprene, for example the T_g of polyisoprene with microstructure of 45% of 3,4- and 55% 1,4- is -34°C.[4] The increase in T_g due to the increasing amount of 3,4-microstructure was also observed by Meyer *et al.*[5] Their study highlighted how the chain stiffness which is responsible for high values of T_g, is enhanced by the presence of the side-chain vinyl groups. The exact microstructure observed for any particular sample of polyisoprene is largely dependent upon the polymerisation mechanism and reaction conditions such as polymerisation solvent and catalyst/initiator. In the present work, anionic polymerisation was used to prepare the polymers and a lithium initiator was used in a non-polar solvent (benzene). Under such conditions a high 1,4-microstructure would be expected.

The value of approximately -58°C observed in the current work for the T_g of the polyisoprene block differs from the value reported in literature for the 100% *cis*-1,4-polyisoprene (-73°C) and this is due to slightly different microstructure obtained. Living anionic polymerisation using a lithium initiator and non-polar solvent would be expected to result in polyisoprene with the following microstructure: 72% 1,4-cis, 20% 1,4-trans and 8% 3,4.[6] The block of polyisoprene of the macromonomers synthesised in this work by living anionic

polymerisation typically have a microstructure which is 93% of 1,4- and 7% 3,4-microstructure. This small amount of 3,4-polyisoprene will affect and increase the T_g of the polymer. In addition the 93% of 1,4-microstructure includes both *cis* and *trans* configurations and the presence of the *trans*-polyisoprene can be another reason for the increase of the T_g. It is also possible that the presence of the two blocks of polystyrene at either the end of the polyisoprene block may also influence and increase the polyisoprene T_g. This may be due to the impact of the rigid, glassy polystyrene domains upon the mobility of the polyisoprene chains.

A variation from the value of the T_g of the homopolymer polystyrene (100°C) was also observed for the polystyrene block of the macromonomers and HyperBlocks (Table 3.1). In these materials the polystyrene T_g was found at a temperature below 100°C, i.e. in the range between 80-90°C. The decrease of T_g for the polystyrene block can be explained with the inclusion of the soft block (polyisoprene) between the two hard blocks (polystyrene). The polystyrene blocks are thus affected to a certain extent by being the end groups at each end of the polyisoprene block. In addition the fact that the polystyrene blocks are relatively short might also account for the low value of polystyrene T_g. A third T_g was observed for one of the macromonomer (P(S-I-S)153_30) at a value of 116°C. The observation of this transition is likely due to the presence of unreacted polystyrene first block that was produced during the synthesis of the ABA triblock macromonomer P(S-I-S)153_30 by the presence of impurities introduced during the addition of the second monomer isoprene.

Thermal analysis of the HyperBlocks clearly identifies the T_gs of the polyisoprene and polystyrene blocks, thereby confirming that the linear segments undergo phase separation into discrete domains of polyisoprene and polystyrene. In order to observe the polystyrene T_g the use of a high heating rate (400°C/min) was required during the thermal analysis of the samples. The T_g values obtained for the HyperBlocks were very similar to the values obtained for the macromonomers. (Table 3.1) One might expect that introducing branching into the structure should affect the glass transition due to a reduction in chain movement and the reduced number of chain ends caused by the presence of the branched points – this might be expected to particularly effect the T_g of the styrene blocks. However, it is important to notice that in this case the complex branched architecture did not prevent microphase separation as indicated by the presence of distinct T_g value for each block.

3.2 Morphology analysis

Block copolymers have the ability to form nano-scale morphologies through microphase separation of the blocks constituting the polymers. This segregation is due to the incompatibility of chemically different blocks linked together by covalent bonds which prevent the macroscopic phase separation of the polymers. The nano-scale self-organisation can occur in melt, solid and micellar solution and it leads to unique properties and applications of block copolymers. For instance, the morphology is strongly connected to the physical properties of the materials and in particular to the mechanical properties; an example of this impact is given by the use of block copolymers as thermoplastic elastomers (TPEs).

Block copolymers self-organise into several morphologies dictated by three main factors i.e. the Flory-Huggins interaction parameter (χ), the molecular weight and the volume fraction of the blocks constituting the block copolymers. Morphologies for block copolymers that have been theorised and experimentally observed include domains of spheres, cylinders, lamellae and co-continuous structures including the gyroid morphology.[7,8] (Figure 3.3)

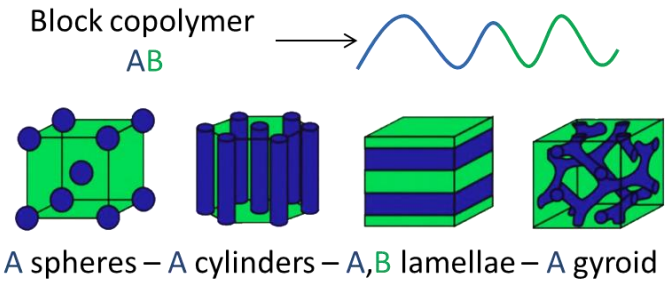

Figure 3.3 Observed morphologies for an AB diblock copolymer.

The type of morphology assumed by block copolymers can be controlled by the choice of the monomers, the blocks molecular weights and the polymeric architecture. Living anionic polymerisation can be used successfully for the synthesis of block copolymers and allows us to control the parameters that influence the morphology of the block copolymers such as molecular weight, molecular architecture, molecular structure and composition.

The equilibrium behaviour for AB and ABA block copolymers, such as the polymers synthesised in the present work, has been described in detail and the phase diagrams of the melts of these two types of linear polymers has been reported by Matsen in 2000. (Figure 3.4)[9]

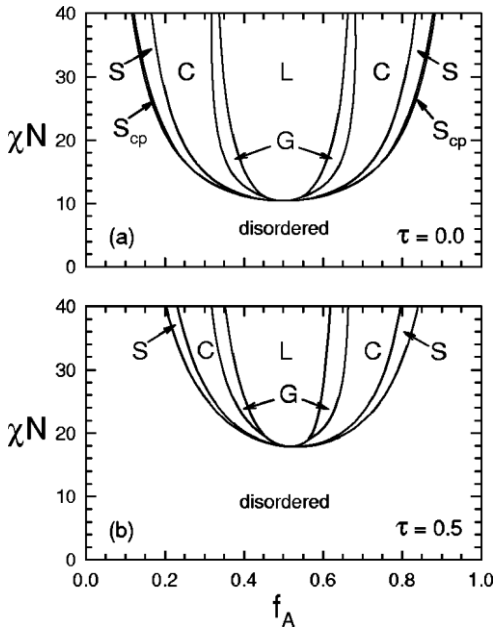

Figure 3.4 Phase diagrams for melts of AB (a) and symmetric ABA (b) block copolymers. The several morphologies are: spherical (S), cylindrical (C), gyroid (G), lamellar (L) and close-packed spheres (S_{cp}). τ represents the asymmetry parameter: $0 \leq \tau \leq 0.5$. These diagrams were calculated by self-consistent field theory (SCFT). (Reprinted with permission from "M. W. Matsen *Journal of Chemical Physics*, **113**, 5539-5544." Copyright [2000], AIP Publishing LLC)

The diagram is calculated by using one of the several theoretical approaches used to study the phase behaviour of block copolymers i.e. the self-consistent field theory (SCFT). In the scheme the degree of segregation χN is plotted as a function of the composition f, where χ is the Flory-Huggins segment-segment interaction parameter and N is the degree of polymerisation. The parameter χ depends on the type of monomers constituting the block copolymer and it is also temperature dependent. The transition from AB diblock copolymer to symmetric ABA triblock copolymer is characterised by the increase of the disordered area in particular at low χN as it is possible to observe in Figure 3.4. In general, the polymer melt is found in a disordered state at small values of χN. By increasing χN a point can be reached where the polymer assumes a heterogeneous ordered structure and this transition is called the order-disorder transition (ODT), which occurs at a critical value of χN. The greater the complexity of the block copolymer, the more variations are observed in a phase diagram. For instance the asymmetric ABA block copolymers studied by Matsen[9] showed several variations in the segregation behaviour in comparison with symmetric ABA block copolymers. Substantial changes in morphology have also been observed in the case of nonlinear block copolymers provided with one or more branch points. The polymers studied in order to understand the influence of branched architecture on the morphology include miktoarm stars[10] and graft copolymers. Of particular note is the work of Mays *et al* who

prepared graft copolymers with a polyisoprene backbone and polystyrene arms[11,12]. It was noticed that the long-range order decreased with the increase in the number of branched points at the same volume fraction of polystyrene. The morphologies formed by the graft copolymer were following the theoretical predictions but the extent of branching influenced the morphology and inhibited the formation of a long-range order.

3.2.1 Transmission Electron Microscopy (TEM)

Poly(styrene-isoprene-styrene) triblock copolymers and Hyperblocks were characterised by Transmission Electron Microscopy (TEM) to investigate the effect of the composition and branched architecture on the solid-state morphology. The morphologies of commercially available TPEs (supplied by Kraton™), comprising linear and star block copolymers of PS and PI, were also explored by TEM and additional morphology studies were carried out on blends of the Kraton™ linear TPE with 10 and 30 wt. % of HyperBlock.

The molecular characteristics of the commercial TPEs can be found in Table 3.2. Commercial TPEs were supplied by Kraton™ Polymers and synthesised by living anionic polymerisation of styrene and isoprene. The two types of TPEs used were Kraton™ D-1160 which is a linear triblock copolymer PS-PI-PS similar to the macromonomers synthesised in this work, and Kraton™ D-1124P which is a three-arm star of PS-PI block copolymers.

Table 3.2 Molecular characteristics of commercial TPEs from Kraton™ Polymers.

SEC in THF	Triple detection[a]			Conventional calibration			
Kraton™	M_n (g mol^{-1})	M_w (g mol^{-1})	**Đ**	M_n (g mol^{-1})	M_w (g mol^{-1})	**Đ**	**PS (%)**
Linear D-1160	89500	95200	1.06	156100	175400	1.12	~20
Star D-1124P	78000	101400	1.30	113600	159500	1.40	~30

a) Data obtained by using dn/dc of polystyrene (0.185)

TEM is a microscopy technique used extensively for the analysis of block copolymers morphology in the solid or melt state. The analysis by TEM of a small area of a sample provides directly a picture of the morphology that diblock and triblock copolymers assumed during the microphase separation process.

Samples for TEM were prepared by dissolving the block copolymers (macromonomer, HyperBlocks and blends of the latter with Kraton™ linear TPE) in toluene (6% w/v for HyperBlocks and 30% w/v for macromonomers and blends) in the presence of the

antioxidant 3,5-di-*tert*-butyl-4-hydroxytoluene (BHT). The solution was subsequently poured onto circular aluminium plates of 1 mm thickness. The solvent was allowed to evaporate at room temperature for few days and then the solution cast films were dried under vacuum to constant weight. In a previously reported procedure for the sample preparation [13] an annealing step was carried out in which the films were maintained at 120°C for 7 days under vacuum in order to reach the equilibrium morphology. In this work we used a slightly different approach in order to understand if the annealing step was really a required step to equilibrate the morphology. Kraton™ D-1124P, PS-PI three-arm star, was solution cast from toluene onto two aluminium plates and dried until constant weight under vacuum. One of the samples was then annealed at 120°C under vacuum for 7 days prior the TEM analysis, whereas the other sample was analysed by TEM without any further treatments. The TEM-micrographs of the two samples of Kraton™ star processed by each method are shown below. (Figure 3.5)

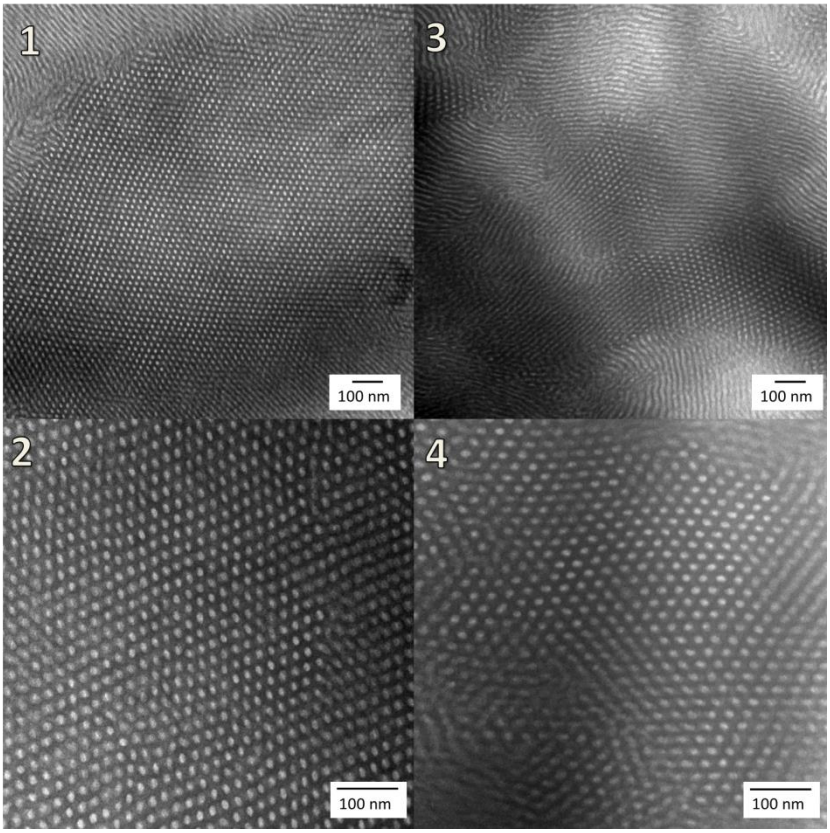

Figure 3.5 TEM micrographs for the sample Kraton™ D-1124P three-arm star (30% PS). 1 and 2 are images for the unannealed film, 3 and 4 are the images for the films annealed at 120°C.

In Figure 3.5 it can be seen that the annealed (3-4) and unannealed samples (1-2) of the star-branched Kraton™ are both microphase separated with identical hexagonally packed

cylindrical morphology. The micrographs show dark and light domains which correspond to the polyisoprene and polystyrene blocks respectively. The dark colour arises by exposing the film to osmium tetraoxide (OsO_4) vapour which stains the unsaturated rubbery component (PI) but not the glassy component (PS). In this type of contrast enhancement method OsO_4 reacts exclusively with the double bonds of polyisoprene forming the following osmate ester:[14]

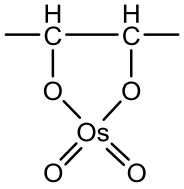

The cylindrical morphology is indicated by the coexistence of both the circles and transverse segments of polystyrene in the polyisoprene matrix. From these images it seems that the solvent cast technique for the preparation of the films allows the polymer to reach its equilibrium morphology without the need of the annealing step.

3.2.1.1 Macromonomer morphology

The morphology of each linear ABA macromonomer has been analysed and allows us to systematically compare the impact of composition and molecular weight upon morphology. In Table 3.3 we recall the polystyrene weight fraction and the molecular weight of each P(S-I-S) block copolymers.

Table 3.3 Molecular weight and dispersity data of the final macromonomers calculated by ^{1}H-NMR spectroscopy and triple detection SEC in THF using dn/dc of polystyrene in THF.

Macromonomers	***P(S-I-S)*** M_n**(g mol^{-1})**		**PS**
	(a)	**(b)**	**(%)**
P(S-I-S)183_20	93100	183000	20
P(S-I-S)114_23	44400	113900	23
P(S-I-S)94_30	61100	93900	30
P(S-I-S)153_30	119200	152800	30
P(S-I-S)65_31	33600	64900	31
P(S-I-S)82_41	46300	81500	41

(c) Data obtained by SEC in THF using a value of dn/dc= 0.185
(d) Data obtained by ^{1}H-NMR spectroscopy in $CDCl_3$ and C_6D_6.

Polymers such as the linear ABA triblock copolymers synthesised in this work have hard/glassy blocks at each end of the polymer chains (polystyrene block) and one soft/rubbery block in the inner part (polyisoprene block). The macromonomer structure can

be schematically represented as in Figure 3.6 where the blocks at each end of the chain have similar molecular weights and the inner block constitutes the bigger part of the linear chain.

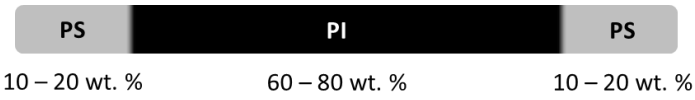

Figure 3.6 Schematic representation of linear macromonomers P(S-I-S). The weight percentage of each block varies from 10 to 20 wt. % for the polystyrene blocks and from 60 to 80 wt. % for the polyisoprene block.

The difference in molecular weights and polystyrene weight fractions results in different morphologies for the linear P(S-I-S) triblock copolymers. Figure 3.7 shows the TEM images for the macromonomers. As already observed in the morphology pictures of Kraton^{TM} star, the rubbery polyisoprene block reacts with heavy metal containing molecules and is stained by OsO_4 resulting in the black matrix of each picture taken by TEM.

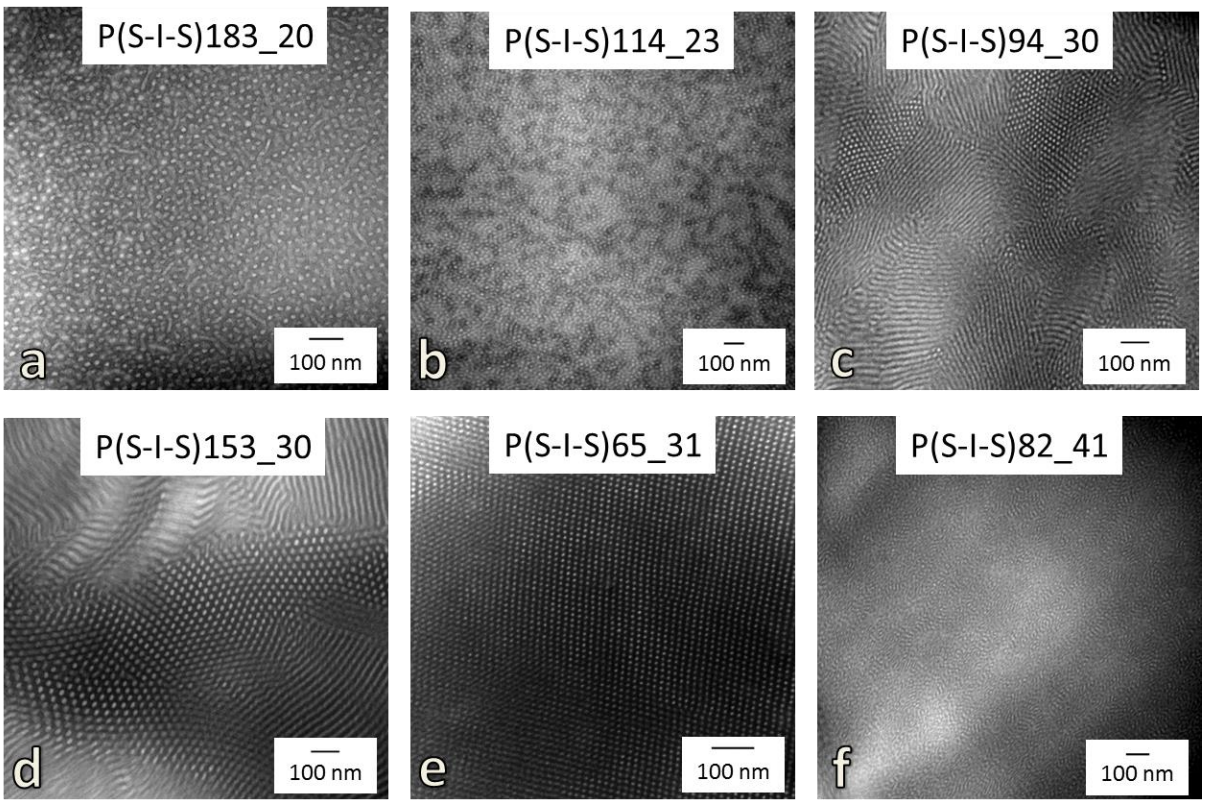

Figure 3.7 TEM images of the macromonomers P(S-I-S) characterised by different molecular weights and polystyrene weight fractions.

The TEM images presented here show how the morphology of the ABA triblock copolymer macromonomers varies by changing the molecular weight and the polystyrene weight fraction. P(S-I-S)94_30, P(S-I-S)153_30 and P(S-I-S)65_31 (Figure 3.7 *c*, *d*, *e*) with a content of polystyrene of 30 wt. % all show a cylindrical morphology. Observing the TEM images it is possible to identify hexagonally packed cylinders in both side-on and head-on orientations.

These three images are similar to the TEM images for Kraton^{TM} D-1124P (Figure 3.5) which has the same content of polystyrene and shows a cylindrical morphology. The change in molecular weight does not seem to affect the morphology of these macromonomers with 30 wt. % of polystyrene. However, it is possible to observe that by decreasing the molecular weight of the macromonomer, the domain sizes of polystyrene cylinders get smaller. This is observed with particular evidence in Figure 3.7 *d* and *e* where the measured domain sizes are respectively of ca. 17 nm and 8 nm (cylinders diameter) corresponding to the decrease of the molecular weight from 153 kg mol^{-1} to 65 kg mol^{-1}. Macromonomers P(S-I-S)183_20 and P(S-I-S)114_23 have a lower polystyrene content (20 wt. %) and they show a more spherical morphology with long-range order although the morphology is not perfect and it is possible that at 20% styrene these samples are on the boundary between the spherical phase and disordered phase (Figure 3.7 *a*, *b*). By observing Figure 3.4 we could think that spheres are theoretically expected for these ABA block copolymers with volume fractions of PS f_{PS}= 0.19 and 0.21 respectively. The volume fractions have been calculated by the following equation $f_{PS} = w_{PS}\,\rho_{PI}/(\rho_{PS}w_{PI} + \rho_{PI}w_{PS})$, where w_{PS} and w_{PI} are the weight fractions and ρ_{PI} and ρ_{PS} are the density of isoprene and styrene respectively.

The different molecular weights of P(S-I-S)183_20 and P(S-I-S)114_23 did not change the resulting morphology. The increase to 40 wt. % in the styrene content for P(S-I-S)82_41 results in a less well-ordered cylindrical morphology. The segregation in microphases is still visible but the long-range order is less obvious; for a linear macromonomer we could expect a better order and this high percentage of disorder could be due to the combination of the styrene content of 40 wt. % and the molecular weight (M_n 46 kg mol^{-1}). By observing Figure 3.4 the linear ABA triblock copolymer P(S-I-S)82_41 could have in this way a morphology on the phase boundary between cylinders and the gyroid phase having a volume fraction f_{PS} of 0.38.

3.2.1.2 HyperBlocks morphology

A dramatic change in the morphology is noticed when the macromonomers are converted into HyperBlocks and branch points are introduced. Figure 3.8 shows the TEM micrographs of the HyperBlocks synthesised from each of the macromonomers mentioned above.

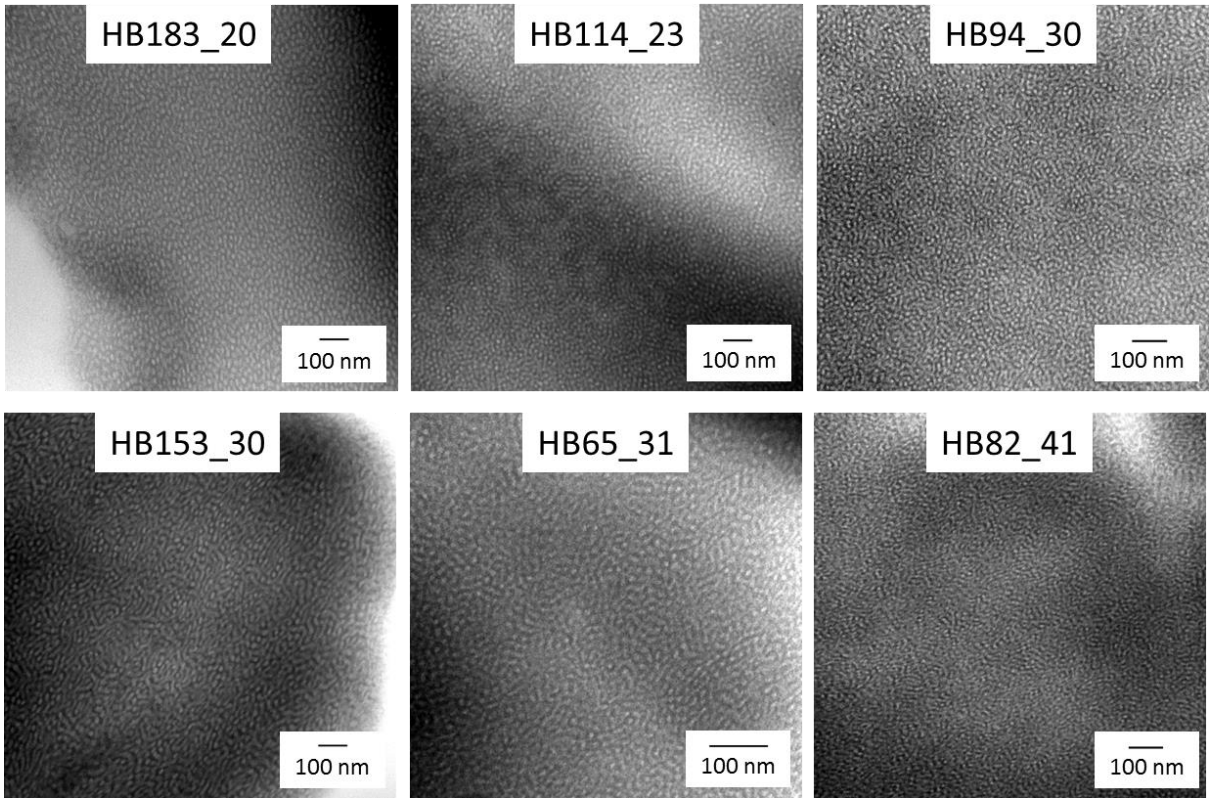

Figure 3.8 TEM micrographs of HyperBlocks synthesised from their linear precursor macromonomers P(S-I-S).

The comparison of the two sets of TEM images (Figure 3.9) shows the development of the morphology of the triblock copolymers due to the transformation of the architecture. The change of the architecture clearly has a dramatic effect on the self-assembly of the block copolymers. Each image in Figure 3.8 shows that the HyperBlocks are microphase separated (and this is confirmed by the DSC data discussed above) but in each case the HyperBlocks lack the long-range order characteristic of the macromonomers. The composition of each HyperBlock is identical to the precursor macromonomer and as a consequence the morphology should be the same following the theoretical predictions (ignoring the impact of architecture). The decrease of the long-range order is therefore due to the complex branched architecture of the HyperBlocks. The effect of branching points on the morphology has been previously reported in the case of graft copolymers made of polystyrene arms and polyisoprene backbone.[11] It was noticed that the long-range order of the graft copolymers decreased with the increase of the number of branch points leading to morphologies similar to the ones reported in this work. In addition the results reported here are consistent with result obtained previously by Hutchings[13] where a similar change in morphology was observed accompanying the transformation of the macromonomer into HyperBlock.

We can observe a direct comparison between the macromonomer precursor and resulting HyperBlock in Figure 3.9. The contrast in morphology between linear precursor and branched HyperBlock is most obvious for the samples in which the styrene content is approximately 30% by weight where the long-range order is strongest in the macromonomer.

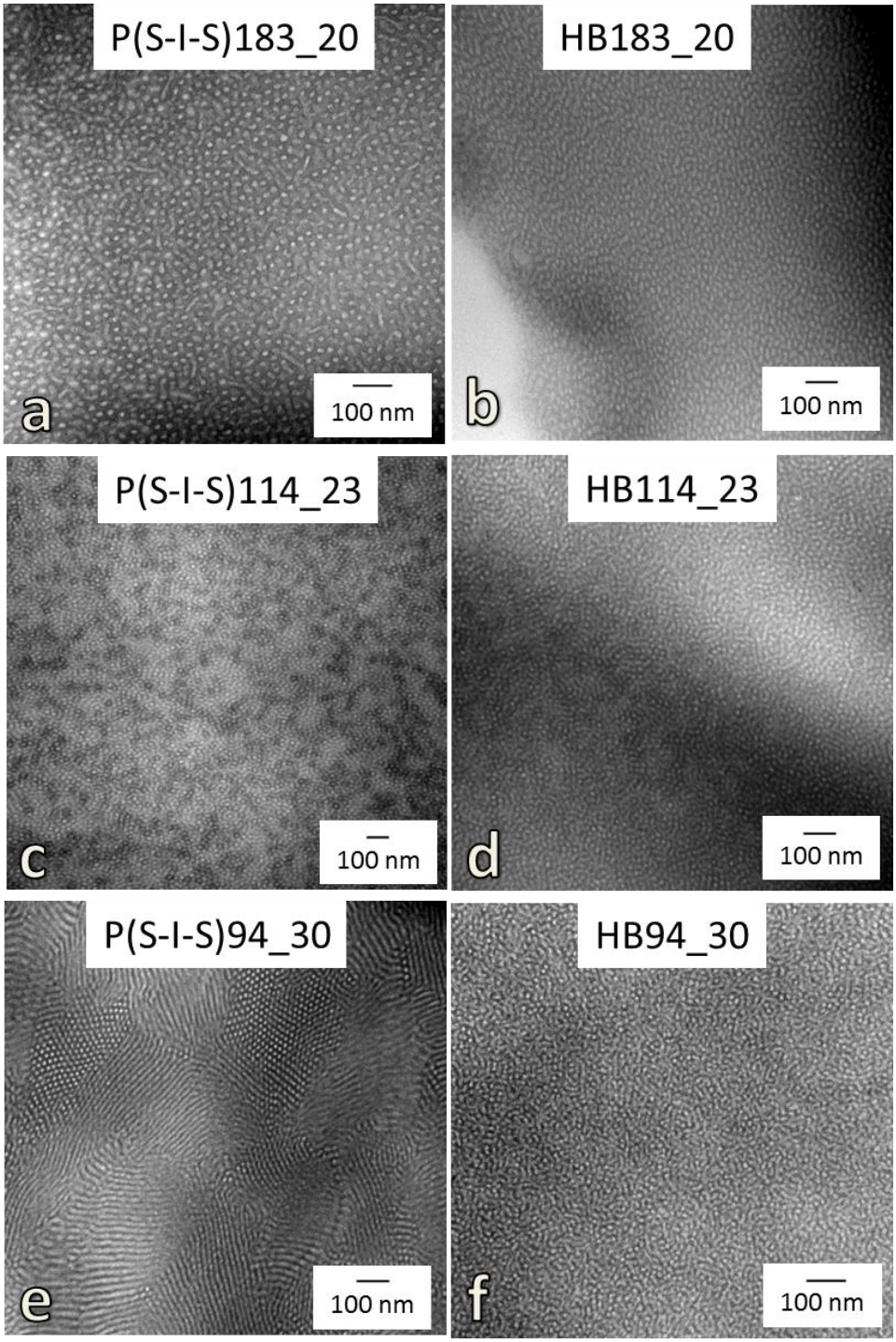

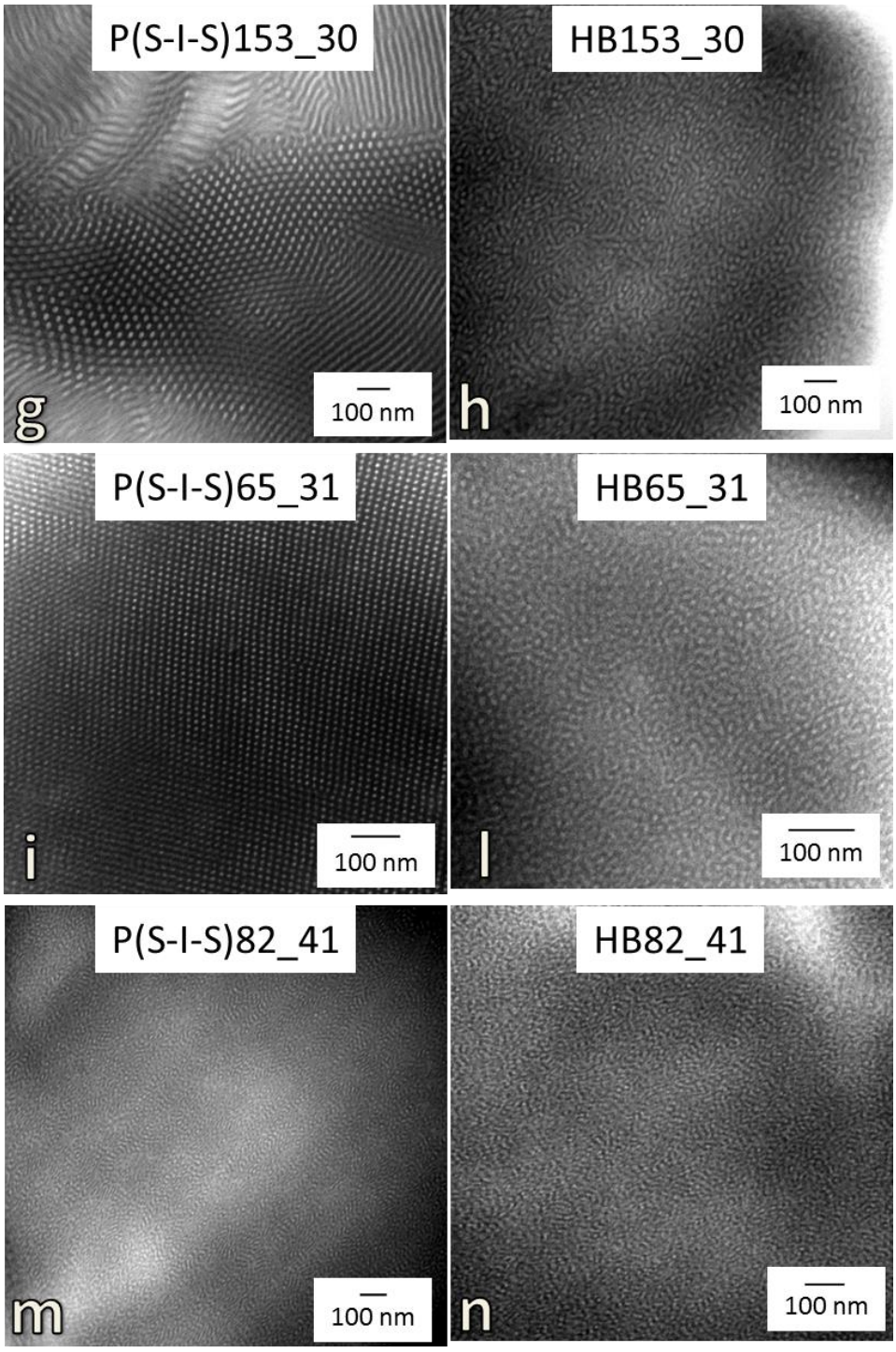

Figure 3.9 TEM micrographs of macromonomers (on the left column a, c, e, g, i, m) compared with HyperBlocks (on the right column b, d, f, h, l, n).

Significant changes to the observed morphology of the macromonomer can be observed for the HyperBlocks HB94_30, HB153_30 and HB65_31 (Figure 3.9 *f*, *h*, *l*). The long-range order in the cylindrical morphology of the corresponding macromonomers is lost and the microphase separation, which is still visible, seems to have a much higher degree of disorder. In the case of the macromonomers/HyperBlocks with a weight fraction of

polystyrene of approximately 0.2, represented in Figure 3.9 *a-d*, the impact of the branching upon morphology with long-range order is less obvious. Moreover, the change of morphology for P(S-I-S)82_41 in the passage to the hyperbranched structure of HB82_41 can be hardly detected. This is more a consequence of the macromonomer having a less ordered morphology, than the branched architecture having no impact. What can be said with certainty is that in all of the above cases, regardless of the composition or molecular weight of the linear macromonomer precursor, the resulting HyperBlocks all show microphase separation but the morphology in each case is characterised by a total lack of long-range order. It is as if the branched architecture imposes a disordered, possibly bi/co-continuous morphology upon the HyperBlocks. Work is ongoing to understand the nature of the HyperBlock "disordered" morphology by small angle X-ray scattering.

3.2.1.3 Morphology of Blends of Linear and Hyperbranched Block Copolymers

Polymer blends are new materials obtained from the mixture of two or more existing polymers and they are characterised by physical properties which differ from the properties of each component. Blends are often produced in order to create materials with unique properties developed in accordance to the applications of the material itself. We have seen above the dramatic impact that the complex branched architecture has in all cases on the morphology of HyperBlocks and it was considered interesting to investigate whether the architecture of HyperBlocks would in any way impact upon the morphology of linear block copolymers when the HyperBlock was added to a blend.

The blends produced in this work were binary blends of various HyperBlocks with the linear Kraton^{TM} TPE (D-1160). The morphology of this commercial linear triblock copolymer PS-PI-PS thermoplastic elastomer is reported in Figure 3.10.

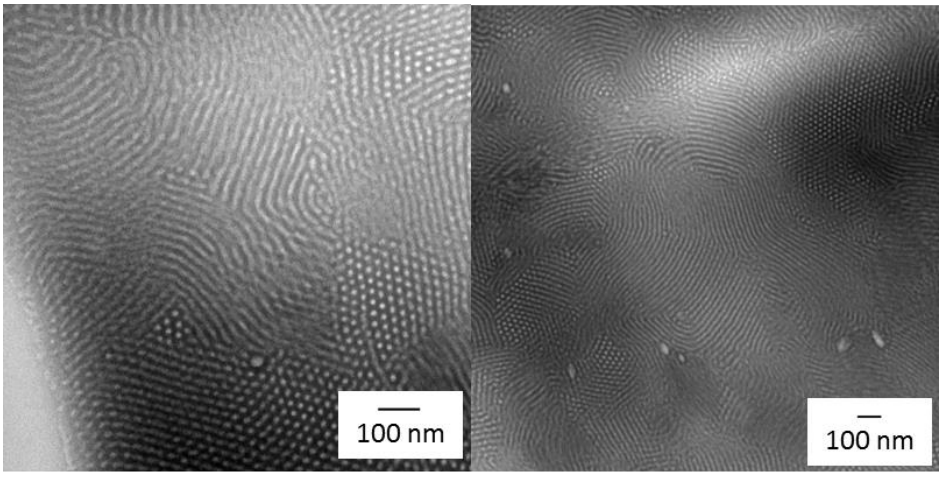

Figure 3.10 TEM micrograph of commercial linear TPE Kraton^{TM} D-1160.

The microphase separation for Kraton^{TM} D-1160 results in a cylindrical morphology with long-range order. In the micrograph (Figure 3.10) the polystyrene cylinders lie parallel and perpendicular to the surface in a polyisoprene matrix as already observed for the macromonomers analysed above. The composition of this commercial TPE is of about 20% polystyrene and its morphology results similar to the macromonomer P(S-I-S)94_30 and more significantly to the macromonomer P(S-I-S)153_30 which has a similar molecular weight. No substantial difference in the domain size can be observed between Kraton^{TM} D-1160 (cylinders diameter 13 nm) and the macromonomers mentioned (cylinders diameter 17 and 8 nm respectively) even if the greater content of polystyrene in the macromonomers should result in a somewhat larger domain size.

In the current work, blends were prepared by co-dissolution in toluene of the Kraton^{TM} D-1160 with the relevant HyperBlock. Blends containing 10% and 30% by weight of HyperBlock were prepared and the impact of the HyperBlock upon the phase-separated morphology of the commercial linear copolymer was investigated by TEM. Blends are multicomponent systems where the polymers take part as components and each of them is strongly influenced by the presence of the other, modifying the overall material properties. The impact of blend composition upon the morphology can clearly be seen by comparing the TEM micrographs of pure Kraton^{TM} D-1160 (Figure 3.10) and the morphology observed for each HyperBlock/Kraton^{TM} D-1160 blend prepared and reported in Figure 3.12 and 3.12.

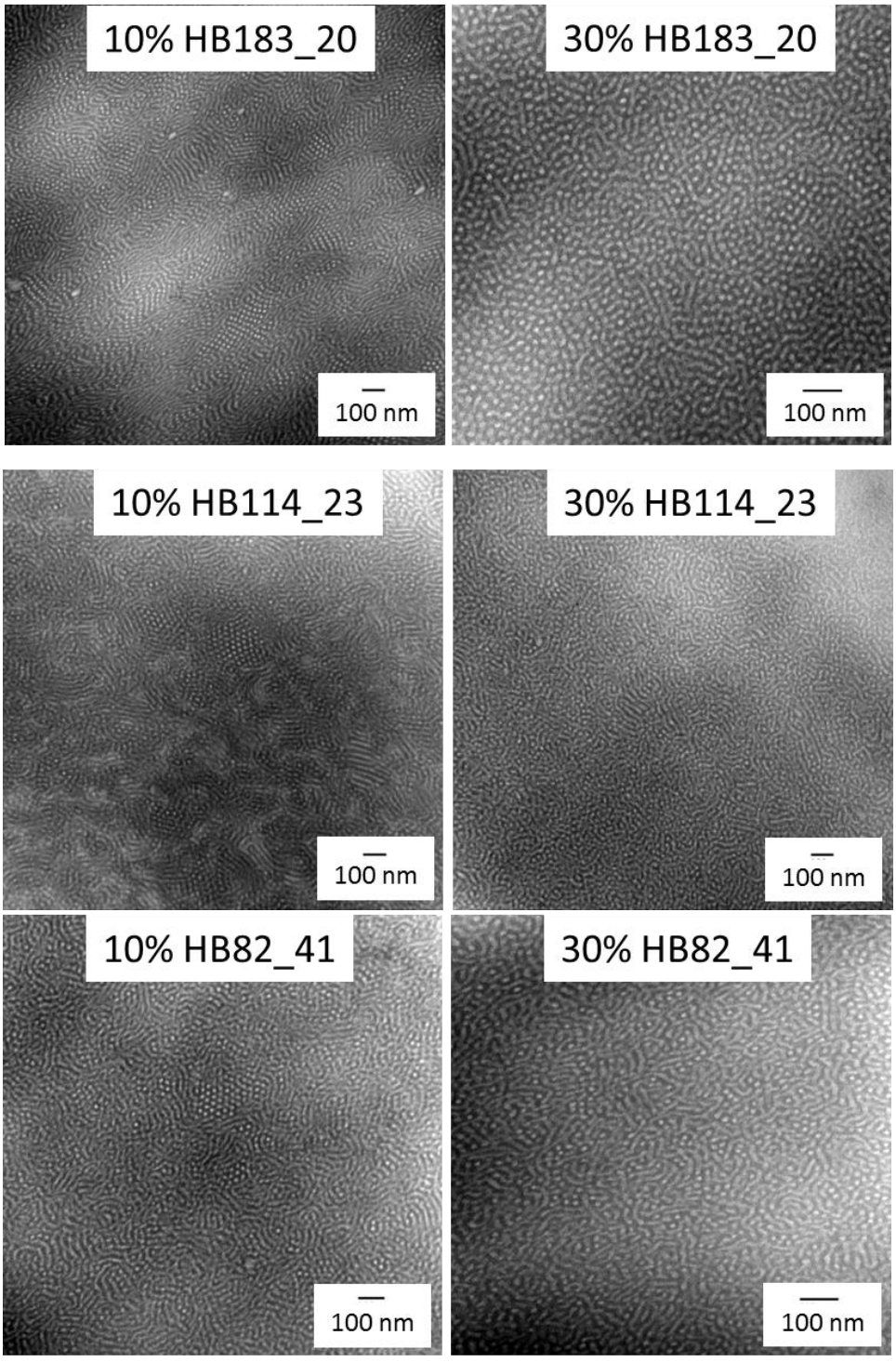

Figure 3.11 TEM micrographs of the binary blends HyperBlock/Kraton^{TM} D-1160. The two types of blends have a content of HyperBlock of 10 and 30 wt. % whose TEM images are reported respectively on the left and right column of the picture. In this figure we compare blends of HyperBlocks with a content of polystyrene of 20 and 40 wt. %.

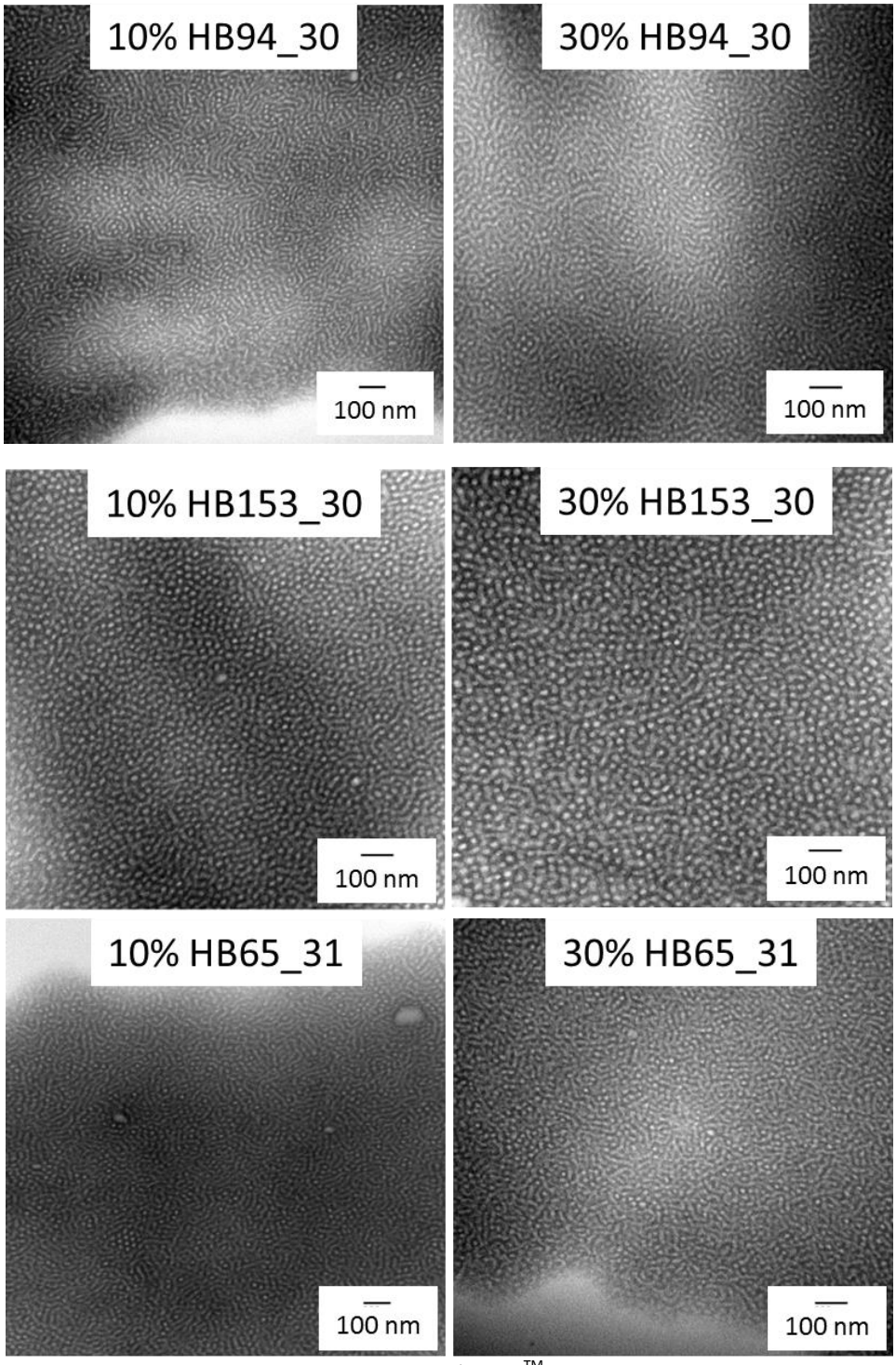

Figure 3.12 TEM micrographs of the binary blends HyperBlock/Kraton^{TM} D-1160. The two types of blends have a content of HyperBlock of 10 and 30 wt. % whose TEM images are reported respectively on the left and right column of the picture. In this figure we compare blends of HyperBlocks with a content of polystyrene of 30 wt. %.

After solvent casting and drying of the films the TEM study reported in Figure 3.11 and 3.12 shows that a microphase separation can be observed in each TEM micrograph for each blend made. Nevertheless it is no longer possible to observe the long-range order that characterised the commercial TPE Kraton^{TM} D-1160 (Figure 3.10). This demonstrates how the presence of even a small amount of HyperBlock in a blend with the linear polymer of the

same nature influences and frustrates the formation of the well-defined morphology. The typical morphology of the linear polymer, which is the main component of the blends, is in fact completely lost. The loss of long-range order is evident in both the 10 and 30 wt. % blends but for the blends at 10 wt. % of HyperBlock small regions of order can be noticed in the morphology pattern in some cases. Therefore the influence of the HyperBlock on the morphology of the Kraton^{TM} D-1160 is once again proved by the disappearance of these small ordered regions in the blends of 30 wt. % HyperBlock, i.e. by the increase of the amount of hyperbranched polymer in the blend. It is as if the presence of the HyperBlock – even as a minor component – can impose the same disorder morphology observed in the pure HyperBlock. Should it turn out that the disordered morphologies are in fact co-continuous then this would imply that relatively small quantities of HyperBlock, derived from macromonomers of any molecular weight and copolymer composition, can impose a disordered and possibly co-continuous morphology upon a simple linear block copolymer. This could have important technological consequences since the co-continuous morphology in a linear block copolymer is represented by a very narrow compositional window in the phase diagram – see Figure 3.4.

3.3 Mechanical Properties of hyperblocks

In Chapter 1 (section 1.3) thermoplastic elastomers (TPEs) were defined and described as an important class of industrial polymers characterised by good mechanical properties. Commercial TPEs are materials with thermoreversible "physical crosslinks" that allow them to be processed as thermoplastics at elevated temperatures and to behave as elastomers at ambient temperatures. TPEs are phase-separated systems, typically block copolymers, where one phase, covalently connected to the second phase, is hard at the temperature of use while the other is a soft elastomeric phase. The "physical crosslinks" formed by discrete glassy phases embedded in a continuous elastomer are responsible for the good mechanical properties of the materials. The hard phase confers to a thermoplastic elastomer its strength and the soft phase provides flexibility and elasticity. The strength of a material is its ability to withstand external forces without breaking. When TPEs break, i.e. at the rupture point, the "physical crosslinks" corresponding to the glassy domains are broken. Typical TPEs are in the form of microphase-separated ABA triblock copolymers where the hard domains are dispersed in a soft domain. Examples are given by polystyrene-polyisoprene-polystyrene (SIS), polystyrene-polybutadiene-polystyrene (SBS) triblock copolymers, linear or star polymers. The presence of more than one branching point in the architecture of TPEs was subsequently developed with the synthesis of multigraft copolymers made of a polyisoprene backbone and polystyrene branches (Figure 3.13) which were regularly spaced and provided with a multifunctional character (tri-, tetra- and hexafunctional branch points).[12,15,16]

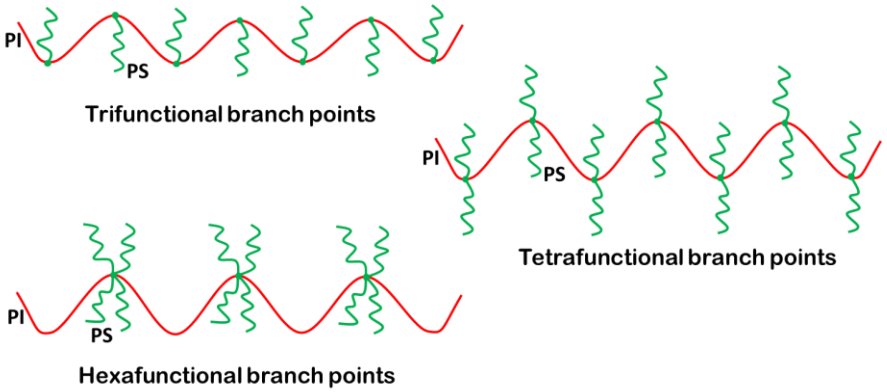

Figure 3.13 Schematic representation of multigraft copolymer of polystyrene (PS in green) and polyisoprene (PI in red) with regularly spaced branch points (tri-, tetra- and hexafunctional branch points).

From the mechanical testing of multigraft copolymers it was observed how both the functionality of the grafting points and the number of junction points along the backbone

influences the mechanical response of the polymers. For instance, for tetrafunctional multigraft copolymers (20 wt. % polystyrene) tensile strength and elongation at break increases linearly with increasing number of junction points. This leads also to a decrease in the long-range order of the morphology showing that a well ordered morphology is not required in order to have good mechanical properties. More recently a new type of multigraft TPEs has been reported by Wang *et al*.[17] This kind of multigraft presented a rigid backbone as the hard domain and soft branches constituting the rubbery matrix in the TPEs showing an opposite structure to the multigraft copolymers mentioned above. In particular the work showed the use of cellulose as rigid backbone and random copolymers poly(*n*-butyl acrylate-*co*-methyl methacrylate) as the grafted arms. By changing the composition of the random copolymer they were able to easily synthesise a wide range of TPEs with desired mechanical properties also with no-long-range order in their morphology. Weidisch *et al*.[18] reported a different type of TPE obtained by the modification of the linear SBS thermoplastic elastomers. The middle rubbery block was substituted by the statistical copolymer poly(styrene-*co*-butadiene). Mechanical tests and morphological studies were carried out in order to investigate the effect of changes in terms of composition of the middle block, overall polystyrene content and molecular weight of the TPEs. By varying these three parameters they showed the possibility to control the mechanical behaviour of modified SBS polymers and to create both highly ductile and brittle block copolymers.

From the above mentioned works it can be asserted that TPEs can be found in the form of linear, star or multigraft copolymers. The constituents are different types of polymers that create rubbery and glassy domains.

Hutchings *et al*. presented a different type of polymer with a hierarchically branched architecture for possible use in the field of thermoplastic elastomers, i.e. the long-chain hyperbranched polymers HyperBlocks. In a previous work[13] it was demonstrated that HyperBlocks possessed potential to be a new class of branched thermoplastic elastomers with their hyperbranched structure and the ABA triblock copolymers of polystyrene and polyisoprene constituting each linear segment. (Figure 3.14) The peculiarity of this hyperbranched materials is found in the glassy domains where the polystyrene blocks are covalently connected and the “physical crosslinks” responsible for the good mechanical properties are therein reinforced by the covalent bonds.

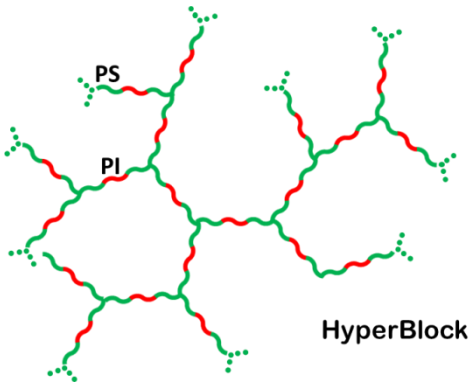

Figure 3.14 Schematic representation of the hyperbranched polymers HyperBlocks. Linear ABA triblock copolymer of polystyrene (PS in green) and polyisoprene (PI in red) are the repeating unit along the structure. The branch points are constituted entirely by polystyrene.

The mechanical tensile testings carried out on a single sample of HyperBlock and on blends of it with a commercial TPE, showed that the pure HyperBlock had a higher ultimate tensile stress (UTS) and a lower elongation at break than the commercial TPEs. Furthermore an interesting result was found in the analysis of a blend of the commercial TPE with 10% w/w of the HyperBlock. The mechanical properties were improved: both the elongation at break and the ultimate tensile stress were higher than the commercial TPE. (Chapter 1 – Figure 1.11)

In the current work a range of both linear precursors macromonomers and HyperBlocks synthesised has been submitted to tensile tests in order to study their mechanical properties and compare them to the commercial thermoplastic elastomer Kraton^{TM} linear D-1160. In addition three types of blends have been analysed: 10, 20 and 30 wt. % of HyperBlocks with Kraton^{TM} D-1160.

3.3.1 Mechanical properties by tensile testing

Materials subjected to a mechanical stress can respond in different ways directly related to their mechanical properties. Tensile test (or tension test) is a type of mechanical test carried out in order to determine the tensile stress-strain properties of the materials. The procedure is simple and several standards that regulate the test can be found for several types of materials, from thermoplastic rubbers to metals. The process of the test, as shown in Figure 3.15, consists in pulling a test piece placed in the tensile-testing machine by applying a constant tension until the test piece breaks. During the uninterrupted stretching of the

specimen, the elongation, i.e. the change in length of the test piece, and the strength of the materials are recorded by a computer-based data acquisition method.

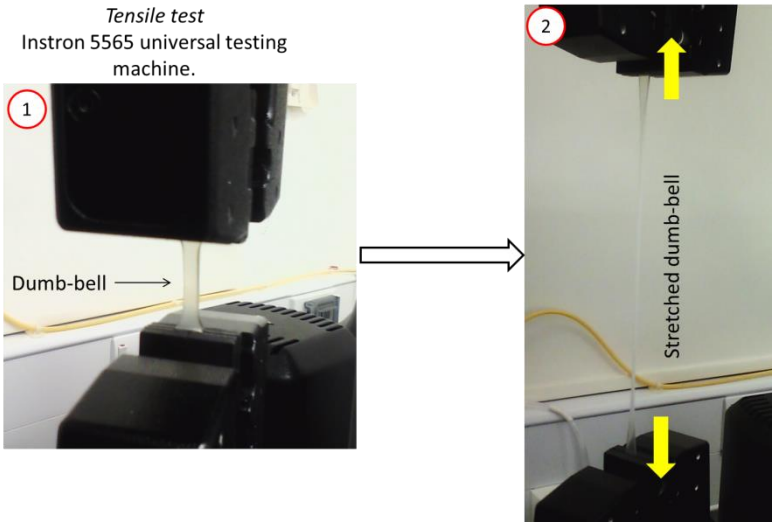

Figure 3.15 Dumb-bell sample before (1) and during (2) the tensile testing carried out with the universal testing machine Instron 5565.

The test piece can have several shapes (e.g. dumb-bells, dog-bones, rings) and in this work it was decided to use the dumb-bell shape represented in Figure 3.16.

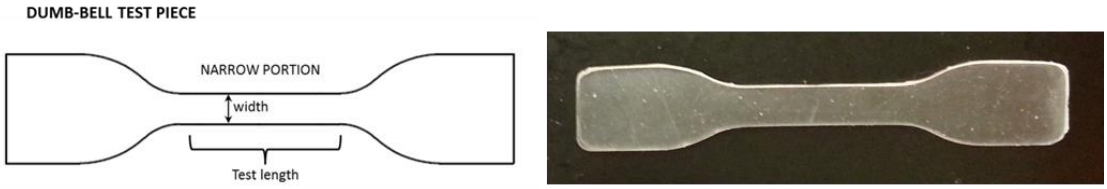

Figure 3.16 On the left schematic representation of a dumb-bell specimen. The narrow portion has an exact width, test length and thickness in accordance to the standard chosen for the test (in this work standard ISO37). On the right a dumb-bell samples prepared with Kraton^{TM} D-1160.

The tensile profile of the material analysed is represented by a stress-strain curve (Figure 3.17) that describes how the material reacts to the applied force. Tensile stress (σ) is expressed in megapascals (MPa) and it is given by the ratio of the applied force (Newton) to the area of the narrow portion (Figure 3.16) of the dumb-bell test piece. Strain (or elongation) (ε) is usually expressed in percentage and represents the increase of the length of the test narrow portion.

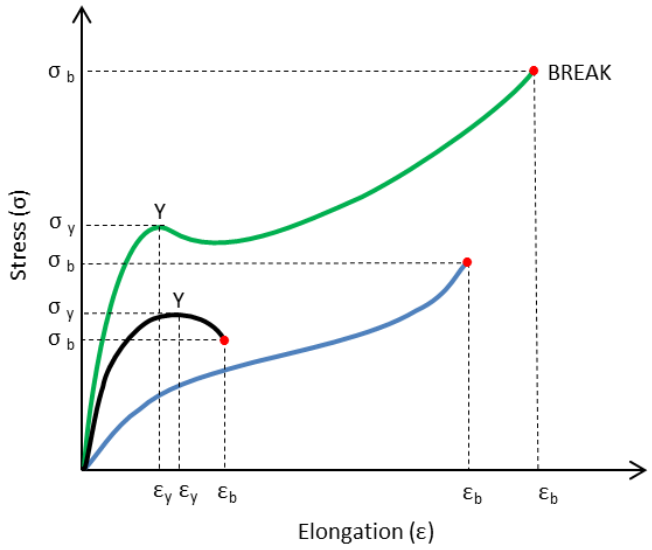

Figure 3.17 Stress-strain curves of the possible behaviour of three different materials. The curves are characterised by the presence of the point of break (red dots) and (but not necessarily) of the yield point (Y).

Stress-strain curves describe the mechanical properties of the materials and its shape depends strongly on the type of material analysed and the experimental conditions of the test. The properties that can be measured and/or calculated from these curves are tensile strength, elongation at break, stress at a given elongation, Young's modulus, elongation at a given stress and elongation and stress at yield. In Figure 3.17 it is possible to observe the yield point (Y) which gives the values of stress and strain at yield. The yield point is found at either a point of inflection (green curves in Figure 3.17) or a maximum (black curve in Figure 3.17) and it represents the point at which the stress does not increases for some further increase in strain. A second important point along the stress-strain curve is represented by the point of break or rupture of the test piece. At this point stress and strain at break can represent the maximum tensile stress (ultimate tensile strength UTS) and the maximum elongation recorded during the test as for the green and blue curves in Figure 3.17. For the black curve in Figure 3.17 the maximum tensile stress is found at the yield point (σ_y) while the tensile stress at break (σ_b) is at a lower value.

The majority of tensile tests show a stress-strain curve where the initial portion is characterised by a linear region where the stress is proportional to the strain. The equation that defines this linear region is the Hooke's law. (Eq. 3.1)

$$E = \sigma/\varepsilon \qquad (3.1)$$

The ratio of the stress (σ) to the strain (ε) is a constant E that corresponds to the slope of the linear region. E is called Young's Modulus and measures the stiffness of the material tested.

The linear region represents the elastic region of the material, in fact, within this region the stretched material can return to its original shape once the applied force has been removed. When the curve stops following Hooke's law, the material enters the plastic region where each deformation that occurs in the specimen is permanent and the deformation remains after removal of the applied force. The yield point (Y) defines the start of the plastic region. A material that breaks before the plastic deformation is a brittle and hard material like, for instance, polystyrene. A tough plastic like polyethylene results in a stress-strain curve resembling the green curve of Figure 3.17 which is characterised by the elastic region, the yield point and the plastic region.

3.3.1.1 Macromonomers tensile tests

Macromonomers P(S-I-S) were tested at a cross-head speed of 200 mm/min and the typical stress-strain curves obtained for each sample tested are shown in Figure 3.18.

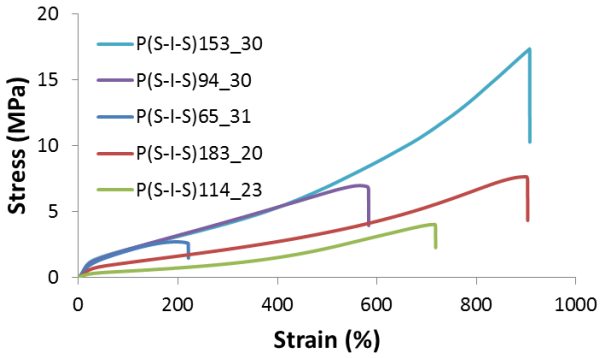

Figure 3.18 Representative tensile stress-strain curves for a series of macromonomers which vary in molecular weight and polystyrene content.

The curves show a clear elastomeric behaviour for each sample as expected for linear SIS polymers. There is an overall increase in tensile strength with increasing polystyrene content and increasing molecular weight of the triblock copolymer. This is due to the increased rigidity and toughness provided by the increasing polystyrene content and the increasing molecular weight of the polystyrene block.

For both the two set of samples containing respectively 20 and 30 wt. % polystyrene, it can be seen that an increase in the molecular weight of the samples results in an increase in both the elongation at break and the tensile strength at break. (Figure 3.19)

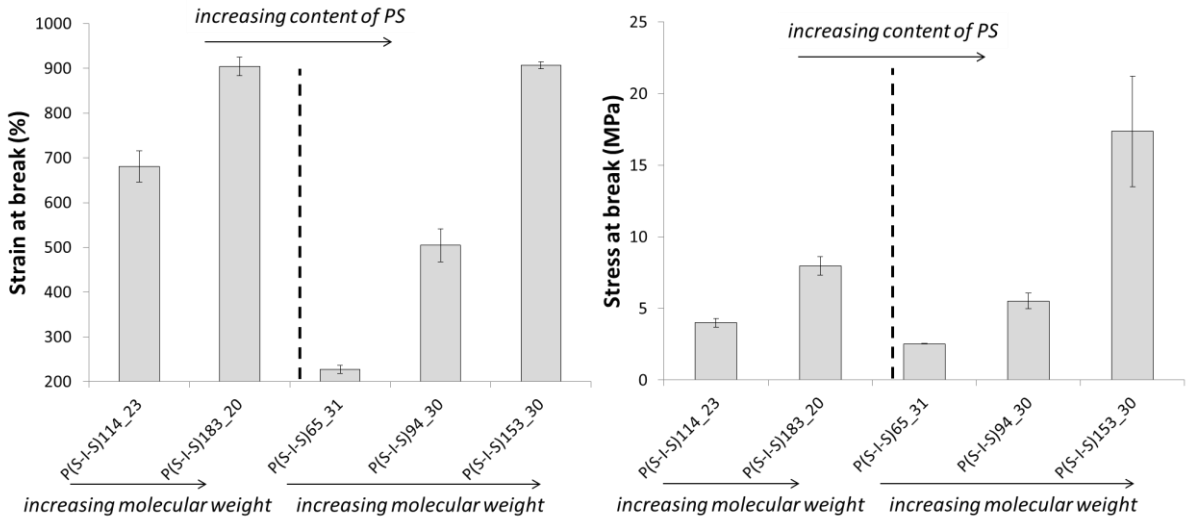

Figure 3.19 Strain and strength at break for the series of macromonomers P(S-I-S) analysed by tensile tests.

The results are in accordance with the morphologies found for each polymer and reported in the previous section 3.2.1.1. The passage from a low to a higher strength at break corresponds to the change of the morphology from spheres ((P(S-I-S)183_20 and P(S-I-S)114_23) to cylinders (P(S-I-S)65_31, P(S-I-S)94_30 and P(S-I-S)153_30) in correspondence to the change of polystyrene content from 20 to 30 wt. %. The Young's modulus of each macromonomer is showed in Figure 3.20.

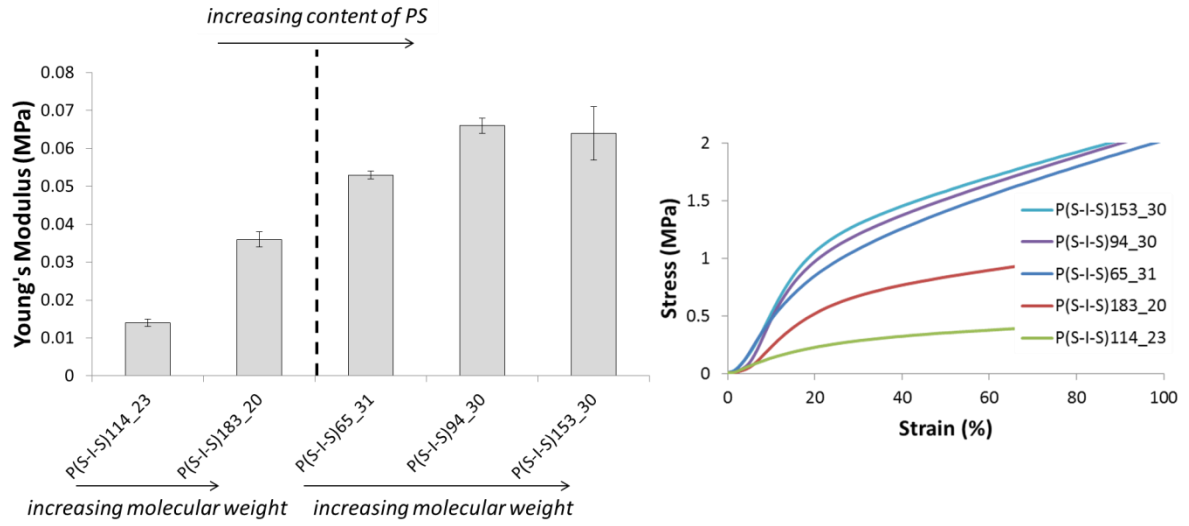

Figure 3.20 Graph of the modulus values obtained from the tensile tests of the macromonomers (left) and expanded stress-strain curve at low deformations in correspondence of the elastic region (right).

Higher values of E are observed for the macromonomers containing 30 wt. % of polystyrene meaning enhanced mechanical reinforcement.

3.3.1.2 Hyperblock and blends tensile tests

Under the same tensile test conditions as describe above, the pure HyperBlock HB114_23 and three blends of the commercial TPE Kraton™ D-1160 (Table 3.2) with respectively 10, 20 and 30 wt. % of HB114_23 were tested. Figure 3.21 shows the variation in terms of tensile strength and strain at break and Young's modulus for the pure HyperBlock and for each blend compared with the precursor macromonomer and Kraton™ D-1160.

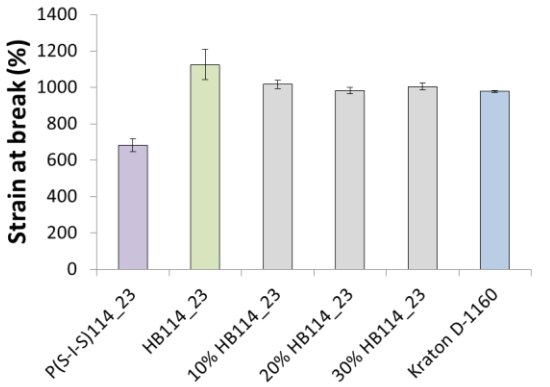

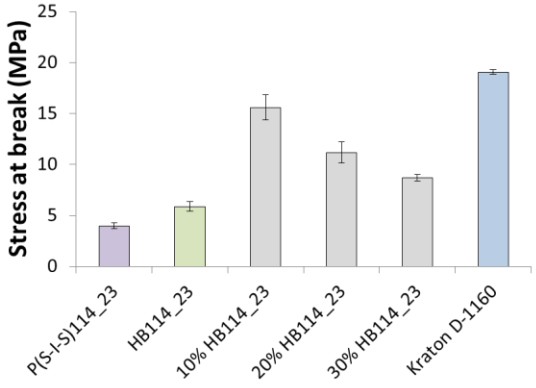

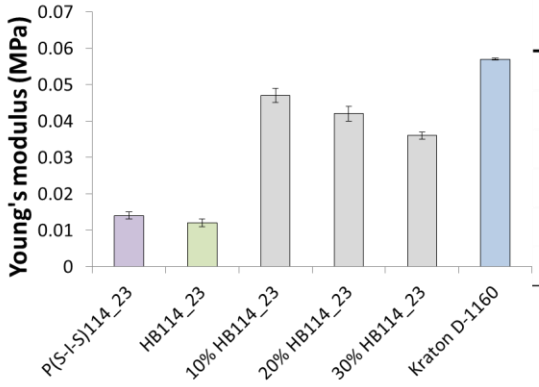

Sample	Young's modulus (MPa), E ± SD	Tensile strength (MPa), σ_{UTS} ± SD	Strain at break (%), ε_b ± SD
P(S-I-S)114_23	0.014 ± 0.001	3.99 ± 0.30	681 ± 35.1
HB114_23	0.012 ± 0.001	5.88 ± 0.48	1125 ± 82.4
10% HB114_23	0.047 ± 0.002	15.60 ± 1.24	1018 ± 22.9
20% HB114_23	0.042 ± 0.002	11.17 ± 1.04	984 ± 17.8
30% HB114_23	0.036 ± 0.001	8.67 ± 0.32	1005 ± 18.6
Kraton™ D-1160	0.057 ± 0.0004	19.06 ± 0.23	978 ± 5.2

Figure 3.21 Comparison of strain and stress at break and Young's modulus of the macromonomer P(S-I-S)114_23 and the resulting HyperBlock HB114_23, the commercial TPE Kraton™ D-1160 and the blends of 10, 20 and 30 wt. % of HB114_23 with the same commercial TPE. The table reports the corresponding data values with standard deviation (SD).

Observing the data in Figure 3.21 it is possible to make several observations regarding the behaviour of polymer specimens submitted to mechanical tests. The conversion of the linear macromonomer P(S-I-S)114_23 to hyperbranched polymer HyperBlock HB114_23 confers to the material higher value of strain at break (from 681 to 1125 %) and higher stress at break (from 3.99 to 5.88 MPa). The Young's modulus shows instead a slightly lower value for the HyperBlock in comparison with the linear macromonomer (0.012 and 0.014 MPa respectively). These data and the representative stress-strain curves in Figure 3.22 show that the presence of the branched points along the structure of the HyperBlock provides enhanced mechanical properties compared to the linear macromonomers.

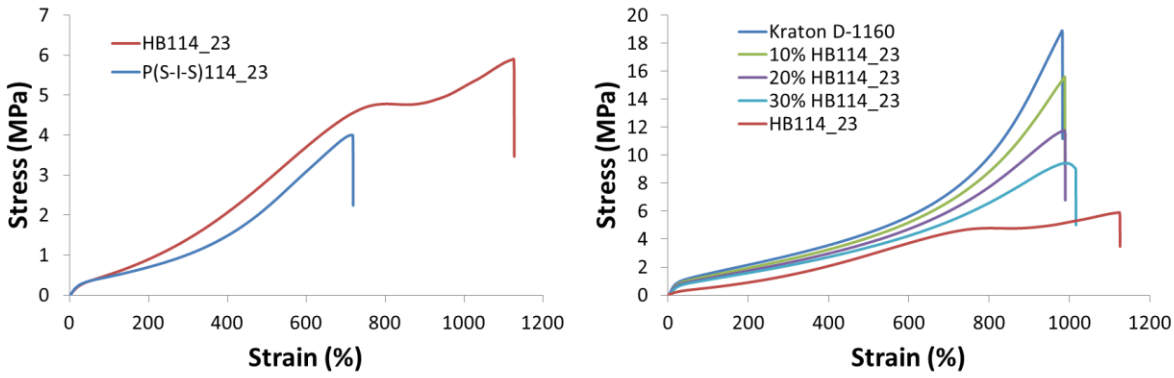

Figure 3.22 Representative tensile stress-strain curves for P(S-I-S)114_23 and HyperBlocks, compared in the graph on the left, and stress-strain curves for Kraton™ D-1160 and blends compared with HB114_23 in the graph on the right.

The "physical crosslinks" formed in the linear macromonomer by chain entanglements are reinforced in the HyperBlock by the covalent bonds that connect together the polystyrene blocks. Thus, the combination of chain entanglement and covalently bonded branch points results in a positive effect on the mechanical properties and it leads to an increase in both the toughness and elasticity of the polymer. The morphologies of the two polymers do not help to explain such a different behaviour in mechanical properties. The macromonomer P(S-I-S)114_23 was characterised by a spherical morphology and the subsequent HyperBlock, HB114_23, even if it had the same content of polystyrene (23 wt. %), showed a macrophase separation with no long-range order. Thus the improvement of the mechanical properties in the HyperBlock cannot be easily explained by means of the morphology results. By comparing the results of P(S-I-S)114_23 (macromonomer) and HB114_23 (HyperBlock) with the data for the commercial TPE (Figure 3.22), it can be seen that whilst the strain at break of the HyperBlock is higher than the value of Kraton™ D-1160, the other two parameters, stress and Young's modulus, are far below the values obtained for Kraton™ D-1160 (table in Figure 3.21). P(S-I-S)114_23 shows lower values for all the three parameters in comparison with Kraton™ D-1160. Each of these materials differs from one another by their polymer architecture and molecular weight. While the content of polystyrene for Kraton™ is about the same of the tested macromonomer and HyperBlock (20 and 23 % respectively), the molecular weight (M_n) calculated by SEC (dn/dc 0.185) is 89500 g mol^{-1} for Kraton™ D-1160 and 44400 g mol^{-1} for P(S-I-S)114_23. In terms of the polymer architecture, the comparison is between two linear polymers (Kraton™ D-1160 and P(S-I-S)114_23) and a hyperbranched polymer (HyperBlock). The morphology analysis by TEM reported in the previous section (Section 3.2) showed a well-defined cylindrical and spherical morphology

for Kraton™ D-1160 and P(S-I-S)114_23 respectively, while a phase separation with no long-range order was observed for the Hyperblock. Thus the different stress-strain curves obtained can be explained in terms of these data. The worse mechanical properties of P(S-I-S)114_23 in comparison to Kraton™ D-1160 are consistent with the change in morphology from spheres to cylinders and the change in M_n that both causes the P(S-I-S)114_23 to have lower elongation and stress at break than the commercial TPE. The stress-strain curve of the HyperBlock can be explained in terms of the change in architecture, as discussed above. In addition the HyperBlock morphology, with no long-range order, highlights the fact that well order morphology is not necessary to achieve good mechanical properties.

Regarding the blends of HB114_23 with Kraton™ D-1160, the results show that the strain at break of each blend is maintained around the value of the pure Kraton™. On the other hand, the stress at break is lower than the value of the Kraton™ for each blend, higher than the value of the pure HyperBlock and decreasing with increasing content of HyperBlock in the blend. Similar trends in behaviour are observed for the Young's modulus that also decreased with an increasing content of HyperBlock in the blends. It is worth noting that a low Young's modulus, denoting a flexible material, is a desirable property in many applications of the TPEs.

Thus, in this case the addition of the HyperBlock HB114_23 to the commercial TPE does not affect the strain at break but it worsens the values of the ultimate stress at break of the commercial TPE. In a certain way the blends show intermediate mechanical properties between the two constituents. Observing Figure 3.22 it is in fact possible to notice a shift of the representative stress-strain curves of the blends from the Kraton™ D-1160 curve toward the HB114_23 curve with increasing amount of HB114_23. This behaviour cannot be explained by the content of polystyrene in the blends. In fact with the increasing amount of HyperBlock in the blends, and so increasing amount of polystyrene, we should notice the opposite behaviour; the material should become tougher instead of more elastic, as it has been observed here.

3.3.1.3 Blends at comparison

Further tensile tests were carried out on blends resulting from the addition of a different HyperBlock to Kraton™ D-1160. After testing blends of Kraton™ D-1160 with HB114_23,

two other HyperBlocks were used: HB94_30 and HB153_30. An overview of all the several blends tested is presented in Table 3.4 along with the values of tensile stress and strain at break and Young's modulus obtained by testing dumb-bell specimens at a constant cross-head speed.

Table 3.4 Mechanical properties of pure Kraton™ D-1160 and blends of Kraton™ D-1160 with HyperBlocks HB114_23, HB94_30, HB153_30. For HB114_23 and HB94_30 three types of blends are listed below, each containing respectively 10, 20 and 30 wt. % of the specific HyperBlock. For HB153_30 only the 10 wt. % blend is reported.

sample	Young's modulus (MPa), E ± SD	Tensile strength (MPa), σ_{UTS} ± SD	Strain at break (%), ε_b ± SD
10% HB114_23	0.047 ± 0.002	15.60 ± 1.24	1018 ± 22.9
20% HB114_23	0.042 ± 0.002	11.17 ± 1.04	984 ± 17.8
30% HB114_23	0.036 ± 0.001	8.67 ± 0.32	1005 ± 18.6
10% HB94_30	0.057 ± 0.002	18.15 ± 1.22	981 ± 19.4
20% HB94_30	0.059 ± 0.005	18.59 ± 1.53	959 ± 10.9
30% HB94_30	0.053 ± 0.008	13.97 ± 0.94	877 ± 2.1
10% HB153_30	0.028 ± 0.001	18.17± 1.69	993 ± 32.5
Kraton™ D-1160	0.057 ± 0.0004	19.06 ± 0.23	978 ± 5.2

With the addition of a different HyperBlock to the commercial TPE it is possible to observe a different trend of the stress-strain curves compared to the blends described above made of Kraton™ D-1160 and HB114_23. In Figure 3.23 a comparison of representative stress-strain curves of Kraton™ D-1160 and different blends containing 10 wt. % of three different HyperBlocks shows the changes in the mechanical properties of the commercial TPE due to the HyperBlock addition.

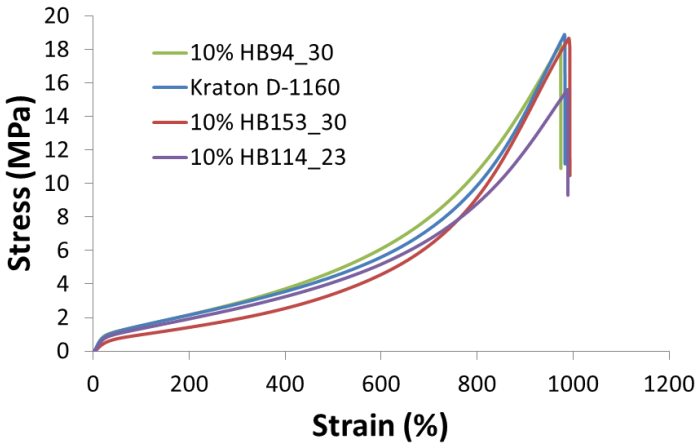

Figure 3.23 Representative tensile stress-strain curves for Kraton™ D-1160 compared with tensile stress-strain curves of three types of blend containing each the same amount (10 wt. %) of different HyperBlocks: HB94_30, HB114_23 and HB153_30.

It can be stated that for each blend the strain at break is maintained around the value of the pure commercial TPE (978%). The stress at break, corresponding to the ultimate tensile

stress, is only slightly lower for the blend with HB114_23. In addition small variations are observed in the shape of the blends curves in comparison to the commercial TPE.

The effect of blending two different types of HyperBlock with the commercial TPE can be observed by comparing the two sets of blends made by using HB114_23 and HB94_30 respectively. The data of stress and strain at break and Young's modulus are reported and compared in the graphs in Figure 3.24.

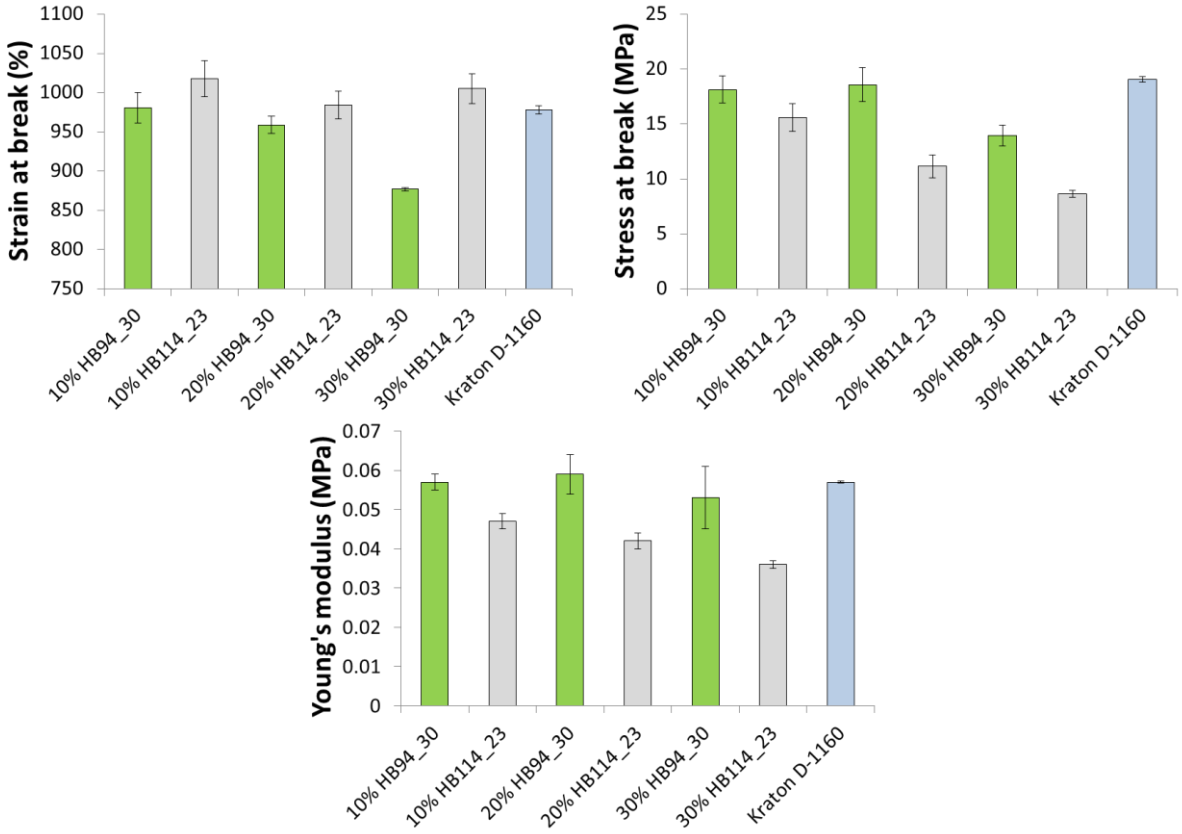

Figure 3.24 Schematic graphs comparing the value of strain and stress at break and Young's modulus for the blends of Kraton^{TM} D-1160 with 10, 20 and 30 wt. % of the two HyperBlocks HB114_23 and HB94_30. Each graph also reports the corresponding value for the pure Kraton^{TM} D-1160.

The blend employing HB94_30 showed lower values of strain at break for each blends (10, 20 and 30 wt. % of HB94_30) in comparison with both Kraton^{TM} D-1160 and blends with HB114_23. In terms of stress at break and Young's modulus the values obtained are higher than the blends employing HB114_23 but almost of the same value of the pure commercial TPE. This difference may be explained with the different content of polystyrene of the two HyperBlocks employed in the blends (23 and 30 wt. %). Higher content of polystyrene reinforces the (Kraton^{TM} D-1160/HB94_30) blends resulting in a less elastic polymer which is more resistant to the force applied in comparison with (HB114_23/Kraton^{TM} D-1160) blends. The pure HyperBlock HB94_30 could not be tested under the same conditions so it was not

possible to compare the mechanical properties with the blends showed here and observe if the blends have intermediate properties as shown by the other set of blends with HB114_23. Nevertheless, also for this set of blends with HB94_30 the morphologies for each blends appeared to be macrophase separated but with no long-range order and once again the morphology appears to be disconnected from the mechanical response. In conclusion it can be noticed that whilst the addition of small quantities of HyperBlock has a dramatic impact upon the morphology, as seen in section 3.2.1.3, the impact upon mechanical properties is limited. In addition, the data here reported for the mechanical tensile testings are representative data. In fact, only part of the materials synthesised could be tested and a fuller investigation into the mechanical properties is ongoing.

3.4 Experimental

3.4.1 Differential Scanning Calorimetry (DSC)

Thermal analysis of the synthesised macromonomers and HyperBlocks was carried out using two different methods, on two different instruments. Firstly using a TA Instruments Q1000 Series differential scanning calorimeter (DSC) and a heating cycle of: room temperature to 150°C at 20°C/min, 150°C to -90°C at 20°C/min, -90°C to 150°C at 20°C/min and between each temperature ramp a 2 minute isothermal period was applied. Measurements were carried out under nitrogen. Secondly, further thermal analysis was carried out using a Perkin-Elmer Pyris 1 DSC instrument calibrated with indium. Thermal behaviour was investigated by heating the samples from room temperature to 200°C at 400°C/min. The heating cycle was: room temperature to 200°C at 400°C/min, 200°C to 20°C at 400°C/min, isothermal step of 4 min at 20°C, 20°C to 200°C at 400°C/min. Measurements were carried out under nitrogen. Sample weights used in both measurements were between 1 and 15 mg.

3.4.2 Transmission Electron Microscopy (TEM)

The preparation of the polymers films submitted for TEM analysis was carried out by solvent casting. Macromonomers, pure HyperBlocks and blends of 10 and 20 wt. % of HyperBlocks with Kraton^{TM} D-1160 were cast from solutions (6% w/v for HyperBlocks and 30% for macromonomers) in toluene onto aluminium plates. The films were allowed to dry at room temperature and atmospheric pressure for one day and then under vacuum to constant weight.

Samples for TEM analysis were prepared by cryo-ultramicrotomy using a Leica EM UC6 Ultramicrotome and Leica EM FC6 cryochamber (Milton Keynes, UK). Cryosections of 50–70 nm thickness were cut using a cryo 35° diamond knife (Diatome, Switzerland) at a temperature between -120°C and -140°C and then manipulated from the knife edge onto formvar coated grid. Sections were stained for 2-4 hrs with osmium tetroxide (OsO_4) vapour then viewed with a Hitachi H7600 transmission electron microscope (Hitachi High Technologies Europe) using an accelerating voltage of 100KV. The TEM measurements were carried out in collaboration with Dr. Christine Richardson, School of Biological and Biomedical Sciences, Microscopy & Bioimaging at Durham University.

3.4.3 Mechanical Testing

Tensile tests were performed according to standard ISO37 – "Rubber, vulcanized or thermoplastic – determination of tensile stress-strain properties". The polymer samples for the analysis of the mechanical properties were prepared by solvent casting. A solution in toluene of each macromonomer, HyperBlock and blend of 10, 20 and 30 wt. % of HyperBlock with Kraton^{TM} D-1160 was cast onto rectangular molds of polytetrafluoroethylene (PTFE) with a base of siliconised paper. The films were allowed to dry at room temperature and atmospheric pressure for at least three days and then under vacuum to constant weight. The rectangular-shaped film obtained was then cut into dumb-bell test pieces by using a fixed-blade cutter and a press. The dimensions of each test piece are in accordance with standard ISO37 specifications and are reported in the following Figure 3.25.

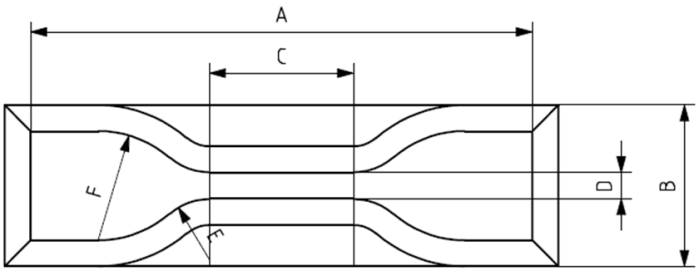

Dimension	Type 3
A Overall length (mm)	50
B Width of ends (mm)	8.5 ± 0.5
C Length of narrow portion (mm)	16 ± 1
D Width of narrow portion (mm)	4 ± 0.1
E Transition radius outside (mm)	7.5 ± 0.5
F Transition radius inside (mm)	10 ± 0.5

Figure 3.25 Dimension of the cutting die used for the dumb-bell test piece Type 3. The dumb-bell test piece dimensions correspond to A, C, D and F.

The standard thickness of the dumb-bell test piece in correspondence of section C was 2.0 ± 0.2 mm for the chosen test piece (Type 3) and a minimum of three test pieces were tested. The thickness was measured using a digital micrometre.

Tensile testing of the samples was performed at 23°C at a constant nominal rate of traverse of the moving grip (cross-head speed) of 200 mm/min. The instrument used was an Instron 5565 universal material testing machine provided with pneumatic grips and rubber-coated jaw faces. The measurements were carried out at the industry Kraton^{TM} Polymers Research placed in Amsterdam thanks to the kind collaboration of Dr. Marianne Stol.

3.5 Conclusions

We have investigated the thermal properties, the morphology and the mechanical properties of macromonomers, HyperBlocks, commercial TPEs and blends of HyperBlocks with a commercial TPE, i.e. linear triblock copolymer of PS-PI-PS Kraton^{TM} D-1160 to establish the impact of polymer architecture upon physical properties.

The thermal analysis of the polymer synthesised during this work showed the presence of two T_gs for both macromonomers and HyperBlocks. The presence of the two T_gs, corresponding to the T_g of the polyisoprene block and polystyrene blocks, confirms the microphase separation of the polymers into discrete domains of polyisoprene and polystyrene. The T_g found for the polyisoprene block was found to be at a somewhat higher temperature (ca. -58°C) than the literature value for 1,4-cis polyisoprene while the polystyrene block showed a T_g lower (ca. 85°C) than the value of pure polystyrene T_g. The shift of the glass transition is mainly due to the influence that each block exerts on each other: the polyisoprene block softens the polystyrene blocks while the polystyrene blocks have the opposite effect on the polyisoprene block.

The study of the solid-state morphology of the linear macromonomers (PS-PI-PS triblock copolymers) showed microphase separation into different morphologies in broad agreement with the theoretical predictions for linear ABA triblock copolymers morphology. By varying the content of polystyrene it was possible to observe spherical morphology [P(S-I-S)183_20 and P(S-I-S)114_23] and cylindrical morphology [P(S-I-S)94_30, P(S-I-S)153_30 and P(S-I-S)65_31]. It was found that the conversion of these linear macromonomers to the highly branched block copolymers, HyperBlocks, resulted in the loss of the long-range, well-ordered morphologies associated with the macromonomers. The highly branched architecture of the HyperBlocks is undoubtedly the factor responsible for frustrating and inhibiting the long range order. The effect of HyperBlocks structure on the solid-state morphology was also observed in blends of Kraton^{TM} D-1160 with 10 or 30 wt. % of HyperBlock whereby the presence of even small amounts (10%) of HyperBlock in these blends dramatically influences and frustrates the formation of the well-defined cylindrical morphology which is characteristic of Kraton^{TM} D-1160.

The mechanical properties of macromonomers and HyperBlocks demonstrated that the highly branched architecture acts (as theorised) by improving the mechanical properties of

the linear precursor thanks to the reinforced “physical crosslinks” given by the covalently bonded polystyrene blocks. In particular we noticed that the conversion of the linear macromonomer P(S-I-S)114_23 to hyperbranched polymer HyperBlock HB114_23 confers to the material higher value of strain at break, higher stress at break and lower Young’s modulus. Furthermore it was demonstrated that the absence of the long-range order in the HyperBlock morphology does not result in worsened mechanical properties of the material. Several variations of blends of HyperBlocks with the commercial TPE Kraton^{TM} D-1160 were also tested. Each blend possessed mechanical properties which were intermediate between the pure HyperBlock and the linear TPE but still comparable to the mechanical properties of the commercial TPE.

3.6 References

(1) Cowie J. M. G., Arrighi V., *Polymers: Chemistry and Physics of Modern Materials*, CRC Press, (**2008**)
(2) Mark J. E., *Polymer Data Handbook*, Oxford University Press, (**1999**)
(3) Kroschwitz J. I., *Concise encyclopedia of polymer science and engineering*, John Wiley & Sons Inc., (**1990**)
(4) Bryan E., Smith R., *Polymer A Property Database*, CRC Press, (**2009**)
(5) Widmaier J. M., Meyer G. C. *Macromolecules*, **1981**, *14*, 450-452
(6) Hsieh H. L., Quirk R. P., *Anionic Polymerization: Principles and Practical Applications*, Marcel Dekker I.: (**1996**)
(7) Bates F. S., Fredrickson G. H. *Annu. Rev. Phys. Chem.*, **1990**, *41*, 525-557
(8) Hamley I. W., *The Physics of Block Copolymers*, Oxford University Press, (**1998**)
(9) Matsen M. W. *J. Chem. Phys.*, **2000**, *113*, 5539-5544
(10) Dyer C., Driva P., Sides S. W., Sumpter B. G., Mays J. W., Chen J., Kumar R., Goswami M., Dadmun M. D. *Macromolecules*, **2013**, *46*, 2023-2031
(11) Beyer F. L., Gido S. P., Buschl C., Iatrou H., Uhrig D., Mays J. W., Chang M. Y., Garetz B. A., Balsara N. P., Tan N. B., Hadjichristidis N. *Macromolecules*, **2000**, *33*, 2039-2048
(12) Zhu Y., Burgaz E., Gido S. P., Staudinger U., Weidish R., Uhrig D., Mays J. W. *Macromolecules*, **2006**, *39*, 4428-4436
(13) Hutchings L. R., Dodds J. M., Rees D., Kimani S. M., Wu J. J., Smith E. *Macromolecules*, **2009**, *42*, 8675-8687
(14) Paul D. R., Bucknall C. B., *Polymer blends*, John Wiley & Sons, (**2000**)
(15) Duan Y., Thunga M., Schlegel R., Schneider K., Rettler E., Weidisch R., Siesler H. W., Stamm M., Mays J. W., Hadjichristidis N. *Macromolecules*, **2009**, *42*, 4155-4164
(16) Weidisch R., Gido S. P., Uhrig D., Iatrou H., Mays J. W., Hadjichristidis N. *Macromolecules*, **2001**, *3*, 6333-6337
(17) Jiang F., Wang Z., Qiao Y., Wang Z., Tang C. *Macromolecules*, **2013**, *46*, 4772-4780
(18) Ganß M., Staudinger U., Thunga M., Knoll K., Schneider K., Stamm M., Weidisch R. *Polymer*, **2012**, *53*, 2085-2098

CHAPTER 4

Synthesis of Asymmetric Stars via the Macromonomer Approach

4.1. Introduction

We describe here the synthesis of a series of model asymmetric and symmetric three-arm stars for structure-property (rheology) studies. In each case the star polymers were produced from polystyrene and the arms were produced by living anionic polymerisation. In each case the stars were three-arm stars, with two identical 'long' arms with a molecular weight of 90 kg mol^{-1} whilst the molecular weight of the third 'short' arm was varied from a value of 10 kg mol^{-1} to 90 kg mol^{-1}. Essentially, this series of stars represents a series of linear polymers of identical molecular weight (180 kg mol^{-1}) with a single branch at the centre of the linear chain. The molecular weight of the single branch is in a range from below the entanglement molecular weight of the polystyrene (M_e= 16 kg mol^{-1})[1], approximately equal to M_e and significantly above M_e. In this way it is possible to determine at what point the rheology of the polymer changes from linear-like to star-like thereby indicating how long a branch needs to be before it begins to impact upon rheology. These rheological measurements were carried out by collaborators and will not be discussed in this thesis and we will focus on the description of the synthesis and characterisation of the stars.

Whilst it would be possible to prepare such a series of stars by the more traditional arm-first methodology and chlorosilane coupling (described in Chapter 1), it would not be possible to produce a series in which the effective chain length of the linear polymer was identical in every case. Clearly for such a study it is preferable that the only variable be the length of the 'short' arm branch. The 'macromonomer' approach described here is the only method capable of producing such a set of stars with the desired degree of control over the molecular structure. The arms were synthesised by living anionic polymerisation and then characterised by Size Exclusion Chromatography (SEC) and Nuclear Magnetic Resonance Spectroscopy (NMR). The star polymers were prepared in a separate coupling reaction, either by a Williamson or copper (I)-catalysed azide-alkyne 'click' coupling reaction and the resulting stars purified by fractionation to obtain well-defined, structurally homogeneous branched polymers. The efficiency of the two coupling methods are compared and the star polymers characterised by both SEC and Temperature Gradient Interaction Chromatography (TGIC).

4.2. Results and discussion

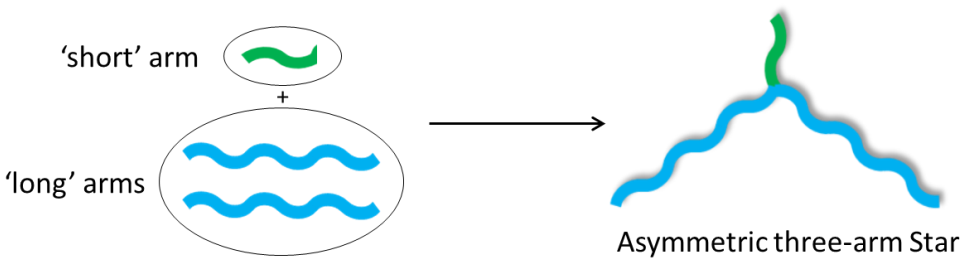

Figure 4.1 General scheme for the synthesis of asymmetric three-arm stars via 'macromonomer' approach.

The general concept of the synthesis of three-arm stars via the 'macromonomer' approach is shown in **Figure 4.1.** It can be seen that the stars are prepared by the coupling of two 'long' arms – each with a reactive functionality at one chain end – to a 'short' arm carrying a difunctional end group. Two different coupling strategies were investigated and compared, each requiring different reactive groups. The synthesis of the arms, the introduction of the appropriate functional groups and the coupling strategies are described below.

4.2.1. Synthesis of the 'arms'

The synthesis of the arms was carried out by living anionic polymerisation but in order to allow the successful subsequent coupling of the arms to create stars, two different procedures were required for the 'long' and the 'short' arms respectively. Each type of arm used a different initiator and the synthesis of the 'short' arm required the use of a particular end-capping agent to introduce the desired chain-end functionalities. In order to produce stars in which the molecular weight of the 'long' arm was identical in each case, the synthesis of the 'long' arm was carried out on a large scale to ensure the same 'long' arm could be used for all the stars created.

The two coupling reactions chosen for the assembly of the stars were the Williamson coupling reaction and the copper (I)-catalysed azide-alkyne 'click' reactions.[2-4] These methods combined with the use of living anionic polymerisation used for the arms synthesis allowed the synthesis of well-defined star polymers with an exact number of arms and narrow molecular weight distributions and more importantly a series of stars in which the 'long' arm was identical in all cases. The Williamson coupling reaction technique has been previously used by our group for the synthesis of other types of branched polymers.[5-7] The

ether linkage formed in this reaction is stable and its formation requires functionalities that can be easily introduced onto the polymer chain ends during the living anionic polymerisation and by deprotection and conversion reactions. The 'click' coupling reaction has been used widely for polymer synthesis and has proved an efficient reaction for the synthesis of several polymer architectures, including block copolymers, cyclic polymers, star-shaped polymers, hyperbranched and dendritic polymers.[8]

4.2.1.1. Synthesis of the end-functionalised polystyrene 'long' arm

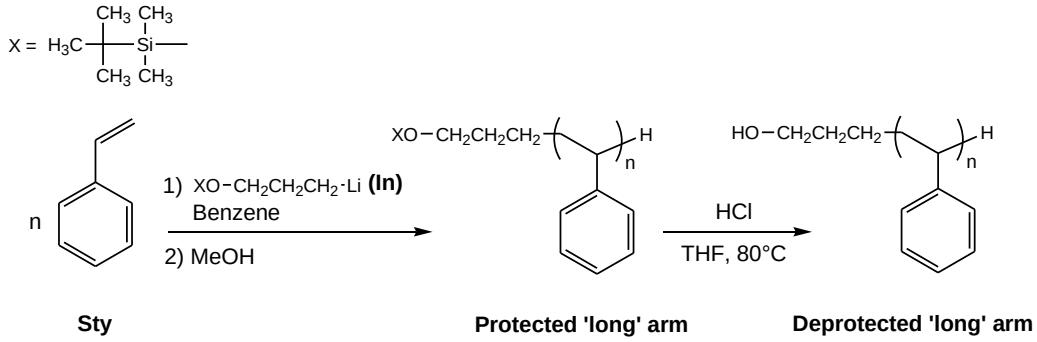

Scheme **4.1** Synthesis of the polystyrene 'long' arm via living anionic polymerisation and subsequent deprotection of the primary alcohol functionality at one chain end of the polymer.

The first step in the synthesis of the stars was the preparation of the end-functionalised polymer that would be the 'long' arm in the stars. The chosen monomer, styrene, was polymerised by living anionic polymerisation under high-vacuum conditions at room temperature with benzene as the solvent. (Scheme 4.1) An initiator (**In**) 3-*tert*-butyldimethylsiloxy-1-propyllithium with a protected primary alcohol functionality was selected to introduce a functional end group which could be modified in subsequent reactions.[5] After addition of the initiator to the solution of styrene in benzene, the appearance of an orange/red colour, typical of living polystyryllithium was observed. The Lewis base N,N,N',N'-tetramethylethylendiamine (TMEDA) was added before the injection of the initiator to ensure rapid initiation of the polymerisation. This was necessary since *n*-alkyllithium initiators of the type employed generally result in polymers with a relatively high dispersity index due to the fact that the rate of initiation is slow in comparison with the rate of propagation. The aggregation of alkyllithium that causes this phenomenon is prevented by the addition of a Lewis base additive such as TMEDA and the rate of initiation increases, resulting in the desired low dispersity of the polymers. The reaction was left stirring overnight to allow complete consumption of the styrene and then terminated with nitrogen-

sparged methanol. The target molecular weight of the 'long' arm was intended to be several (5 – 6) times M_e and the resulting polymer had a molecular weight (M_n) equal to 89,900 g mol^{-1} and a dispersity index of 1.03. The polymer was also analysed by ^{1}H-NMR spectroscopy (see Figure 4.2).

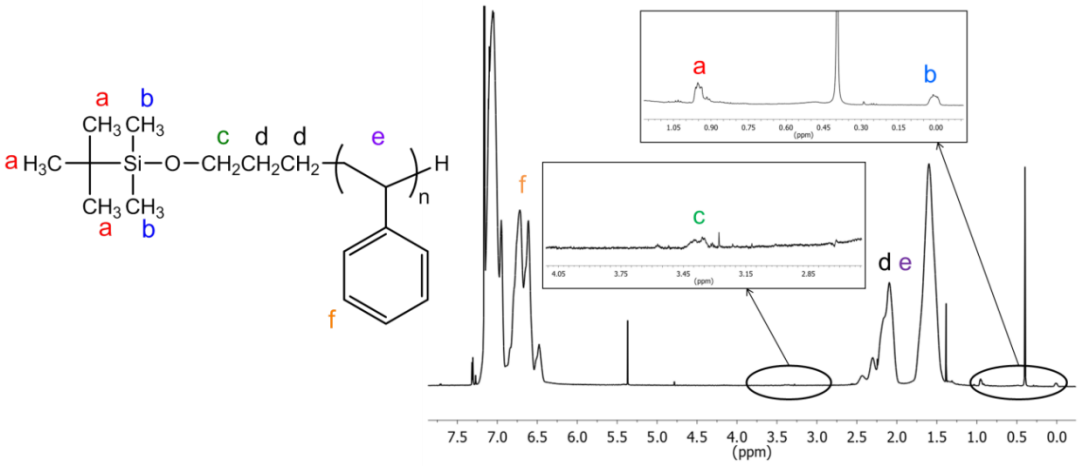

Figure 4.2 ^{1}H-NMR spectrum of the protected polystyrene 'long' arm in C_6D_6 (700 MHz). (Peak at 0.4 ppm corresponding to H_2O protons)

The initiator carries a primary alcohol functionality protected by a silyl group and the corresponding ^{1}H-NMR signals from the protecting group can be identified on the spectrum at 0.0 ppm [(C**H**$_3$)$_2$SiO] and at 0.9-1.0 ppm [(C**H**$_3$)$_3$C-Si]. One more characteristic signal is observed at 3.3-3.5 ppm representing the protons adjacent to the protected primary alcohol [C**H**$_2$OSi]. The presence of these signals is proof of the existence of the protected primary alcohol functionality at the chain-end of the polymer – moreover since this functionality is introduced via the initiator every chain will have this functionality. The polystyrene 'long' arm was synthesised in a large scale reaction with about 100 g of monomer to ensure enough starting material for the synthesis of the entire series of stars.

The next step was the deprotection of the 'long' arm which was carried out under mild acid conditions (Scheme 4.1). The polymer was dissolved in THF and after addition of concentrated HCl was left stirring under reflux overnight.[9] The progress of the deprotection reaction can be observed by ^{1}H-NMR spectroscopy of the polymer (Figure 4.3) which shows the decrease of the peaks at δ 0.0 ppm [(C**H**$_3$)$_2$SiO] and at δ 0.9-1.0 ppm [(C**H**$_3$)$_3$C-Si] corresponding to the *tert*-butyldimethylsilyl protection groups until their complete removal. The peak corresponding to the end group [C**H**$_2$-OSi] shifts from δ 3.3-3.5 ppm to δ 3.0-3.3 ppm representing the protons next to the deprotected primary alcohol functionality [C**H**$_2$OH].

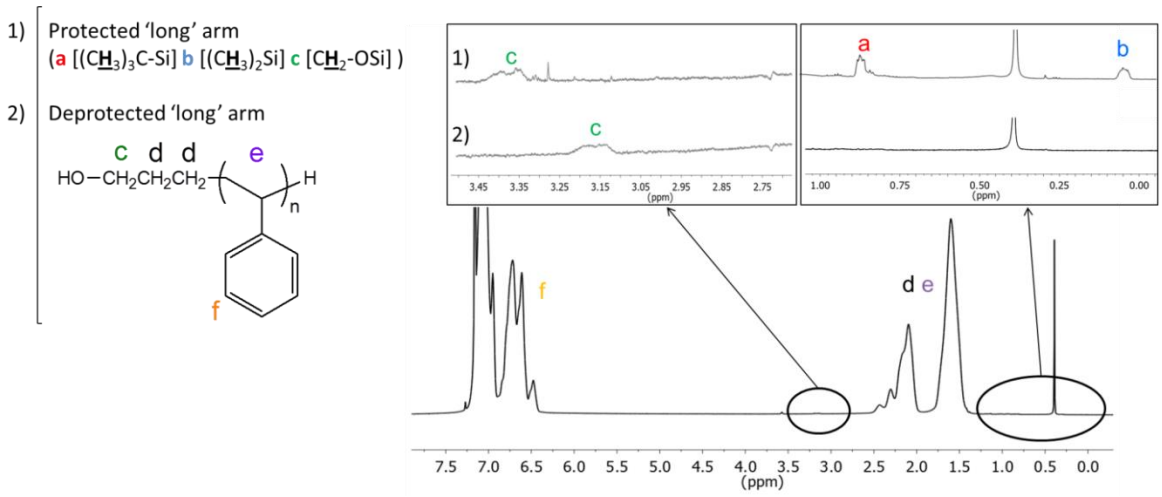

Figure 4.3 ^{1}H-NMR spectra of the deprotected polystyrene 'long' arm in C_6D_6 (700 MHz). Comparison of the main spectra fragments before and after deprotection is reported.(Peak at 0.4 ppm corresponding to H_2O protons)

4.2.1.1.1. Introduction of chain end functionality for Williamson coupling

In order to synthesise the stars via a Williamson coupling reaction it was necessary to convert the deprotected primary alcohol group into an alkyl bromide group. A bromide group has been shown to be particularly effective for such coupling reactions in previous work on the reaction[6]. The bromination was carried out using CBr_4/PPh_3 via the Appel reaction and the conversion followed by ^{1}H-NMR spectroscopy. (Scheme 4.2)

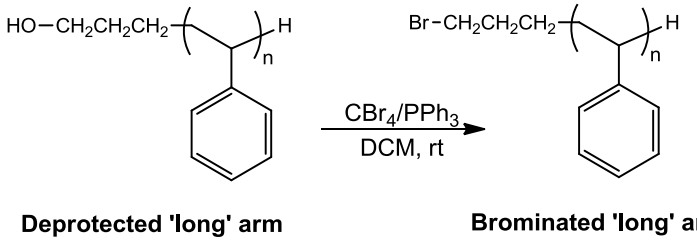

Scheme 4.2 Conversion of the primary alcohol functionality of the polystyrene 'long' arm to bromide functionality.

In Figure 4.4 it is possible to observe the signal of the protons next to the primary alcohol [C**H**$_2$-OH] at δ 3.0-3.3 ppm that disappears and is replaced by a new peak at δ 2.7-2.85 ppm of the methyl protons next to the bromide functionality [C**H**$_2$-Br].

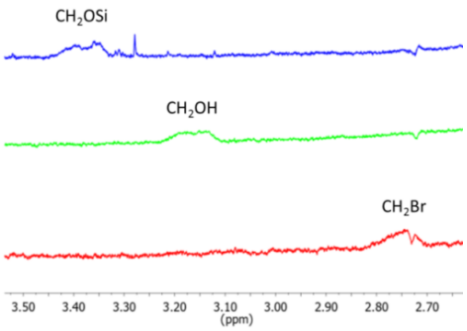

Figure 4.4 Fragments of the ^{1}H-NMR spectrum in C_6D_6 (700 MHz) of the 'long' arm showing the shift of the peak representing the chain end functionality during the conversion from protected alcohol [C**H**$_2$OSi] to the alkyl bromide [C**H**$_2$Br].

4.2.1.1.2. Introduction of chain end functionality for azide-alkyne 'click' coupling

In order to carry out the coupling reaction by a 'click' mechanism it is necessary to convert the bromide functionality at the chain end of the 'long' arm into an azide functionality. This functional group modification was carried out in DMF in the presence of sodium azide (NaN_3). (Scheme 4.3)

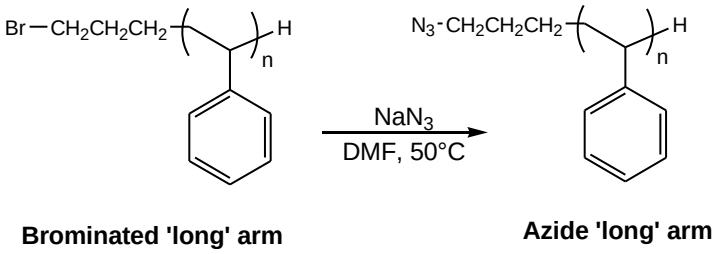

Scheme 4.3 Azido-functionalisation of the polystyrene 'long' arm.

A similar procedure was described in previous work[10] where the synthesis of a functionalised polybutadiene via living anionic polymerisation was carried out utilising the same protected alkyllithium initiator employed for the 'long' arm synthesis. For the functionalised polybutadiene this reaction was carried out in a mixture of DMF and THF in order to solubilise the polybutadiene which is insoluble in DMF. In the present case the solubility of polystyrene in DMF made the use of THF unnecessary. DMF is an excellent solvent for the azidation step due to its ability to promote the nucleophilic substitution reaction S_N2.

The progress of the reaction was checked by ^{1}H-NMR spectroscopy (Figure 4.5) and the reaction was stopped when the disappearance of the peak at δ 2.7-2.85 ppm [C**H**$_2$-Br] was observed.

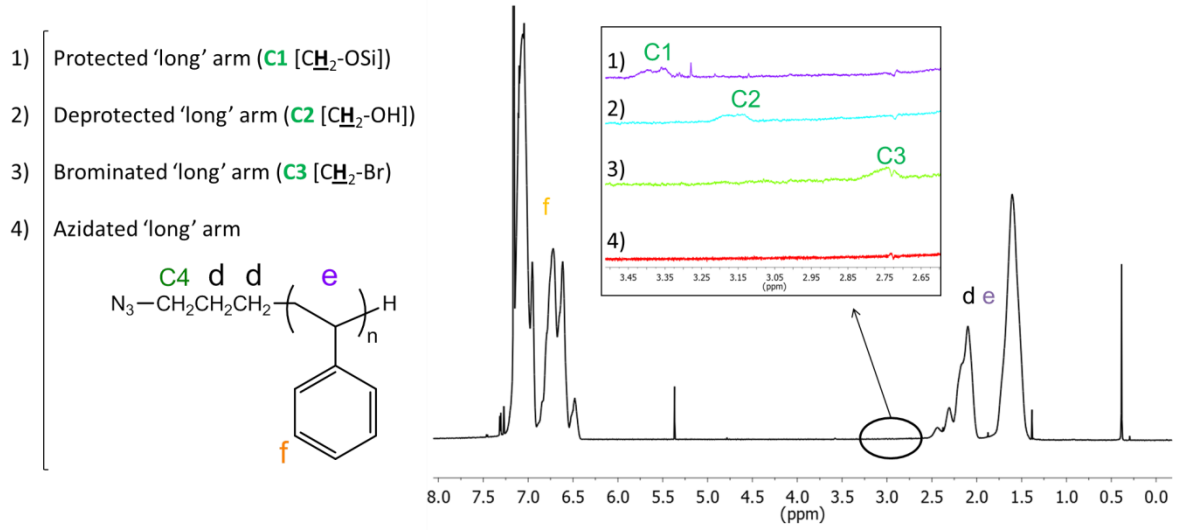

Figure 4.5 ^{1}H-NMR spectrum in C_6D_6 (700 MHz) of PS 'long' arm. Comparison of the spectra collected during the conversion of the end group from protected alcohol [C**H**$_2$OSi], to primary alcohol [C**H**$_2$OH], to alkyl bromide [C**H**$_2$Br] and to the final alkyl azide [C**H**$_2$N$_3$].

Although the disappearance of the peak representing [C**H**$_2$-Br] was clear as shown in Figure 4.5 it was not possible to observe the appearance of any new peaks representing the protons next to the azide group [C**H**$_2$-N$_3$]. As observed before[10] the substitution of the bromide group with an azide group shifts the peak of the protons next to the functionality to lower values of ppm. In our case this shift pushes the [C**H**$_2$-N$_3$] peak into the region where there are the intense peaks due to the aliphatic protons of the polystyrene that completely mask the low intensity peak of the protons next to the azide.

4.2.1.2. Synthesis of the end-functionalised polystyrene 'short' arm

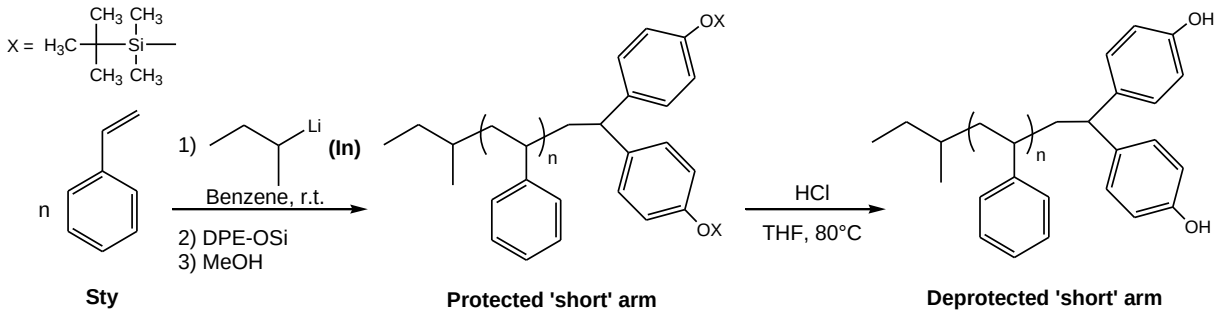

Scheme 4.4 Synthesis of the protected polystyrene 'short' arm via living anionic polymerisation and following deprotection of the two phenol functionalities.

The procedure for the synthesis of the 'short' arm again exploits the living anionic polymerisation of styrene. (Scheme 4.4) *Sec*-butyllithium was used as the initiator that upon addition to the solution of styrene in benzene caused a change in colour of the solution which became orange/red. The polymerisation was left stirring overnight to ensure the

complete consumption of the styrene. To the living solution was then added the end-capping agent 1,1-*bis*(4-*tert*-butyldimethylsiloxyphenyl)ethylene (DPE-OSi) that was injected as a solution in benzene, purified prior to injection by the dropwise addition of *sec*-butyllitium in the presence of the Lewis base TMEDA.[5] The addition of *sec*-butyllithium until a permanent (but weak) red colour indicates the absence of any impurities in the DPE-OSi solution. This functionalised diphenylethylene derivative results in the introduction of two protected phenol functionalities which are used in the subsequent coupling reactions for the synthesis of the star polymers. It was possible to add an excess of DPE-OSi with respect to the concentration of propagating chain ends due to the fact that although it will react with the living polystyrene chain end, it is too sterically bulky to propagate[11] and in this way we could ensure a nearly quantitative reaction with the living polymer chain ends. As a consequence of the addition of DPE-OSi the solution turned a dark red colour and, because of the slow rate of reaction of DPE-OSi with polystyryllithium, it was left stirring for five days before termination with nitrogen-sparged methanol. A series of four 'short' arms with varying molecular weights were prepared by the described method and the resulting polymers were analysed by both SEC and by ^{1}H-NMR spectroscopy and a typical NMR spectrum of the end-capped polystyrene short arm with the phenol groups protected is given below. (Figure 4.6)

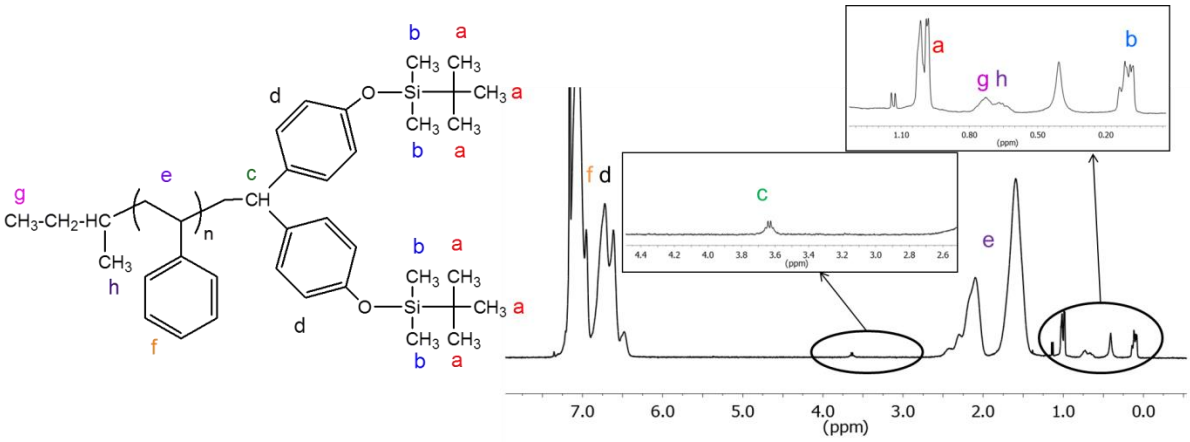

Figure 4.6 Typical ^{1}H-NMR spectrum of a protected polystyrene 'short' arm PS16 in C_6D_6 (400 MHz). (Peak at 0.4 ppm corresponding to H_2O protons)

The characteristic peaks corresponding to the protected phenol groups attached to the polymer chains can be observed at δ 0.0-0.2 ppm [(C**H**$_3$)$_2$Si] and at δ 0.9-1.1 ppm [(C**H**$_3$)$_3$C-Si]. In addition it is possible to observe the peak at δ 3.5-3.7 representing the proton [C**H**(Ph)$_2$] of the DPE-OSi end-capping group following termination with methanol. The peak visible at δ

0.6-0.8 ppm corresponds to the methyl groups [C**H**$_3$CH$_2$] and [C**H**$_3$CH] introduced by the initiator used for the polymerisation. For a quantitatively end-capped polymer the integral values of peaks at δ 0.0-0.2 ppm and δ 0.6-0.8 ppm should be in a ratio of 2:1 (DPE-OSi:In).

The silyl-protected phenol groups on the resulting polymers were deprotected (Scheme 4.4) by mild acid hydrolysis as described above (Section 4.2.1.1). In Figure 4.7 it is possible to observe in the ^{1}H-NMR spectrum of the resulting deprotected 'short' arms, the disappearance of the signals corresponding to the *tert*-butyldimethylsilyl protection groups at δ 0.0-0.2 ppm [(C**H**$_3$)$_2$Si] and at δ 0.9-1.1 ppm [(C**H**$_3$)$_3$C-Si]. It is also possible to observe the appearance of new peaks in the spectrum of the 'short' arm at δ 3.7-3.9 corresponding to the phenol groups [**H**OPh].

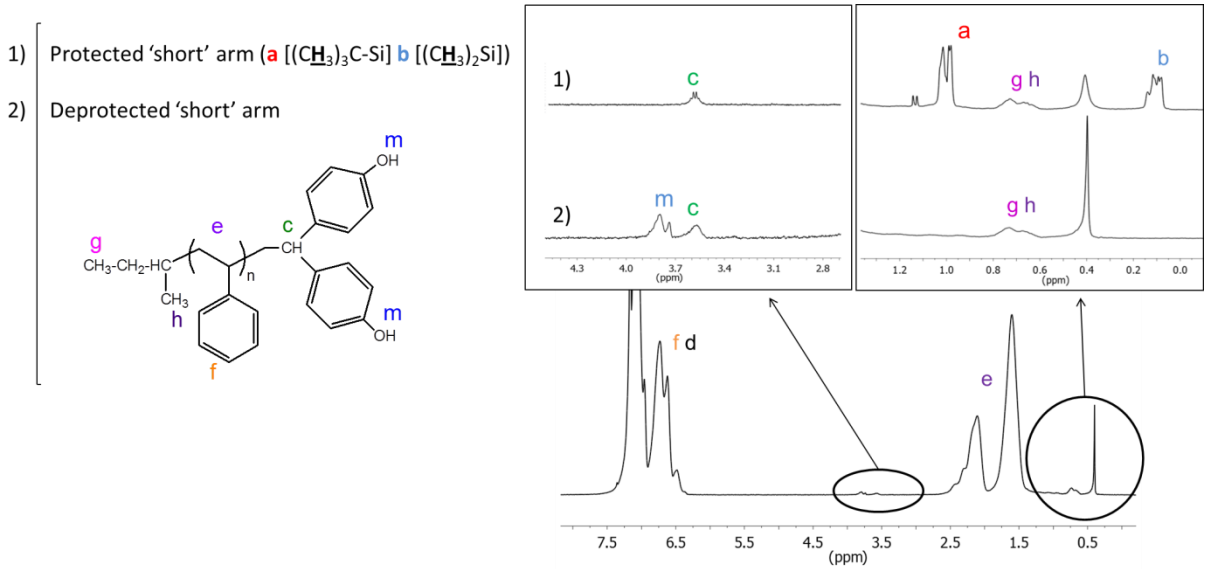

Figure 4.7 ^{1}H-NMR spectra of deprotected 'short' arms PS16 synthesised in C_6D_6 (400 MHz). Comparison of the main spectra fragments before and after deprotection. (Peak at 0.4 ppm corresponding to H_2O protons)

Following deprotection the phenol groups can be used directly in a subsequent Williamson coupling reaction.

A series of polystyrene 'short' arms with different molecular weights was produced and the molecular weights obtained by SEC are shown in Table 4.1. We will refer to the short arms with the name PSX were X stands for the molecular weight in kg mol^{-1}.

Table 4.1 Molecular weight and dispersity values of the polystyrene short arms.

Short arm	M_n (g mol^{-1})	M_w (g mol^{-1})	Đ
PS10	10000	10500	1.05
PS16	16200	16800	1.04
PS20	19600	20500	1.05
PS32	32100	33700	1.05

4.2.1.2.1. Introduction of chain end functionality onto 'short' arm for azide-alkyne 'click' coupling

Just as the chain end functionality on the 'long' arm needs to be suitably modified to enable a 'click' coupling reaction, so do the functionalities on the short arms need to be converted - in this case the two phenol functionalities are converted into two alkyne functionalities. This functional group modification of the 'short' arm was carried out via a Williamson coupling reaction (Scheme 4.5) with propargyl bromide in the presence of Cs_2CO_3 in DMF.

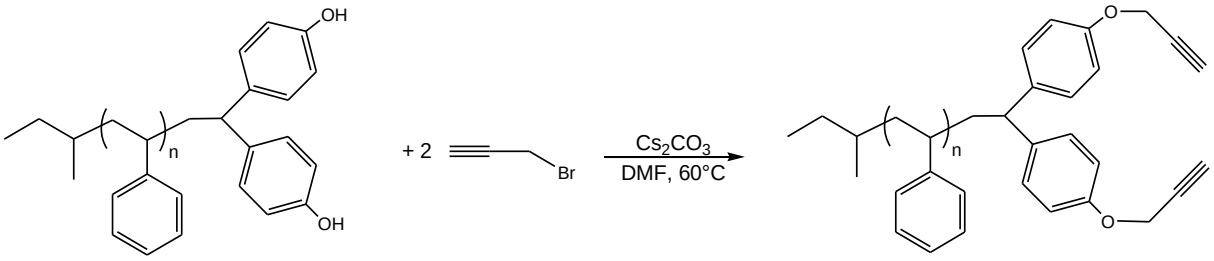

Deprotected 'short' arm **Propargyl bromide** **Propargyl 'short' arm**

Scheme 4.5 Conversion of the two phenol functionalities of the 'short' arm into two alkyne functionalities.

The end group modification reaction was followed by ^{1}H-NMR spectroscopy (Figure 4.8) which showed the appearance of the peaks at δ 4.1-4.3 ppm due to the presence of the new alkyne functionality [C**H**$_2$C≡CH]. This has been verified by the value of the integrals of peak *a* and *c* in Figure 4.8 having a ratio of 4:1. The peak corresponding to the alkyne protons is not visible because they are in the region of the polystyrene chain protons.

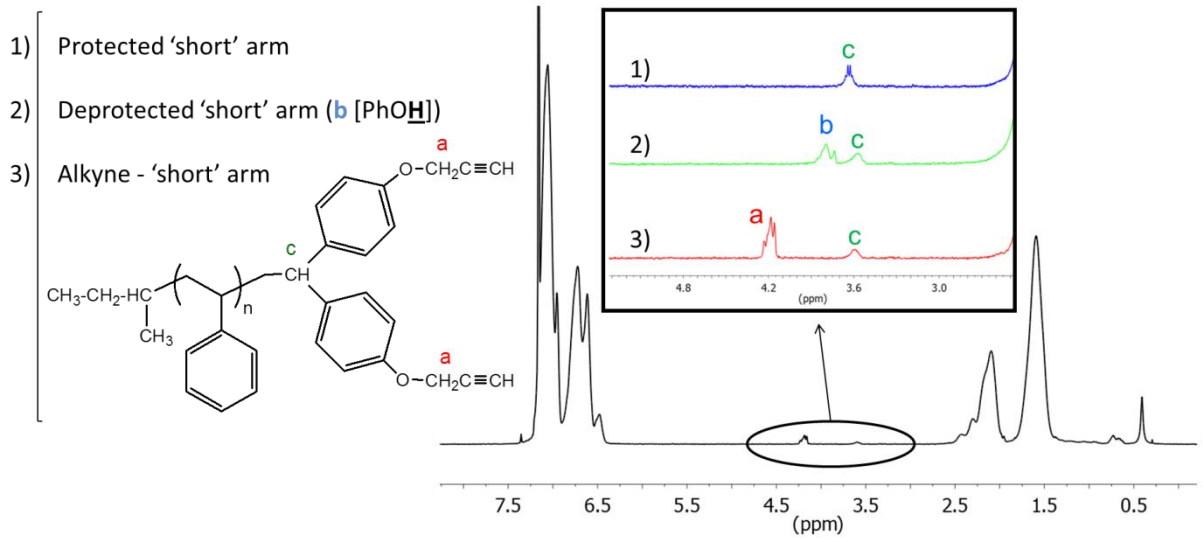

Figure 4.8 ^{1}H-NMR spectra of the 'short' arm provided with two alkyne functionalities in C_6D_6 (400 MHz). Comparison of the spectra acquired during the transformation of the chain-end functionalities from protected phenol groups to alkyne groups.

4.2.2. Synthesis of Stars

After the preparation of well-defined polymer arms with the appropriate chain end functionalities, the assembly of the stars is conducted using two different approaches. The arms are coupled either by a Williamson coupling reaction or by a copper (I)-catalysed azide-alkyne 'click' reaction. The two coupling strategies were carried out as described in the following sections for the synthesis of four asymmetric three-arm stars and one symmetric three-arm star. The stars synthesised are named "StarX" where X denotes the molar mass of the 'short' arm. The symmetric star (Star90) is produced from 3 'long' arms. As well as describing the two synthetic strategies we will compare the relative efficiency of the two approaches.

4.2.2.1. Synthesis of Stars via a Williamson Coupling Reaction

The synthesis of stars by a Williamson coupling reaction consists of a nucleophilic substitution reaction between an alkyl bromide (the bromide being the leaving group) and a phenol (the nucleophile) that results in an ether linkage. (Scheme 4.6)

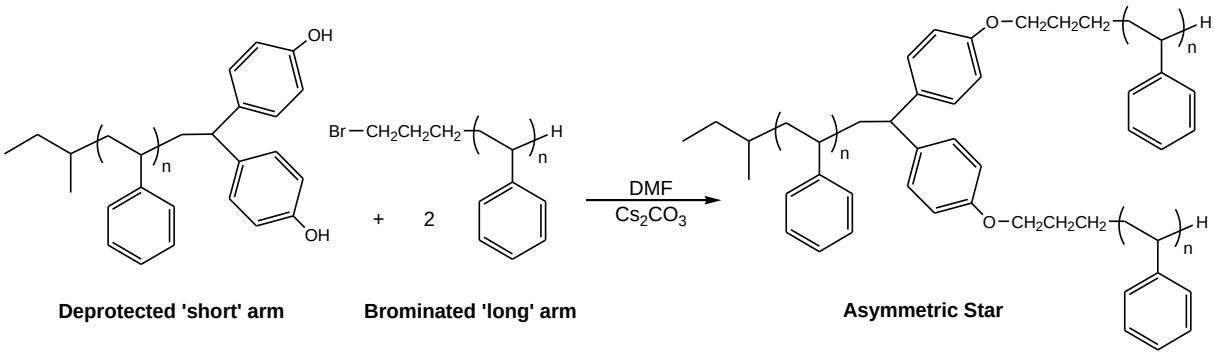

Scheme 4.6 Williamson coupling reaction for the synthesis of asymmetric star polymers.

The 'short' arm carries the phenol functionalities that react with the bromide functionalities of two different polymer chains corresponding to two 'long' arms. The substitution reaction is carried out in DMF in the presence of cesium carbonate (Cs_2CO_3)[6] with an excess of the 'long' arm. The molar ratios of the reagents are 1 : 2.5 : 10 respectively for 'short' arm, 'long' arm and Cs_2CO_3 - a slight molar excess of the 'long' arm being used to drive the reaction towards complete coupling. The extent of coupling was followed by extracting small samples periodically and subjecting them to SEC analysis as shown in Figure 4.9. As the reaction proceeded the intensity of the first peak at 14 ml representing the 'long' arm decreased and was accompanied by the appearance of a second peak (13.3 ml) corresponding to the resulting star. It is also possible that a third (unresolved) peak exists between the peak of the 'long' arm (retention volume 14 ml) and the peak corresponding to the star (retention volume 13.3 ml). The presence of this 'unresolved peak' would correspond to a linear polymer chain made by the 'short' arm coupled to only one 'long' arm chain arising from an incomplete coupling reaction. It is likely that any such intermediate product would be present in low concentrations and given the relatively small difference in molecular weight between the 'long' arm (c. 90 kg mol^{-1}) and a linear polymer arising from the coupling of one 'long' arm to a 'short' arm (c. 100 kg mol^{-1}) it is extremely unlikely that this peak would be observed by SEC. However, experience tells us that it is likely that such an intermediate product may be present – see later discussion on TGIC analysis of stars.

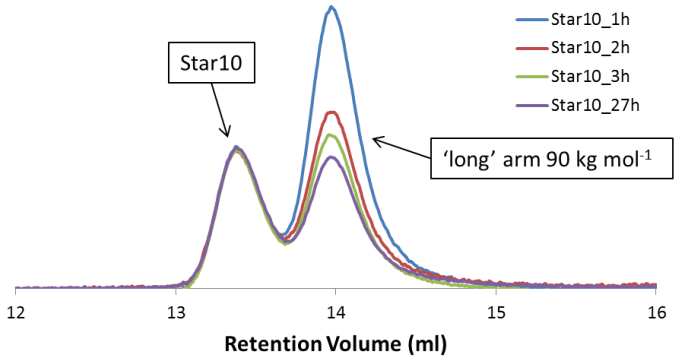

Figure 4.9 SEC (RI detector) chromatogram of Star10 synthesised by Williamson coupling reaction with PS10 and the 'long' arm as starting materials at a temperature of 60°C. Samples are taken after 1, 2, 3 and 27 hours.

The conditions chosen for the first attempt of the star synthesis by Williamson coupling reaction (Scheme 4.6) were found in a previous work where the same reaction was used for the synthesis of hyperbranched polymers.[7] The 60°C temperature worked very well for this type of reaction and it was optimal in the attempt of avoiding side reactions due to the degradation of the DMF at higher temperature.[5] Although it is clear from the data in Figure 4.9 that the reaction proceeded with reasonable efficiency, appearing to be almost complete after 3 hours, attempts were made to improve the ultimate extent of the coupling reaction. With this aim in mind different reaction conditions have been tested. A series of coupling reactions were carried out in which the reaction temperature and the solution concentration were varied – the reaction parameters chosen for this series of reactions are given in Table 4.2.

Table 4.2 Reaction temperature and solution concentration experimented for the synthesis of Star10 via a Williamson coupling reaction.

Experiment	T(°C)	Concentration (% w/v)	TIME (h)[(a)]
1	60	10	27
2	80	10	23
3	150	10	4.5
4	150	20	5
5	150	5	19

(a) Times at which the reaction was stopped – no more changes in the SEC chromatograms.

The effect of the temperature was investigated first. In experiments 1, 2 and 3 the coupling reaction was carried out in a solution of DMF at a fixed concentration of 10 wt. % of polymer. Experiment 1 was conducted at 60°C and for the experiments 2 and 3 the temperature was increased to 80°C and 150°C respectively. Analysis of the resulting polymer mixtures by SEC shows that the higher temperature influences positively the conversion to

stars both in terms of the extent and rate of coupling. As shown in the SEC chromatograms in Figure 4.10 *a)* the peak at high retention volume (14 ml) corresponding to the unreacted 'long' arm decreases with the increase in temperature.

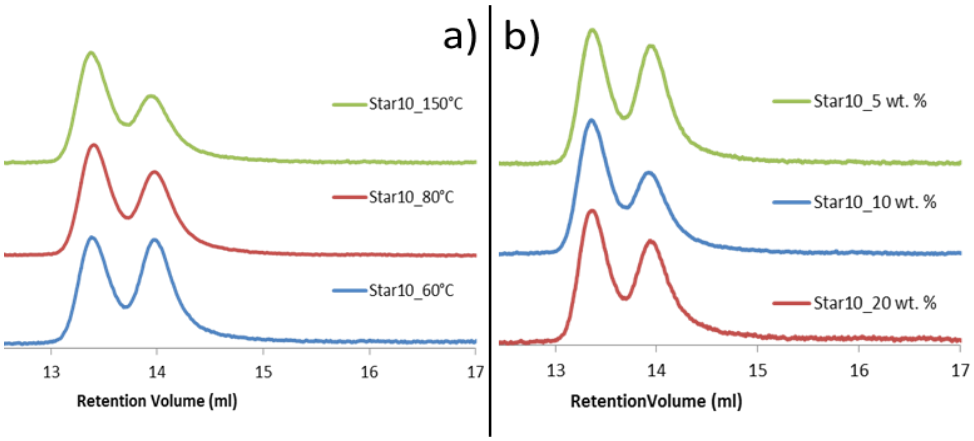

Figure 4.10 SEC (RI detector) chromatograms of Star10 synthesised via Williamson coupling reaction representing **a)** the effect of the changes in temperature at a fixed solution concentration of 10 wt. % and **b)** the effect of the changes in solvent concentration at a fixed temperature of 150°C.

The SEC chromatogram of experiment 3 (green chromatogram in Figure 4.10 *a*) shows in fact for this peak the lowest intensity demonstrating a higher conversion of the 'long' arm to star. As mentioned before, in each of these experiments it is still possible to assume the presence of the third peak representing the partially coupled polymer.

Furthermore it was possible to observe an increase in the rate of the coupling reaction with temperature whereby the reaction performed at 150°C (exp. 3 – Table 4.2) resulted in a higher extent of conversion of the 'long' arm in a shorter time in comparison to experiment 1 and 2 that required longer time to reach a lower degree of conversion.

The effect of the solution concentration was subsequently investigated. The temperature was fixed at 150°C and the concentration was varied from 5 wt. % in experiment 5 to 20 wt. % in experiment 4. From the SEC chromatograms (Figure 4.10 *b)*) it is observed that neither decreasing the concentration to 5% nor increasing to 20% resulted in any improvement. The highest degree of 'long' arm conversion was observed for experiment 3 with a 10 wt. % polymer solution. For the reaction at low concentration the lower extent of coupling may be due to the fact that the polymer chains are more dilute but it is also worthy of notice that Williamson coupling reaction is not a very consistent reaction. The same polymer reacted by Williamson coupling reaction at the same conditions can give a different result each time. For this reason it is not possible to conclude that Williamson coupling reaction works better or worse at a given concentration with only these three data.

However in accordance with the results obtained from the investigation described above, it was decided that a temperature of 150°C at a solution concentration of 10 wt. % was the most suitable condition for the conversion of the three-arms into star polymers via Williamson coupling reaction. Following this conclusion we applied the same procedure and conditions to the synthesis of Star16, Star20 and Star32 (Figure 4.11). The results for the synthesis of Star16 showed a lower degree of conversion than the one obtained for Star10 (Figure 4.10) and repeated reactions at the same conditions did not show any better results.

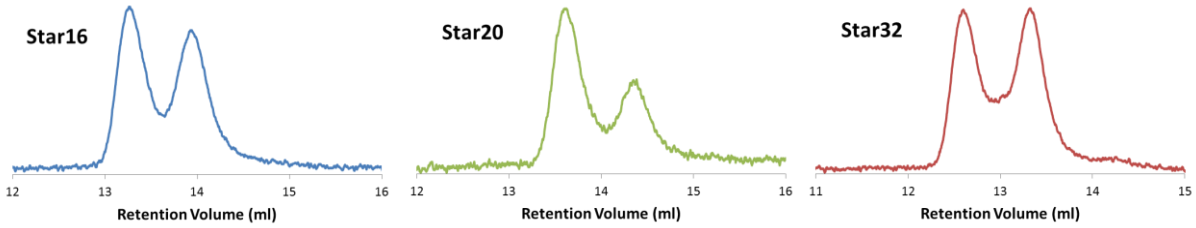

Figure 4.11 SEC (RI detector) chromatograms of Star16, Star20 and Star32 synthesised by Williamson Coupling reaction at a temperature of 150°C and a solvent concentration of 10 wt. %.

Star20 showed a good conversion to star at the chosen conditions but a second attempt of the coupling on a bigger scale reaction showed a much lower degree of conversion than the previous small scale reaction.

Star32 proved to be the most difficult star to synthesise via Williamson coupling reaction. The degree of conversion was lower than in the other cases and the SEC chromatogram (Figure 4.11) indicates the presence of a peak at 14.3 ml indicating that not all of the 'short' arm had reacted.

4.2.2.2. Synthesis of Stars via azide-alkyne 'click' Reaction

The synthesis of stars by an azide-alkyne 'click' reaction (Scheme 4.7) proceeds by the addition reaction between the azide functionality carried by the 'long' arm and the alkyne functionality carried by the 'short' arm resulting in the formation of a 1,2,3-triazole linkage.

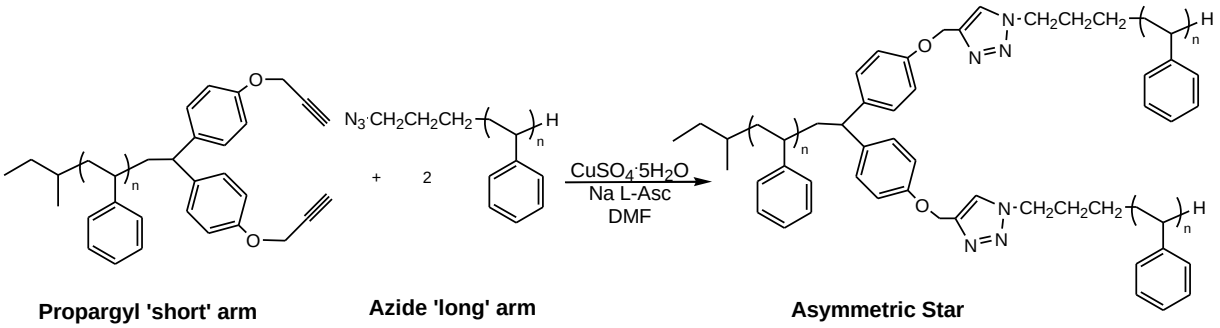

Scheme 4.7 Azide-alkyne 'click' reaction for the synthesis of star polymers.

The reaction was carried out in DMF in the presence of the catalyst copper(II) sulphate pentahydrate ($CuSO_4 \cdot 5H_2O$) and the reducing agent sodium ascorbate (Na L-Asc).[10] The 'short' arm is reacted with a similar excess of 'long' arm used in Williamson coupling reaction (1:2.5). As previously, the extent of coupling reaction was followed by extracting samples and characterising them by SEC.

Synthesis of asymmetric three-arm stars

The azide-alkyne 'click' reaction was exploited for the synthesis of the asymmetric three-arm stars Star16 and Star32. After the introduction of azide and alkyne functionalities at the chain end of the 'long' arm and 'short' arm respectively, the two arms were coupled in DMF under a variety of conditions in order to optimise the conversion into stars.

In the case of Star16, the propargyl functionalised 'short' arm PS16 was reacted with an excess (2.5:1 with respect to PS16) of the azide functionalised 'long' arm as shown in Table 4.3. Three different reactions were carried out at a fixed temperature of 50°C and solvent concentration of 10 wt. %.

Table 4.3 Reaction conditions for the several experimented azide-alkye 'click' reactions conducted for the synthesis of Star16.

Experiment	T (°C)	Solvent (% w/v)	[$CuSO_4 \cdot 5H_2O$]:[short arm]	[Na L-Ascorbate]:[short arm]	TIME (h)
1	50	10	1.25	2.5	-
2	50	10	1.25[(a)]	2.5[(a)]	48
3	50	10	2	4	35

(a) More catalyst in the same molar ratio of 1.25 : 2.5 : 1 with respect to PS16 was added to the reaction during the reaction time.

The amount of catalyst in each experiment was varied and in the first instance (experiment 1) the molar ratio of copper sulphate and ascorbate reducing agent was 1.25 and 2.5 respectively with respect to the moles of 'short' arm. The reaction proceeded successfully as can be observed in the first SEC chromatogram shown in Figure 4.12. A sample of the

product of experiment 2, which was started with the same amount of the two component catalytic system, was analysed after one day by SEC and it did not show the same conversion as previously seen in expt. 1. In an attempt to improve this initial conversion we added more catalyst to the reaction mixture. After a further day of reaction the SEC chromatogram showed that the reaction had progressed to a higher extent of reaction as observed in Figure 4.12 where the SEC chromatograms after one and two days are superimposed.

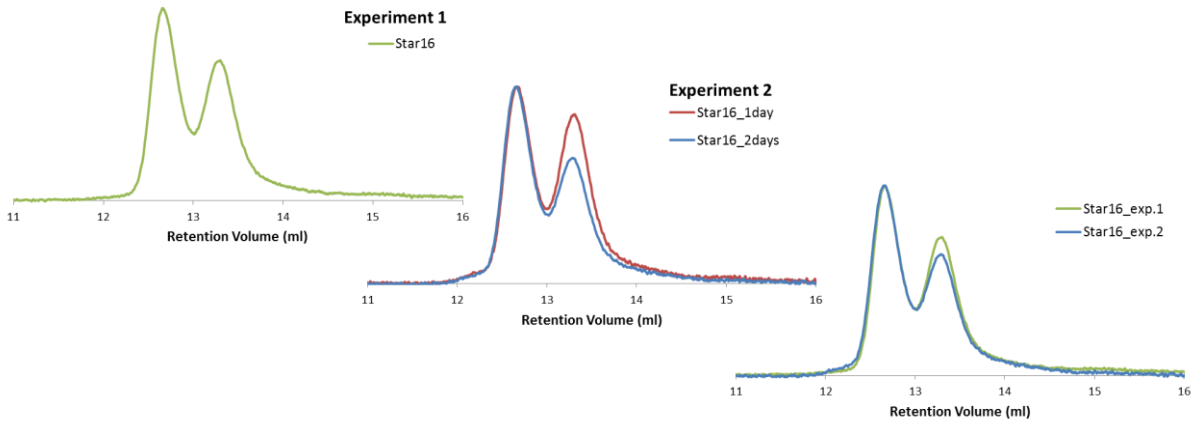

Figure 4.12 SEC chromatogram (RI detector) of Star16. I the middle, comparison of the polymer mixture of the same reaction sampled after 1 day and 2 days. On the right, comparison of the two final polymers mixtures obtained from experiment 1 and 2.

The comparison between experiment 1 and 2 (Figure 4.12) shows a slightly better conversion in experiment 2 and in particular the result of a second addition of catalyst in experiment 2 suggests that the amount of catalyst can strongly influence the progress (rate and extent) of the reaction. In fact the success of the 'click' reaction is strictly connected to the concentration of Cu(I) that must be high at all times during the reaction. Reactions of disproportion of Cu(I) to Cu(II) and Cu(0) or oxidation of Cu(I) to Cu(II) can occur due to the presence of oxygen which must be avoided. These side reactions were found to be a problem above all for the reactions carried out in solution or with less reactive reagents.[12] The presence of the reducing agent is a way to overcome the problem and regenerate Cu(I) and in this work the addition of higher ratios of the catalytic system probably helped to reach the high concentration of the active species Cu(I) required to yield the star. In a third experiment the molar ratio of the catalytic system was further increased (see Table 4.3) with dramatic effect. The reaction underwent a significant improvement with a very high, almost quantitative degree of conversion after only 2.5 hours. The reaction was allowed to proceed further but after 30 hours SEC analysis of the reaction showed only a modest increase in the

extent of reaction suggesting the reaction was almost complete after 2.5 hours. In the chromatograms below (Figure 4.13) it is possible to observe the peak of the star formed and the low intensity of the unreacted 'long' arm present. By sampling the reaction it was noticed that the decrease of the peak at higher retention time was substantial and very quick, occurring within 2.5 hours of the start of the reaction.

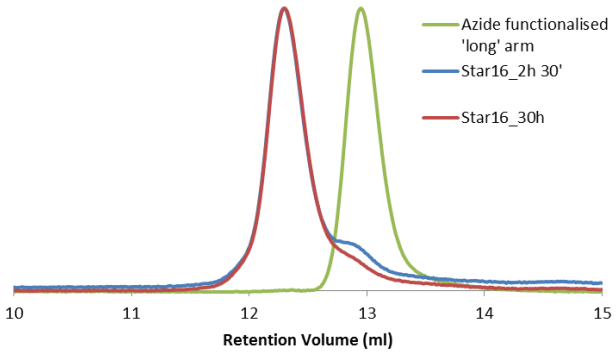

Figure 4.13 SEC chromatogram (RI detector) of Star16 for the experiment 3. Comparison of the pure 'long' arm and the polymer mixture of Star16 sampled during the reaction at 2.5 and 30 hours.

After the successful synthesis of Star16 via a 'click' coupling reaction, a series of reactions were carried out to ascertain whether the 'click' coupling approach would be more successful than the Williamson coupling for the synthesis of Star32. The 'short' arm (PS32) was reacted in DMF with an excess of 'long' arm (1:2.5) and the mole ratio of catalyst was varied in a similar fashion to the synthesis of Star16 (see Table 4.4). However since the extent of reaction was initially less than for Star16, the reaction temperature and solvent concentration were also varied.

Table 4.4 Reaction conditions for the several experimented azide-alkye 'click' reactions conducted for the synthesis of Star32.

Experiment	T(°C)	Solvent (% w/v)	$[CuSO_4 \cdot 5H_2O]$:[short arm]	[Na L-Ascorbate]:[short arm]	TIME (h)
1	50	10	1.25[(a)]	2.5[(a)]	41
2	60	10	2[(a)]	4[(a)]	69
3	60	20	2	4	48
4	60	20	3	6	47

(a) More catalyst was added during the reaction time in a molar ratio of (1 : 7.5 : 15) (exp. 1) and (1 : 1.16 : 2.32) (exp. 2) with respect to PS32.

Experiment 1 (Table 4.4) for the synthesis of Star32 was carried out under the same conditions as Experiments 1 and 2 for Star16 (Table 4.3). The addition of further catalyst in a molar ratio of 1 : 7.5 : 15 with respect to PS32, a higher ratio than the one used at the

beginning of the reaction, did not show any improvement and the reaction was stopped at a very low conversion to star. (Figure 4.14)

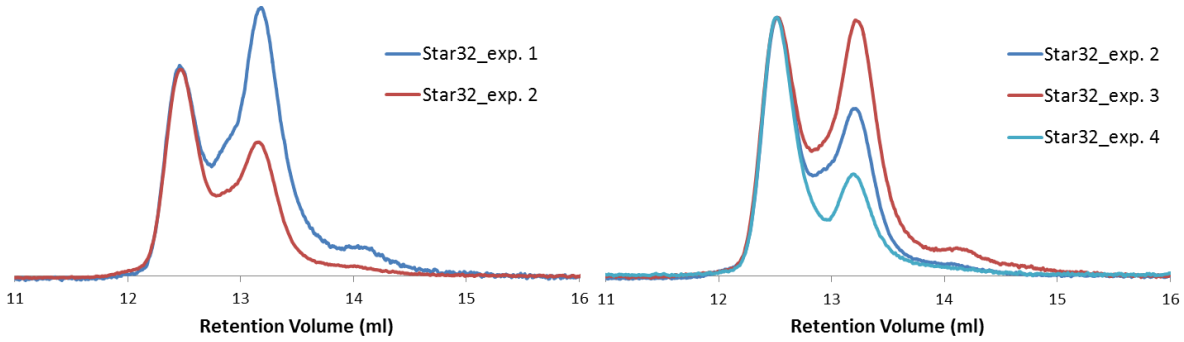

Figure 4.14 SEC chromatogram (RI detector) of Star32. On the left: comparison of the final polymer mixture resulting from exp. 1 and 2. On the right: comparison of the final polymers mixtures obtained from experiment 2, 3 and 4.

Taking into account the results obtained for the synthesis of Star16 by 'click' coupling reaction, it was decided to increase the amount of catalyst in a subsequent reaction – the reaction temperature was also increased to 60°C. SEC analysis of samples extracted at various times during the reaction indicated a slow reaction rate. After 20 hours the conversion was still low and so in an attempt to improve it, more catalyst was added in a molar ratio of (1 : 1.16 : 1.32) with respect to PS32. The addition improved the conversion. A second addition of catalyst in the same amount of the previous addition after another 26 hours was unproductive and after 2 days and 21h the reaction was stopped. The conversion obtained at the end was improved in comparison with experiment 1 (Figure 4.14). Changing the solution concentration from 10 wt. % to 20 wt. % experiment 3 showed no improvement at all – in fact the conversion was poorer than the previous experiment. However, in experiment 4 an increase in solution concentration coupled with an increase in the molar ratio of catalyst resulted in a significant improvement in the extent of reaction.

Observing the SEC chromatograms of Figure 4.14 it is also possible to see a peak in between the two major peaks – this is particularly evident in experiment 1. As mentioned before this is likely to be due to the presence of the incomplete coupling in the synthesis of the star, i.e. a linear polymer made of PS32 and only one chain of polystyrene 'long' arm attached.

Synthesis of symmetric three-arm star

In addition to the synthesis of the asymmetric three-arms stars described above, the synthesis of one symmetric three-arm star was carried out with the 'long' arm utilised for

the asymmetric stars. For this synthesis, also carried out by an azide-alkyne 'click' coupling reaction, the preparation of a trifunctional core carrying three alkyne groups is required. 1,1-Tris(4-hydroxyphenyl)ethane (B3OH) was reacted in DMF with an excess of propargyl bromide in the presence of Cs_2CO_3.(Scheme 4.8)

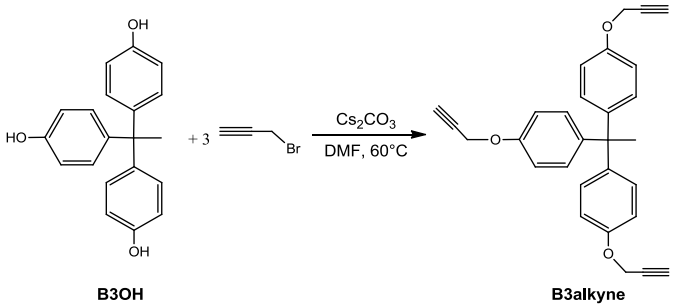

Scheme 4.8 Synthesis of alkyne functionalised B3 core for the synthesis of symmetric stars.

The reaction was followed by TLC which showed several spots corresponding to the starting material (B3OH), the partially modified molecule and the desired B3alkyne core. The product was purified by flash chromatography on SiO_2 with toluene as eluent. The first fraction constituting the pure B3alkyne core was collected and dried. The product was analysed by ^{1}H-NMR and ^{13}C-NMR spectroscopy that demonstrated its purity.[13] (Figure 4.15)

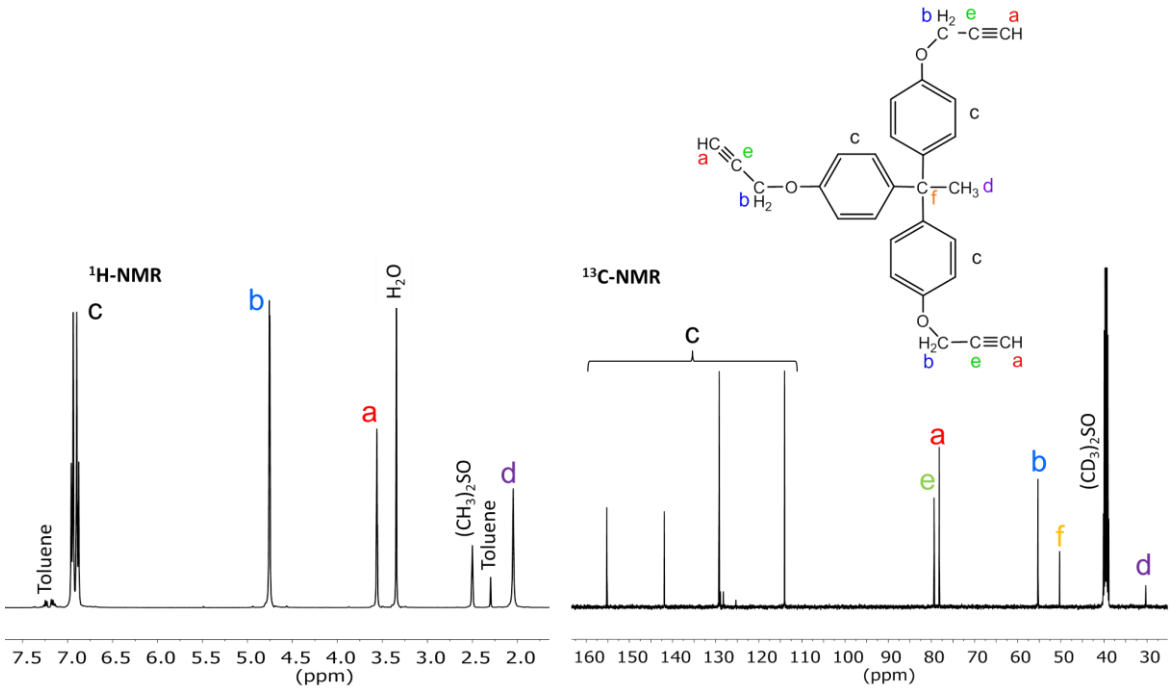

Figure 4.15 ^{1}H-NMR spectrum (left) and ^{13}C-NMR spectrum (right) in DMSO (400 MHz) of the alkyne - B3 core.

The synthesis was confirmed by the integrals calculation that gave the following results: 2.05 ppm [3H], 3.55-3.60 ppm [3H], 4.7-4.8 ppm [6H], 6.85-7 [12H].

The coupling reaction for the synthesis of the symmetric star was conducted at a temperature of 60°C and a solution concentration of 20 wt. %. At the beginning of the reaction the catalytic system had a molar ratio of (1:4:8) with respect to the B3 core utilised. (Figure 4.16)

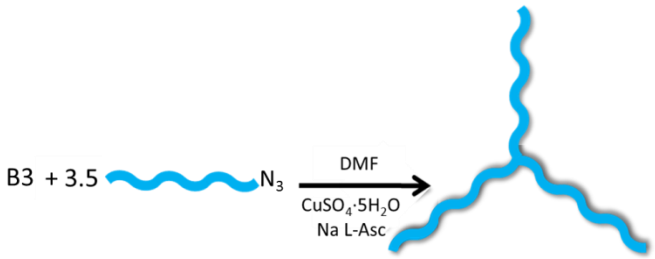

Figure 4.16 Azide-alkyne 'click' reaction for the synthesis of symmetric three-arms star.

The synthesis was carried out twice under the same conditions. In the first small scale reaction (1 g) it was noticed that the reaction was slower in comparison to the stars synthesised before. This low rate it may be due to the longer polymer chains involved, in fact the three-arms that had to be joined together in this reaction were all of the same molecular weight of 90 kg mol^{-1}, i. e. the 'long' arm of all the rest of the reactions discussed before. As shown in the SEC chromatogram below (Figure 4.17), the reaction had a low conversion after 1 hour and 50 minutes but after 18 hours the conversion had improved. After a further 25 hours the conversion was slightly better so we left the reaction for longer (ca. 4 days) but with no further improvement. Moreover the subsequent addition of more catalyst (in a molar ratio of 1 : 1.9 : 4.4 with respect to the B3 core) did not affect further the conversion.

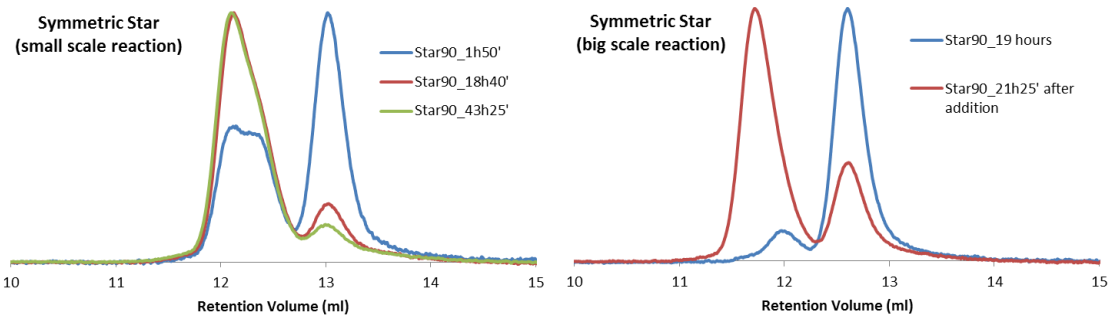

Figure 4.17 SEC chromatograms (RI detector) of the synthesis of the symmetric star. Shown are the SEC chromatograms of samples withdrawn at different times during the reaction.

A second reaction was carried out on a larger scale (about 7 g) and initially the reaction was slow and the conversion was still low after 19 hours. It was decided to add more of the catalytic system in a molar ratio of (1 : 2.7 : 5) with respect to the B3 core and 21 hours and

25 minutes after the addition of this second batch of catalyst, the reaction was checked and it showed a good conversion but with a larger amount of unreacted 'long' arm in comparison with the small scale reaction (Figure 4.17). We left the reaction for 5 days and we added more catalyst in a molar ratio of (1 : 1.2 : 2.6) but no further changes were observed.

Both the reactions were only checked periodically during the reaction so it is not certain exactly when the reactions reach their maximum conversion. In the large scale reaction the low conversion obtained after 19 hours is maybe due to the catalytic system not being active from the beginning due to the presence of oxygen resulting in possible oxidation and disproportion.

The results of the first reaction were more successful than the second one in terms of conversion of the 'long' arm but observing the SEC chromatogram it is possible to observe a shoulder in the peak at higher retention volume. This shoulder represents the linear polymer made of two 'long' arm connected together and it does not appear as clearly in the second reaction's chromatogram. So the first reaction had a higher conversion of linear arms into coupled product but the amount of star created may not be as much as in the second reaction.

4.2.3. TGIC Analysis of Stars

Temperature gradient interaction chromatography (TGIC) is a chromatographic method for polymer characterisation reported the first time by Prof Taihyun Chang in 1996.[14] This type of liquid chromatography was revealed to be a useful tool, in combination with Size Exclusion Chromatography (SEC) for the characterisation of polymers of different types in particular branched polymers. SEC and TGIC differ in the separation mechanism utilised for the analysis of solute molecules. They both use porous packing materials as a stationary phase and the specific conditions adopted in the analysis determine which type of mechanism is involved and so the type of technique used. In Figure 4.18 it is possible to observe the chromatographic retention behaviour of the polymers in three different types of chromatography: SEC, LCCC and IC.

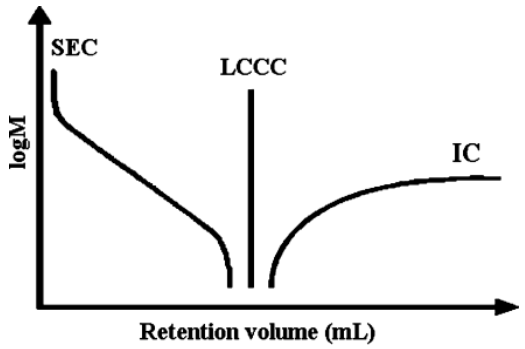

Figure 4.18 Polymer molecular weights separation in three different chromatographic methods: Size Exclusion Chromatography (SEC), Liquid Chromatography at Critical Condition (LCCC) and Interaction Chromatography (IC).

In SEC mode the order of elution of the polymers goes from high molecular weight to low molecular weight polymers and they are all eluted before the solvent peak. In IC mode, polymers are eluted after the solvent peak and the order is the opposite to SEC mode with low molecular weight polymers eluted first. The reason can be found in the type of interactions that governs the distribution of the solute between the stationary and the mobile phases. In SEC the retention of the solute is dominated by entropy but in IC is dominated by enthalpy. When these two parameters that drive the separation of the polymers exactly compensate each other we are in the unique case of LCCC, i.e. liquid chromatograph at the critical condition. Under these conditions the separation mechanisms are annulled and the polymer chains with different molecular weights elute all together.

SEC is the most common liquid chromatographic technique for the calculation of polymer molecular weight and molecular weight distribution. The separation mechanism is based on the distribution of the molecules between the mobile (solvents) phase and the pores of the stationary phase. It is possible to define the process as an entirely entropic process and SEC separates the polymer chains in terms of their molecular size and the loss of conformational entropy when a polymer chain enters a pore. Although this technique is very efficient for the analysis of linear homopolymers, it shows a reduced resolution when non-linear and non-homogeneous polymers are analysed. Since SEC separates polymers based on molecular size rather than molecular weight, the technique cannot distinguish polymer molecules with similar hydrodynamic volumes and this is a particular problem for the analysis of branched polymers. In TGIC the separation process is driven by enthalpic interactions between the solute and the stationary phase, making the analysis of polymers by their chemical nature and molecular weight possible. TGIC is a type of IC where these interactions are controlled by varying the temperature during an isocratic elution and the interactions are to a first

approximation, proportional to the molecular weight and not to the hydrodynamic volume. In comparison with SEC, this technique shows a better resolution (especially for branched polymers) but is much less universal, in fact optimal separation conditions need to be found for each single polymer type and the choice has to be made in order to maximize the resolution of TGIC. The enthalpic interactions have to be controlled for each polymer by choosing the stationary and mobile phases and the temperature gradient elution in order to achieve a good separation of the solute molecules. SEC instead is carried out under good solvent conditions and there should be no enthalpic interactions between the polymer and column. Moreover SEC can utilise a wide variety of good solvents for different polymers. It is possible to observe a big difference in resolution between SEC and TGIC analysis in Figure 4.19 below, taken from the work reported by Chang *et al*. in 1996.[14] Ten polystyrene standards with molecular weights in the range from 1.7 to 2890 kg mol^{-1} were analysed by isocratic elution using a 49/51 (v/v) mixture of THF/CH_3CN as the mobile phase while the temperature was varied from 0°C to 44°C. The column used was a C18 bonded silica column (Alltech, Nucleosil, 100 Å pore, 250 x 4.5 mm) and the flow rate was 0.5 ml/min.

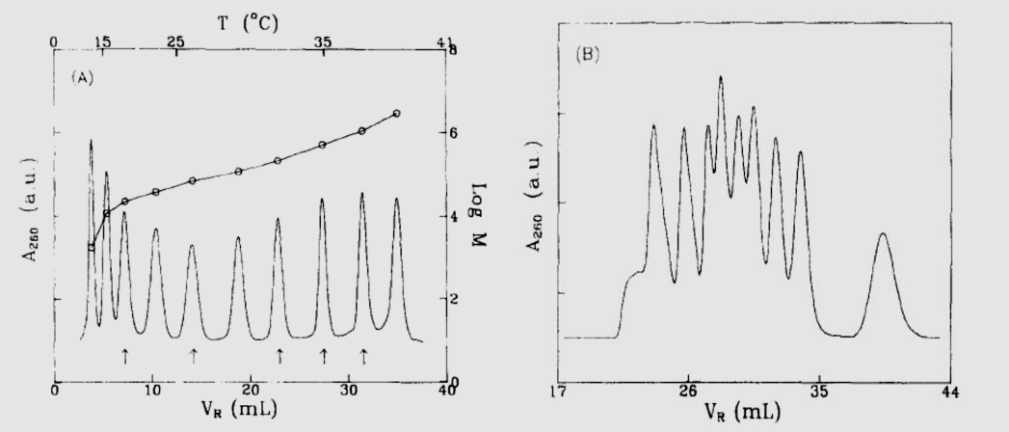

Figure 4.19 TGIC (A) and SEC (B) chromatograms for ten polystyrene standards. In the first chromatogram (A) it is also reported the temperature program at the top of the graphic and the calibration curve of log M versus the retention volume (V_R). "Reprinted from Polymer, 37, H. C. Lee, T. Chang, *Polymer molecular weight characterization by temperature gradient high performance liquid chromatography*, 5747-5749, Copyright (1996), with permission from Elsevier."

It is clear that the resolution of the same mixture of linear polystyrene samples is better in the case of TGIC analysis in comparison with SEC analysis. In this study it was also pointed out that the underlying mechanism of separation was not clear. The solvents used for the TGIC were good solvents for PS but at the lower temperatures exploited at the start of the experiment the highest molecular weight sample was not soluble - so it would appear that the polymer-solvent interactions may also contribute to the separation mechanism and

should not be ignored. Similar high resolution was obtained in another study for the TGIC analysis of PMMA samples[15] and in addition it was noticed that a change in the type of stationary phase could influence the TGIC separation analysis demonstrating that the stationary phase has an important role in the separation and it is not a passive support.

TGIC can be carried out as either a reverse-phase or normal-phase chromatography. The two types of technique work with different stationary and mobile phase. Reverse-phase chromatography utilises a non-polar, hydrophobic stationary phase such as silica modified with RMe_2SiCl, where R is a straight chain alkyl group like $C_{18}H_{37}$, and a mobile phase that is more polar than the stationary phase. Normal-phase TGIC instead utilises a polar, hydrophilic stationary phase such as bare silica and a mobile phase whose polarity is changed according to the polymers analysed. Reverse-phase (RP) TGIC has been used for the characterisation of imperfections in model branched polymers and it has been demonstrated as a useful tool to reveal impurities that SEC is not able to resolve. RP-TGIC is often carried out close to or even below theta conditions i.e. under poor solvent conditions and for this reason, polymers can precipitate and the actual mode of separation is more complex than often described. Normal-phase (NP) TGIC can result in the same good resolution seen with RP-TGIC but in addition it is very sensitive to functional groups on polymers making it possible to separate polymers by their functionalities as well as molecular weight.[16]

A schematic representation of TGIC apparatus can be observed in the figure below (Figure 4.20).

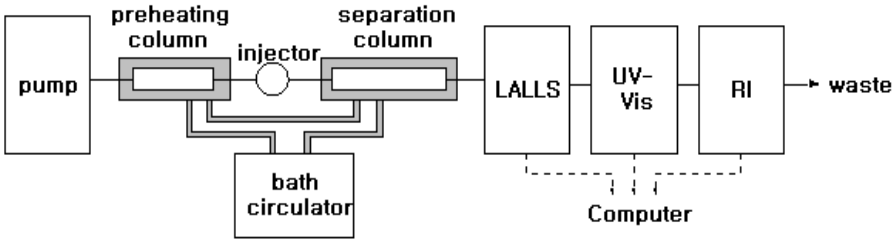

Figure 4.20 Schematic picture illustrating the TGIC apparatus.

This system makes it possible to control the column temperature – one of the key parameters that can influence the resolution of the separation of the polymer solute.

TGIC has been employed for the characterisation not only of linear polymers like PS, PMMA and PI[17] but also branched polymers[18,19] demonstrating its ability to separate polymer

molecules that differ in their molecular weight but not very much in their hydrodynamic volume. So while SEC fails to separate such polymers, TGIC can succeed thanks to the interactions that regulate the separation of the polymers in terms of their molecular weight without being influenced by the molecular architecture. Some of the classes of branched polymers which have been successfully characterised by TGIC include H-shaped polymers[20,21], star polymers[22,23], dendritcally branched polymers[24], mikto-arm star block copolymers[25] and highly branched polymers[26]. In the case of the star polymers, TGIC was used for the characterisation of polystyrene six-arm stars by Chang *et al*.[23] It is shown in this study how TGIC can resolve each peak representing the unreacted arm and each coupled species from two arms to six. The improved resolution obtained with TGIC compared to SEC analysis is remarkable, confirming the great potential of TGIC to resolve polymers differing in the molecular weight but similar in the hydrodynamic volume.

In the current work we decided to characterise the polystyrene star polymers by TGIC to check the purity of the final product and quantify the level of residual impurities. It has been mentioned above, that the product of many, if not all, of the coupling reactions is likely to contain small quantities of part coupled star, i.e. a linear polymer comprising of one 'long' arm coupled to the 'short' arm or two 'long' arms in the case of the symmetric star. We have also seen that SEC analysis is not capable of identifying the presence (or otherwise) of this intermediate product due to the small differences in hydrodynamic volume. The primary objective of this exercise was to produce a series of perfect stars with identical 'long' arms for structure-property correlation studies – by perfect stars we mean free of any structural heterogeneity.

TGIC analysis was carried out on each star before the subsequent purification by fractionation which was carried out in an attempt to eliminate the partially coupled star and the unreacted 'long' arm. The analysis was conducted by reverse-phase TGIC with a Nucleosil C18 column and the eluent composition of CH_2Cl_2/CH_3CN 55/45 (v/v). The temperature was varied during the elution to control the interactions between the polymer molecules and the stationary phase, the flow rate was maintained constant at 0.25 ml/min.

The high resolution of TGIC made possible the observation of three peaks corresponding to the unreacted 'long' arm, the partially coupled star and the three-arm stars as it can be observed in Figure 4.21.

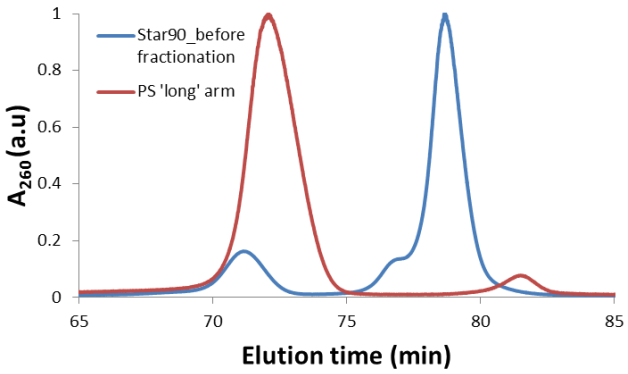

Figure 4.21 Overlay of the TGIC chromatograms of Star90 before the purification by fractionation and of the 'long' arm recorded by UV detector.

The overlay proves that the peak at ca. 71 min present in the crude Star90 corresponds to the unreacted 'long' arm. The molecular weight calculated by TGIC was 91 kg mol^{-1} which is also in excellent agreement to the one obtained by SEC (89 kg mol^{-1}). In Figure 4.22 it is possible to observe the TGIC analysis of each star before the purification by fractionation.

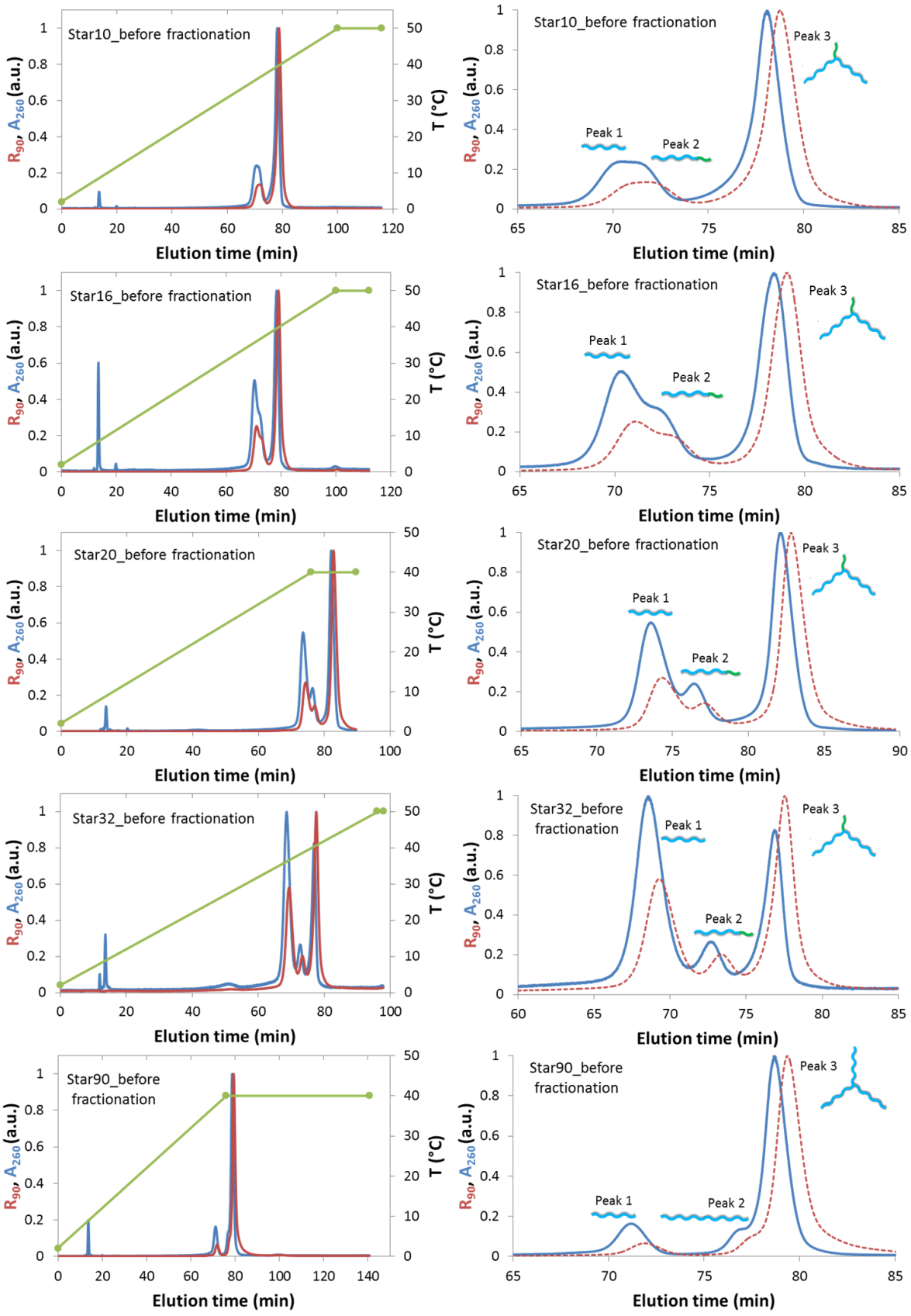

Figure 4.22 TGIC chromatograms of polystyrene three-arm stars before purification by fractionation recorded with UV detector (A_{260}) and RALS detector (R_{90}). Profile temperature can be observed on the left chromatograms and on the right the expanded chromatograms are reported in order to observe the presence of the three peaks due to stars and impurities.

As can be observed from the chromatograms in Figure 4.22 the first peak (at the lowest retention time) corresponding to the 'long' arm is always well resolved. On the contrary, the second peak corresponding to the partially coupled star appears as a shoulder of one of the two main peaks in all cases except Star32. It is possible to notice the shift of this second peak from being a shoulder on the 'long' arm peak in Star10 to be a well resolved peak in Star32 and become a shoulder on the three-arm star peak in Star90 chromatogram. Its shift to higher molecular weight highlights the increase in the molecular weight of the 'short' arm in each star. SEC analysis of the impure stars revealed the presence of a peak corresponding to partially coupled star only in Star90 and Star32 where a shoulder appeared on the main peak representing the star. This is due to the fact that SEC is incapable of distinguishing between polymers with small differences in molecular size i.e. with almost identical hydrodynamic volume.

4.2.4. Purification of the Stars

In both of the two types of coupling reactions (Williamson and 'click') carried out to synthesise the star polymers described above, an excess of 'long' arm was used with respect to the 'short' arm in order to favour the formation of the three-arm star. Despite using an excess, the coupling reaction in some cases is incomplete, resulting in a product comprising of the desired stars along with partly coupled material and unreacted (excess) arms. Unreacted arms and partly coupled polymer formed during the reaction can be separated from the stars by fractionation. Fractionation was achieved using a combination of toluene and methanol as solvent/nonsolvent and a solution concentration of 0.5% w/v was used for each polymer mixture. The procedure described later in the experimental part was repeated three times for each star to ensure the complete removal of the low molecular weight impurities. The success of the fractionation was initially followed by SEC. The SEC chromatogram showed how the peaks of the impurities decreased resulting in the isolation of a purified polymer star. (Figure 4.23) Further analysis of the "purified" star with TGIC allowed a more detailed observation of the success of the purification process and more importantly allowed quantitative analysis of the presence of any trace of residual impurities.

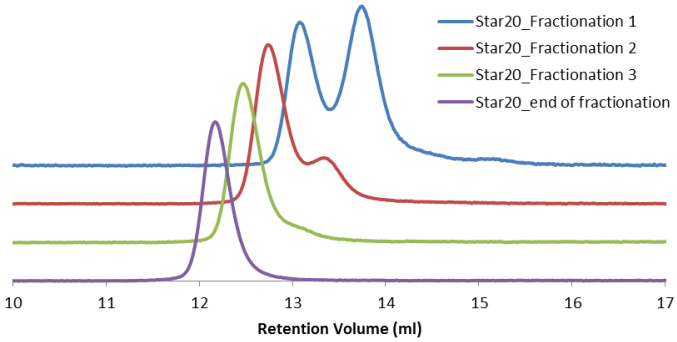

Figure 4.23 SEC chromatograms (RI detector) of the Star20 polymer mixtures from the starting crude material to the final 'pure' star after being processed through three fractionations.

In Figure 4.23 it is possible to observe the SEC chromatograms of Star20 at various stages of purification by fractionation. After the first fractionation most of the low molecular weight impurity polymers were removed (excess of 'long' arm and 'short' arm) and the best fractions collected in this procedure, i.e. the fractions where the amount of impurities was lower, were combined together (second chromatograms in Figure 4.23 from the top) for an additional fractionation. The same procedure was repeated for the third fractionation after which the SEC analysis would suggest that the purification is complete and 'pure' Star20 has been isolated. Shown below in Figure 4.24 are the SEC chromatograms of the crude product and the purified star obtained by fractionation for each star prepared in the current work.

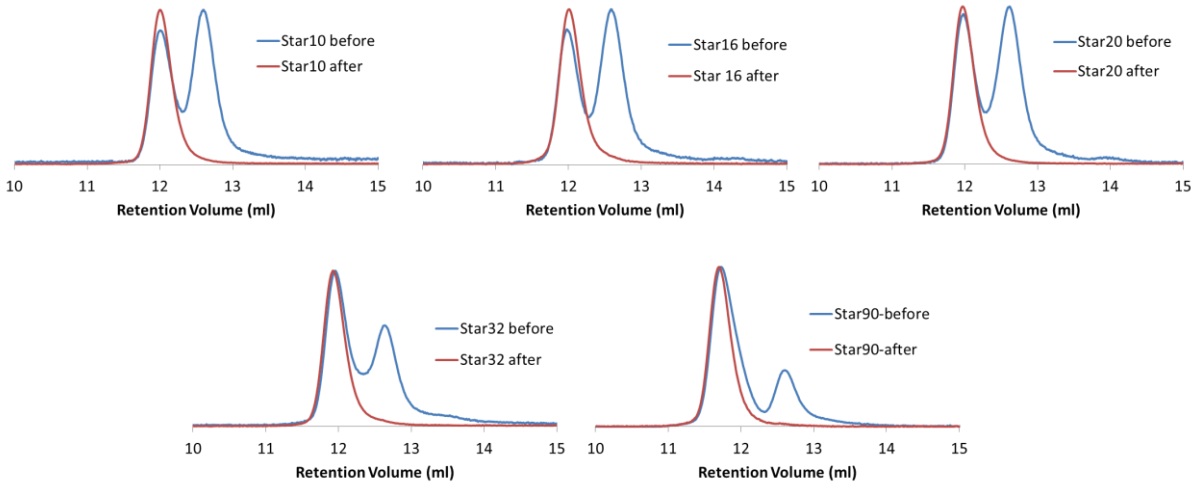

Figure 4.24 SEC chromatograms (RI detector) for each star before and after three fractionations. The last chromatogram Star90 corresponds to the symmetric three-arm star.

In each case the SEC chromatogram of the purified star appears to be monomodal. The final characteristics of the stars synthesised and purified by fractionation are shown in Table 4.5.

Table 4.5 Molecular weight data for the polystyrene arms and the purified asymmetric and symmetric three-arm stars obtained by SEC.

	Molecular weight data for arms						**Molecular weight data for stars**		
StarX	'Long' arm			'Short' arm PSX					
	M_n (g mol^{-1})	M_w (g mol^{-1})	Đ	M_n (g mol^{-1})	M_w (g mol^{-1})	Đ	M_n (g mol^{-1})	M_w (g mol^{-1})	Đ
10	89900	92400	1.03	10000	10500	1.05	193300	197700	1.02
16	89900	92400	1.03	16200	16800	1.04	198800	205100	1.03
20	89900	92400	1.03	19600	20500	1.05	202000	208300	1.03
32	89900	92400	1.03	32100	33700	1.05	211000	218300	1.03
Symmetric star									
90	89000	92400	1.03	-	-	-	279700	289100	1.03

The monomodal peak and the narrow dispersity index (1.03/1.02) for each star obtained by SEC analysis would historically have led to the assumption of a high degree of purity obtained for the three-arm stars. However, as already observed in the analysis of crude stars by TGIC, SEC is incapable of revealing the presence of all those polymers with a similar hydrodynamic volume that constitute the impurities in the polymer stars. For this reason the fractionated stars were submitted to TGIC characterisation and, as observed in the analysis of other branched polymers by TGIC[14], the fractionation process failed to remove completely all the impurities.

As shown in Figure 4.25, TGIC revealed the presence of small quantities of residual impurities with lower molecular weights corresponding to the unreacted 'long' arm and the partially coupled star.

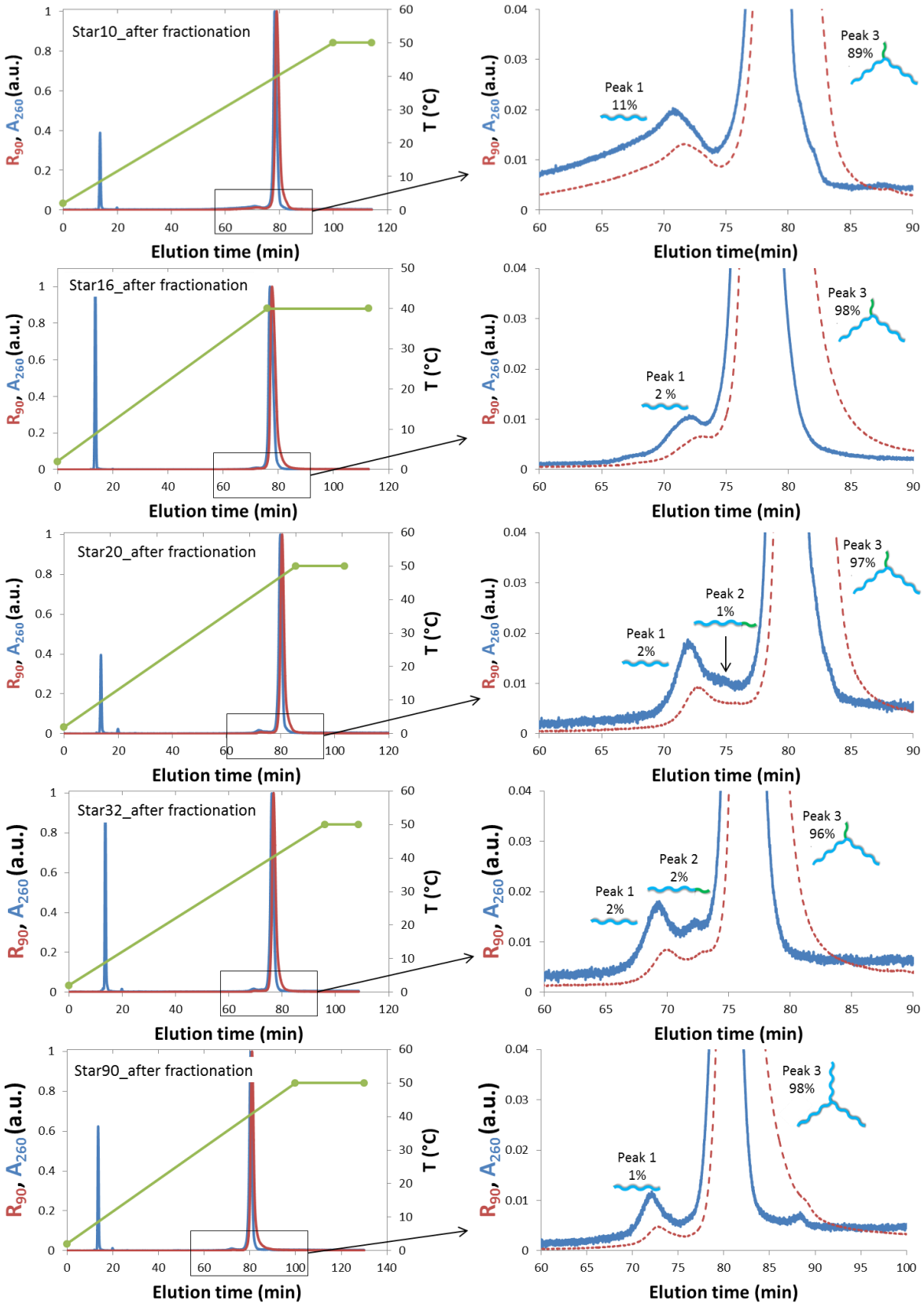

Figure 4.25 TGIC chromatograms of polystyrene three-arm stars after purification by fractionation recorded with UV detector and RALS detector. Profile temperature reported on the graphics on the left and expanded chromatograms on the right in order to observe the presence of remaining impurities. The percentage numbers are calculated by deconvolution of the chromatograms using a Gaussian distribution and represent the relative concentration of each species.

From this analysis it was possible to quantify the amount of impurities present in each star. Deconvolution of the TGIC chromatograms suggested that the desired star was present at a very high concentration at a total weight percent of 89% in Star10, 96% in Star32, 97% in Star20 and 98% in Star16 and 90. The impurities were present but at a very low concentration and they were due mainly to the unreacted 'long' arm. For instance in Figure 4.26 the comparison between the crude Star90 and the purified Star90 after fractionation shows that the remaining impurity corresponds to the 'long' arm and it is visible thanks to the expanded chromatogram highlighting the low concentration of the impurity.

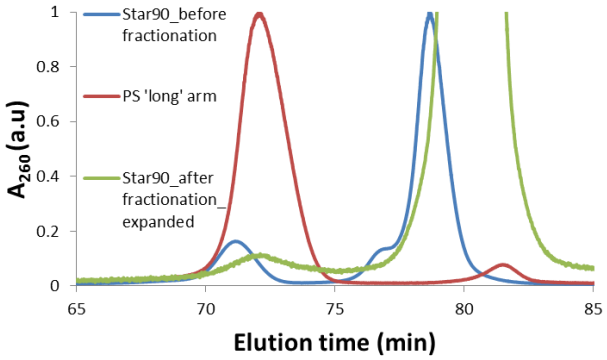

Figure 4.26 TGIC chromatograms of Star90 before and after purification by fractionation and the chromatogram of the 'long' arm overlaid. The 'pure' Star90 has been expanded in order to see the traces of impurities present in the star.

The impurities due to the partially coupled star can be observed in Star20 and 32 in Figure 4.25 having a total weight percent of 1% and 2% respectively. In the chromatogram of Star16 it is possible to observe an impurity peak assigned to the 'long' arm thanks to the fact that the molecular weight estimated by TGIC (M_n 89.8 kg mol^{-1}) was in a good agreement with the molecular weight calculated by SEC (M_n 89.9 kg mol^{-1}). However it is possible to observe next to this peak the presence of another peak at lower elution time. The total weight percent of this impurity has not been calculated but comparing it with the previous peak it can be estimated to be far less than 2%. The possibility of quantifying the presence of the impurities in a polymer thanks to TGIC is important in order to observe the impact of these impurities on the rheology of the polymers. Nevertheless the effect of such low percentage upon rheology measurements has been demonstrated to be negligible. In Hutchings *et al.* report[24] on DendriMacs, TGIC analysis allowed the quantification of the impurities present in the polymer. The quantities of impurities were considered in the computational prediction of the DendriMac rheology and the predictions agreed very well with the experimental rheology. In addition it was also noticed that the experimental rheology was also similar to

the computational prediction of the rheology of a pure DendriMac. The impact of the impurities on the rheology of DendriMacs was found to be significant in the computational predictions only when the impurities were present at a concentration equal to more than 25%.

4.2.5. Comparison between Williamson and 'click' coupling reaction in the synthesis of the stars

The two routes chosen for the synthesis of star polymers described above are both highly efficient conjugation reactions. The two reactions utilised were a Williamson coupling reaction and the copper (I)-catalysed azide-alkyne 'click' reaction. In the current study we investigated the efficiency of each coupling reaction under varying experimental conditions. Star10 and 20 were synthesised exclusively by Williamson coupling reaction, the symmetric star exclusively by the 'click' reaction but Star16 and 32 were synthesised by both types of reactions to allow a comparison of the two methods.

The first advantage given by the use of Williamson coupling reaction in comparison to the 'click' coupling reaction can be found in the number of synthetic steps required to achieve the synthesis of three-arm stars. The required functionalities to allow the arms to be coupled by Williamson reaction can be introduced in fewer steps in comparison with 'click' reaction, which requires two more steps for the introduction of azide and alkyne functionalities. After the introduction of the functionalities required in order to carry out a Williamson coupling reaction, several reactions were carried out to make Star10, at various temperatures and solvent concentrations. The reactions showed how the Williamson coupling reaction can be a good approach for the star synthesis. The optimal reaction conditions proved to be 10 wt. % at 150°C and were adopted for the other stars. The small scale reaction for the synthesis of Star20 showed a conversion that was difficult to reproduce on a large scale reaction. The same reaction conditions were then repeated for the synthesis of Star16 and 32. The conversions obtained in these last two cases were not as high as expected. In particular the reaction for the synthesis of Star32, that involves the use of the highest molecular weight 'short' arm, proved difficult to produce the desired final product in high yield. In fact the SEC chromatograms show the presence of the unreacted 'short' arm peak and a peak between the two main peaks indicating the incomplete star. These disappointing attempts for the

synthesis of Star16 and 32 led us to consider the possibility of choosing a new type of coupling reaction.

Attracted by the reportedly[4,8] high efficiency and versatility of the well-known and widely exploited 'click' reaction, we decided to test its potential in the coupling of Star16 and 32. We started with the use of specific reaction conditions[10] such as the catalytic system [$CuSO_4 \cdot 5H_2O$:Na L-Asc] in a molar ratio of (1:2), the 'long' arm in excess with respect to the 'short' arm (1:2.5) and the solvent DMF. We observed an improvement of the conversion at the first attempt to synthesise Star16 by 'click' coupling. In a series of reactions the amount of catalyst was varied keeping constant the molar ratio [$CuSO_4 \cdot 5H_2O$:Na L-Asc] (1:2) but changing the molar ratio of this catalytic system with respect to the 'short' arm utilised from (1 : 1.25 : 2.5) to (1 : 2 : 4). These changes resulted in a good conversion as shown in the SEC chromatogram in Figure 4.27. In this figure it is possible to observe the comparison of this result with the best result we could get from Williamson coupling reaction.

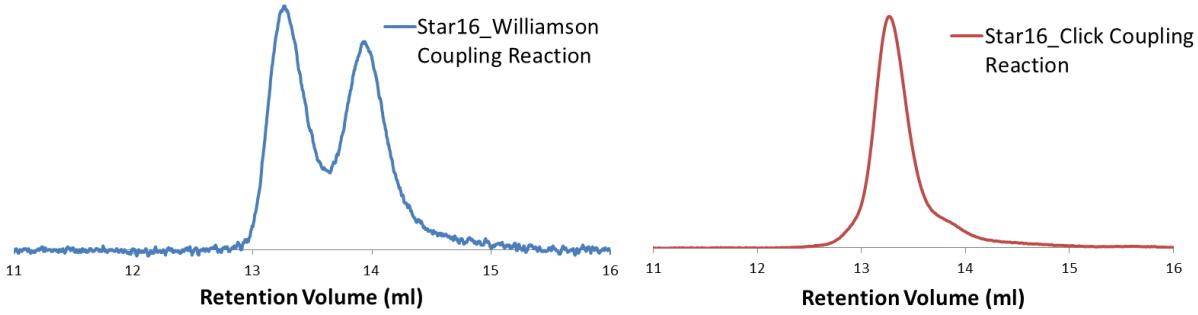

Figure 4.27 SEC chromatograms (RI detector) of Star16 synthesised by Williamson coupling reaction at 150°C and 10 wt. % (left) and 'click' coupling reaction at 50°C and 10 wt. % (right).

To obtain a high conversion in the synthesis of Star32 by 'click' coupling, we needed further modifications to the reaction parameters. The temperature and the solvent conditions were investigated as well as the amount of catalyst. At the end of this study there was a significant improvement in the conversion to star. In Figure 4.28 it is clear that the conversion is far superior in the 'click' coupling reaction.

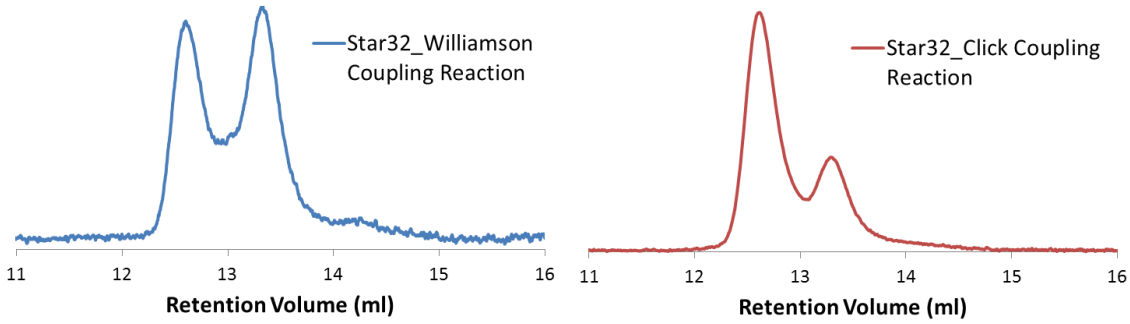

Figure 4.28 SEC chromatograms (RI detector) of Star32 synthesised by Williamson coupling reaction at 150°C and 10 wt. % (left) and 'click' coupling reaction at 60°C and 20 wt. % (right).

The advantage of using 'click' as a coupling reaction instead of Williamson is clear. The former reaction was found to be more reproducible, more efficient and also yielded stars with greater conversions. The reaction time is much lower and the use of high temperatures can be avoided: 50/60°C against the 150°C used for Williamson coupling.

4.3. Experimental

4.3.1. Materials

Benzene (Aldrich, HPLC grade, ≥ 99%), styrene (Sigma-Aldrich, ≥ 99%), dichloromethane (in-house purification) were dried and degassed over calcium hydride (CaH_2) (Acros Organics, 93%) and stored under high vacuum. 3-*tert*-butyldimethylsiloxy-1-propyllithium in cyclohexane (InitiaLi 103, FMC Corporation), triphenylphosphine (Sigma-Aldrich) and carbon tetrabromide (Sigma-Aldrich, 99%), cesium carbonate (Sigma-Aldrich), sodium azide (Sigma-Aldrich ≥ 99.5%), copper sulfate pentahydrate ($CuSO_4 \cdot 5H_2O$) (Sigma-Aldrich), (+)-sodium L-ascorbate (Sigma-Aldrich), 1,1,1,-Tris(4-hydroxyphenyl)ethane (Sigma-Aldrich 98+%) and N,N,N'N'-Tetramethylethylenediamine were used as received. Dimethyl formamide (DMF) (Sigma-Aldrich 99.8%) was stored on molecular sieves (Sigma-Aldrich) under inert atmosphere. *Sec*-butyllithium (Sigma-Aldrich) 1.4 M solution in cyclohexane, was used as received. Propargyl bromide (Sigma-Aldrich) 80 wt. % solution in toluene was used as received. Tetrahydrofuran, toluene, methanol (AR grade) and hydrochloric acid (~36 wt. %) (all Fischer Scientific) were used as received. 1,1-Bis(4-*tert*-butyldimethylsiloxyphenyl)ethylene (DPE-OSi) was synthesised in two steps from dihydroxybenzophenone according to the procedure of Quirk and Wang.[9]

4.3.2. Synthesis of Polystyrene 'long' arm

The reaction was carried out using a specially designed reaction vessel for carrying out anionic polymerisation colloquially known as a "christmas tree" (Figure 4.29).

Figure 4.29 "christmas tree" reaction vessel for living anionic polymerisation.

The polystyrene arms were synthesised by living anionic polymerisation using standard high vacuum techniques. Benzene (500 ml) and styrene (103.14 g, 0.99 mol) were distilled under vacuum into the 1L reaction flask of the christmas tree. To the monomer solution was injected through a septum, TMEDA (0.309 ml, 2.1 mmol) in a molar ratio of 2:1 with respect to the initiator. After that the initiator 3-*tert*-butyldimethylsiloxy-1-propyllithium 0.47 M in cyclohexane (2.25 ml, 1.06 mmol) was injected into the flask. The reaction was stirred at room temperature overnight and then terminated with nitrogen-sparged methanol. The polymer was recovered by precipitation into methanol (8:1 with respect to benzene) and then dried under vacuum. The polymer has been characterised by ^{1}H-NMR spectroscopy and SEC chromatography. Yield 95%.

PS 'long' arm M_n= 89900 g mol^{-1}, M_w= 92400 g mol^{-1}, Đ= 1.03

^{1}H-NMR (C_6D_6, δ in ppm): 3.3-3.5 [C**H**$_2$OSi], 0.9-1.0 [(C**H**$_3$)$_3$C-Si], 0.0 [(C**H**$_3$)$_2$SiO].

4.3.2.1. Polystyrene 'long' arm deprotection

In a 1l flask, the protected 'long' arm (66.53 g, 0.74 mmol) was dissolved in THF (660 ml, 10% w/v solution). To the solution was added concentrated HCl (0.74 ml, 7.4 mmol) in a 10:1 molar ratio with respect to the 'long' arm and after the addition the solution was stirred under reflux at 80°C overnight. The completion of the reaction was checked with ^{1}H-NMR spectroscopy analysis, and then it was stopped. The deprotected polymer was precipitated

into methanol, redissolved in THF and precipitated again and dried under vacuum. Yield 94%.

^{1}H-NMR (C_6D_6, δ in ppm): 3.0-3.3 [C**H**$_2$OH].

4.3.2.2. Polystyrene 'long' arm bromination

In a 500 ml flask, the deprotected 'long' arm (15.65 g, 0.17 mmol) and triphenyl phosphine (PPh_3) (0.14 g, 0.53 mol) were azeotropically dried three times with benzene under vacuum. Dichloromethane (DCM) (150 ml) was added to form a 10% w/v solution. Meanwhile, carbon tetrabromide (CBr_4) (0.22 g, 0.66 mol) was collected in another flask and DCM (5 ml) was added and then it was brought to atmospheric pressure with nitrogen. The CBr_4 was injected to the polymer solution through a septum at a temperature of 0°C maintained with a water/ice bath. The reaction was allowed to rise to room temperature and left to stir at room temperature for 24 hours. A sample was removed to check the completion of the reaction with ^{1}H-NMR spectroscopy analysis before stopping the reaction. The polymer was precipitated into methanol, redissolved in THF and precipitated again and dried under vacuum. Yield >98%.

^{1}H-NMR (C_6D_6, δ in ppm): 2.7-2.85[C**H**$_2$Br].

4.3.2.3. Conversion of the bromide to azide functionality

In a 250 ml flask, brominated 'long' arm (10.05 g, 0.11 mmol) was dissolved in 100 ml of dimethylformamide (DMF) to form a 10% w/v solution and heated at 50°C. To the solution was added sodium azide (0.036 g, 0.55 mmol) in a 1:5 molar ratio with respect to the 'long' arm and it was left stirring overnight. The completion of the reaction was checked with ^{1}H-NMR spectroscopy analysis, and then it was stopped. The azide functionalised polymer was precipitated into methanol and redissolved in THF, precipitated again and dried under vacuum. Yield 94%.

^{1}H-NMR (C_6D_6, δ in ppm): disappearance of the peak at 2.7-2.85[C**H**$_2$Br].

4.3.3. Synthesis of Polystyrene 'short' arm

4.3.3.1. Synthesis of PS10

Benzene (50 ml) and styrene (4.98 g, 47.82 mmol) were distilled under vacuum into a 250 ml reaction flask of the christmas tree. To the monomer solution was injected the initiator *sec*-butyllithium 1.4 M in cyclohexane (0.45 ml, 0.63 mmol) through a septum. The reaction was stirred at room temperature overnight and then to the solution was added 1,1-*bis*(4-*tert*-butyldimethylsiloxyphenyl)ethylene (DPE-OSi) (0.56 g, 1.27 mmol) as a solution in benzene in a molar ratio of 2:1 with respect to the initiator. Before the addition of DPE-OSi, the desired amount of DPE-OSi was weighed into a flask which was sealed and evacuated. Benzene was distilled in under vacuum and removed to azeotropically dry the DPE-OSi before the DPE-OSi was redissolved in benzene. To this was added an equimolar amount of TMEDA with respect to the initiator (0.093 ml, 0.62 mmol) and the mixture titrated with *sec*-butyllilthium until a persistent deep red colour was seen. The end-capping reaction was stirred at room temperature for 5 days and then terminated with nitrogen-sparged methanol. The polymer was precipitated into methanol, redissolved in THF, precipitated again and then dried under vacuum. The polymer has been characterised by ^{1}H-NMR spectroscopy and SEC chromatography. Yield 98%.

PS10 M_n= 10000 g mol^{-1}, M_w= 10500 g mol^{-1}, Đ= 1.05

^{1}H-NMR (C_6D_6, δ in ppm): 3.5-3.7 [**H**C(Ph)$_2$], 0.0-0.2 [(C**H**$_3$)$_2$Si], 0.6-0.8 [C**H**$_3$CH$_2$], 0.6-0.8 [CHC**H**$_3$], 0.9-1.1 [(C**H**$_3$)$_3$C-Si].

4.3.3.2. Synthesis of PS16

PS16 was prepared according to the procedure described above in 4.3.3.1.The solution was made of benzene (50 ml) and styrene (5.24 g, 50.31 mmol). The initiator *sec*-butyllithium 1.1 M in cyclohexane (0.30 ml, 0.33 mmol) was injected. The reaction was stirred at room temperature overnight and then 1,1-*bis*(4-*tert*-butyldimethylsiloxyphenyl)ethylene (DPE-OSi) (0.29 g, 0.66 mmol) was added to the solution. The reaction was stirred at room temperature for 5 days and then terminated. Yield 98%.

PS16 M_n= 16200 g mol^{-1}, M_w= 16800 g mol^{-1}, Đ= 1.04

^{1}H-NMR (C_6D_6, δ in ppm): 3.5-3.7 [**H**C(Ph)$_2$], 0.0-0.2 [(C**H**$_3$)$_2$Si], 0.6-0.8 [C**H**$_3$CH$_2$], 0.6-0.8 [CHC**H**$_3$], 0.9-1.1 [(C**H**$_3$)$_3$C-Si].

4.3.3.3. Synthesis of PS20

PS20 was prepared according to the procedure described above in 4.3.3.1. The solution was made of benzene (50 ml) and styrene (5.08 g, 48.78 mmol). The initiator *sec*-butyllithium 1.1 M in cyclohexane (0.19 ml, 0.21 mmol) was injected. The reaction was stirred at room temperature overnight and then 1,1-*bis*(4-*tert*-butyldimethylsiloxyphenyl)ethylene (DPE-OSi) (0.19 g, 0.43 mmol) was added to the solution. The reaction was stirred at room temperature for 5 days and then terminated. Yield 98%.

PS24 M_n= 19600 g mol^{-1}, M_w= 20500 g mol^{-1}, Đ= 1.05

^{1}H-NMR (C_6D_6, δ in ppm): 3.5-3.7 [**H**C(Ph)$_2$], 0.0-0.2 [(C**H**$_3$)$_2$Si], 0.6-0.8 [C**H**$_3$CH$_2$], 0.6-0.8 [CHC**H**$_3$], 0.9-1.1 [(C**H**$_3$)$_3$C-Si].

4.3.3.4. Synthesis of PS32

PS32 was prepared according to the procedure described above in 4.3.3.1. The solution was made of benzene (50 ml) and styrene (5 g, 48 mmol). The initiator *sec*-butyllithium 1.4 M in cyclohexane (0.11 ml, 0.15 mmol) was injected. The reaction was stirred at room temperature overnight and then 1,1-*bis*(4-*tert*-butyldimethylsiloxyphenyl)ethylene (DPE-OSi) (0.13 g, 0.30 mmol) was added to the solution. The reaction was stirred at room temperature for 5 days and then terminated. Yield 94%.

PS32 M_n= 32100 g mol^{-1}, M_w= 33700 g mol^{-1}, Đ= 1.05

^{1}H-NMR (C_6D_6, δ in ppm): 3.5-3.7 [**H**C(Ph)$_2$], 0.0-0.2 [(C**H**$_3$)$_2$Si], 0.6-0.8 [C**H**$_3$CH$_2$], 0.6-0.8 [CHC**H**$_3$], 0.9-1.1 [(C**H**$_3$)$_3$C-Si].

4.3.3.5. Polystyrene ‘short’ arms deprotection

Protected PS10 short arm (5.1 g, 0.51 mmol) was treated in the same way as described above 4.3.2.1 for the ‘long’ arm. Concentrated HCl (1.02 ml, 10.2 mmol) was added and the reaction was stirred overnight. The completion was checked with ^{1}H-NMR spectroscopy analysis before stopping the reaction. Yield>95%.

^{1}H-NMR (C_6D_6, δ in ppm): 0.6-0.8 [C**H**$_3$CH$_2$], 0.6-0.8 [CHC**H**$_3$], 3.5-3.9 [**H**OPh], 3.5-3.7 [**H**C(Ph)$_2$].

PS16, PS20 and PS32 were deprotected following the same procedure described above for PS10 and characterised by ^{1}H-NMR spectroscopy.

4.3.3.6. Conversion of the phenol functionalities to alkyne functionalities

This reaction was carried out as follows for both PS16 and PS32 polymers.

In a 50 ml flask under inert atmosphere of nitrogen, deprotected PS16 short arm (1.01 g, 0.062 mmol) and cesium carbonate (0.051 g, 0.157 mmol) were dissolved in 5 ml of DMF (20% w/v solution) previously dried on molecular sieves. To the solution was then added propargyl bromide (0.018 g, 0.15 mmol). The reaction was heated with an oil bath at 60°C and it was stirred overnight. The completion of the reaction was checked with ^{1}H-NMR spectroscopy analysis, and then it was stopped. The polymer was precipitated into methanol and redissolved in THF, precipitated again and dried under vacuum. Yield 94%.

^{1}H-NMR (C_6D_6, δ in ppm): 0.6-0.8 [C**H**$_3$CH$_2$], 0.6-0.8 [CHC**H**$_3$], 3.5-3.7 [C**H(**Ph)$_2$], 4.1-4.3 [C**H**$_2$C≡CH].

4.3.4. Synthesis of asymmetric three-arm stars

4.3.4.1. Williamson coupling reaction

4.3.4.1.1. Synthesis Star10

In a 250 ml flask, under an inert atmosphere of nitrogen brominated 'long' arm (2.25 g, 0.025 mmol), 'short' arm PS10 (0.1 g, 0.01 mmol) and cesium carbonate (Cs_2CO_3) (0.033 g, 0.101 mmol) were dissolved in 23 ml of DMF previously dried on molecular sieves. The reaction was heated with an oil bath at 150°C and it was stirred with a mechanical stirrer. The progress of the reaction was followed by SEC analysis and when the peak corresponding to the 'long' arm no longer decreased the reaction was stopped. The polymer was precipitated into methanol and redissolved in THF, precipitated again and dried under vacuum. Yield 98%.

Star10: M_n= 143300 g mol^{-1}, M_w= 168300 g mol^{-1}, Đ 1.18.

4.3.4.1.2. Synthesis Star16

Star16 was prepared according to the procedure described above in 4.3.4.1.1. Brominated 'long' arm (2.05 g, 0.023 mmol), 'short' arm PS16 (0.15 g, 0.009 mmol) and cesium carbonate (Cs_2CO_3) (0.030 g, 0.092 mmol) were dissolved in 21 ml of dried DMF. Yields 97%.
Star16: M_n= 162500 g mol^{-1}, M_w= 184700 g mol^{-1}, Đ 1.14.

4.3.4.1.3. Synthesis Star20

Star20 was prepared according to the procedure described above in 4.3.4.1.1. Brominated 'long' arm (2.00 g, 0.022 mmol), 'short' arm PS20 (0.17 g, 0.009 mmol) and cesium carbonate (Cs_2CO_3) (0.029 g, 0.089 mmol) were dissolved in 21 ml of dried DMF. Yields 99%.
Star20: M_n= 191700 g mol^{-1}, M_w= 216100 g mol^{-1}, Đ 1.13.

4.3.4.1.4. Synthesis Star32

Star32 was prepared according to the procedure described above in 4.3.4.1.1. Brominated 'long' arm (2.04 g, 0.023 mmol), 'short' arm PS32 (0.29 g, 0.009 mmol) and cesium carbonate (Cs_2CO_3) (0.030 g, 0.092 mmol) were dissolved in 20 ml of dried DMF. Yields 97%.
Star20: M_n= 172200 g mol^{-1}, M_w= 198400 g mol^{-1}, Đ 1.15.

4.3.4.2. Azide-alkyne 'click' reaction

4.3.4.2.1. Synthesis Star16

In a 250 ml flask under inert atmosphere of nitrogen azide functionalised 'long' arm (2.04 g, 0.023 mmol) and alkyne functionalised 'short' arm PS16 (0.15 g, 0.009 mmol) were dissolved in 20 ml of DMF which was previously dried on molecular sieves to form a 10% w/v solution. The reaction was heated with an oil bath at 50°C and it was stirred with a mechanical stirrer. To the solution was added first sodium ascorbate (0.008 g, 0.04 mmol) and then the catalyst $CuSO_4 \cdot 5H_2O$ (0.005 g, 0.020 mmol) in few drops of water. The progress of the reaction was followed by SEC analysis and when the peak corresponding to 'long' arm no longer decreased the reaction was stopped. The polymer was precipitated into methanol and redissolved in THF, precipitated again and dried under vacuum. Yield 96%.
Star16: M_n= 195800 g mol^{-1}, M_w= 204300 g mol^{-1}, Đ 1.04.

4.3.4.2.2. Synthesis Star32

Star32 was prepared following the same method as described above in 4.3.4.2.1. Azide functionalised 'long' arm (3.23 g, 0.036 mmol) and alkyne functionalised 'short' arm PS32 (0.46 g, 0.014 mmol) were dissolved in 16 ml of dried DMF to form a 20% w/v solution. After heating the reaction to 60°C, sodium ascorbate (0.017 g, 0.086 mmol) and then $CuSO_4 \cdot 5H_2O$ (0.011 g, 0.044 mmol) in water solution were added. The reaction was stopped after 23 hours. Yield 99%.

Star32: M_n= 153400 g mol^{-1}, M_w= 17300 g mol^{-1}, Đ 1.13.

4.3.5. Synthesis of symmetric three-arm star

4.3.5.1. Synthesis of 1,1,1-tris(4-propargyloxyphenyl)ethane (B3 core)

In a 250 ml flask, under an inert atmosphere of nitrogen 1,1-tris(4-hydroxyphenyl)ethane (B3OH) (1 g, 3.26 mmol) and cesium carbonate (2.13 g, 6.54 mmol) were dissolved in 30 ml of dried DMF to form a 20% w/v solution. After the addition of propargyl bromide (1.80 g, 15.13 mmol) the reaction was heated with an oil bath at 60°C. The progress of the reaction was followed by TLC analysis and it was stopped after 48h. The solution was then filtered and the solid washed with toluene. The solvent of the organic phase was removed by rotary evaporation and the product was purified by SiO_2 flash chromatography using toluene as eluent. The first fraction corresponds to the desired product, the 1,1,1-tris(4-propargyloxyphenyl)ethane (B3 core). The product was dried using a rotary evaporator and then analysed by ^{1}H-NMR and ^{13}C-NMR spectroscopy. The yield was 35%.

^{1}H-NMR (DMSO, δ in ppm): 2.05 [s, $Ph_3CC\underline{\mathbf{H}}_3$], 3.55-3.60 [tr, C≡C**H**], 4.7-4.8 [d, $C\underline{\mathbf{H}}_2C{\equiv}CH$], 6.85-7 [m, **H**-Ph].

^{13}C-NMR (DMSO, δ in ppm): 155.21, 141.92, 129.20, 114.03 [aromatic **C**H], 79.38 [**C**≡CH], 78.17 [C≡**C**H], 55.31 [$\underline{\mathbf{C}}H_2C{\equiv}CH$], 50.27 [$Ph_3\underline{\mathbf{C}}CH_3$], 30.31 [$Ph_3C\underline{\mathbf{C}}H_3$].

4.3.5.2. Synthesis Star90 via 'click' coupling reaction

In a 250 ml flask under inert atmosphere of nitrogen, azide functionalised 'long' arm (7.05 g, 0.078 mmol) and propargyl B3 core (0.0098 g, 0.023 mmol) were dissolved in 36 ml of DMF which was previously dried on molecular sieves to form a 20% w/v solution. The reaction

was heated with an oil bath at 60°C and it was stirred with a mechanical stirrer. To the heated solution was added first sodium ascorbate (0.037 g, 0.19 mmol) and then the catalyst $CuSO_4 \cdot 5H_2O$ (0.022 g, 0.088 mmol) both in few drops of water. The progress of the reaction was followed by SEC analysis. After 19h more sodium ascorbate (0.022 g, 0.11 mmol) and then catalyst $CuSO_4 \cdot 5H_2O$ (0.015 g, 0.060 mmol) were added to the reaction. When the peak corresponding to the 'long' arm no longer decreased the reaction was stopped. The polymer was precipitated into methanol and redissolved in THF, precipitated again and dried under vacuum. Yield 99%.

Star90: M_n= 170300 g mol^{-1}, M_w= 214300 g mol^{-1}, Đ 1.29.

4.3.6. Stars Fractionation

In a 3 litre separating funnel the polymer (<10 g) was dissolved in 2 litres of toluene and the separating funnel transferred into a temperature controlled water bath. Methanol was added dropwise to the solution until it became cloudy. The temperature was increased from 20°C to 22°C at which point the solution became clear. More methanol was added until the solution turned cloudy again. The solution was heated until a suitable temperature where it cleared again and then it was left to cool to the set temperature of 20°C overnight. The lower layer fraction obtained was then collected and precipitated into methanol. The polymer was dried under vacuum and analysed by SEC. The procedure was repeated until the SEC chromatogram showed a high intensity of the peak corresponding to the unwanted low molecular weight 'long' arm. The fractionation process was repeated three times for each polymer star synthesised (Star10, Star16, Star20, Star32 and Star90) until disappearance of the peaks corresponding to the 'long' arm.

Star10: M_n= 193300 g mol^{-1}, M_w= 197700 g mol^{-1}, Đ 1.02.

Star16: M_n= 198800 g mol^{-1}, M_w= 205100 g mol^{-1}, Đ 1.03.

Star20: M_n= 202000 g mol^{-1}, M_w= 208300 g mol^{-1}, Đ 1.03.

Star32: M_n= 211000 g mol^{-1}, M_w= 218300 g mol^{-1}, Đ 1.03.

Star90: M_n= 279700 g mol^{-1}, M_w= 289100 g mol^{-1}, Đ 1.03.

4.3.7. Characterisations

4.3.7.1. Size Exclusion Chromatography (SEC)

Measurements of molecular weight and dispersity of the polymers synthesised were carried out by size exclusion chromatography (SEC) on a Viscotek TDA 302 with triple detectors: refractive index, light scattering and viscosity. The columns used were PLgel 2 x 300 mm 5 μm mixed C, that have a linear range of molecular weight from 200-2,000,000 g mol^{-1}. The solvent was THF, the flow rate was 1.0 ml/min at a temperature of 30 °C. The calibration was carried out with a narrow molecular weight polystyrene standard purchased from Polymer Laboratories. A value of 0.185 (obtained from Viscotek) was used for the dn/dc of polystyrene. All data reported in this work are obtained by using triple detection calibration.

4.3.7.2. Temperature Gradient Interaction Chromatography (TGIC)

Temperature gradient interaction chromatography analysis was carried out using reverse phase analysis. The column utilised was a C18 bonded silica (Nucleosil C18, 100Å pore 250×4.6 mm I.D., 5 μm) and the eluent was CH_2Cl_2/CH_3CN (Sigma-Aldrich, HPLC grade) in a ratio 55/45 (v/v). The flow rate was set to 0.25 ml/min. The polymer solution concentration of TGIC samples was about 2 mg/ml dissolved in the eluent mixture and the injection volume was 100 μl. The detectors utilised were LS detector (Viscotek) and UV detector (Knauer). The temperature of the column was controlled by a Thermo Scientific circulating bath and a thermostat. The dn/dc utilised was 0.213 which was obtained from a previous reported measurement.[23] The calibration was done by using a narrow PS standard (66 kg mol). The TGIC measurements were carried out by Mrs Onome Swader which was working as a Postdoc in Dr. Lian Hutchings group at Durham University.

4.3.7.3. Nuclear Magnetic Resonance (NMR)

^{1}H-NMR spectra were measured on Varian VNMRS 700 MHz or Burker DRX-400 MHz spectrometer using either C_6D_6, DMSO or $CDCl_3$ as solvents.

4.4. Conclusions

We have synthesised a series of model asymmetric and symmetric three-arm stars using the combination of living anionic polymerisation and the 'macromonomer' approach. The stars were comprised of two identical 'long' arm of 90 kg mol^{-1} and a varying 'short' arm whose molecular weight was varied from below the entanglement molecular weight of polystyrene (M_e) to above M_e. The technique of living anionic polymerisation used for the synthesis of each single arm, allowed us to obtain well-defined polymers in terms of molecular weight and molecular weight distribution. The 'macromonomer' approach proved to be a very useful method to be employed in order to create this series of stars where the 'long' arm was exactly the same for each star synthesised. In this way the resulting stars were good model polymers for rheological studies which were carried out elsewhere in order to understand the effect of the 'short' arm with varying molecular weight on the rheological properties. The arms were joined together successfully by both Williamson coupling reaction and copper (I)-catalysed azide-alkyne 'click' coupling reaction. Slightly better results were shown for the 'click' coupling reaction that resulted in a greater conversion to stars in the case of Star16 and Star32 and that in addition allowed us to work at lower temperature in comparison to Williamson coupling reaction.

After the coupling reactions carried out with each of described two methodologies, the stars were characterised by both size exclusion chromatography (SEC) and temperature gradient interaction chromatography (TGIC) before and after purification by fractionation. The comparison of the chromatograms obtained by the two different characterisation techniques highlighted the better resolution that can be obtained by TGIC. In addition the comparison showed that the stars were not completely pure after the purification by fractionation, as it had appeared initially by observing the SEC chromatograms of the 'pure' stars. It was observed that the final product still contained traces of unreacted 'long' arm and partially-coupled star. TGIC made possible the observation of these impurities in the stars and, more significantly from a point of view of the subsequent rheological characterisations, the quantitative estimation of amount of these impurities. Thus, TGIC proved to be a necessary technique to be used in combination with SEC for the complete characterisation of polymers and, in particular, branched polymers in order to have well characterised model polymers for the study of the properties.

4.5. References

(1) Larson R. G., *The structure and rheology of complex fluids*, Oxford University Press, (**1999**)
(2) Rostovtsev V. V., Green L. G., Fokin V. V., Sharpless K. B. *Angew. Chem. Int. Ed.*, **2002**, *41*, 2596-2599
(3) Kolb H. C., Finn M. G., Sharpless K.B. *Angew. Chem. Int. Ed.*, **2001**, *40*, 2004-2021
(4) Moses J. E., Moorhouse A. D. *Chem. Soc. Rev.*, **2007**, *36*, 1249-1262
(5) Hutchings L. R., Dodds J. M., Roberts-Bleming S. J. *Macromolecules*, **2005**, *38*, 5970-5980
(6) Clarke N., De Luca E., Dodds J. M., Kimani S. M., Hutchings L. R. *Eur. Polym. J.*, **2008**, *44*, 665-676
(7) Hutchings L. R., Dodds J. M., Rees D., Kimani S. M., Wu J. J., Smith E. *Macromolecules*, **2009**, *42*, 8675-8687
(8) Kempe K., Krieg A., Becer C. R., Schubert U. S. *Chem. Soc. Rev.*, **2012**, *41*, 176-191
(9) Quirk R. P., Wang Y. *Polym. Inter.*, **1993**, *31*, 51-59
(10) Kimani S. M., Hardman S. J., Hutchings L. R., Clarke N., Thompson R. L. *Soft Matter*, **2012**, *8*, 3487-3496
(11) Hseih L. H., Quirk R. P., *Anionic Polymerization, Principles and Practical Applications*, Marcel dekker, New York (**1996**)
(12) Meldal M., Tornøe C. W. *Chem. Rev.*, **2008**, *108*, 2952-3015
(13) Huang H., Niu H., Dong J.-Y. *Macromolecules*, **2010**, *43*, 8331-8335
(14) Lee H. C., ChangT. *Polymer*, **1996**, *37*, 5747-5749
(15) Lee W., Lee H. C., Chang T., Kim S. B. *Macromolecules*, **1998**, *31*, 344-348
(16) Lee W., Cho D., Chun B. O., Chang T., Ree M. *J. Chromatogr. A*, **2001**, *910*, 51-60
(17) Lee W., Lee H. C., Park T., Chang T., Chae K. H. *Macromol. Chem. Phys.*, **2000**, *201*, 320-325
(18) Chang T. *J. Polym. Sci., Part B: Polym. Phys.*, **2005**, *43*, 1591-1607
(19) Hutchings L. R. *Macromolecules*, **2012**, *45*, 5621-5639
(20) Perny S., Allgaier J., Cho D., Lee W., Chang T. *Macromolecules*, **2001**, *34*, 5408-5415
(21) Li S. W., Park H. E., Dealy J. M., Maric M., Lee H., Im K., Choi H., Chang T., Rahman M. S., Mays J. *Macromolecules*, **2011**, *44*, 208-214
(22) Lee H. C., Lee W., Chang T., Yoon J. S., Frater D. J., Mays J. W. *Macromolecules*, **1998**, *31*, 4114-4119
(23) Lee H. C., Chang T., Harville S., MaysJ. W. *Macromolecules*, **1998**, *31*, 690-694
(24) Hutchings L. R., Kimani S. M., Hoyle D. M., Read D. J., Das C., McLeish T. C. B., Chang T., Lee H., Auhl D. *ACS Macro Lett.*, **2012**, *1*, 404-408
(25) Park S., Cho D., Im K., Chang T., Uhrig D., Mays J. W. *Macromolecules*, **2003**, *36*, 5834-5838
(26) Im K., Park S., Cho D., Chang T. *Anal. Chem.*, **2004**, *76*, 2638-2642

CHAPTER 5

Concluding remarks

Conclusions

In this thesis well-defined polymers with branched architectures were synthesised by using living anionic polymerisation and post-polymerisation coupling reactions. The resulting branched polymers were characterised by various techniques. In particular the work focused on two different types of branched polymers: asymmetric three-arm stars, i.e. polystyrene polymers provided with one single branch point and comprised of arms of non-uniform length, and HyperBlocks, i.e. polystyrene-polyisoprene-polystyrene triblock copolymers with highly (hierarchical) branched architectures.

The synthesis of these well-defined polymers was possible thanks to the combination of the living anionic polymerisation technique and the versatile 'macromonomer' approach that allowed us to control the molecular weight, dispersity, composition, microstructure and branched architecture of the polymers synthesised. HyperBlocks and three-arm stars were both constructed from well-defined macromonomers (with A and/or B chain-end functionalities) which were assembled into the branched architectures by coupling reactions. The Williamson coupling reaction and the copper (I)-catalysed azide-alkyne 'click' coupling reactions were the two types of coupling exploited for the synthesis. Both of the two reactions were possible thanks to the presence of chain-end functionalities (A and B) introduced during the living anionic polymerisation of the linear (macromonomer) precursors. A protected initiator (3-*tert*-butyldimethylsiloxy-1-propyllithium) and a difunctional end-capping agent (1,1-*bis*(4-*tert*-butyldimethylsiloxyphenyl)ethylene) (DPE-OSi) were used to introduce the appropriate end groups. A similar approach – namely the use of end-functionalised macromonomers has been previously used[1] and in this work they proved again their great usefulness in the synthesis of branched polymers.

Specifically, HyperBlocks were produced by coupling ABA triblock copolymers of polystyrene-polyisoprene-polystyrene synthesised by living anionic polymerisation. The 'macromonomer' approach, involving the synthesis of the macromonomers first and their coupling after, allowed us to fully characterise the linear polymer segments between the branch points in the resulting long-chain hyperbranched polymers. Large scale reactions (50 grams) were carried out and a series of macromonomers with a varying content of polystyrene (from 20 to 41 wt. %) and a varying molecular weight (from ca. 65000 to 183000 $g \cdot mol^{-1}$) were synthesised. From these precursors a series of HyperBlocks was obtained

which were highly polydisperse in terms of both molecular weight and molecular architecture. The final hyperbranched polymers have a degree of polymerisation (number of macromonomers per HyperBlock) DP_n of between 2.9 and 6.7 and DP_w between 7.9 and 24.6, high values of Đ and molecular weights (M_w) of at least 600 kg·mol^{-1}. For the synthesis of the HyperBlocks the copper (I)-catalysed azide-alkyne 'click' coupling reaction was investigated in addition to the Williamson coupling reaction already used in the previous work.[1] The procedure for the chemical modification of the chain-end groups was described together with the characterisation of the AB_2 macromonomers modified with azide and alkyne groups.

Furthermore a modification was carried out to the procedure for the synthesis of the macromonomers reported in the previous work.[1] In order to improve the dispersity of the first polystyrene block of the ABA macromonomers (broad Đ due to the use of the *n*-propyllithium initiator), THF was added in a small amount and then removed before the addition of isoprene. The removal was necessary to avoid the production of a polyisoprene block with a less desirable high 1,2 microstructure . This procedure worked very well on a small scale reaction and the first block PS block was produced with a 1.14 – c.f. 1.45 by the previously published method. However it was not possible to reproduce this benefit when the reaction was scaled up

The characterisation of both macromonomers and HyperBlocks was accomplished using DSC (for thermal analysis), tensile testing (mechanical analysis) and TEM (morphology studies). The results were compared and examined in order to understand the influence of composition, molecular weight and branched architecture on the physical properties of HyperBlocks. The thermal analysis carried out by differential scanning calorimetry (DSC) showed that both macromonomers and HyperBlocks had two distinct T_gs corresponding to polyisoprene and polystyrene blocks proving that both macromonomers and HyperBlocks undergo microphase separation into discrete domains of polyisoprene and polystyrene. The solid-state morphology studies were particularly interesting and comparisons were made between the morphologies observed for the linear macromonomers, HyperBlocks and blends of Hyperblocks with a commercial linear thermoplastic elastomer (Kraton^{TM} D-1160). TEM indicated that each class of polymer (linear, branched and blends) underwent microphase separation but, while the macromonomers were characterised by various types morphology with long-range ordered, such as cylinders and spheres, the HyperBlocks

showed a microphase separation with no long-range order. This result is undoubtedly due to the highly branched architecture that frustrates and inhibits the formation of morphologies with long-range order. The fact that similar disordered/co-continuous morphologies were observed for all HyperBlocks – regardless of the molecular weight and composition of the linear block copolymer precursors is a rather dramatic observation. Ordinarily, co-continuous morphologies in block copolymers are rather difficult to obtain since there is a rather narrow compositional window within which these morphologies are found – that is assuming a well-defined phase diagram exists for the copolymer in question. Where such a phase diagram does not exist, successfully targeting a particular composition to generate a co-continuous morphology is challenging. It would appear that, should a co-continuous morphology be desirable for a particular application, the synthesis of a complex branched block copolymer of the type described in this work offers a solution to overcome the challenge of optimising block copolymer composition.

Moreover, the potential benefit of using a complex branched polymer to deliver a co-continuous morphology is further demonstrated by the TEM analysis of blends of HyperBlocks with Kraton^{TM} D-1160, a linear PS-PI-PS TPE characterised by a cylindrical morphology with long-range order. The addition of as little as 10% (by weight) of HyperBlocks to this commercial TPE resulted in the imposition of a disordered morphology by the HyperBlock upon the linear polymer. This is a rather extraordinary result and offers an attractive strategy for using small quantities of (potentially expensive) branched polymers to impose co-continuous morphologies upon commodity block copolymers. Finally, tensile testing of the HyperBlocks and blends revealed interesting aspects about the mechanical properties of these polymers. In fact the HyperBlocks showed improved mechanical properties in comparison to the linear precursor macromonomer. Higher strain and higher stress at break were observed demonstrating that the polystyrene branched points in the hyperbranched structure reinforce the “physical crosslinks” responsible for the good mechanical properties of TPEs. Furthermore the HyperBlock (and blends) analysed suggest that it is not necessary to have long-range order in phase separated morphology to have good mechanical properties. Blends of 10, 20 and 30 wt. % of HyperBlocks with the commercial TPE Kraton^{TM} D-1160 were also tested. The mechanical properties showed

intermediate values between the two polymers constituting the blends but still comparable to the mechanical properties of the commercial TPE.

Regarding the second type of branched polymer synthesised during this work, a series of three-arm stars,[2] made entirely of polystyrene, was successfully synthesised by coupling two identical 'long' arms of 90 kg mol^{-1} and a 'short' arm whose molecular weight was varied from below the entanglement molecular weight of polystyrene (M_e) to above M_e. The 'macromonomer' approach made possible the use of the same 'long' arm for each star synthesised enabling the synthesis of a series of stars, identical in every way with the only exception being molecular weight of the short arm – thus making them an optimal series of model polymers for probing the rheological properties of simple branched polymers. Living anionic polymerisation was utilised for the synthesis of each polystyrene arm and made possible the production of well-defined polymers in terms of molecular weight and molecular weight distribution. The coupling of the arms was carried out successfully by both Williamson coupling reaction and copper (I)-catalysed azide-alkyne 'click' reaction. Slightly better results in terms of degree of coupling were obtained for the azide-alkyne 'click' reaction which also allowed us to work at lower temperatures. The characterisation of the star-branched polymers was carried out by using several techniques. During the synthesis, ^{1}H-NMR spectroscopy and size exclusion chromatography (SEC) were employed for the fully characterisation of arms and resulting stars. Purification by fractionation of the stars was required in order to remove impurities arising predominantly by the excess of 'long' arm used during the coupling reaction. Before and after purification each three-arm star synthesised was also characterised by temperature gradient interaction chromatography (TGIC), a technique that showed to be an important and powerful tool in combination with SEC for the analysis of branched polymers. The better resolution obtained by TGIC made it possible to observe each single species present in the crude stars before purification. Unreacted 'long' arm and partially-coupled stars were the impurities identified to be removed in order to obtain three-arm stars with high degree of structural purity. Analysis by TGIC of the polymers after purification revealed that although SEC analysis has suggested that fractionation had indeed removed all of the unwanted impurities/imperfections, in reality, very low levels of impurity and heterogeneity remained. Furthermore TGIC allowed

the quantitative estimation of the amount of impurities presents and it was possible to observe high percentages of pure product (up to 98%). Thus, the possibility to quantify the levels of residual impurities, is fundamental for the preparation of model polymers for the study of properties. Whilst we would always aim to produce a perfectly homogeneous model polymer, the next best thing is a perfectly characterised, nearly homogenous polymers.

In conclusion with this work we could demonstrate that it is possible to plan a synthesis in order to obtain the desired physical properties for a material. The choices made from a chemical point of view such as the selection of the monomers and the method of synthesis led to the production of ABA triblock copolymers known as thermoplastic elastomers. Moreover by changing parameters such as composition, molecular weights and architecture it was possible to observe changes in the microstructure of the polymers and the impact upon the mechanical properties of TPEs. Therefore the chemical nature of the polymers with particular nano and microstructures resulted in the production of materials with specified properties. However, the lack of analytical techniques able to fully characterise the resulting products constitutes a great obstacle for the formulation of new materials and the full understanding of the relationship between structure and properties. Temperature gradient interaction chromatography used in this work is an example of what is required to gain a complete understanding of the polymers synthesised and it must be the beginning of the accurate analysis of the materials in polymer science.

Future Work

Possible future works can be hypothesised for further development in the field of branched polymers such as the polymers constituting the main object of this study: three-arm stars and HyperBlocks.

Asymmetric three-arm stars

Synthesis of three-arm stars by using a different type of monomer. Polystyrene asymmetric three-arm stars of this study were analysed in terms of rheology elsewhere in order to understand the effect of the different short arms on the rheology response. Polystyrene was chosen for the value of entanglement molecular weight (M_e = 16 kg mol^{-1}) which was convenient for the rheological analysis. It could be interesting to make analogous stars from other classes of polymer with different entanglement molecular weight to establish whether the relation between structure and properties are universal.

Synthesis of asymmetric three-arm stars from diblock/triblock copolymers utilising the same 'macromonomer' approach used in this study. Being a very good technique for the synthesis of well-defined branched polymers, using block copolymers could lead to a new series of asymmetric three-arm stars with high structural purity. These might be interesting materials to study as they would be possible architectures of intermediate complexity between linear block copolymers and HyperBlocks. In addition further analysis by temperature gradient interaction chromatography (TGIC) would expand the research also in the field of the TGIC analysis of three-arm star polymers made by block copolymers.

A deeper study of the coupling reaction could be carried out. In particular the study of azide-alkyne 'click' reaction could be deepened by trying to find other conditions in terms of temperature of reaction, solvent and concentration of the polymer mixture. The aim would be to ensure a good degree of coupling also for the 'short' arm with higher molecular weights. In addition, other coupling methods could be found by using other chain-end functional groups, such as thiol groups for thiol-yne 'click' chemistry.

HyperBlocks

Further mechanical tensile testing measurements on the full set of HyperBlock samples and blends of the latter with the commercial thermoplastic elastomer (TPE) Kraton^{TM} D-1160 would help to expand our understanding of the relationship between mechanical properties and branched architecture. Testing the HyperBlocks characterised by different content of polystyrene, analysed already from a point of view of the morphology, could give more information on the relationship between composition and mechanical properties of polymers with the same hyperbranched architecture.

More studies on the morphology of HyperBlocks and blends of HyperBlocks with Kraton^{TM} D-1160 should be carried out by using a different technique like small angle X-ray scattering (SAXS). Such analysis would give further information about the exact nature of the co-continuous morphologies observed in this study by TEM.

The HyperBlocks in this study have been made of polystyrene and polyisoprene. In future it would be interesting to explore whether the HyperBlock architecture could be expanded into other polymer types. . A further understanding on the relationship between branched architecture and composition could be gained. The 'macromonomer' approach and living anionic polymerisation are good techniques to be used for the synthesis of different triblock copolymers made of polybutadiene, for instance, replacing the polyisoprene block. But also diblock or tetrablock copolymers could be used as macromonomers.

New types of coupling reaction of AB_2 macromonomers could be exploited. The aim would be to find a coupling methodology able to give higher degrees of polymerisation for the hyperbranched polymers constructed from macromonomers with high molecular weights (e.g. higher than 100 kg mol^{-1}). We investigated the copper (I)-catalysed azide-alkyne 'click' reaction but new methodologies could be used like, for example, the thiol-yne 'click' chemistry which has been already used for hyperbranched polymers synthesis.[3]

A possible new approach to the synthesis of the linear precursor macromonomers can be exploited. A convergent approach to the synthesis of the P(S-I-S)macromonomers can be introduced in order to decrease the defects arising from the modification reactions carried out after the living anionic polymerisation step. The functionalities required for the 'click'

reaction, such as alkyne groups, can be added to the end-capping agent (DPE-OSi) before the addition of the latter to the living polymer. Possible protection reactions may be required. In this way it is possible to functionalise, characterise and purified more easily the end groups before the end-capping reaction, eliminating the possible defects derived from an incomplete conversion of the phenol functionalities to alkyne groups and a difficult characterisation.

HyperBlocks, being polydisperse polymers, would be interesting but extremely challenging materials for TGIC analysis. TGIC could give a better understanding of the range of molecular species present.

References

(1) Hutchings L. R., Dodds J. M., Rees D., Kimani S. M., Wu J. J., Smith E. *Macromolecules*, **2009**, *42*, 8675-8687
(2) Agostini S., Hutchings L. R. *Eur. Polym. J.*, **2013**, *49*, 2769-2784
(3) Konkolewicz D., Gray-Weale A., Perrier S. *J. Am. Chem. Soc.*, **2009**, *131*, 18075-18077